Soil deformations caused by soft-ground tunnelling

Nigel H. Glossop

SOIL DEFORMATIONS CAUSED BY SOFT-GROUND TUNNELLING

Nigel H. Glossop

Department of Geological Sciences

University of Durham

Submitted in partial fulfillment of the requirements of the degree of Doctor of Philosophy

May, 1978

ACKNOWLEDGMENTS

I would like to express my gratitude to my supervisor, Dr. P.B. Attewell, for giving me the opportunity to carry out the research described in this thesis and for his helpful advice and encouragement.

I would also like to thank the following people and organisations, without whose help the research would not have been possible:

The Transport and Road Research Laboratory for their financial assistance.

The Northumbrian Water Authority and all site personnel for their assistance and cooperation during the field investigations.

Mr. Keith Sizer, M.Sc., Mr. John Bewick, M.Sc., and Mr. Tony Gowland, postgraduate colleagues, for their assistance both in the laboratory and in the field.

Dr. I.W. Farmer, Reader in Mining Engineering, University of Newcastle-upon-Tyne, for his encouragement and support.

The technical staff of the Engineering Geology Laboratories, University of Durham, particularly Mr. Bernard McEleavey and Mr. Philip Kaye for their assistance on site.

Dr. Sandra L. Wolfson for typing the manuscript and for her confidence and friendship.

ABSTRACT

This thesis discusses the interaction between methods of tunnelling in soil and sources of ground loss. Two distinct phases of settlement in cohesive soils are identified. Short term settlements are caused by loss of ground into the tunnel and long term settlements are caused by consolidation of the ground around the tunnel. A stochastic model of ground movements caused by volume loss into the tunnel is developed in order to explain in-situ observations. Consolidation settlement is estimated with the aid of flow nets developed by finite difference numerical modelling. These nets are also used to estimate the contribution of seepage to tunnel face instability.

Field observations of ground movements caused by tunnelling in soft, cohesive ground were made at three sites. These measurements were taken in order not only to add to the store of case history evidence already available, but also in a direct attempt to confirm or disprove the theoretical model. Tunnelling conditions were different in each case. One tunnel was shield-driven in laminated clay, one was shield-driven with the aid of compressed air support in alluvial organic silt, and one was driven without a shield in stiff, stony clay. These case histories confirm that settlement troughs of Gaussian configuration were developed, agreeing with the stochastic model, and that long-term consolidation may develop in clay soils on the removal of compressed air support from the tunnel.

TABLE OF CONTENTS

LIST OF TABLES

LIST OF FIGURES

CHAPTER 5.

LIST OF PLATES

LIST OF SYMBOLS

A	Half width of tabular void (Schmidt, 1969)
A_f	Area of face (seepage calculations)
C (x,z)	Curvature of settlement trough
C_c	Compression index
C_u	Undrained shear strength
D	Tunnel diameter
D_e	Length of sample (extrusion test)
d	Partical diameter in "stochastic" medium
e_o	Original void ratio
F_s	Seepage force
H, h	Piezometric head
I_l	Liquidity index
I_w	Plasticity index
i	Distance of point of inflection of settlement trough from centre-line
i_s	Seepage gradient
k	Soil permeability
k_a	Empirical constant (Schmidt, 1969)
L	Distance from face to point of grout injection
L_w	Liquid limit
l_e	Length of extruded plug (extrusion test)
m_c	Soil moisture content
N_f	Number of flow paths in flow net
N_h	Number of potential drops in flow net
n	Empirical constant (Schmidt, 1969)
OFS	Simple overload factor
P_a	Air pressure in tunnel
P_s	Seepage pressure

P_w	Plastic limit
p_o	Original effective stress in soil
Q	Rate of water flow through soil
R	Tunnel radius
R_a	Rate of advance of tunnel
R_i	Rate of intrusion of soil
S (x,z)	Settlement at coordinates (x,z)
S_h (x,z)	Lateral displacement at coordinates (x,z)
T (x,z)	Tilt at coordinates (x,z)
T_g	Time elapsed between excavation and grout injection
V_a	Volume of ground lost into annulus around shield and lining
V_d	Flow velocity
V_e	Volume of soil element on which seepage force (F_s) acts
V_f	Volume of soil lost into face
V_s	Volume of settlement trough
$V_s\%$	Volume of settlement trough expressed as percentage of tunnel volume
W	Half width of drawdown trough around drained trench
x,z,y	Cartesian co-ordinates with origin at point of ground loss in "stochastic" medium
Z	Depth to tunnel axis
Z_i	Depth to tunnel invert
α	Angle between seepage force and horizontal
γ	Soil density
γ_w	Water density
Δ/l	Deflection ratio (Attewell, 1977a)
Δp	Change in effective stress
Δ_v	Volume change as a proportion of original volume

ε_h (x,z)	Horizontal strain at coordinates (x,z)
θ	"Angle of repose" of "stochastic" medium
λ	Vertical spacing of particles in "stochastic" medium
σ_{ef}	"Extrusion failure" stress in extrusion test
σ_f	Failure stress in extrusion test
σ_o	Overburden stress
ω	Horizontal spacing of particles in "stochastic" medium

Chapter 1

SOFT GROUND TUNNELLING AND ASSOCIATED SETTLEMENTS

1.1) Introduction

In recent years the importance of soft ground tunnelling as an engineering operation has increased considerably, particularly in urban environments. As excavation and lining methods have improved, so tunnelling has become economically more attractive relative to other methods of underground construction. However, the real impetus for this improvement and the major source of economic and environmental advantage for tunnelling methods has been the increasing need to avoid any disturbance at the surface. This need is partly social, as people become less prepared to accept the disturbance associated with, for example, cut-and-cover workings. The major factor is, however, economic, as the cost of disruption to existing services, roads, housing and so on, and the cost of reinstating them, has risen dramatically. In many cases, of course, it is impossible to use any other method, as for example under existing major buildings that must not be destroyed.

The above factors have been augmented by a growth in the number of tunnels needed. Whilst the installation of new services continues, there is a growing need for the replacement or an increase of existing ones. This is the case in the North-East of England, where in order to reduce pollution of the River Tyne it has been necessary to construct a new system of interceptor sewers totalling about 60 km (see Appendix B and Figure 1.1). The majority of soft

tunnels constructed in this country are sewers. These are generally fairly small diameter tunnels, usually about two metres but sometimes up to four metres, excavated at depths between five and thirty metres. Tunnelling is fairly cheap for these sizes (Smith and Bevan, 1972). Another advantage of constructing sewers in tunnel rather than from the surface is that the sewer alignment is not restricted to existing roads and open spaces. This can be very important for gravity fed sewers where gradients may be quite critical.

The other major application of soft ground tunnelling is in the construction of road or rail tunnels where the alignment often precludes construction from the surface. These tunnels are generally somewhat larger than sewer tunnels and are often constructed using specially built equipment (see Section 1.2). This usually means that they are much more expensive to construct than sewer tunnels.

The main problems to be overcome in any tunnelling project are instability of the work area, changes in the face material (particularly if these occur unexpectedly), lining integrity, and surface settlement and related ground movements which may cause consequential damage to structures. The controls on face stability and lining integrity are now reasonably well understood, problems associated with these factors being connected, in the most part, with the excavation mechanics in the tunnel and the structural mechanics of the support. Improvements in face stabilisation methods, construction techniques, and lining still continue with such methods as the bentonite shield (Walsh and Biggart, 1976), continuous lining methods such as slip-formed concrete (Halvorsen, Kesler and Paul, 1976), and so on. Probably the least understood problem associated

with soft ground tunnelling at the present time is that of surface settlement and associated damage to structures. The problem of settlement takes on increasing importance as more tunnels are constructed in the urban environment. In consequence there is a current need for a method of predicting the ground surface movements that will be associated with the construction of tunnels. There is also a need for a better understanding of the fundamental mechanisms by which the ground may be displaced into the excavation, in order that methods of limiting settlement may be developed where necessary. The ground displaced into the tunnel may conveniently be regarded as a volume loss associated with the tunnelling procedure. It should be noted here that a major factor affecting the amount of this ground loss, and hence to some extent the amount of surface settlement, is the expertize and diligence of the construction team themselves, both engineers and miners. The contribution made to the total settlement by imperfect workmanship or poor procedures is of course an imponderable factor in any specific case. In the estimation or prediction of volume loss associated with any given tunnel it should always be borne in mind that the predicted volume may be considerably exceeded if the standard of workmanship is inadequate. This is probably a particularly critical factor in non-cohesive ground where ground loss into the tunnel may be much more rapid.

1.2) The prediction of ground surface movements

The prediction of the ground surface movements associated with tunnel construction can be separated into two phases. The first involves the prediction of the volume of ground "lost" during the

course of the tunnelling process. The second consists of determining how - and to what extent - this volume of lost ground is transmitted to the surface. It will be found convenient in many cases to consider the transmission or migration of voids or lost ground from the tunnel to the surface, although, in fact, it would be more precise to discuss the downward movement of the mass of ground towards the tunnel. To all intents and purposes the two are equivalent.

Sources of ground loss, as noted from field observations, are discussed in Chapter 6. The more general question of ground loss into a tunnel is discussed below. Since this is to a large part dependent on details of the construction of the tunnel, a brief discussion of tunnelling methods is also included.

1.3) Tunnel construction methods

Soft ground tunnels in the U.K. are usually driven with the aid of a form of protective shield of the type pioneered by Greathead (Plate 1.1). A diagrammatic cross-section of a typical shield is shown in Figure 1.2. The shield is cylindrical in shape, generally with a hood at the leading edge and which often incorporates a "bead" in order to facilitate steering (see Section 1.8). There is also an un-reinforced section at the rear, the tailskin, inside which the lining segments are built. The shield is moved forward by hydraulic jacks bearing on lining rings that have earlier been erected. The use of such a shield is now almost universal, both in Europe and the United States. Its principle purpose in most cases is not to support the ground, but to provide security for the miners, the possibility of collapse of the work area being unacceptable. Although quite

understandable, this universal use of tunnelling shields may have several undesirable side effects. As Peck (1969) points out, it may lead to the dissipation of much needed expertize in conventional hand-mining, experience which is invaluable in the sections of a tunnel where a shield cannot be used, for example the first stages of a tunnel when it may be necessary to excavate a chamber for the erection of the shield. It is also possible that the use of a shield may result in larger ground losses, and hence larger settlements than would be caused by careful hand mining (see Section 1.5.3).

In some cases tunnelling machines are used for the ground excavation itself. In difficult ground conditions, closed-face machines which support most of the face may be used (see Section 1.5.1). In good ground open-face machines or roadheaders are more common. Machines have limitations, however, the chief of these being cost and also their poor performance on mixed faces or in ground for which they were not specifically designed. For this reason, the most common means of excavation in soft ground is the use of hand operated pneumatic spades, or "clay-spades." This is likely to remain the case until cheaper, more versatile and more reliable machines have been developed. In extremely poor ground, such as running sands or very soft silts, specialised closed face or bentonite shield machines may be used, often in conjunction with compressed air (Dawson, 1963).

The use of compressed air in cohesionless soils has little or no effect on ground loss (Peck, 1967). In cohesive soils it may have a fourfold effect. Firstly, it provides support to the face, reducing the overload factor (Sections 1.5 and 1.9). Secondly, by reducing or eliminating the seepage gradients, it reduces the chances

of erosion due to water flow. Thirdly, by partially "drying out" the face it may reduce the plasticity of the soil, thus reducing the intrusion rate (Section 1.5.1). Fourthly, by reducing the rate of water flow into the tunnel, dewatering of the soil and hence consolidation settlement will be minimised (Section 1.5.6). This latter effect may be negated if water is allowed to seep into the tunnel when the air pressure is removed (Chapters 5 and 6).

1.4) Tunnel linings

Most tunnels are lined in two stages. The first stage is a primary lining constructed as soon as possible after the excavation process. The function of this lining is to provide support for the ground and to inhibit the entry of water. The second stage is the secondary or final lining, whose purpose is to provide whatever finish is required for the inside of the tunnel, for example a smooth internal bore in the case of a sewerage tunnel. This secondary lining is generally not load bearing and has no effect on ground settlement.

The primary lining in circular soft ground tunnels usually consists of precast concrete segments or cast iron segments bolted together and caulked, and erected within the tailskin of the shield (Ward, 1966; Deere et al, 1969). This procedure inevitably leaves an annular void around the outside of the assembled lining. This void is filled with grout, or sometimes pea-gravel (with or without subsequent grout injection) and any areas remaining ungrouted will contribute to the overall ground settlement. In the case of tunnels constructed without a shield, if a conventional bolted lining is used it is still necessary to cut the tunnel slightly oversize to allow for the erection

of the lining segments. This may result in a smaller void than would be left behind a shield but grouting is still necessary. An alternative method where no tailskin is used is to jack the lining directly onto the soil and hold it in place using wedges or "Dutchmen." This method requires no bolting and no grouting, although it demands a perfectly smooth circular excavation for it to be used successfully. All the above linings are flexible to a certain extent. This is particularly true of jacked, un-bolted linings which depend for much of their strength on the deformation of the surrounding ground. This deformation will be reflected somewhat in the surface settlement (see Chapter 2).

An alternative method of tunnelling to the above, one which is used in extremely soft ground, is pipe-jacking. In this method a cutting shoe is attached to the front of the leading lining ring, or pipe, and the entire lining is jacked forward as excavation progresses. Using this method it should be possible to avoid most settlement, the only source of ground loss being intrusion into the face, although the jacking process itself may result in some disturbance, possibly even ground heave. In the past, pipe-jacking has been restricted to short, straight drives, typically beneath railway embankments or major roads. However, by using a beaded cutter, and filling the resulting void around the lining with bentonite as a lubricant, it has been possible to reduce dramatically the skin friction of the lining rings and so increase the drive lengths. O'Roarke (1978) quotes drive lengths up to 323 m at rates of up to 41 m/day for pipe-jacked sewers in Chicago.

1.5) Sources of settlement above tunnels

Bartlett and Bubbers (1970) list the sources of settlement above a tunnel as

1. Natural settlement of recent strata.
2. Remoulding of clay caused by tunnel construction, resulting in consolidation.
3. Ground water lowering by well-point systems.
4. Redistribution of material on the return of ground water.
5. Drainage of ground through seepage into the tunnel.
6. Movement of ground towards the working face.
7. Squatting of the primary lining.
8. Loss of ground and limitations of grouting during tunnel construction.
9. Movement due to other activity in the area unconnected with the construction of the tunnel.

To these may be added

10. Movement of ground radially towards the shield if a bead is present.
11. Movement of ground towards the shield due to ovality of hole caused by steering and normal shield "look-up."

All of these sources except 1, 2 and 9 can be counteracted to some extent either at the design stage or by careful construction. Different sources of settlement are emphasised by different ground conditions. In order to discuss the sources of settlement in more detail, we shall split them up into the following broad headings:

a) Settlements due to ground instability.

b) Settlements due to shield design.

c) Settlements due to construction procedures.

d) Settlements due to lining design.

e) Settlements due to ground de-watering.

In reality, the distinction between some of these categories may become blurred. However, each category produces different problems and requires a different solution.

1.5.1) Settlements due to ground instability

Several different types of soil instability can be distinguished in soft-ground tunnels. In slightly cohesive sands and silts, ravelling may occur. This consists of progressive "flaking away" of the face or more usually the roof of the tunnel. If this process is allowed to become established, large cavities may form above the tunnel, ultimately resulting in considerable settlement at the surface. Ravelling ground is easily stabilised by the provision of direct support to the ground, and so is seldom a problem in shield-driven or continuously lined tunnels (Peck, 1969).

Running ground occurs in purely frictional materials such as dry sand or loose gravel. If unconstrained, these materials run into the face until they reach their angle of repose, thus causing considerable settlements (Peck, 1969). It is possible to excavate these materials either by using poling boards ahead of the face or by using a full-face shield to support the ground (Kell, 1963). In either case excessive face-take may occur, so causing large settlements. This form of ground loss is particularly difficult to

recognise, particularly where a tunnelling machine is in use. It is often preferable, particularly where settlement is a critical factor, to attempt to stabilise the ground by grouting.

If seepage pressures are permitted to build up in the above types of grounds, the soil may become what is termed a "flowing ground." If this occurs the ground will run into the face like a liquid, filling the entire heading (Peck, 1969). Clearly, this type of failure must be avoided at all costs. It is possible to tunnel through this kind of material using a full-face shield and allowing the soil to extrude through shutters on the face itself. This procedure must be conducted with great care if settlement or heave at the surface is to be avoided. Usually an attempt will be made to stabilise the ground by drainage, by the use of compressed air (Dawson, 1963), or occasionally by chemical grouting (Anderson and McCusker, 1972), to enable conventional tunnelling techniques to be used.

In cohesive soils (clays and silty or sandy clays) plastic failure will occur at the face when a certain stress level is exceeded. This type of stability criterion, developed by Broms and Bennermark (1967) and developed further by Attewell and Boden (1971) is discussed in more detail in Section 1.8. Failure due to this type of instability consists of rapid incursion of the ground into the excavation, "loss" of the face, and will result in very large settlements. Ground of this type is usually stabilised by the use of compressed air, sometimes in conjunction with a bentonite shield.

It is clear from the above that settlements due to ground instability are large, and usually connected with catastrophic

failure of the excavation. Where the ground is supported physically, for example using a full-face shield or poling boards, surface settlement will be dependent almost entirely on constructional details. Where this is not the case it is normal to stabilise the ground artificially, and in this case the sources of settlement will be those listed in Sections 1.5.2 to 1.5.7.

1.5.2) Settlements in stable ground

Most soft ground tunnels are constructed either in naturally cohesive soil or in ground which has been rendered cohesive artificially. Whilst this type of ground may become unstable under certain circumstances (Section 1.8), these soils will generally stand unsupported at the face, at least for a short period of time. However, as considered in Section 1.13, it is to be expected that slow, plastic intrusion into the void will occur. This small amount of movement into the tunnel will inevitably be reflected in surface settlement and is considered in Sections 1.5.3 and 1.5.4.

1.5.3) Settlements due to the use of a shield

Several sources of ground loss are associated with the use of a tunnelling shield. A typical shield is illustrated in Figure 1.2. As is shown, there is generally a bead around the cutting edge of the shield. The object of this bead is to ensure that the ground only touches the shield at the bead itself and where the base of the shield rests on the bottom of the excavation. This has two effects, firstly to reduce the skin friction acting on the shield, thus making it easier to push forward, and secondly the void around the skin of

the shield facilitates steering. In order for the bead to be effective in carrying out both of these functions, it must be deep enough to ensure that even at low cutting rates the ground does not have sufficient time to intrude onto the tailskin itself. This means that if the shield is functioning properly, no support is provided for the ground until such time as the void behind the lining is grouted. In this case, when the inward movement of the ground is completely unrestricted, the ground loss, and hence settlement due to this factor, is proportional to the distance between the bead and the first grouted ring, and the rate of tunnel advance (see Section 1.10). In the case of very soft ground it may well prove impractical, or even impossible, to prevent the soil moving in onto the tailskin, in which case it may well be best to dispense with the bead. In ground as soft as this it should not be too difficult to steer the shield without a bead, and the lack of a bead should help to reduce ground losses to a certain extent.

In boulder clay "gouging" may be another source of voids around the tunnel. Boulders may be pushed forward by the cutting edge of the shield, ploughing a large groove through the clay outside the shield. In softer ground it is not uncommon to grout each ring individually, immediately after it leaves the protection of the tailskin. Grout may seep into the void around the outside of the skin and if this is allowed to build up it can have the same "gouging" effect as boulders. It is possible for grout to build up over a period of time to such an extent that steerage becomes difficult and a considerably oversize excavation is formed (A.P. Benson, Personal Communication).

In many cases, particularly in soft ground, the shield is driven with "look-up." This means that the longitudinal axis of the shield is inclined slightly upwards from the horizontal. This procedure is necessary to counteract the natural tendency of a shield to nose downwards into the clay under its own weight, and results in the cutting of a slightly oval hole. Where a bead is installed, the look-up is unlikely to have any effect, but if no bead is in use the elliptical excavation forms an extra source of ground loss. Another, probably minor source of ground loss is the use of poling plates and so on for protection in poor ground (Hasmire and Cording, 1972).

Remoulding of a zone of clay around the tunnel during the advance of the shield will most probably occur. This remoulded ground may be compressed under the existing state of stress, particularly in soft or sensitive clays, and may therefore act as another source of volume loss.

1.5.4) Settlements due to construction procedures

Inevitably a void will be formed behind the tailskin around the lining rings. This void may well be quite large, of the order of 50 mm or more in the roof, where it will be widest, and is generally grouted with pea gravel, portland cement, or a mixture of both soon after the shield has passed. The amount of closure which this void will undergo depends primarily upon three factors. These are:

a) The time that the void is left unsupported.

This will depend upon the rate of advance of the shield or heading and the average distance between the face and the point of injection of the grout. The standing time can be reduced by increasing

the mean rate of advance and by reducing the unsupported length of tunnel to a minimum by grouting as soon as possible and by using as short a shield as is feasible (Kell, 1963).

b) The efficiency of the grouting.

It is clear that in most cases grouting of the void is not entirely perfect, it being difficult, for example, to grout right up into the crown of the tunnel. It is common to have to "back-grout" the lining at a later stage. Given time, the voids in or around the grout will close up, so adding to the total settlement.

c) Contraction of the grout.

It is possible that whilst setting the grout undergoes a certain amount of shrinkage. This will, of course, contribute to the ultimate settlement.

Care in construction can reduce to a minimum the sources of settlement described in this section, particularly the removal of boulders to reduce "gouging" and driving with the minimum "look-up" possible. A certain degree of ovality in the excavation will result from any steering corrections or grade corrections which must be made, and therefore the steering and level should be kept as precise as possible. It should be noted that this ovality will be less pronounced with a short shield than with a long one.

The use of a pilot tunnel may increase the total settlement considerably, since although it is much smaller than the main tunnel it will increase the total length of time that the ground is unsupported.

1.5.5) Settlement due to lining design

It is now generally accepted that in most soft ground situations a flexible primary lining will prove most economical (Deere et al, 1969). The type of permanent lining is one of the major factors in the tunnel economy and may affect the choice of excavation method and primary lining (Beauleau, 1972). It is unlikely to have any effect on total settlement, since generally by the time it is installed the primary lining will have stabilised.

Although steel ribs with timber lagging form a common method of primary lining in the U.S.A., in Europe steel or concrete segments are much more popular in soft ground. The disadvantage of the former method is that it is difficult not to leave voids behind the timber lagging, even if this is grouted, and these voids will contribute towards the surface settlement. Also, it is impossible to erect this type of lining within the tailskin of a shield.

The most common type of tunnel lining for use in soft ground consists of segmental rings of either cast iron or pre-cast concrete. Cast iron segmental linings were used extensively in the London Underground (Ward and Thomas, 1965), although nowadays concrete is more common. These linings are normally bolted in place, although boltless linings can be used if they are not erected within the tailskin.

Typically, a tunnel lining undergoes a decrease in vertical diameter, accompanied by an increase in horizontal diameter as the load comes on; that is the lining squats. These deformations may take, according to some of the published literature, some years to develop. The total "squat" of the tunnel may be of the order of 20 mm,

dependent on the stress in the ground and the flexibility of the lining (Ward and Thomas, 1965). This deformation will result in a slight decrease in volume of the tunnel and must therefore contribute somewhat to the total settlement.

The flexibility is advantageous in that it enables the radial stresses to be more evenly distributed through the lining and helps mobilise some of the shear strength of the soil or encourage arching in frictional materials. The lateral dilation of the shield will put the soil into the Rankine passive state (Terzaghi and Peck, 1967) and will therefore mobilise considerable soil resistance (Drucker, 1943).

1.5.6) Settlement due to ground de-watering

The above factors a to d of Section 1.5 all contribute to the total settlement by acting as sources of volume loss, whereas the last factor, e, causes a volume change in the ground above the tunnel. As was noted in Section 1.5 and can clearly be seen from the field measurements taken at Willington Quay (see Chapter 5), settlements associated with de-watering of the ground tend to develop over a long period of time and are often associated with the removal of compressed air.

The magnitude of this consolidation settlement depends on several factors, including the compressibility of the ground, its permeability, and the ability of the tunnel to provide a suitable drainage path. The estimation of this type of settlement is considered in Chapter 3. The contribution of consolidation to the total settlement may be quite large, as it was, for example, at Willington Quay

(Chapter 5) and over the Potomac interceptor (Rebull, 1972), and is likely to be associated with the release of compressed air from the excavation, where this is used. Where compressed air is not used, in clays of low permeability, it is possible that very long-term consolidation settlements may occur. As discussed in Chapter 3, this may account for the long-term increase in settlements associated with the London Underground excavations at Green Park (O'Reilly, Personal Communication).

1.6) Volumetric strain in the ground

It has been reported by several sources (Peck, 1969; Schmidt, 1969; Attewell and Farmer, 1972) that in cohesive soils where significant de-watering does not take place, the volume of the settlement trough is approximately equal to the volume of ground lost at the tunnel (i.e., that the settlement process does not result in any permanent volumetric strain). Although this may not be perfectly true, the results presented in this thesis seem to confirm it in a general sense (Chapters 5 and 6).

If we accept this assumption of zero volumetric strain, and also assume that either the ground experiences no de-watering or that any consolidation can be recognised and dealt with separately, then it is reasonable to attempt to calculate the magnitude of the ground losses associated with the above factors as a first step in predicting the total settlement due to a particular tunnel. The transmission of this volume loss to the surface and the shape of the resulting settlement trough are considered in Chapter 2.

1.7) The calculation of settlement volume

It has been common in the past to assume, for the purposes of settlement calculations, that the volume of the settlement trough, and hence the volume of ground lost at the tunnel, is equal to 2-3% of the total tunnel volume (Bartlett and Bubbers, 1970; Muir-Wood, 1975; Attewell, 1977). Field measurements indicate that this is a reasonable "order-of-magnitude" figure, but it would clearly be more satisfactory to find a somewhat less arbitrary method of calculating settlement volume. In Chapter 6 an empirical relationship between the OFS (Attewell and Boden, 1971) and the volume loss expressed as a percentage of total tunnel volume has been developed. Nonetheless it is of value at least to attempt to consider ground loss into a tunnel in rather more fundamental terms.

In a shield-driven tunnel the sources of volume loss can conveniently be apportioned in the following way.

1. Ground loss into the face.
2. Ground loss into the annulus around the shield and ungrouted lining.
3. Ground loss into voids left in or around the grout.
4. Compression of the grout.
5. Deformation of the lining.

The volume loss due to 1 and 2 above depends upon the size of the tunnel, the rate of advance, the average time elapsed before grouting and the rate of intrusion of the soil, the relations being:

$$V_f = \frac{\pi D^2}{4} \frac{R_i}{R_a} \qquad (1.1$$

$$V_a = \pi D . R_i T_g \qquad (1.2$$

where V_f = volume lost into the face

V_a = volume lost into the annulus

D = tunnel diameter

R_i = soil intrusion rate

R_a = tunnel advance rate

T_g = average time between face excavation and grouting.

All the above factors are readily available, except for the soil intrusion rate (R_i).

1.8) Estimation of the rate of soil intrusion into a tunnel

In order to estim te the rate of soil intrusion into a tunnel we must develop a model of soil deformation around a tunnel. In the case of purely frictional material we can assume that any material allowed to enter the excavation will do so virtually instantaneously and that similarly all voids will be filled instantaneously. In this case the volume loss is directly and solely dependent upon the details of the construction method. However, in this case arching may well develop (Széchy, 1970) if large scale ground loss into the tunnel is avoided, and this will tend to reduce the observed settlement (see Section 2).

We can regard cohesive soils as visco-elastic media. If the state of stress around the tunnel boundaries is within the yield envelope (Schofield and Wroth, 1968) then we can regard the soil as behaving elastically. In this case the deformations would be expected to be quite small and independent of the length of time the clay is left unsupported. However, most tunnels will stress the soil beyond its yield envelope into the viscous or plastic region, where

the deformation of the soil becomes time-dependent.

1.9) Face stability and the overload factor

Broms and Bennermark (1967) investigated the intrusion of clay at depth into vertical openings (analogous to a tunnel face) by extruding clay out of, or into, a small hole in the side of a cylinder. They discovered that "failure" occurred at a loading some 6-8 times the undrained shear strength of the soil (Figures 1.3 and 1.4), i.e.,

$$\frac{(\sigma_o - p_o)_f}{c_u} = 6 - 8$$

where σ_o = applied stress

p_o = confining pressure

c_u = undrained shear strength.

Deere et al. (1969) termed this ratio the simple overload factor or OFS.

From theoretical analysis of semi-circular shear failure at a tunnel face Broms and Bennermark found a theoretical OFS of 6.28, agreeing well with the experimental results. However, several authors (Moretto, 1969; Peck, 1969; Ward, 1969; Kuesel, 1972) have noted unstable conditions at somewhat lower stability ratios.

Attewell and Boden (1971) have proposed the adoption of another stability ratio based on extrusion testing. This type of test involves extruding the clay through a small hole in the side of a cylinder (see Figure 1.5). It is found that as the load on the sample is increased "failure" occurs when $\frac{\sigma_{ef}}{c_u}$ exceeds 4.5,

where σ_{ef} is the stress at failure. "Failure" in this test is considered to occur at the point where the rate of intrusion accelerates (see Figure 1.6). Attempts have been made to relate $\frac{\sigma_{ef}}{c_u}$ to the liquidity index (I_l) (Attewell and Boden, 1971; Attewell and Farmer, 1972). The relationship shown by Attewell and Farmer (1972), along with tests carried out by the author on samples from Willington Quay, is shown in Figure 1.7. Although a trend is apparent, the scatter of the points is probably too great to enable the prediction of face stability from liquidity index. Nonetheless, the extrusion test is extremely useful, since it can be used to predict the rate of intrusion at a tunnel face for any given depth to axis, and this rate is invaluable in any attempt to relate ground loss to tunnel construction procedures.

1.10) Intrusion into a "stable" tunnel

Deformations of the type described above are quite large and may be catastrophic. It is normal for tunnel designers and contractors to maintain the overload factor below 5 or 6 either by increasing the cohesion of the soil by ground treatment or by the use of compressed air. Although this results in a "stable" face, the stress state in the soil close to the tunnel is still outside the yield envelope and therefore the soil will still intrude into the void in a viscous manner. Observations at Hebburn, presented in Chapter 5, indicate that the rate of intrusion into the face of a tunnel is constant, so confirming the observations of Attewell and Boden for stress-controlled tests. Goldstein and Misumsky (1961) also show that the viscous flow component of strain should increase linearly with time.

Attewell and Farmer (1972) plot relationships between σ_v / σ_f and the rate of extrusion for the extrusion test. A summary of these is reproduced as Figures 1.8 and 1.9. Although there is clearly a correlation between them, the scatter of results is rather large. It is considered that further work is necessary on the prediction of intrusion rates before accurate prediction of volume loss into tunnels is practicable.

Observations at Green Park indicate an intrusion rate at a depth of 30 m of approximately 0.0055 mm/hr for a stability ratio ($\gamma Z/c_u$) of 2.07. This agrees reasonably well with experimental predictions (Attewell and Farmer, 1972). At Hebburn, where in-situ measurements of intrusion rate were taken, a rate of 0.22 mm/hr at a stability ratio of 2.02 was observed, again in reasonable agreement with experimental evidence (Chapter 5). It is possible to use these figures as very approximate guidelines to intrusion rates in stiff or laminated clays, along with Figures 1.8 and 1.9, in the absence of better evidence.

It is clear that the amount of ground loss to be expected after the lining has been grouted will depend very much on the care with which the operation is carried out. Volume losses due to grout contraction or lining deformation are likely to be small (Sections 1.5.4 and 1.5.5). Volume loss into voids in and around the grout depends on the quality of the grouting and can only be assessed empirically. On the basis of the case histories reported in this thesis, it is suggested that up to 40% of the total volume of the ground lost may occur after grouting has been carried out.

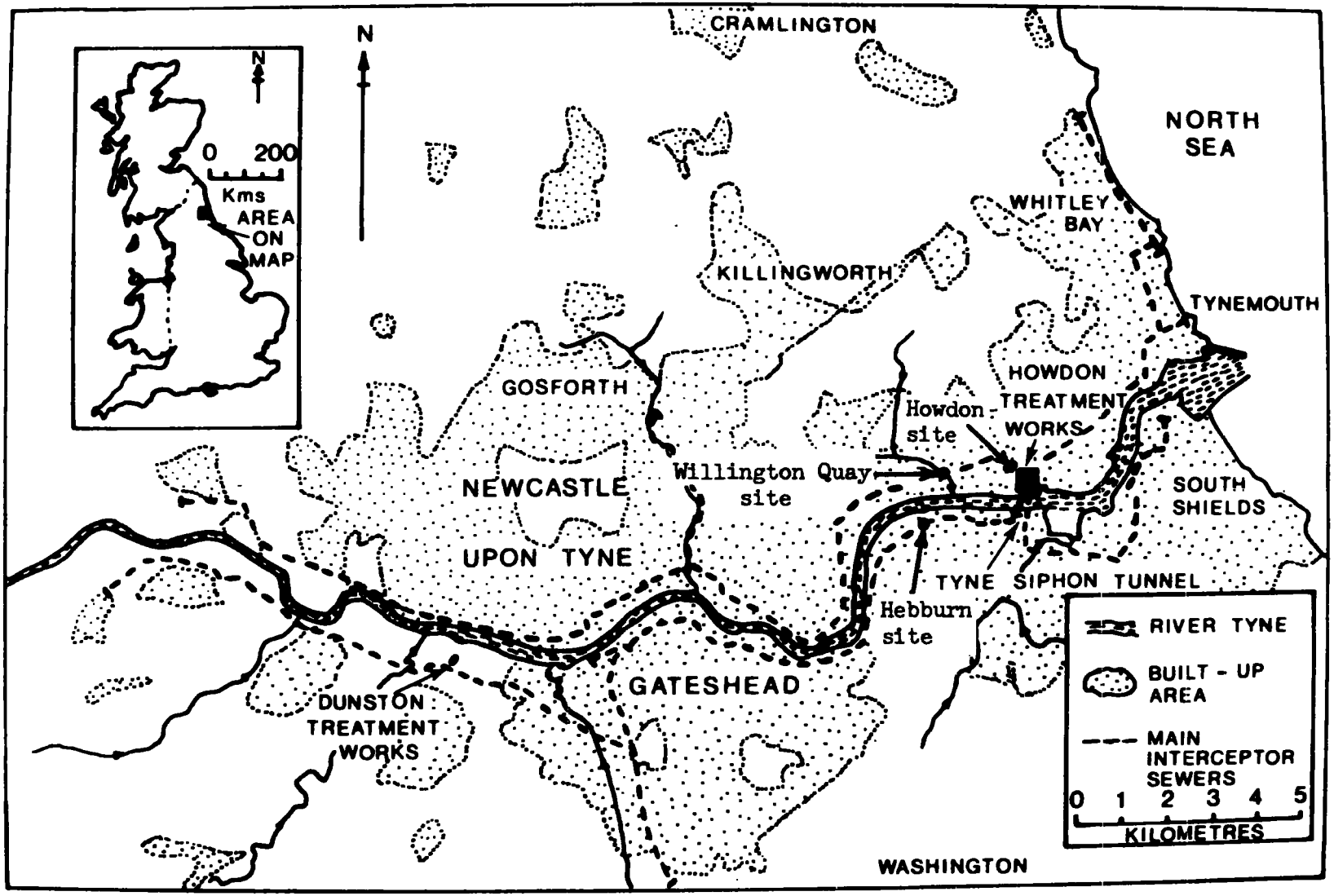

Figure 1.1
Site location map

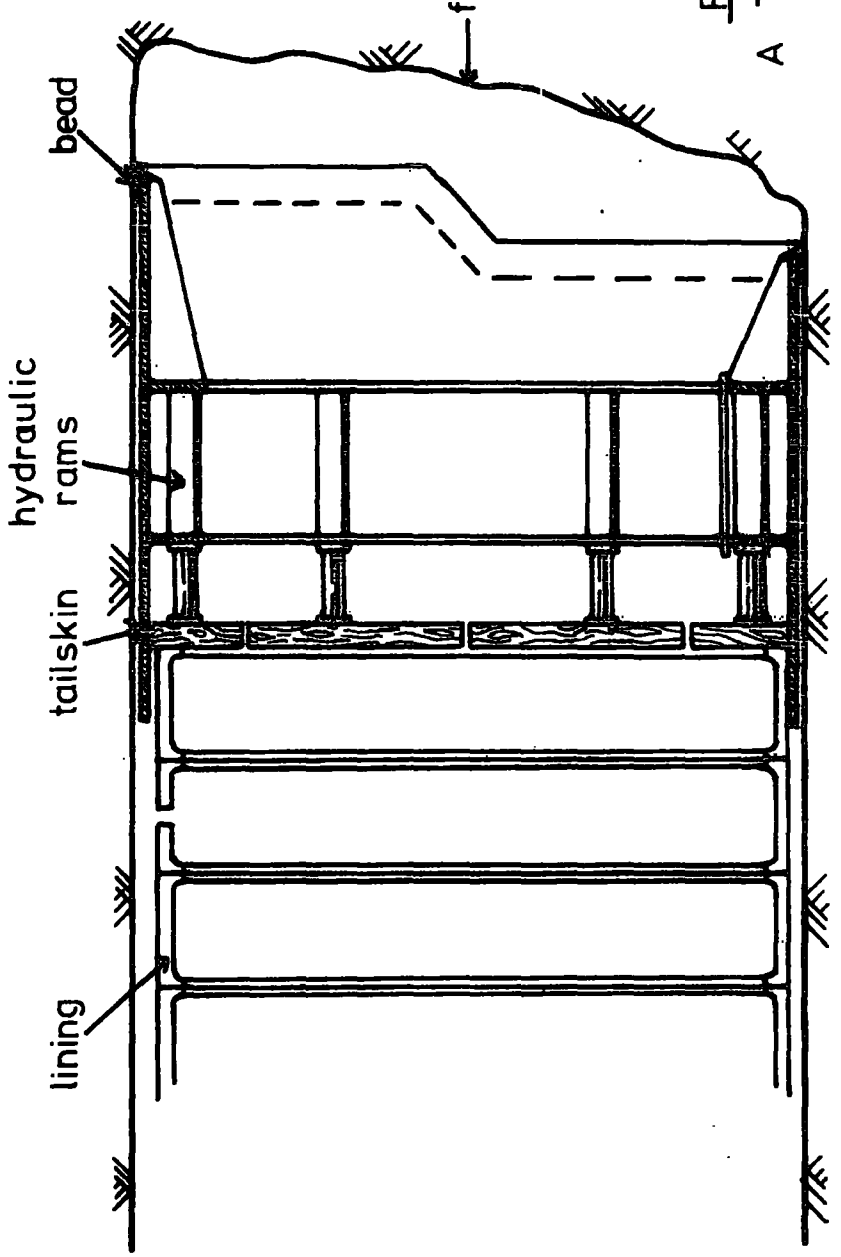

Figure 1.2
A Typical Shield

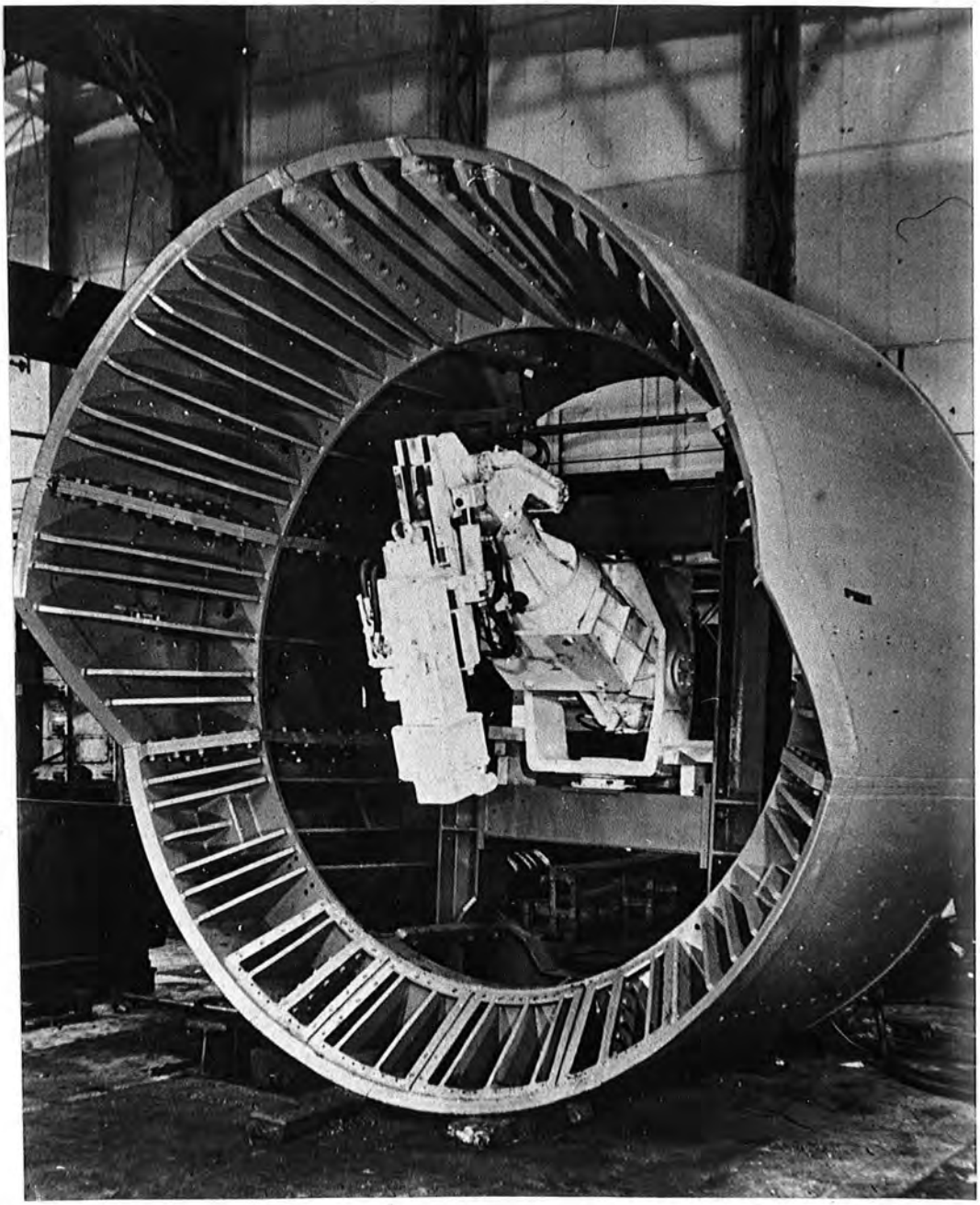

Plate 1.1

A typical shield.

Markham tunnelling shield of the type used for L.T.E. Jubilee Line. This shield is shown in carcass-form only, and with an excavation boom. Photograph by courtesy of the Markham Company, Chesterfield, Derbyshire.

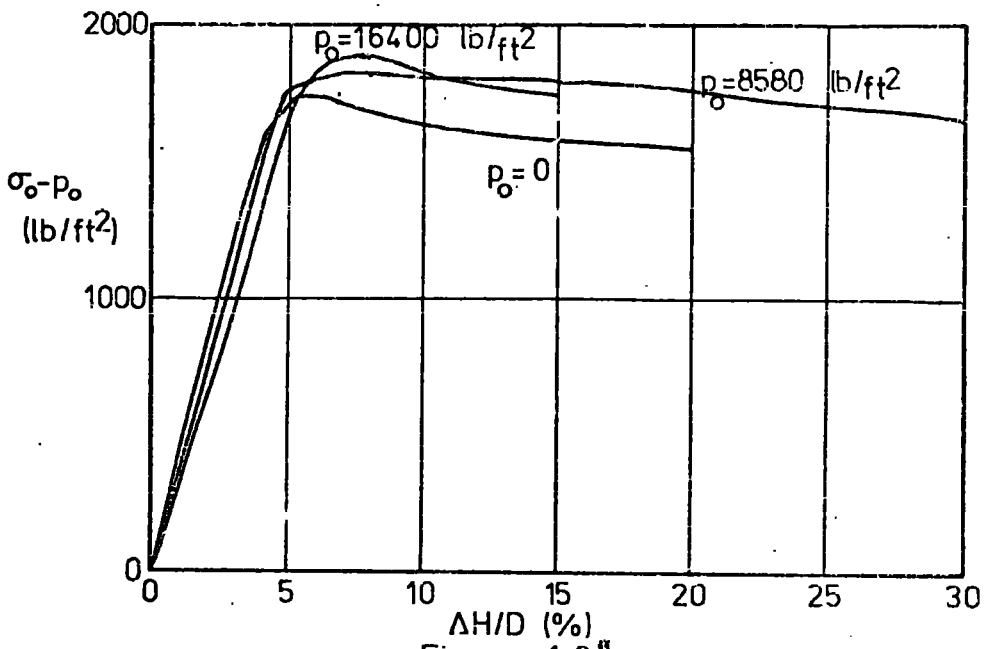

Figure 1.3*
Deviator stress Vs axial defn.

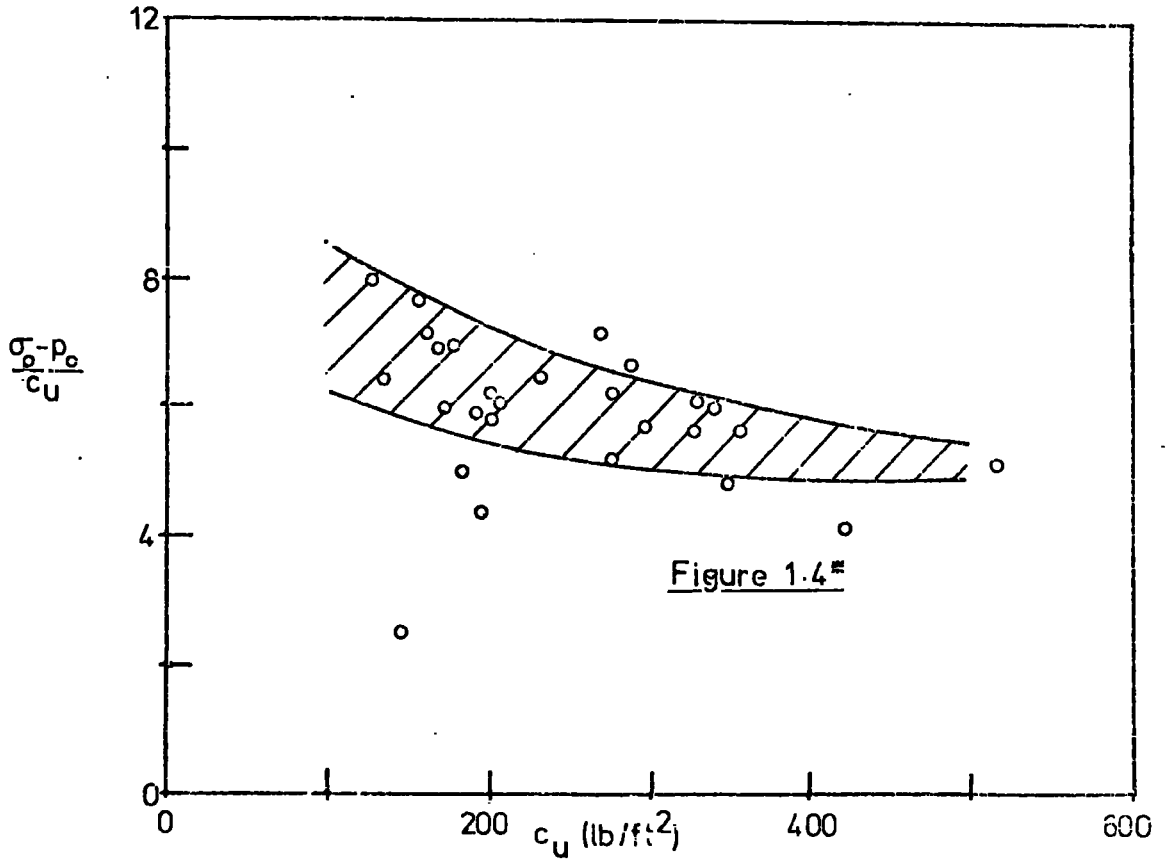

Figure 1.4*

* after Broms and Bennermark (1967)

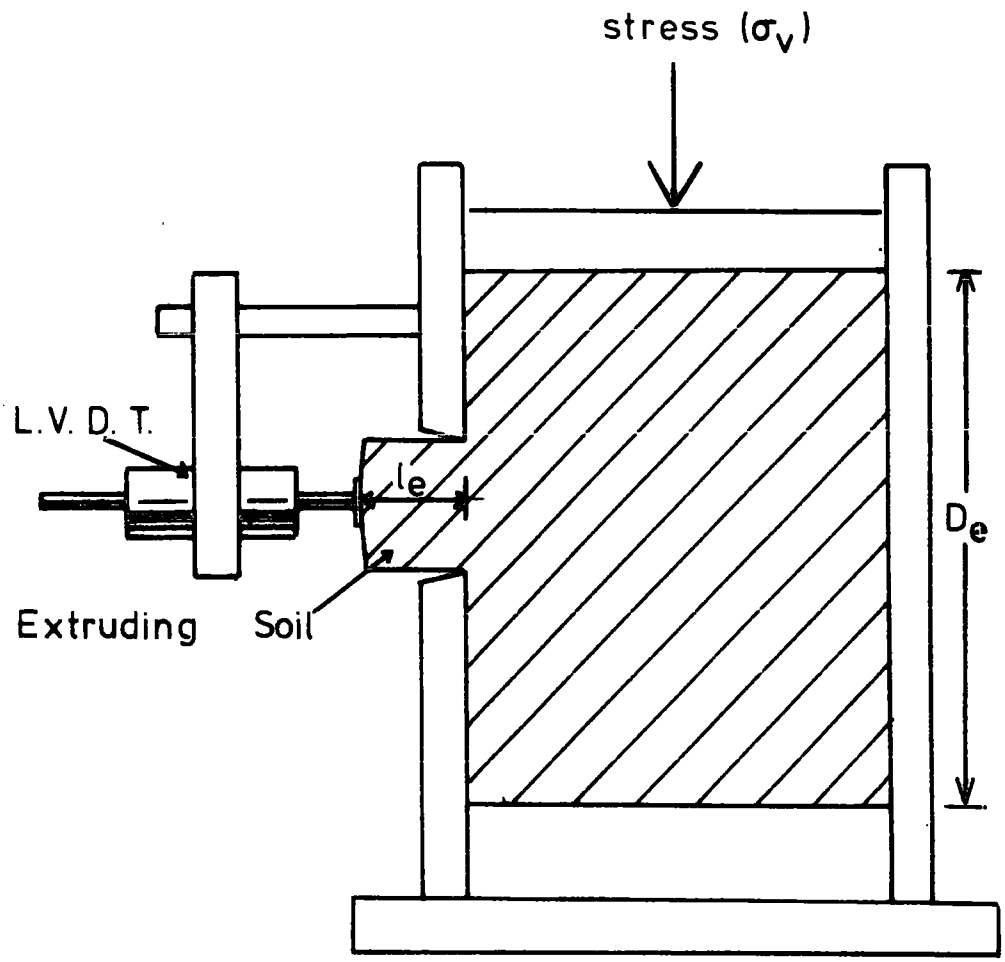

Figure 1.5
The Extrusion Test

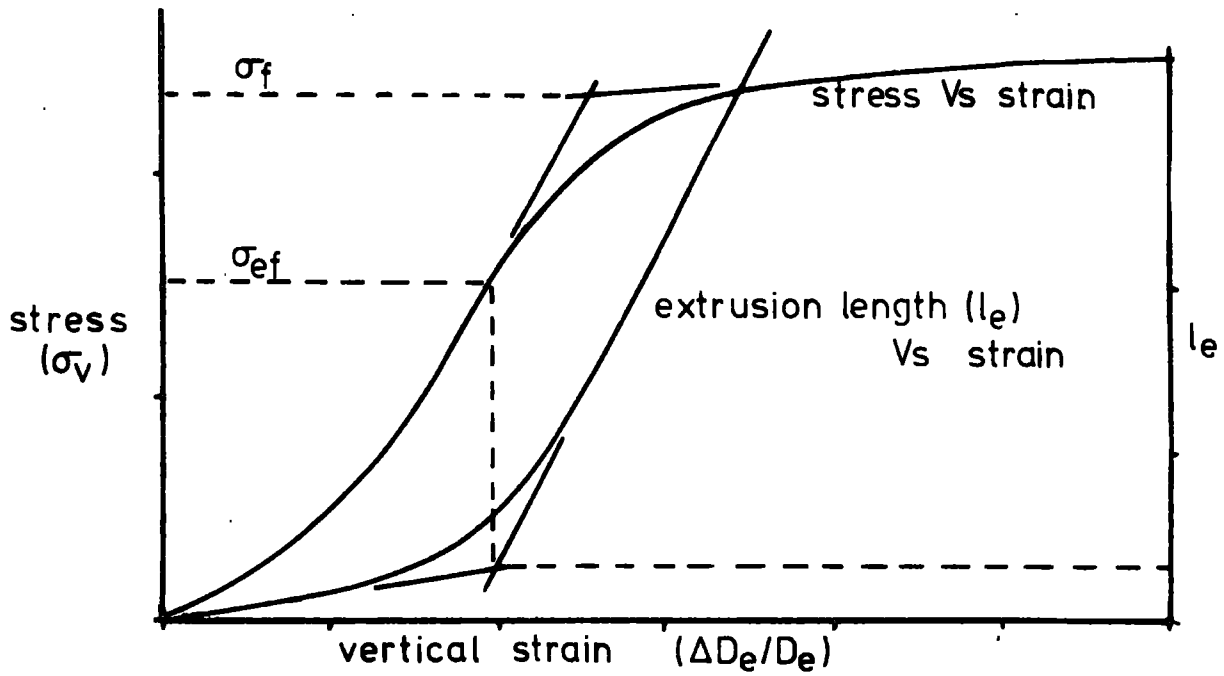

Figure 1.6
Extrusion Test Results

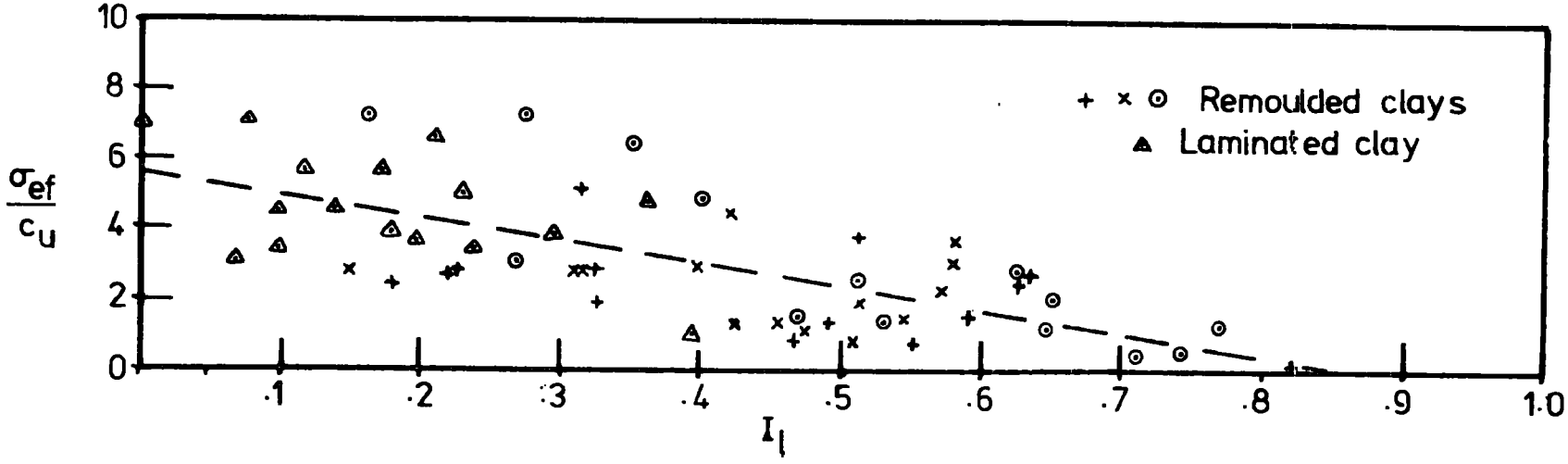

Figure 1.7

Stability ratio Vs liquidity index

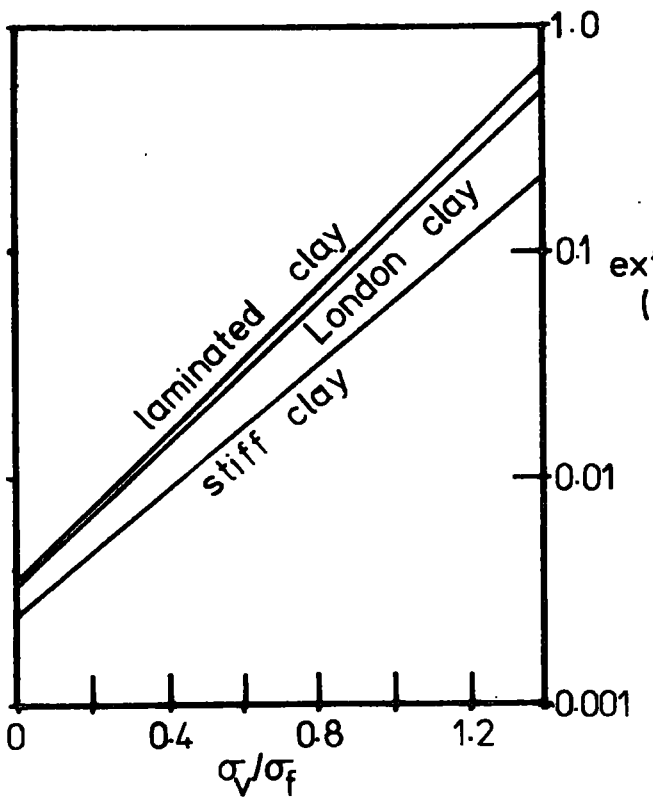

Figure 1·8

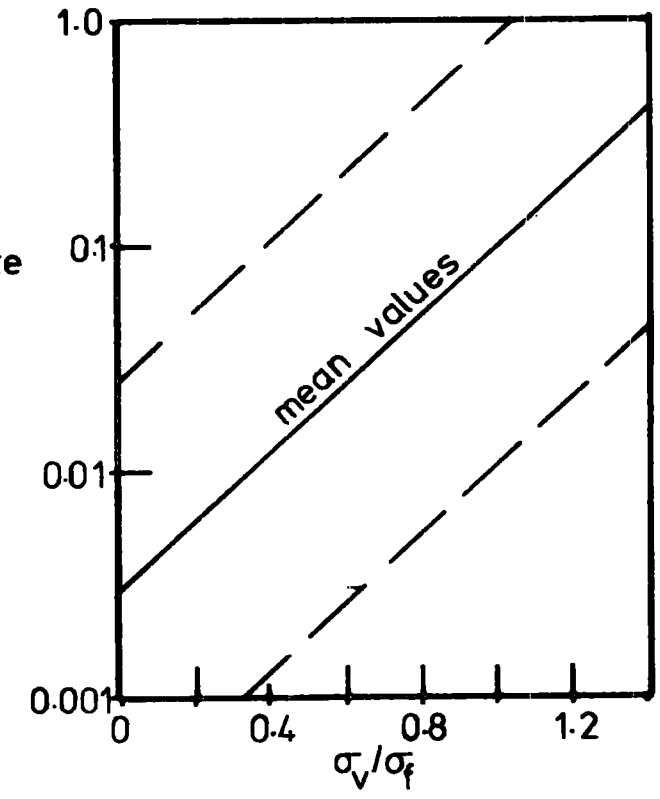

Figure 1·9

Extrusion rate Vs stability ratio

Chapter 2

SETTLEMENT DEVELOPMENT

2.1) Introduction

Chapter 1 has outlined methods for the estimation of the volume of ground that will be lost during the construction of a tunnel in soft ground. In order to predict the nature and magnitude of the settlement trough that can be directly equated to this loss it is now necessary to develop a model which will describe how this volume loss is transmitted to the ground surface. The general requirements for this model are:

a. To predict the shape and magnitude of the transverse surface settlement trough above the excavation;

b. To predict the distribution and magnitude of lateral movements across the settlement trough, and hence;

c. To predict the distribution and magnitude of any surface strains above the tunnel.

Ideally it should also be possible to use the model to predict the development of settlement, displacement and strain at any given point on the ground surface during the construction of the tunnel and to estimate the magnitudes of ground movements at depth. It is also desirable that the model should be applicable to generalised openings of any shape.

In Sections 2.4.2 to 2.4.5 a theoretical model fulfilling many of these requirements is developed for the prediction of ground movements over a tunnel. A comparison of the predictions of this model with

field evidence is discussed in Chapter 6.

2.2) Subsidence* over coal excavations

Many attempts have been made to model the development of subsidence, both theoretical and empirical, over longwall coal seam excavations. These are reviewed by Voigt and Pariseau (1970) and have broadly speaking consisted of the following approaches:

2.2.1) Empirical studies

Probably the largest accumulation of data on mining subsidence is represented by the Subsidence Engineers Handbook, published by the National Coal Board, although of course there are many published reports of individual case histories. The Subsidence Engineers Handbook collates a vast volume of observations and presents them as design curves, applicable to more general cases of longwall mining in the British coal measures. No attempt is made to explain the overall nature of the ground movements, and its application to tunnelling in soft ground is strictly limited.

2.2.2) Theoretical studies

Analytical studies have been carried out considering the ground as an elastic (Hackett, 1959; Berry, 1969) or visco-elastic (Marshall and Berry, 1966) medium. These solutions generally involve many simplifying assumptions about the properties of the ground and the shape of the opening. Generally, agreement with field observations is limited (Voigt and Pariseau, 1970). Even in rock it has been suggested

*Conventionally the small vertical movements generally associated with tunnelling are referred to as "settlements" whereas the larger scale disturbance associated with coal mining is known as subsidence. This convention is adopted throughout this thesis.

that the development of a plastic, "post-yield" zone around the advancing face has considerable influence on the development of surface settlement (Voigt and Pariseau, 1970). Finite element models have also been developed, for example by Zienkiewicz (1976). The major problem with this type of model has been the difficulty in calculating the in-situ properties of the ground in question. It is often necessary to estimate these properties from empirical observations.

2.3) Settlement development above tunnels

Although there is much less literature concerning the development of settlement above tunnels in soft ground, the studies which do exist may be split up into the same broad headings of empirical and theoretical models, along with observations of physical laboratory models.

2.3.1) Empirical studies

Principal sources of case history data are listed by Peck (1969) and Attewell (1977). Both of these authors have attempted to derive relationships between the settlement trough geometry (maximum settlement and trough width) and the tunnel geometry (depth to axis and tunnel diameter). No data are presented on surface strains or lateral displacements. Both authors suggest that the surface settlement trough can be adequately described by a Gaussian distribution, an observation confirmed by the data presented in Chapter 5. This distribution is fully described by two parameters, the trough volume, assumed to be equal to the volume loss at the excavation, and the standard deviation of the curve, which for this distribution corresponds with its point of

inflection (i). Deere (1969) suggests the empirical relation*

$$\left(\frac{Z}{D}\right) = \left(\frac{2i}{D}\right)^{0.8} \qquad (2.1$$

where Z = depth to axis level,

D = tunnel diameter,

i = point of inflection.

Figure 2.1 shows the relation between Z/D and 2i/D for the data quoted by Peck (1969). It is clear that the data shows considerable scatter and that the zones for different materials can only be considered to be rough guidelines. A simpler relation is derived from the data presented by Attewell (1977) in Chapter 6. This type of empirical relation, whilst not providing any elucidation of the possible mechanisms involved in settlement over tunnels, does nonetheless provide guidelines against which theoretical models can be tested.

2.3.2) Laboratory experiments

Laboratory models have been used to study tunnel behaviour, notably at Cambridge (Cairncross, 1973; Atkinson et al., 1974) and at Illinois (Cording et al., 1976). These have used both purely frictional soils (dry sand) and overconsolidated clay (kaolin). Cylindrical cavities in these materials have been stressed to failure, using either a surcharge above the cavity or by generating large body forces in a centrifuge. As has been noted by Attewell (1977) these have shown only limited agreement with field measurements, the frictional soils giving particularly narrow troughs. This possibly reflects the fact that whilst movements above a real tunnel are extremely small in relation to the dimensions of the tunnel, the model tests, of necessity, induce relatively large movements. These possibly result in a different

*Derived on the basis of case history data available prior to 1969.

mode of ground failure from the relatively small plastic deformations observed in the full size situation. This comment should not be taken to imply that there is no place for physical modelling in soft ground tunnel research. However, if used, its emphasis should be on qualitative representation of movement rather than detailed quantitative analysis of the model.

2.4) Theoretical models

As outlined in Chapter 1 there is at present no simple model available to predict ground movements caused by soft ground tunnelling. Finite element models as described by Girijavallabhan and Reese (1968) are restricted by the requirement that all strength parameters for the ground must be known or assumed at all points in the ground. Also a specific solution must be found for each case. Nonetheless, reasonably good agreement with field observations has been found using finite element models (Attewell et al., 1975).

2.4.1) The stochastic model

Several workers, most notably Litwiniszyn (1964) and Sweet and Bogdanoff (1965) have developed models based on a "stochastic" theory of ground movement. A "stochastic" process is one obeying statistical rather than deterministic laws, normally with time as the dominant independent variable (Parzen, 1960). Examples range from queuing times to brownian motion. It should be noted, however, that the independent variable need not necessarily be time, as was stated by Berry (1964), but may, as in the case of the settlement model, be a "space parameter" (Bartlett, 1955).

2.4.2) Litwiniszyn's model

The term "stochastic medium" was coined by J. Litwiniszyn and his co-workers in a series of papers published from 1955 onwards. In these papers an analogy was noted between the general equations of a particular class of stochastic processes (which includes brownian motion) and laboratory observations of settlement profiles obtained under certain conditions. The method was based on mathematical assumptions about the relations between settlements at different depths. A differential equation for the development of settlement was derived and solved, but characteristic functions in the equation must be found empirically. No analytical solution was obtained and the use of probabilistic methods was not attempted. The model has many shortcomings, which are discussed at length by Berry (1964), and provides only an empirical solution.

2.4.3) Sweet and Bogdanoff's model

A stochastic model of ground settlements in granular materials derived using probabilistic methods was presented by Sweet and Bogdanoff in 1964. Since this provides the basis for the model developed by the author, the theory is discussed briefly below.

Sweet and Bogdanoff considered a medium of infinite extent with a co-ordinate system orientated so that the x-axis is horizontal and the z-axis is vertical with positive upwards and the origin at a distance Z below the surface corresponding to the source of the disturbance. If the subsidence at z=0 is described by the function $R(x',0)$ and the subsidence at z is given by the function $S(x,z)$ then a stochastic medium will give a subsidence distribution function such

that

$$F(x,b) = P[S(x,z) \leq b] \qquad (2.2$$

The medium is considered to be a uniform array of spheres or discs as shown in Figure 2.2. If a particle is removed from location (0,0) then either particle (+1, 1) or particle (-1, 1) must fall into the resulting void. In other words, the void may be considered to migrate, either upwards and left or upwards and right. The probability of either of these events is $\frac{1}{2}$. The void will migrate in this way until it reaches the ground surface. The motion of the void can be considered to be a one-dimensional random walk (Chandrasekhar, 1943; Kac, 1947) with the vertical space co-ordinate replacing the time co-ordinate, that is, the void is constrained to move one unit upwards between each observation rather than moving one unit forward in time.

In the general case the void will migrate upwards until it reaches the ground surface or meets a lattice point already occupied by a void. If this occurs the void's motion is no longer random, its path being dictated by the positions of already existing voids. This is illustrated in Figure 2.3. A void reaching any of the positions b to e is forced to migrate to position a. Voids reaching positions g to h must move to position i, whilst those at l to n must move to m. This means that any irregularity in the settlement profile, such as that at i, will eventually be smoothed out. It also means that the trough tends to develop into a "V" shaped profile where the slope angle of the sides, or "angle of repose," is equal to θ in Figure 2.2.

Let R = Event [void travels from (0,0) to (x,z)] ,

Q_i = i voids have left (0,0),

and $W(x,z) = P\left[\frac{R}{Q_1}\right]$ is the probability of event R

when 1 particle has left (0,0).

For the motion of the first void through the lattice the motion is an unrestricted one-dimensional random walk and is described by:

$$W(x,z) = \binom{N}{(K+N)/2} \left(\tfrac{1}{2}\right)^N \qquad (2.3$$

where N = number of steps = z/λ

and K = number of horizontal increments = x/ω

This relation is a binomial distribution with parameter $\frac{1}{2}$. The motion of subsequent voids cannot be described perfectly by the above relation since their paths are restricted by the final positions of all previous voids. Although no solution to this problem was found by Sweet and Bogdanoff it can be seen that the settlement profile will tend towards a "V" shape, a deterministic result.

In most cases of subsidence due to sub-surface ground loss the volume of subsidence is small in comparison with the total volume of ground involved, maximum settlement at the surface being of the order of $\frac{1}{2}\%$ or less of the depth to source. We can assume that for these small settlements the motion of each void is entirely independent and can be described by equation 2.3. The probability of n voids arriving at (x,z) when m leave (0,0) is:

$$P_n[x,m] = \binom{m}{n} [W(x,z)]^n [1 - W(x,z)]^{m-n} \qquad (2.4$$

which is a binomial distribution with parameter W(x,z). Thus, the

probability distribution of the settlement is:

$$P\ [\ S(x,z) = n\lambda\ ] = P_n\ [\ x,m\ ] \qquad (2.5$$

and the settlement distribution function is:

$$P\ [\ S(x,z) \leq n\lambda\ ] = \sum_{i=0}^{m} P_i\ [\ x,m\ ] \qquad (2.6$$

The expected settlement is:

$$S(x,z) = E\ [\ S(x,z)]$$

$$= \sum_{n=0}^{m} n\lambda P_n\ [\ x,m\ ]$$

$$= m\lambda W(x,z) \qquad (2.7$$

This means that the shape of the settlement profile is defined by the function W(x,h), which is a binomial distribution (equation 2.3). Substituting z/λ for N and x/ω for K in equation 2.3 we find:

$$W(x,z) = \binom{z/\lambda}{x/2\omega + z/2\lambda} (\tfrac{1}{2})^{z/\lambda} \qquad (2.8$$

In the case where the particle size is small relative to the total amount of settlement, and when a large number of particles is involved, the number of steps (z/λ) becomes large and the binomial distribution tends to a normal distribution (Kreyszig, 1970), vis:

$$W(x,z) \rightarrow (2\lambda/\pi z)^{\frac{1}{2}} \exp(-(x/\omega)^2 \lambda/2z) \qquad (2.9$$

$$S(x,z) = \lambda m(2\lambda/\pi z)^{\frac{1}{2}} \exp(-(x/\omega)^2 \lambda/2z)$$

$$= (V_s/\omega)(\lambda/2\pi z)^{\frac{1}{2}} \exp(x^2\lambda/2z\omega^2)) \qquad (2.10$$

where V_s = area between the settlement curve and the original surface.

Since $\omega = d \cos \theta$

$$= d\,(1 + \tan^2 \theta)^{-\frac{1}{2}}$$

and $\lambda = d \sin \theta$

$$= d \tan \theta\,(1 + \tan^2 \theta)^{-\frac{1}{2}}$$

then $S(x,z) = V_s/(\sqrt{2\pi}\, i)\left\{\exp\left(-(x^2/2i^2)\right)\right\}$ (2.11

where $i = \sqrt{z\, d/\left\{\tan \theta\,(1 + \tan^2 \theta)^{\frac{1}{2}}\right\}}$ (2.12

This is a normal, Gaussian distribution with the point of inflection at i from the centre-line and represents the settlement due to the loss of a volume V_s of ground from a point source at a height z above that source. Sweet and Bogdanoff generalise equation 8.10 to give the settlement due to a general disturbance at depth z below the surface and having the distribution R(x',0). They find the following relation:

$$S(x,z) = 1/(\sqrt{2\pi}\, i) \int_{-\infty}^{\infty} \exp\left\{-(x - x')^2/2i^2\right\} R(x',0)\, dx \qquad (2.13$$

2.4.4) The stochastic model for cohesive soil

From equation 2.12 we can see that for frictional materials:

$$i = \sqrt{z}\, K \qquad (2.14$$

where $K = \left\{d/\tan \theta\,(1 + \tan^2 \theta)^{\frac{1}{2}}\right\}^{\frac{1}{2}}$

θ = "material constant" of the soil.

Equation 2.14 states that the width of the settlement trough is proportional to the square root of the height of the trough above tunnel axis multiplied by a material constant dependent on the "angle of repose" of the material and its particle size and having dimension $L^{\frac{1}{2}}$. It should be noted that this will tend to predict a relatively

narrow settlement trough. The above parameters are not suitable when cohesive materials are under consideration. Some workers, notably Schmidt (1969), have introduced an empirical term "$k\sqrt{A}$" dependent upon the overall size of the void, thus:

$$i = k\sqrt{A}\, z$$

$$\text{giving} \quad i/A = k\sqrt{2}\,(z/2A)^{\frac{1}{2}} \qquad (2.15$$

This is generalised to the form:

$$i/A = K_a(z/2A)^n \qquad (2.16$$

where A = half-width of opening,

K_a = "material constant" ≈ 1

$n = 0.8$ (empirical value)

The generalisation from 2.15 to 2.16 is made to "account for non-linearities and departures from stochastic theory." This procedure is unsatisfactory since the addition of a term in "A" in this way makes the equations non-linear, that is, a summation of the disturbances caused by many small sources at depth "h" does not give the same result as the calculation of settlement due to an equivalent large source at the same depth using the above equation 2.16. The fundamental stochastic equations <u>are</u> linear, and any modification of the theory to accommodate cohesive soils should take this into account.

We would expect the trough width, as expressed by i, to depend directly on the depth of the source and the material properties of the soil, but only in an additive sense on the width of the opening. The case histories presented in Chapters 4 and 5 of this thesis suggest the very simple relation:

$$i = z/2 \qquad (2.17$$

for cohesive soils.

If this is substituted into equation 2.10 the resulting source function

$$S(x,z) = 2V_s/(\sqrt{2\pi}\,z)\,\exp(-2x^2/z^2) \qquad (2.18$$

can be used to find the settlement at any point over the void.

It is implicitly assumed in the above model that any void created at the source will ultimately create an equivalent "unit of settlement" at the surface, that is, that volume loss at the tunnel equals settlement volume at the surface, and that the medium undergoes no volumetric strain. Whilst it is difficult to justify these assumptions from a theoretical point of view, field evidence, as discussed in Chapter 6, does seem to support them in a general sense.

2.4.5) The prediction of settlement over a generalised opening

Equation 2.16 can be used directly for the calculation of settlement above a tunnel if we assume that all settlement is caused by an infinitesimally small source located at the centre of the tunnel. This model assumes plane strain conditions in the ground, a reasonable assumption for the final case where all settlement is complete (see Section 2.4.6). The assumption of a point source is unrealistic, however, and is likely to lead to error, especially where settlement is calculated relatively close to the tunnel and the effect of the void shape would be expected to be greatest. A more sophisticated and realistic model may be formulated by calculating the settlement over a tabular void of width equal to the tunnel diameter (cf. Litwiniszyn, 1964; Schmidt, 1969). However, by using a numerical approach any shape of opening can be modelled.

The numerical method that is adopted regards the opening as

being made up of a very large number of point sources evenly distributed throughout the opening and each making an equal contribution to the total settlement. The settlement is calculated separately for each source using equation 2.18 and the settlements are summed to give the final settlement profile. This procedure is analogous to the use of influence functions in the prediction of subsidence above longwall coal workings. In this procedure the influence functions are used to deduce the effect of an irregularly-shaped plan of extraction, in a horizontal sense, whereas for tunnels the sources are distributed in a vertical sense. This numerical integration was performed on an IBM 370 computer using the program listed in Appendix E.

Using this program the source of ground loss was modelled in three ways: as a point source, a tabular source (similar to a coal seam), and a cylindrical source (similar to a tunnel), for several depth-to-diameter ratios. Plots of these solutions are shown in Figures 2.4 to 2.6. At large values of z/D (depth-to-diameter ratio) the settlement profiles generated for each of the three models are very similar and at these ratios it would be reasonable, therefore, to use the simple point source/Gaussian distribution model, for which analytical solutions are available. For smaller z/D values (less than about 1.5), several differences become apparent. The trough above the point source remains similar to a Gaussian distribution but becomes narrower and deeper. The other two models begin to diverge from this Gaussian shape. Both produce a trough which is shallower and wider than that over the point source. The settlement trough over a tabular void develops towards a flat centre section with limbs which take the form of a cumulative normal distribution centred over the edges of the source,

although this will only occur at unrealistically small values of z/D. Above an annular source the settlement trough tends to develop two points of maximum settlement, approximately over the springlines of the tunnel. This is due to the fact that at low values of z/D the width of the settlement trough due to each point source becomes so small that the "overlap" of the separate troughs is no longer sufficient to mask the effect of the larger contributions that are made by the sidewalls of the tunnel. This effect would seldom be of relevance to the calculation of surface settlements above tunnels, since they are very unlikely to be constructed at such extremely shallow depths. It may be of importance, however, when attempting to calculate the volume of ground loss associated with a tunnel from the movement of deep settlement rings close to the excavation.

2.4.6) The prediction of tilt, curvature, strain, and lateral displacement

The use of the stochastic model is not restricted to the calculation of vertical settlement above an opening. In order to calculate other parameters we shall first consider the tunnel to be a point source of ground loss at a depth Z, creating a settlement trough as defined by equation 2.18. The tilt at a point (x,z) can be found by differentiating the settlement with respect to x:

$$\begin{aligned} T(x,z) &= \partial S(x,z)/\partial x \\ &= (-4x/z^2)(2V_s/\sqrt{2\pi}z)\exp(-2x^2/z^2) \\ &= (-4x/z^2)\, S(x,z) \end{aligned} \qquad (2.19$$

This expression has a negative sign since for positive values of x (i.e. to the right of the origin) the trough tilts in a negative

direction (i.e. to the left).

For small tilts the ground curvature at a point (x,z) is approximately equal to the second differential of the settlement with respect to x:

$$C(x,z) = \partial_2 S(x,z)/\partial x^2$$

$$= \partial T(x,z)/\partial x$$

$$= (-4x/z^2)(-4x/z^2)(2V_s/\sqrt{2\pi}z)\exp(-2x^2/z^2)$$

$$+ (-4/z^2)(2V_s/\sqrt{2\pi}z)\exp(-2x^2/z^2)$$

$$= (4x^2/z^2 - 1)(4/z^2)\,S(x,z) \qquad (2.20$$

It has earlier been stated that a necessary assumption in the calculation of ground settlement using the stochastic theory is that the transfer of deformation involves zero ultimate volumetric strain. The implications of this assumption are discussed in Chapter 6. We make use of this assumption in the calculation of horizontal ground strain. The assumption can be stated mathematically as:

$$\varepsilon_x(x,y,z) + \varepsilon_y(x,y,z) + \varepsilon_z(x,y,z) = 0$$

If plane strain conditions are assumed to exist, then we can write:

$$\varepsilon_y(x,y,z) = 0$$

$$\varepsilon_h(x,z) = \varepsilon_x(x,y,z) = -\varepsilon_z(x,y,z)$$

and since:

$$\varepsilon_z(x,y,z) = \partial S(x,z)/\partial z$$

then:

$$\varepsilon_h(x,z) = -\left\{(4x^2/z^3)(2V_s/\sqrt{2\pi}z^2)\exp(-2x^2/z^2)\right.$$

$$\left. - (2V_s/\sqrt{2\pi}z^2)\exp(-2x^2/z^2)\right\}$$

$$= -\left\{(4x^2/z^3) - (1/z)\right\}\ S(x,z)$$

$$= (1 - 4x^2/z^2)\ S(x,z)/z \qquad (2.21$$

Having found the horizontal strain we can then find the horizontal displacement $S_h(x,z)$ since:

$$S_h(x,z) = \int_{-\infty}^{x} \varepsilon_h(x,z)\,\partial x$$

$$= \int_{-\infty}^{x} \left\{(8x^2 V_s/\sqrt{2\pi}\, z^4)\ \exp(-2x^2/z^2)\right.$$

$$\left. - (2V_s/\sqrt{2\pi}\, z^2)\ \exp(-2x^2/z^2)\right\}\,\partial x$$

$$= (8V_s/\sqrt{2\pi}\, z^4) \int_{-\infty}^{x} x \left\{x\ \exp(-2x^2/z^2)\right\}\,\partial x$$

$$- (2V_s/\sqrt{2\pi}\, z^2) \int_{-\infty}^{x} \exp(-2x^2/z^2)\ \partial x$$

$$= (8V_s/\sqrt{2\pi}\, z^4)\ \left\{(-xz^2/4)\ \exp(-2x^2/z^2) + \text{constant}\right.$$

$$\left. - \int_{-\infty}^{x} (z^2/4)\ \exp(-2x^2/z^2)\ \partial x\right.$$

$$- (2V_s/\sqrt{2\pi}\, z^2) \int_{-\infty}^{x} \exp(-2x^2/z^2)\ \partial x$$

$$= (2V_s/\sqrt{2\pi}\, z^2)\ \exp(-2x^2/z^2) + \text{constant}$$

$$+ (2V_s/\sqrt{2\pi}\, z^2) \int_{-\infty}^{x} \exp(-2x^2/z^2)\ \partial x$$

$$- (2V_s/\sqrt{2\pi}\, z^2) \int_{-\infty}^{x} \exp(-2x^2/z^2)\ \partial x$$

$$= (x/z)\ S(x,z) \qquad (2.22$$

The constant in the equations is equal to zero, since we know from the symmetry of the model that

$$S_h(0,z) = 0$$

The above equations (8.17 to 8.20) can be thought of as source functions in the same sense as Equation 8.16. They predict tilt, curvature, strain and horizontal displacement over an infinitesimally small source of ground loss. The whole tunnel can be modelled in this way only at reasonable distances (greater than about 1.5D, see Figures

2.4 to 2.6). At smaller distances a numerical approach must be used. For tilt and horizontal displacement (probably the two most important factors) it is possible to calculate numerically in the same way as for settlement, by summing the tilts or displacements caused by many point sources. This is not possible in the cases of curvature or strain. These must be calculated from previously calculated settlement and displacement curves. The curvature can be calculated in a straightforward manner from the settlement curve. The lateral displacement can be calculated graphically or numerically from the lateral displacement curve. It should be noted that "real" lateral strain is calculated from the measured lateral displacement curve in precisely the same way.

In most real tunnelling situations it is reasonable to model the tunnel as a point source. This has the advantage that the source functions (equations 8.17 to 8.20) can be used directly to express the various parameters of ground movement around and above a tunnel, dispensing with the need to use a computer. The numerical methods are really only required for the calculation of ground movements close to the tunnel or over very shallow tunnels (Z/D less than about 1.5). Normalised plots of settlement, curvature, strain, tilt and displacement generated from the source functions (equations 2.16 to 2.20) are shown in Figures 2.7 and 2.8. The main characteristics of these curves are as follows:

Settlement

$$S_{max} = \frac{0.8V}{Z} \quad \text{at} \quad x = 0 \qquad (2.23$$

$$S = 0 \quad \text{at} \quad x = \infty$$

Lateral strain

$$E \text{ max (compressive)} = \frac{S \text{ max}}{Z} \quad \text{at } x = 0 \qquad (2.24$$

$$E \text{ max (tensile)} = -0.45 \frac{S \text{ max}}{Z} \text{ at } x = \sqrt{3}\, i \qquad (2.25$$

$$E = 0 \text{ at } x = i \text{ and } x = \infty$$

Lateral displacement

$$S_h \text{ max} = 0.303\ S \text{ max} \quad \text{at } x = i \qquad (2.26$$

$$S_h = 0 \text{ at } x = 0 \text{ and } x = \infty$$

Curvature

$$C \text{ max} = \frac{4}{Z^3} \ S \text{ max at } x = 0 \qquad (2.27$$

Tilt

$$T \text{ max} = \frac{-1.212}{Z} \ S \text{ max at } x = i \qquad (2.28$$

2.5) Structural damage due to settlement

It is clear from the foregoing two chapters that it is possible, at least approximately, to predict the size and shape of the distribution of settlement, displacement and lateral strain above a tunnel in clay. The value of this prediction depends on our ability to

estimate the amount of structural damage likely to accrue from these deformations and hence assign tolerable limits to the various parameters. Several authors have considered this problem, in particular Skempton and McDonald (1956), Polshim and Tokar (1957) and Burland and Wroth (1975). Attewell (1977) has reviewed the problem of settlement damage with particular reference to tunnelling. The amount of damage suffered by a structure will depend upon many factors, in particular the nature of the structure, its coupling with the ground and its age. The structure's function will also influence the seriousness with which any damage is regarded. Even quite a low degree of purely "cosmetic" damage to domestic housing may be regarded as quite unacceptable by its occupiers, and will also be intolerable in hospitals, public buildings and so on. On the other hand, "architectural" damage to industrial premises may be regarded much less seriously, and remedial treatment in these cases may well be relatively inexpensive. Functional disruption or structural damage must always be taken seriously and avoided at all costs. Details of construction will influence the rigidity and strength of a building to such an extent that it is impractical to lay down any strict rules concerning allowable deformations. Also a structure's age and history may have considerable effect upon the threshold of permissible distortion. Nonetheless, maximum tolerable values of the various parameters such as tilt, strain and displacement have been proposed for particular types of structure. Ground deformations may also damage services such as sewers, gas mains and so on, as well as railways. Again, damage will depend upon the construction of the services as well as the nature and magnitude of the movements.

2.5.1) Damage due primarily to vertical movements

Uniform vertical settlement of a structure is seldom, if ever a cause of damage. Differential settlement, on the other hand, may cause damage in a number of different ways.

a. Damage due to tilt

The simplest form of differential settlement is the uniform tilt of a structure (see Figure 2.9). If the structure is sufficiently rigid, this is unlikely to cause damage, although in practice a structure is unlikely to be sufficiently rigid to resist distortion altogether. It may, however, set up bending strains or shear strains in particularly flexible buildings. The structures most likely to be affected are tall narrow structures such as chimneys or high unsupported walls (when tilted in their own plane). The amount of allowable tilt will depend on the strength and the geometry of the structure and must be calculated for each case individually.

b. Damage due to angular distortion

Where the degree of differential settlement is non-uniform, that is, where the tilt varies across the structure, the building will be subject to more complex stresses and strains.

Angular distortion, ω, as defined by Skempton and MacDonald (1956) is a measure of the shear strain to which a structure is subjected. Its value will vary over the settlement trough (see Figure 2.10). Various authors (Skempton and MacDonald, 1956; Polshin and Tolkar, 1957) have used its maximum value as a damage criterion. Attewell (1977) suggests limiting values of ω of 0.004 for open-frame structures, 0.002 for steel and concrete infill frame structures and 0.001 for load bearing walls or continuous brick cladding. Any degree

of simple tilt should be subtracted from the overall value of ω before its damage potential is assessed (see Figure 2.10).

2.5.2) Damage due to ground curvature

The curvature of the ground may also be a damaging factor since both hogging and sagging may generate tensile strains to which many structures are particularly sensitive. Attewell (1977) suggests the use of the deflection ratio (Δ/l) to define this curvature (see Figure 2.11) and suggests critical thresholds corresponding to 0.075% tensile strain of 0.0003 to 0.001. Since the value of the deflection ratio depends on the length over which it is measured, it may be better to measure curvature directly, where this is possible. Ground curvature has been used as a damage criterion by the National Coal Board for many years (N.C.B., 1975). Ullrich (1974) suggests a minimum permissible curvature of between 20 km and 2 km, depending on the sensitivity of the structures concerned and the degree of damage which is tolerable.

2.5.3) Damage due to lateral movements

Lateral movements themselves are unlikely to be a direct cause of damage to structures, although they may affect the alignment of railway lines and services. Most buildings, however, are quite sensitive to horizontal strains. Burland and Wroth (1975) relate tensile strain to visible cracking in a structure. Although this may not represent "failure" of the structure as such, a threshold value of acceptable tensile strain of 0.05% to 0.1% is suggested. Compressive strain is less likely to cause damage, although in severe cases

distortion of door and window frames may occur.

2.5.4) Damage due to settlement over tunnels

The distribution of settlement, tilt, strain and curvature over a typical tunnel settlement trough is shown in Figures 2.7 and 2.8. It can be seen that at any point on the profile a combination of these parameters will affect its "damage potential." The relative proportions of tilt and angular distortion (ω) will depend upon the rigidity, geometry and location of the structure relative to the profile. These distortions will combine with hogging or sagging stresses. The distribution of lateral strain across the profile means that the hogging strains experienced by a structure outside the point of inflection of the limb of the trough will be aggravated by the tensile strain in the ground, whereas at the centre of the trough, the compressive strains will tend to reduce or nullify any tension generated by sagging. Compressive strains above the neutral axis will tend to be increased.

From the above it seems clear that for buildings sensitive to tilt or angular distortion (shear strain), the most critical part of the profile is around the point of inflection, and the most important parameter is the maximum tilt (T max). On the other hand, for buildings sensitive to tensile strain, maximum damage is likely to occur outside the point of inflection, where maximum convex curvature (hogging) and maximum tensile strain coincide. This point occurs at a distance of $\sqrt{3}$ i from the centre line (see Section 2.4.6).

Figure 2.1

Z/D Vs i/R

(after Peck, 1969)

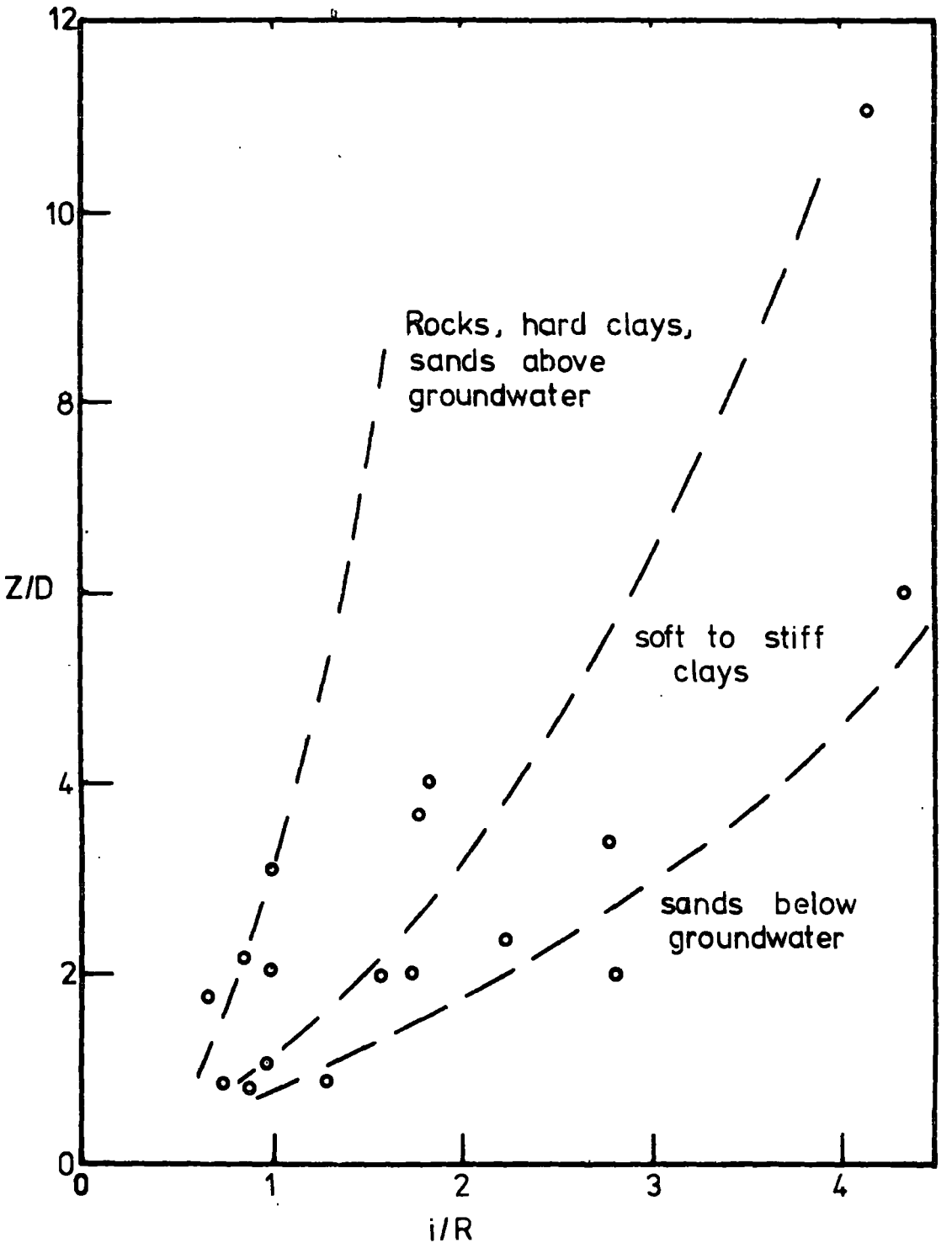

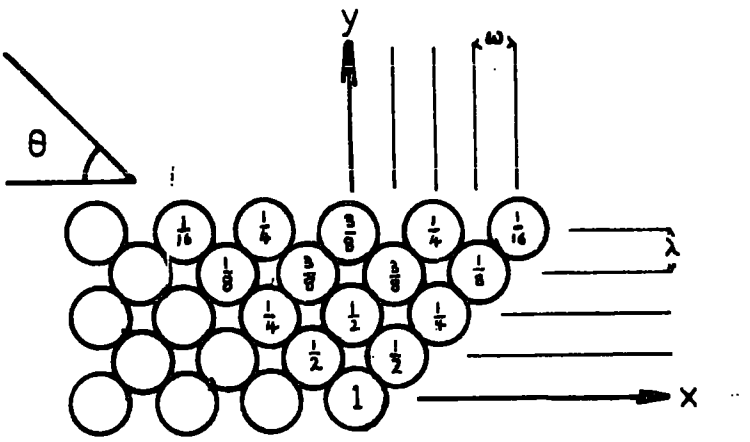

Figure 2.2
The Stochastic Medium

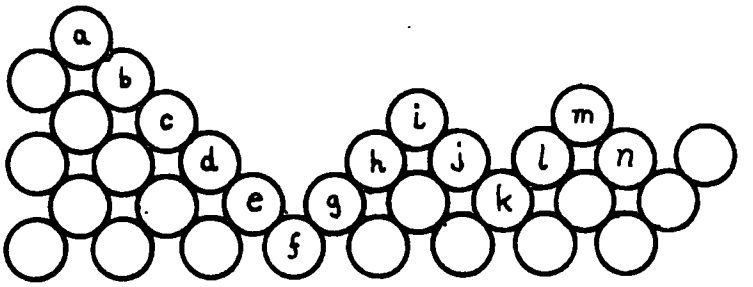

Figure 2.3
The Smoothing Effect

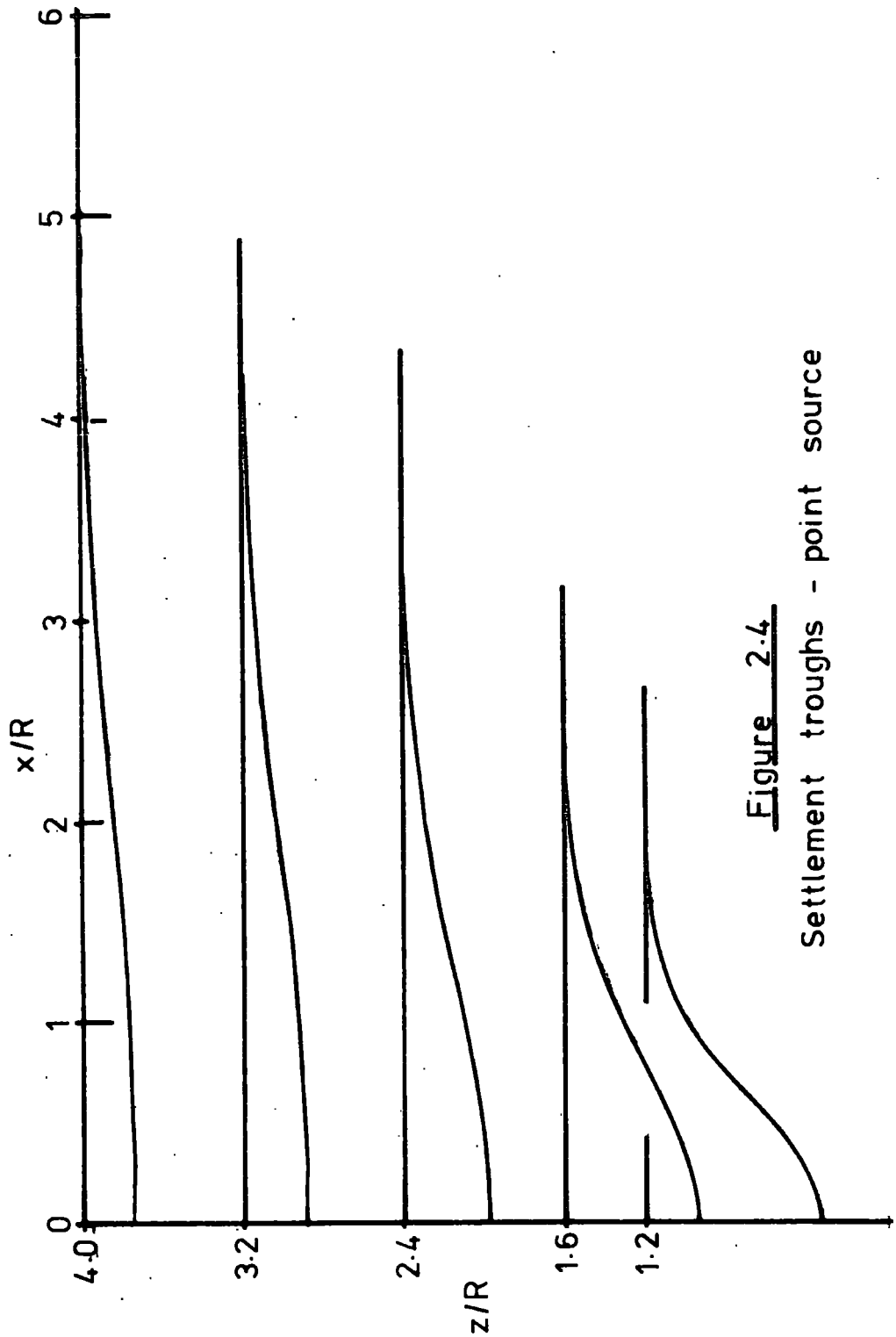

Figure 2.4

Settlement troughs - point source

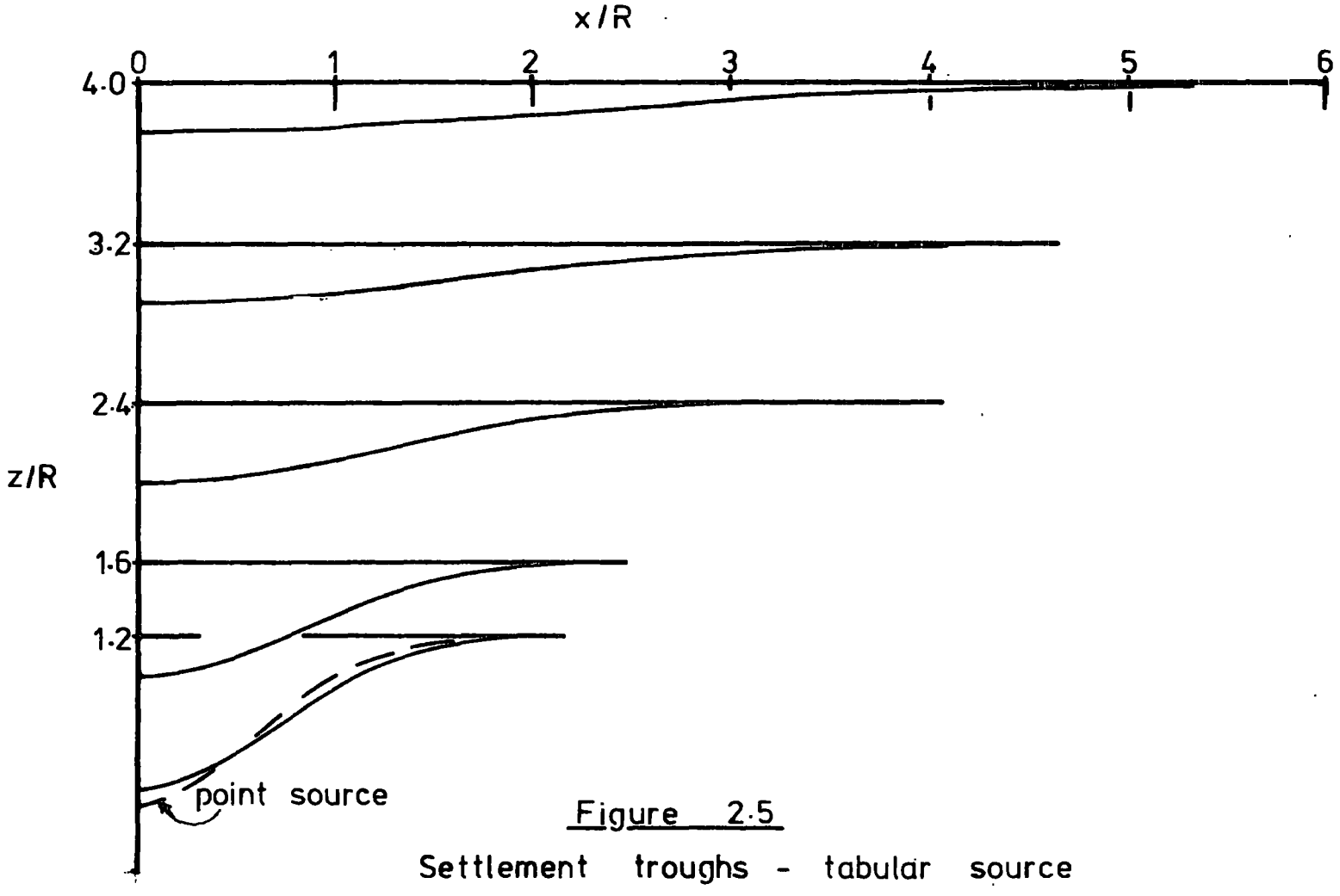

Figure 2·5

Settlement troughs - tabular source

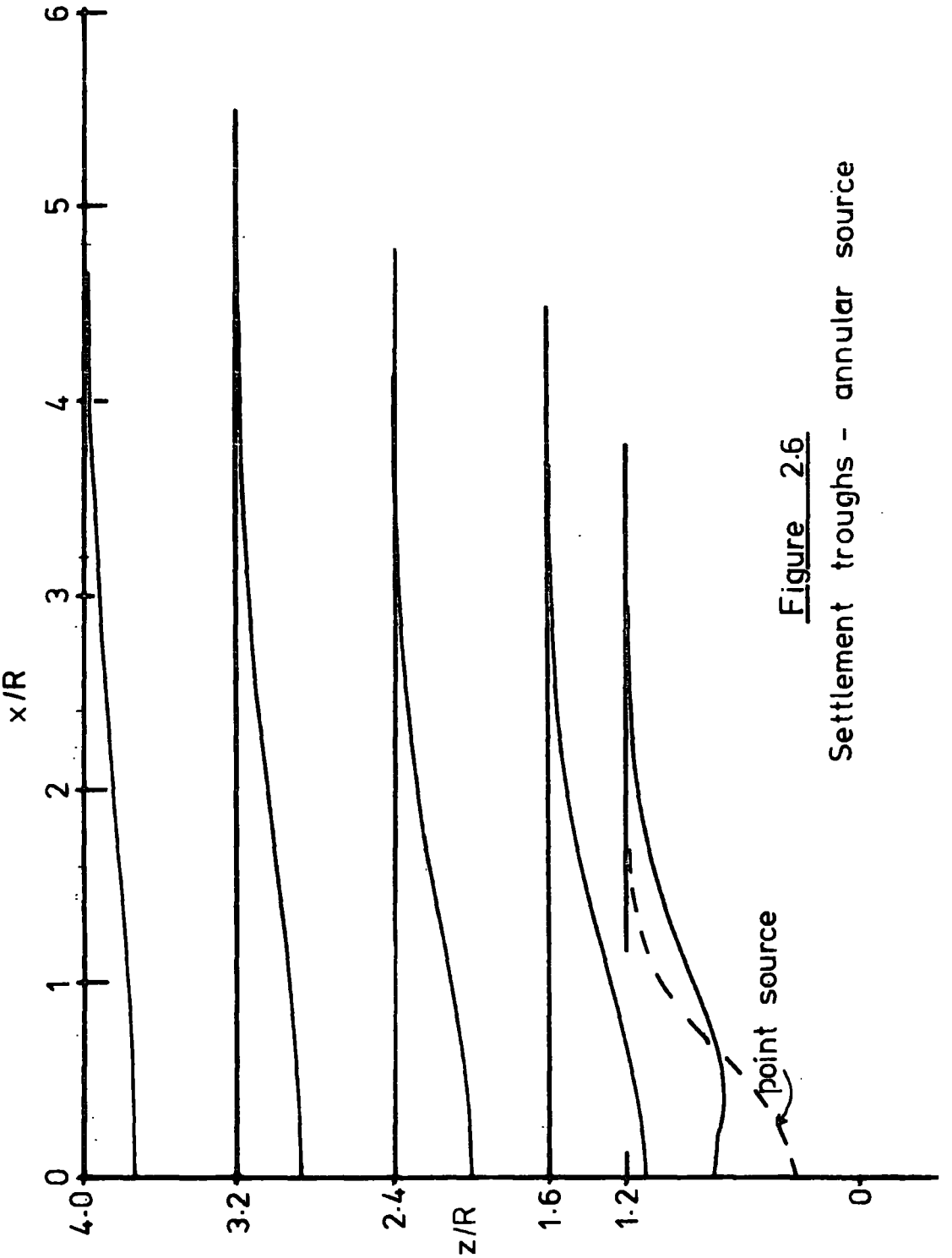

Figure 2.6

Settlement troughs - annular source

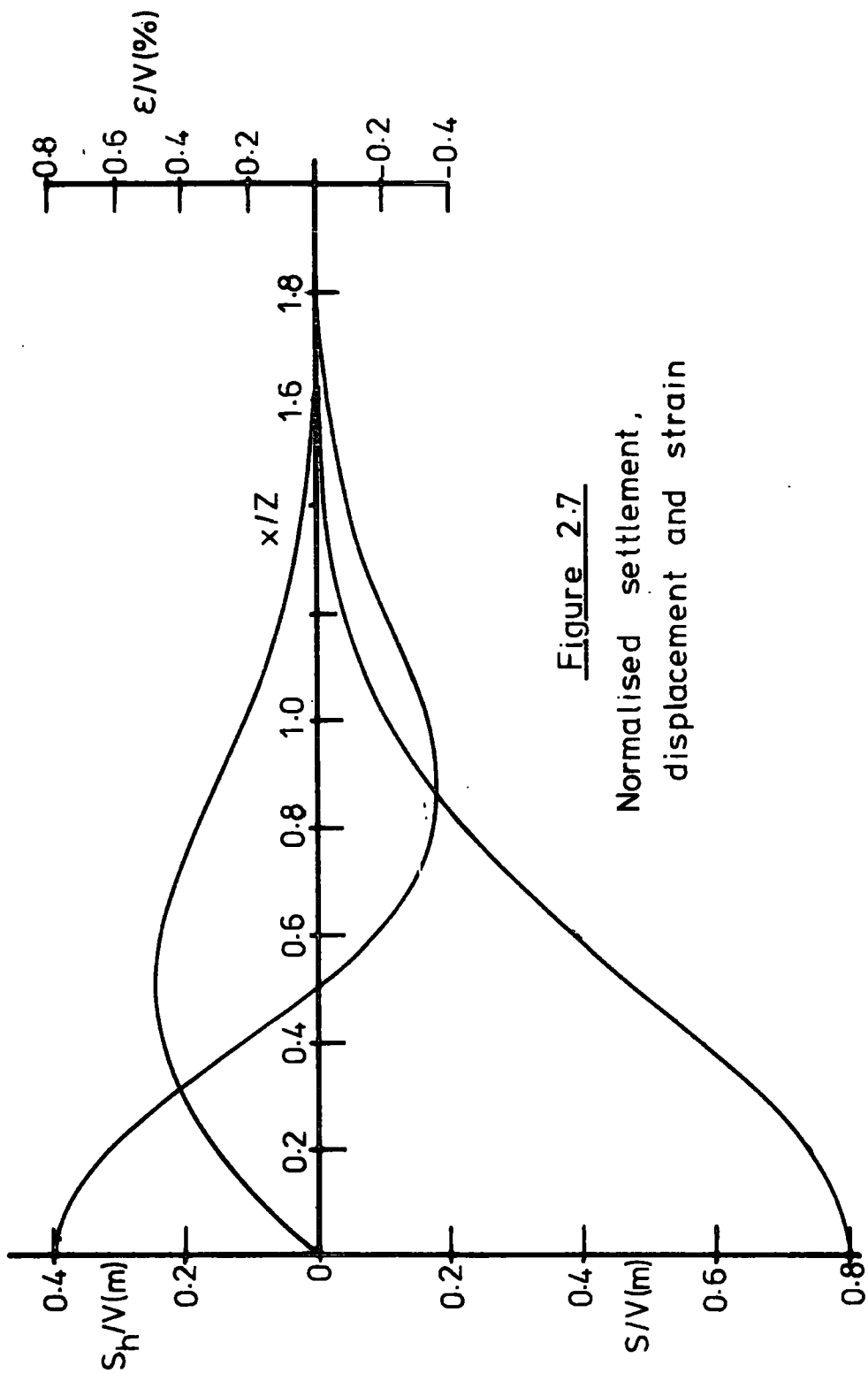

Figure 2.7

Normalised settlement, displacement and strain

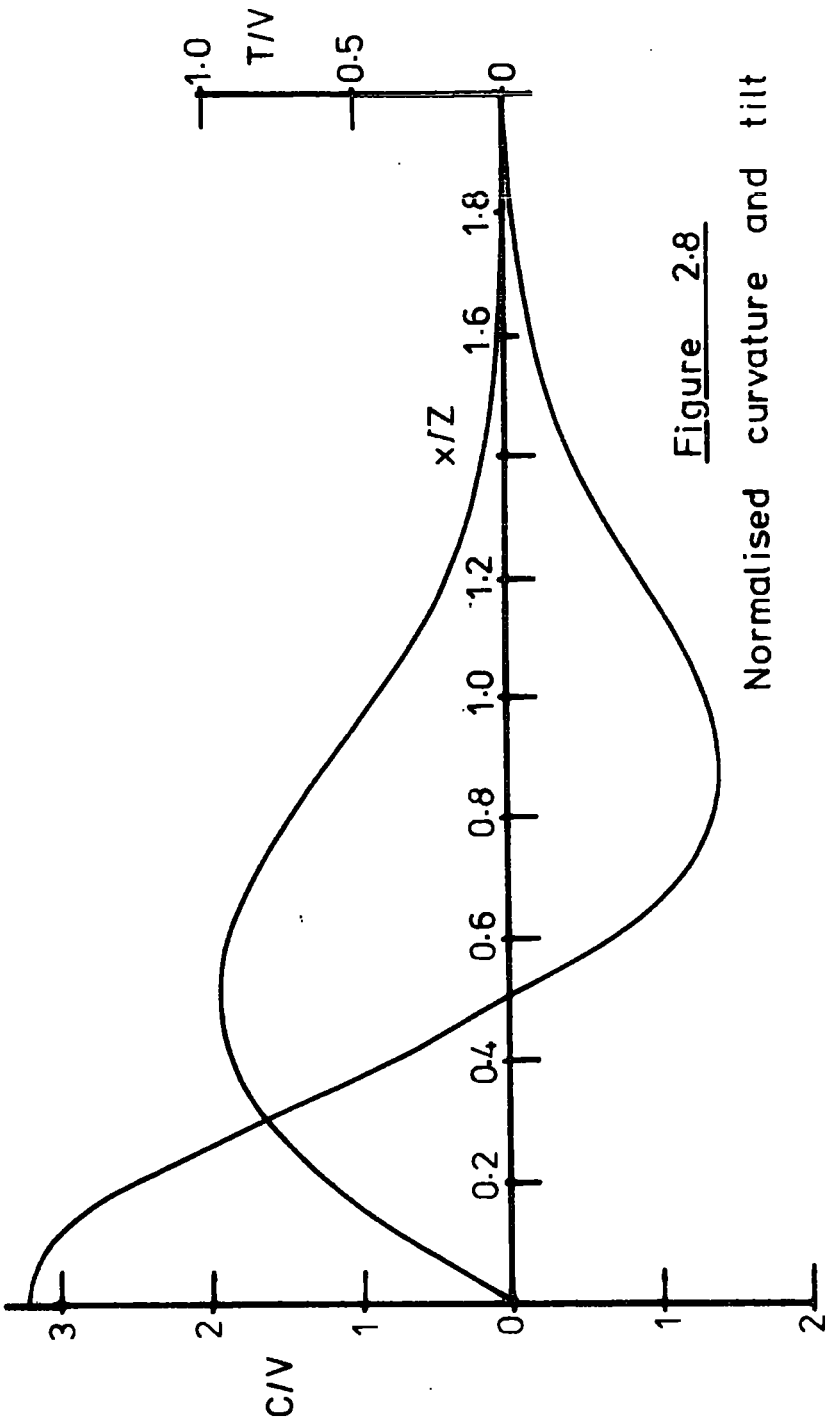

Figure 2.8

Normalised curvature and tilt

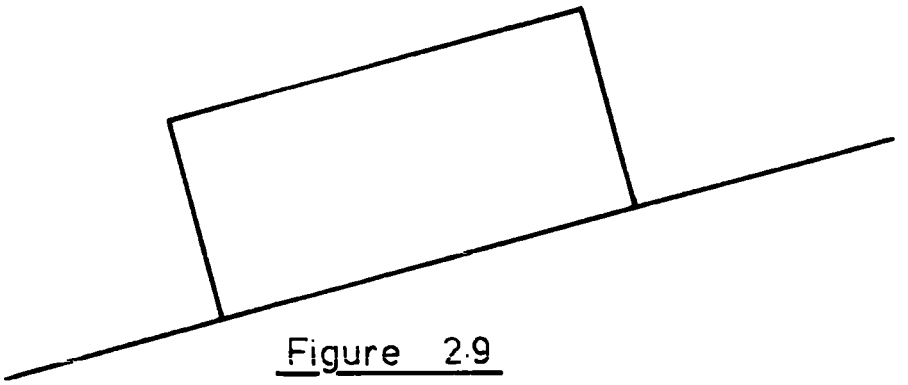

Figure 2.9
Uniform tilt

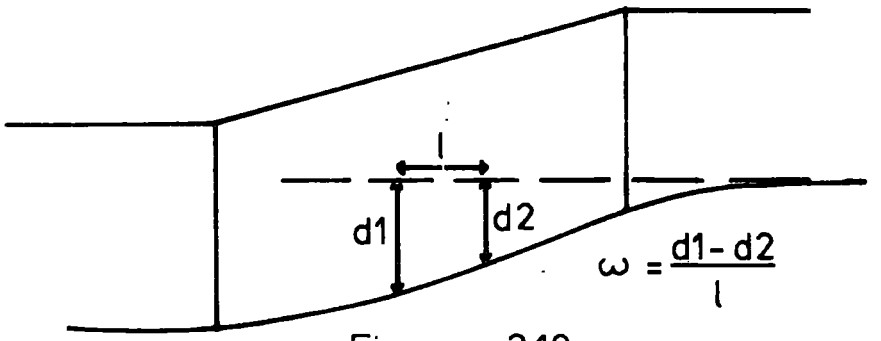

Figure 2.10
Angular distortion

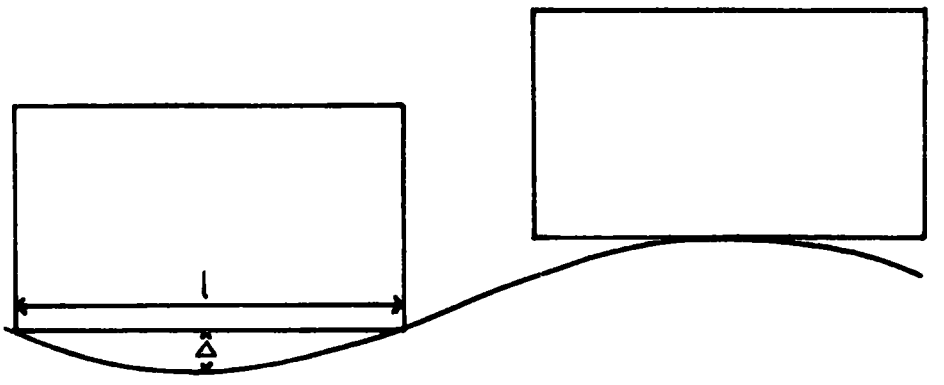

Figure 2.11
Hogging and sagging

Chapter 3

SEEPAGE PHENOMENA AROUND TUNNELS

3.1) Introduction

Tunnel stability, and subsequent settlement, may be affected by the drainage of water into the excavation when the tunnel is constructed below the water table. Two distinct phenomena can be identified. The first is the reduction of the stability of the face and the annulus around the shield, due both to seepage forces and a reduction of the frictional resistance of the soil. Not only may this cause an increase in the volume loss into the tunnel, and hence an increase in settlement, but it may also prove to be a source of danger to the miners. The second effect is due to the lowering of the water table, which may be expected to accompany drainage into the tunnel. This will cause an increase in the effective stress acting on the soil particles and may in consequence result in a certain degree of consolidation in normally consolidated soils. Once again, this will be reflected as settlement at the ground surface, although it will not necessarily take the form of a normal probability curve in this case. In the past, little research has been carried out on this subject, notable exceptions being the work of Sizer (1976) and Glossop and Farmer (1978). As noted by O'Rourke (1978) there is now a pressing need for a serious examination of the effects of pore water on settlements associated with tunnels, and in particular for the collection and publication of field measurements.

Of the case histories reported in this thesis only one, that

at Willington Quay, was carried out in reasonably permeable ground below the water table, where consolidation settlements and face instability may have been expected to occur, and the effects of this are reported in Chapters 5 and 6. At the end of this chapter the Willington Quay case history has been used as an example in the calculation of flow nets and seepage effects.

3.2) Seepage into the excavation area

In a permeable material below the water table it is inevitable that there will be some seepage into the unlined section of the tunnel, through both the face and the tunnel walls. A necessary consequence of this seepage will be the generation of seepage forces within the soil in the direction of flow, that is towards the excavation. It is to be expected these seepage forces will decrease with increasing permeability (Section 3.2.1). However, it is generally the case that in uncemented soils the unconfined compressive strength tends to decrease with increasing permeability, sands and silts showing less cohesion than clay soils, with a consequent increase in the simple overload factor (see Section 1.15). In these situations ground treatment or compressed air is often used, and this will have a twofold effect, both in reducing the OFS and in reducing the seepage forces. This second effect is seldom considered in tunnel stability calculations, but will be discussed in Section 3.2.4. It is first necessary to estimate the unrestricted seepage forces that may be expected to act on the soil around a tunnel, and in order to do this the seepage gradients must be calculated from a flow-net.

3.2.1) The construction of flow nets around tunnels

As described by Cedergren (1967), flow nets may be constructed "by eye," by the use of resistance paper, or by a resistance network (the electrical analogue), by physical modelling, or by using numerical methods, principally either finite elements or finite differences. The construction of flow nets by eye, whilst potentially a reasonably accurate procedure in simple cases, requires considerable practice and is less useful in complex situations. It is also inapplicable to the three-dimensional case. For more complicated boundary conditions electrical analogues are more suitable. These may be constructed using shallow baths of brine (Lane, Campbell and Price, 1934), resistive inks (Butterfield and Howey, 1973) or resistance paper (Wyckoff and Reed, 1935). They all require that a physical model be constructed, and are once again limited to the two-dimension case. Three dimensional models using complex resistance networks are feasible, but are difficult to construct and are limited to the specific case for which they were designed.

This shortcoming also applies to physical modelling. Models consisting of sand-filled tanks instrumented with small piezometers have been constructed, for example by Wrigley (1975), but these models create problems due to possible permeability anisotropy in the sand. Whilst perhaps suitable for detailed testing of specific cases, they are less useful as tools for more general research.

Several numerical methods for the analysis of ground water flow have been proposed, for example by Abbot, Ashamalla and Rodenhuis (1972), Jeppson (1972), Zienkiewicz, Mayer and Cheung (1966) and Tomlin (1966). Of these, the most adaptable are finite element methods and finite

difference methods.

3.2.2) The finite difference model

For the construction of the flow net around a tunnel excavation it was decided to use the finite difference method. For the case of seepage into a cylindrical void of infinite length, a two dimensional model in a plan perpendicular to the axis of the cylinder is quite adequate (see Appendix F). This could be carried out using any of the above methods. However, in order to resolve the flow net around the end of a tunnel excavation, that is in the zone around the shield, it is necessary to use a three dimensional model. Due to its simplicity and ease of application, a finite difference model was considered to be the most suitable method.

The finite difference method is described briefly by Smith (1974) for the two-dimensional case. A simple computer program to carry out the analysis was written by the author and is presented in Appendix F. In order to reduce computing time, which can be quite large for iterative procedures such as the finite difference method, particularly when used in a three-dimensional case, the model was simplified as far as possible. Although it is possible to use a triangular mesh, to facilitate the insertion of complex boundary shapes into the model, as described by Tomlin (1966), it was considered preferable in the interests of simplicity to use a rectangular network of nodes. Although this severely limits the possible boundaries, restricting them to vertical or horizontal planes in the simple case, it is considered to be acceptable, since in the great majority of cases we will be concerned with horizontal tunnels driven through horizontally

layered materials below more or less level surfaces. It does mean, however, that the tunnel must be represented as having either a square or a cruciform cross section (Figure 3.1), unless the mesh size is very small in comparison with the tunnel diameter. As discussed in Section 3.2.3, the resulting inaccuracies in the flow net do not appear to be too great, whilst the resultant saving in computer time is considerable. It is hoped to refine the model by using a variable mesh size, with smaller spacings around the tunnel, at a later date.

The program is capable of calculating for a number of horizontal layers of varying permeability, the maximum possible number depending on the mesh size, and for layers of anisotropic permeability. A limitation on this facility is that the principal permeability axes, that is the directions of maximum and minimum permeability, must be vertical and horizontal, the horizontal permeability being the same in all directions. The program can be used with various unlined-length-to-diameter ratios, and assumes that once lined and grouted, the tunnel becomes impermeable. As will be shown in Section 3.3, this is not necessarily the case, and it is possible, as an alternative, to calculate for a completely unlined tunnel.

A more serious limitation of the simple finite difference method is that the upper boundary must represent either an impermeable boundary or an equipotential surface rather than a phreative surface. In all the examples the latter has been assumed. Strictly speaking this means that continuous recharge must occur at the upper surface of the flow net to maintain steady state conditions, or the flow net can only be regarded as transient. This means that drawdown of the phreatic surface is not predicted, and that the equipotential surfaces generated

approximate to those which would occur if recharge of the soil water was sufficiently rapid to prevent any appreciable lowering of the water table, or if the soil permeability is sufficiently low to result in extremely slow drawdown, which as shown in Section 3.3.1 may well be the case. This represents a "worst case" solution, in that the pore water pressure gradients generated for this situation would be expected to be greater than would be the case if drawdown had occurred.

As can be inferred from the above, the resulting flow nets can only be regarded as at best an approximate guide to water flow into a tunnel. They do provide, however, a means of calculating, at least in an approximate sense, the contribution of pore water to the potential instability of a tunnel excavation.

3.2.3) The flow net around a tunnel excavation

Typical flow nets generated by the above programme are shown in Figures 3.2 and 3.3. These figures show vertical sections, or planes, through the centre-line of the tunnel (Figure 3.2) and through the tunnel face (Figure 3.3). The equipotential lines were drawn by the NUMAC computer, using a contouring program provided by F.J. Rens of Durham University. The flow lines were drawn in by hand. It should be noted that the flow lines shown in Figure 3.3 only indicate the approximate direction of water flow, since the actual flow lines would not be contained within the plane of the paper. For example, the flow lines in the face itself will pass almost perpendicular to the plane of the paper, as shown in Figure 3.2. The condition modelled in Figures 3.2 and 3.3 is the simplest case, that of a tunnel being excavated in a single layer of homogenous, isotropic material. A 2 m external diameter shield,

with the face 3 m ahead of the point of grout injection is modelled. The axis level is assumed to be 10 m below the water table. After grouting the tunnel lining is assumed to be totally impermeable. These parameters are of course freely variable within the program. The flow nets show the way in which water flows inward towards the face and towards the void around the shield. It can be seen that below the tunnel water will flow upwards towards the void. The pore pressure gradient increases close to the tunnel, in this case reaching a maximum of about 2. In the following section it will be shown how this flow net can be used to estimate the contribution of pore water seepage to the instability of the face.

3.2.4) Tunnel face stability

As discussed in Chapter 1, whilst the actual mechanism of failure at a tunnel face is unclear, it is possible empirically to set up a relation between the limiting depth of a tunnel and the unconfined compressive strength of a soil, and this equation can be modified to take into account the support offered to the face by compressed air. Clearly, seepage towards the tunnel face will create seepage forces within the soil which will tend to render the face less stable. In order to calculate the magnitude of these seepage forces it is necessary to estimate the volume of soil on which they act, that is, to estimate the size and shape of the zone of soil which could be said to have failed. Figure 3.4 shows the failure mechanism suggested by Broms and Bennermark (1967). In this case the volume of the failing soil is approximately $\pi^2 r^3/2$. The hydraulic gradient within this zone estimated from Figure 3.2 is roughly 3, acting at an angle of about 15^o below the

horizontal. The seepage force acting towards the tunnel face is:

$$F_s = \gamma_w i_s V_e$$

$$= \gamma_w \cdot i_s \cos \alpha \cdot \frac{\pi^2 R^3}{2} \qquad (3.1$$

where F_s = seepage force,

γ_w = unit weight of water,

i_s = seepage gradient (m of water/m)

V_e = volume of soil element,

R = tunnel radius,

and α = angle of seepage force with the horizontal.

This is equivalent to an additional inwards pressure of:

$$P_s = \frac{F_s}{A} = \gamma_w \cdot i_s \cos \alpha \cdot \frac{\pi R}{2} \qquad (3.2$$

$$= 45 \cdot R \quad kN/m^2$$

where P_s = seepage pressure at face,

and A = area of the face.

For a 2 m diameter tunnel this gives an additional "de-stabilising" stress of 45 kN/m^2. The OFS (Section 1.13) can now be written as:

$$OFS = \gamma \frac{Z + P_s - P_a}{Cu} \qquad (3.3$$

If no compressed air is used, the effect would be to reduce the OFS for a 2 m diameter tunnel at a depth of 10 m by approximately 15%. This reduction is not very great, considering the approximate nature of the OFS itself but should possibly be taken into account in critical situations. It should be noted, however, that this calculation only applies to the geometry of Figure 3.2. The seepage force is directly related to the radius of the tunnel and we would therefore expect the

effect of seepage to be greater on a larger tunnel. This would appear to be the case, for example, at Willington Quay (see Section 3.4). If compressed air is used to balance the head of water, the seepage gradients, and hence the seepage forces, will be reduced more or less to zero. In this way the use of compressed air has the twofold effect of providing a supporting pressure at the face and eliminating seepage forces towards the tunnel. If the air pressure is sufficiently high to drive moisture out of the soil close to the excavation, it will also have the effect of increasing the strength of the soil, but in a dominantly non-cohesive soil a dried zone could begin to run.

3.3) Consolidation

Even in good ground, where the pore-pressure gradients are too low to create any problem of instability at the face, drainage of the soil around the tunnel may result in a certain degree of consolidation. Although it is possible for some consolidation to occur due to drainage into the excavation itself we would normally expect consolidation to be a relatively long-term process, and must therefore consider drainage into or around the lined tunnel. Very often, and as noted earlier, tunnels below the water table will be constructed with the assistance of compressed air. The air pressure is normally calculated to just balance the water pressure experienced at axis level, and would be expected largely to eliminate significant drainage into the excavation area itself during construction. However, on completion of the tunnel drive it is usual to release the pressurisation prior to the installation of the secondary lining. At this stage drainage into the tunnel, accompanied by consolidation, may begin to take place. It will

be shown in Section 3.3.1 that consolidation may be caused by quite a slight degree of leakage through the lining. Although large amounts of consolidation would be expected to be associated with normally consolidated clays and silts, it has been suggested that a small amount of settlement may occur even in quite highly overconsolidated clays such as London Clay, where over the long term settlements have more or less doubled (O'Reilly, 1977, personal communication). This may account for long term settlements over tunnels in the London Clay.

3.3.1) The lined tunnel as a drain

It is possible that the tunnel may act as a drain in two distinct ways. The first and most obvious way is by leakage through the primary lining into the tunnel itself. In the case of segmental linings, whether steel or concrete, this leakage will occur through the joints between the segments. Although the annulus around the lining would normally be grouted, it should not be expected that this will form an impermeable membrane around the tunnel. Caulking of the segment joints will reduce the amount of leakage somewhat, but as is shown in Section 3.3.1, even a small amount of leakage may result in considerable consolidation.

Drainage into the tunnel would be expected to cease if and when a permanent lining, for example cast-in-situ concrete, is installed. However, it is possible that the tunnel may continue to drain the surrounding ground by transmitting water laterally, either through the grout annulus or through the zone of disturbed soil in the immediate vicinity of the tunnel. Both of these zones may well have a considerably higher permeability than the undisturbed soil, and may

therefore provide continuity with areas of lower piezometric head. The tunnel may, for example, pass through well-drained sands or gravels and may allow drainage into these. Whilst this may only cause the drainage of a volume of soil quite close to the tunnel itself, consolidation of this zone will be reflected as additional settlement at the surface. This type of consolidation may occur over a very long period of time and as mentioned previously may even cause a small amount of settlement in overconsolidated clays.

Figure 3.6 indicates a typical flow net around a lined tunnel. It was drawn, using the program described in Appendix F, for an infinitely long tunnel and is therefore unaffected by the tunnel face. This flow net, since it represents the drop in piezometric head at any point in the ground, can also be considered as showing the distribution of the increase in effective stress acting on the soil at any point due to drainage into the tunnel. The actual drop in head, or increase in effective stress, will depend upon the permeability of the lining relative to that of the surrounding soil. For a tunnel in which the primary lining offers no barrier to the ingress of water, the rate of inflow (q) per metre of tunnel can be calculated using the following relation:

$$q = k\, H \frac{N_f}{N_d} \qquad (3.4$$

where k = soil permeability,

H = total head of water (see Figure 3.5),

N_f = number of flow paths,

and N_d = number of equipotential drops.

N_f/N_d is known as the shape factor and is dependent on the

geometry of the particular tunnel in question. For the example shown in Figure 3.6 the rate of inflow will vary between about 200 litres/day/m for a silt with permeability of 10^{-7} m/sec to 2 litres/day/m of tunnel for a clay with permeability of 10^{-9} m/sec, at a depth of 10 m.

Whilst the above conditions may occasionally prevail (see, for example, Glossop and Farmer, 1978, and O'Rourke, 1978), more normally we would expect the original water table to occur at some intermediate height in the porous medium and therefore to be subject to potential drawdown. If appreciable lowering of the water table does occur, this might be expected to reduce the degree of consolidation at depth due to the consequent reduction in effective stress whilst at the same time increasing consolidation in the drained zone itself. The principle of consolidation due to drawdown is explained more fully by Terzaghi and Peck (1967).

An estimate of the amount of drawdown to be expected may be obtained by considering drainage into an infinitely long trench (Figure 3.5). This procedure is in many ways analogous to the calculation of drawdown due to pumping out a well. Darcy's law states that the rate of flow (Q) through a porous medium can be expressed as:

$$Q = i_s A \qquad (3.5$$

where i_s = seepage gradient,

and A = cross sectional area of flow element.

If we assume that the drawdown surface takes the form of a Dupuit curve, that is, that flow is parallel to the phreatic surface, then from Equation 3.5 we find that:

$$Q = 2k\, i_s h$$

$$= 2k \frac{dh}{dy} h \qquad (3.6$$

using the notation of Figure 3.5. Integrating equation 3.6 we obtain:

$$Q \int_{y_1}^{y_2} dy = 2k \int_{h_1}^{h_2} h\, dh$$

$$Q = \frac{k(h_2^2 - h_1^2)}{y_2 - y_1} \qquad (3.7$$

For the boundary conditions $h_1 = H$ at $y = 0$ and $h_2 = H_o$ at $y = W$ (where W is the half width of the "drawdown trough"),

$$Q = \frac{k(H_o^2 - H^2)}{W} \qquad (3.8$$

For a tunnel it is necessary to assume that the drawdown $(H_o - H)$ is less than the depth to invert $(Z + D/2$ or $Z_i)$. This means that the maximum possible rate of flow per metre of tunnel is

$$Q_{max} = \frac{k(2H_o Z_i + Z_i^2)}{W} \qquad (3.9$$

This assumes that the phreatic surface is drawn down as far as the invert of the tunnel.

Equations 3.6 to 3.9 assume that the tunnel acts in the same way as a trench extending to the bottom of the permeable layer. In reality, inflow into the tunnel may be limited by the size of the tunnel itself. It is possible to estimate the rate of inflow into the tunnel using a flow net in conjunction with equation 3.1. Figures 3.6 to 3.8 show flow nets for tunnels with more extreme values of depth to diameter ratio (Z/D) of 1.5 and 9.5 respectively in a semi infinite

porous medium. They can be used to calculate the rate of flow into the tunnel on the assumption that the fall in the phreatic surface is relatively small. The shape factor (N_f/N_d) for the different geometries varies between 2.7 and 1.5. Using a value of 2.2 in equation 3.4 we can calculate that the rate of inflow will range from 2.2×10^{-7} Z_i m/sec/m advance for a typical silt to 2.2×10^{-9} Z_i m/sec/m for a typical clay. This is equivalent to 30 litres/day/m^2 to 0.3 litres/day/m^2 respectively for a 2 m diameter tunnel at a depth of 10 m. The flow nets also indicate that the flow lines extend below the tunnel to a maximum depth of approximately 3.5 Z_i and outwards at the surface to a distance of about 6 Z_i. In fact a small amount of flow will occur beyond these limits, but as over 90% of the flow occurs within the outer flow line it is reasonable to use the above values as approximate indicators of the trough half-width (W) and the depth of influence (H_o). Substituting these values into Equation 3.9 we find the maximum possible rate of inflow into the tunnel:

$$q \text{ max} = 1.33 \, kZ_i \qquad (3.10$$

This is equivalent to an inflow of 1.33×10^{-7} Z_i m/sec/m for silt to 1.33×10^{-9} Z_i for the typical clay. Since this is only slightly less than the maximum rate of inflow calculated from equation 3.1, it would appear that unrestricted drainage into a tunnel is likely to cause significant drawdown, possibly down to tunnel invert level. It is impossible from the above calculations to estimate the actual amount of drawdown to be expected, since any change in the position of the phreatic surface will result in a change in the shape of the flownet and a consequent change in the rate of inflow into the tunnel. Nonetheless, the magnitude of the rate of inflow calculated from equation 3.10 would

indicate that the ultimate drawdown is likely to be quite large relative to the tunnel depth.

In order for this drawdown to be effective in producing consolidation it must occur quite quickly, to provide time for the consolidation process to occur before the permanent lining is constructed and the original pore-water regime beoomes re-established. It is therefore necessary to calculate the rate of drawdown to be expected in materials of various permeabilities. The overall velocity of flow (V_d) through a porous medium can be expressed as follows:

$$V_d = k\, i_s \qquad (3.11$$

If i_s is equated to the pressure gradient at the surface, then the rate of drawdown can be established. It can be seen from the flow nets (Figures 3.6 to 3.8) that the pore pressure gradient over the centre-line at the surface is approximate unity. This means that the maximum rate of drawdown is approximately equal to the permeability of the soil. For consolidating soils (silts and clays) this rate will vary between 10^{-1} and 10^{-3} metres per day. In other words, a drawdown of 10 m would take between 100 days and 27 years. This suggests that appreciable drawdown will only occur in fairly coarse silts where the primary lining offers no restriction to drainage.

Figures supplied to the author by Dr. O'Rourke (Table 3.1) suggest that normal caulking methods can reduce the water inflow through a segmental lining to an average of about 0.2 to 0.4 litres/day/m^2. This implies that for a 2 m diameter tunnel at an axis depth of 10 m in clay, caulking will be unable to prevent drawdown. On the other hand, in a silt of permeability 10^{-7} m/sec the drawdown associated with this inflow rate can be calculated from Equation 3.8:

$$H = (H_0^2 - \frac{Wq}{k})^{\frac{1}{2}} \qquad (3.12$$

$$= 35^2 - \left[\frac{60 \times 2.2 \times 10^{-7}}{10^{-7}}\right]^{\frac{1}{2}}$$

$$= 32.1 \text{ m}$$

This gives a fall in the phreatic surface of 1.9 m, implying that consolidation in a silt of permeability 10^{-7} m /sec can be largely eliminated by suitable caulking of the lining.

The above calculations would seem to suggest that in most cases consolidation due to drawdown of the phreatic surface above a tunnel is unlikely to occur, and that the flow nets shown in Figures 3.6 to 3.8 are adequate. In this case, consolidation will depend solely on the increase in effective stress represented by the equipotential surfaces on the flow nets, and will be greatest close to the tunnel where the potential drop, and hence the increase in effective stress, will be greatest.

3.3.2) Settlement due to consolidation

It is clear from the previous discussion that consolidation of the soil may be facilitated by quite a small degree of leakage through the primary lining in ground of low permeability. It is also clear that equipotential surfaces of the flow net can be regarded as equivalent to surfaces of equal effective stress increase. Strictly speaking, seepage forces will have the effect of reducing the effective stress increase below the tunnel, where the flow is directed upwards, and of increasing it above the tunnel where the flow, and hence the seepage force, is acting downwards. The degree of consolidation at any point in the ground will be dependent upon the compression index of the soil

at that point and the increase in effective stress, equal to the fall in pore pressure, in the following way:

$$\Delta V = \frac{C_c}{1 + e_o} \log_{10} \frac{p_o + \Delta p}{p_o} \qquad (3.13$$

where ΔV = percentage volume change,

C_c = compression index of soil,

e_o = original void ratio of soil,

p_o = original effective stress on soil particles,

and Δp = change in effective stress.

An example of the use of this equation is given in Section 3.4. In this case the greatest degree of consolidation would be expected to occur close to the tunnel where the increase in effective stress is greatest. Conversely, to the sides of the tunnel where the equipotential lines approach the vertical, consolidation will have a tendency to increase upwards to some extent, since in these zones p_o is decreasing more rapidly than Δp. The overall result of this would be to produce a "settlement trough" at the ground surface. If the zone of consolidation is restricted to the area close to the tunnel itself, then the consolidation settlement profile would be expected to be quite similar in shape to the normal probability curve produced by conventional volume-loss settlement. In the more general case, where the consolidating zone may stretch some distance away from the tunnel, a wider trough would be expected to develop. Since this trough will be superimposed upon a normal settlement trough, the resulting shape may be quite complex. Observations on a shallow tunnel in Belfast Sleech (Glossop and Farmer, 1978) have shown an increase in trough width from

15 m to 60 m due to consolidation. A smaller increase was observed at Willington Quay (see Chapter 5).

Except in the case where a tunnel receives no permanent impermeable lining, appreciable drawdown of the phreatic surface would only be expected to occur in fairly granular materials, with permeability greater than about 10^{-7} m/sec. This would represent a fine sand or coarse silt. Drawdown in these materials would not be expected to result in appreciable consolidation, and in any case would be restricted by the limited permeability of the primary lining itself.

3.4) Willington Quay

As an example of how the above calculations may be used, and of their limitations in practice, examples have been worked using the Willington Quay case history. Unfortunately data on pore pressures at this site are sparse and it is consequently impossible to rigorously test the conclusions drawn from the calculations.

3.4.1) Face stability

Figure 3.9 shows the flow net around the shield at Willington Quay, assuming that there is no drawdown of the phreatic surface. As discussed in Section 3.2.3 this probably represents the "worst case" in terms of seepage forces. The soil is modelled in three layers as shown on the diagram, to represent the fill, silt and clay, the ratio of their permeabilities being 1000:10:1. The permeability of the boulder clay is assumed to be 10^{-9} m/sec, that of the organic silt 10^{-8} m/sec and that of the fill 10^{-6} m/sec. The water table is taken as 10.75 m above axis level, with boulder clay 1 m below invert. The pressure

gradient in the "failure zone" ahead of the face is approximately 2 acting at 22^{o} to the horizontal. Using equation 3.1 we calculate the additional force on the "failure zone" due to seepage to be 861 kN. This is equivalent to a "face pressure" of 61 kN/m^2 and will increase the OFS (without air pressure) from 9.5 to 12.4, a change of 30%. The OFS when air pressure is used is 5.2 (see Chapter 4). In this case the high OFS meant that compressed air was necessary even without taking seepage forces into account. It would seem that for this geometry, the seepage forces should be taken into account for OFS values without compressed air of above about 4.5.

3.4.2) Consolidation

The flow net around the lined tunnel at Willington Quay is shown in Figure 3.10. The shape factor measured from this diagram is 1.8. This value is quite low due to the presence of a layer of relatively impermeable clay just below invert level. Assuming a permeability of 10^{-8} m/sec for the silt we find from equation 3.4 that the potential drop at the tunnel will equal 3.4 m of water, for a leakage rate of 0.4 litres/day/m^2. The compression of the layer of silt directly above the tunnel can then be calculated from equation 3.13. Assuming a compression index (C_c) of 0.3 and a void ratio (e) of 1 we find:

$$S = H \frac{C_c}{1 + e_o} \log_{10} \left(\frac{P_o + \Delta p}{p_o} \right) \qquad (3.14$$

$$= 8 \times \frac{0.3}{2} \times \log_{10} \left\{ \frac{(7\gamma - 4\gamma_w) + 1.72\gamma_w}{(7\gamma - 4\gamma_w)} \right\} \text{ m}$$

$$\approx 1.2 \log_{10} (1.172) \text{ m}$$

$$\approx 83 \text{ mm.}$$

The observed consolidation was about 60 mm (see Chapter 6). This is a reasonably good agreement taking into account the assumptions made in the calculation, and suggests that it is possible to roughly estimate the amount of consolidation to be expected above a tunnel from an estimate of the ground properties and the amount of leakage through the lining.

Tunnel	Diameter m	Water Head m	Average water inflow coefficient litres/m^2/day	Notes
Tyne	10.2	38	0.4	Lead caulking
Dartford I	9.3	33	0.18-0.26	" "
Clyde	9.6	28	0.2 -0.25	" "
Toronto a. Running tunnels	5.2	15	0.2	PCl4 caulking
b. Stations	7.8	15	0.008	" "

(Data provided by Dr. T.D. O'Rourke,

University of Illinois)

Table 3.1

Leakage measured at various tunnels with segmental iron linings

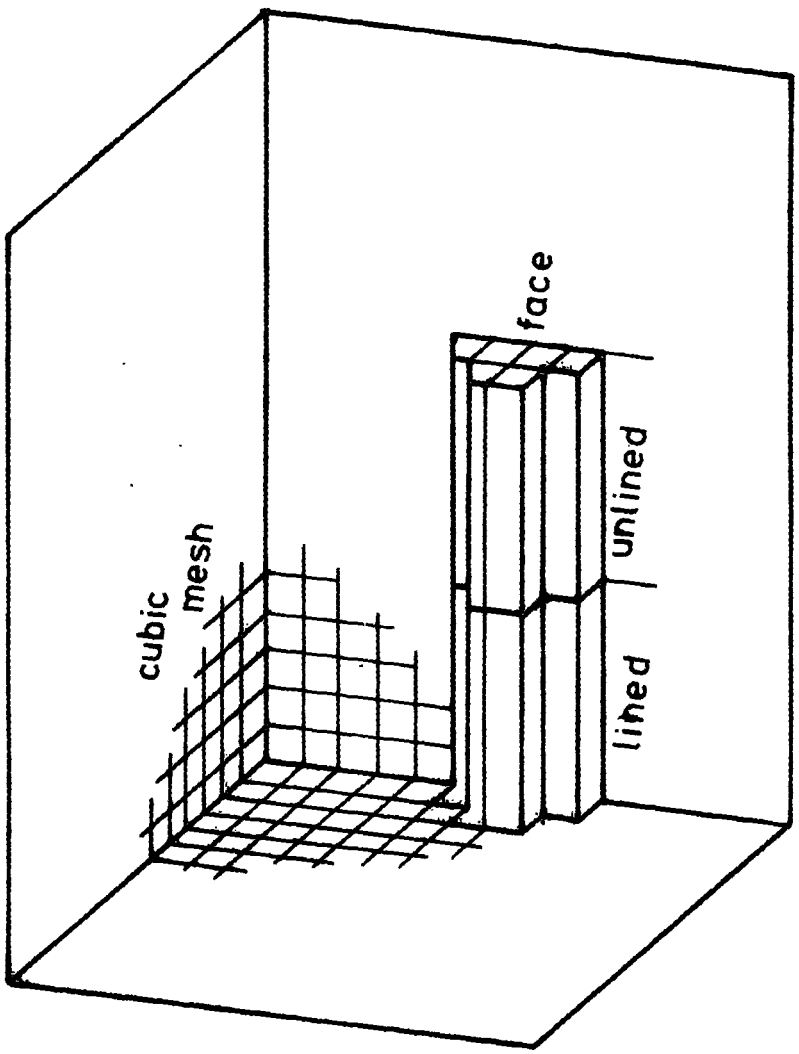

Figure 3.1
The finite difference mesh

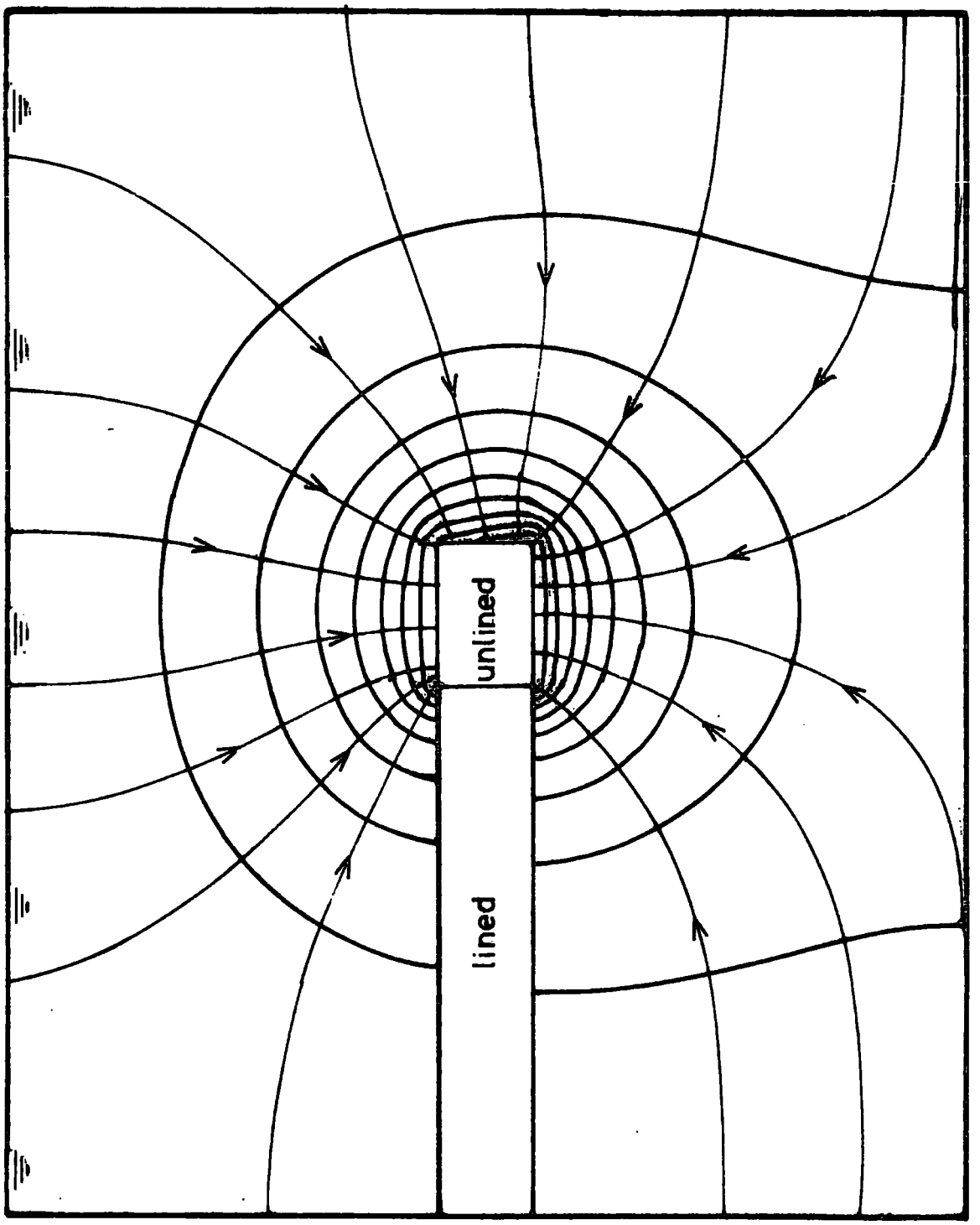

Figure 3.2

Flow net in the plane of the tunnel centre-line (H/D = 5)

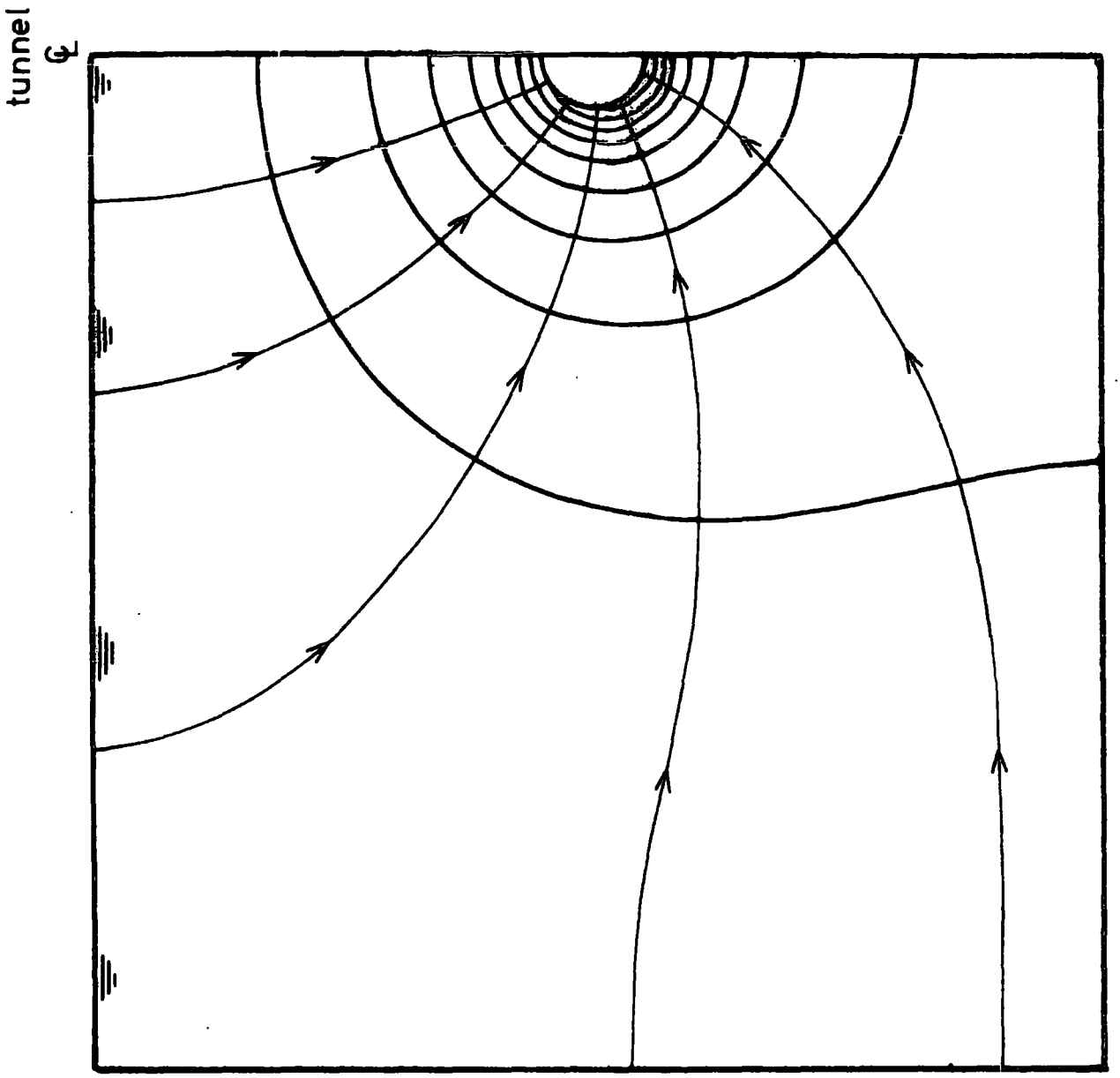

Figure 3.3

Flow net in the plane of the tunnel face

(H/D = 5)

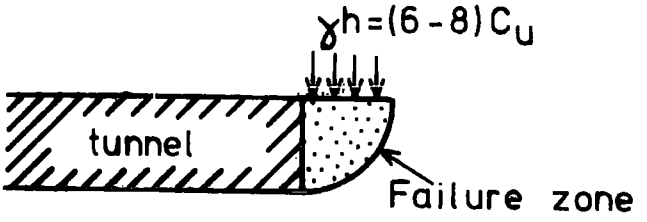

Figure 3.4

Failure of tunnel face

(modified from Broms & Bennermark, 1967)

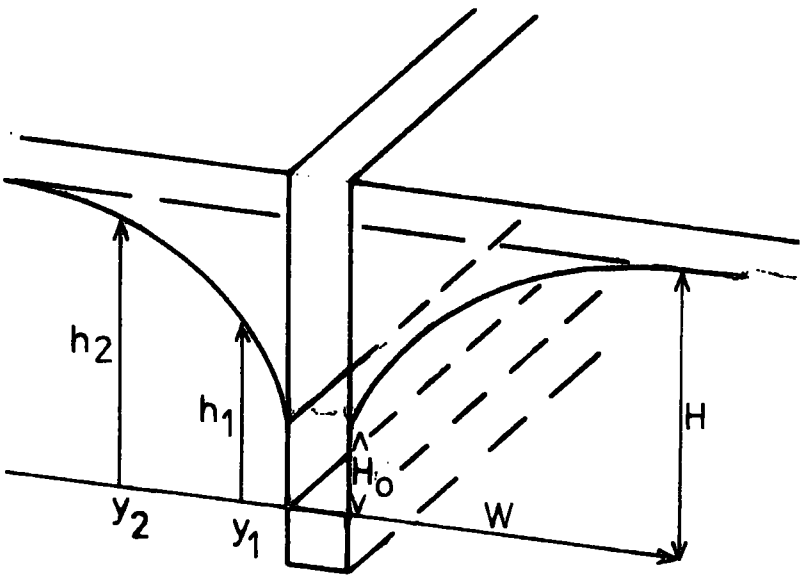

Figure 3.5

Drainage into an infinite trench

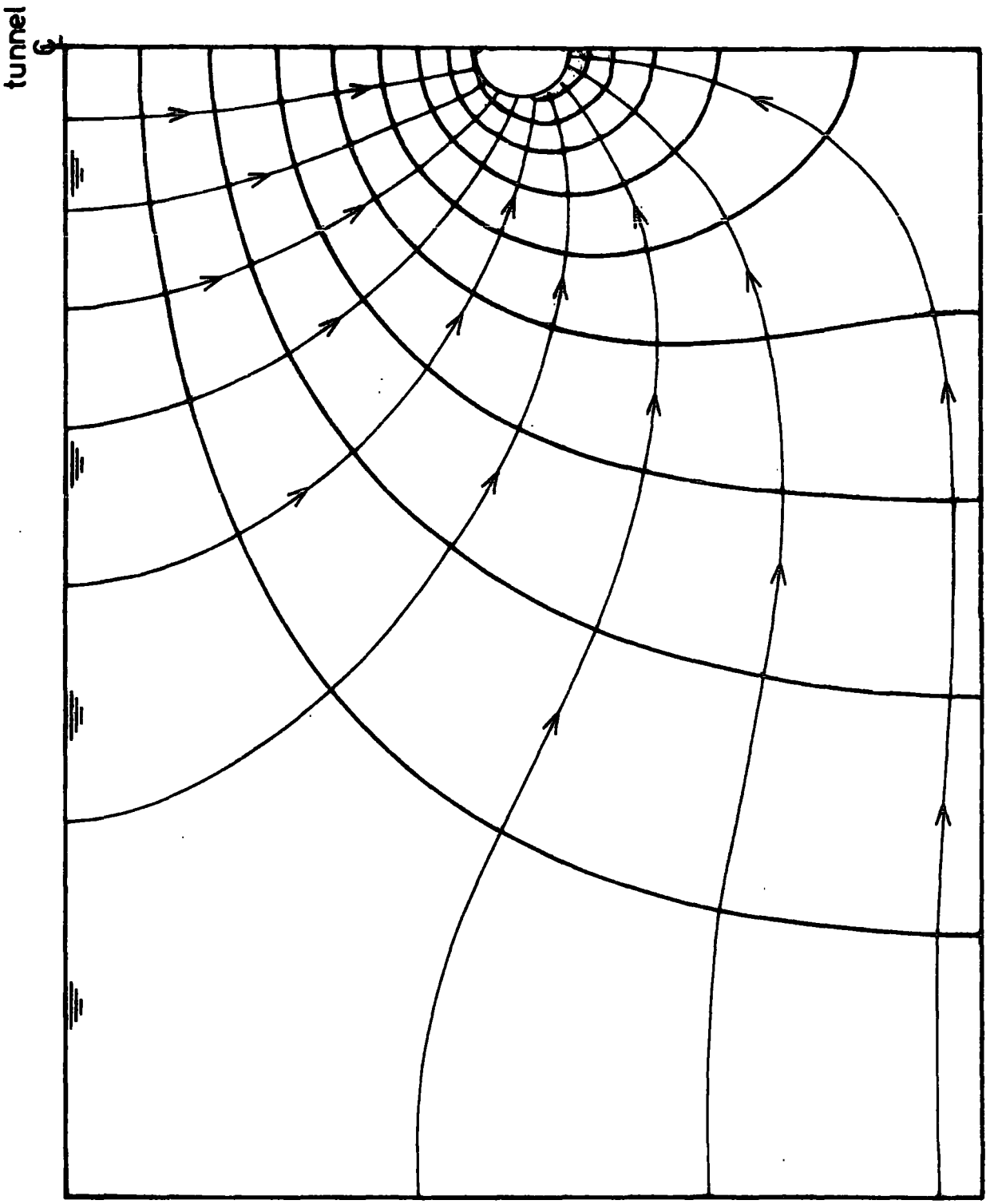

Figure 3.6

Flow net around a typical tunnel (H/D = 5)

Figure 3·7

Flow net around a shallow tunnel (H/D = 1·5)

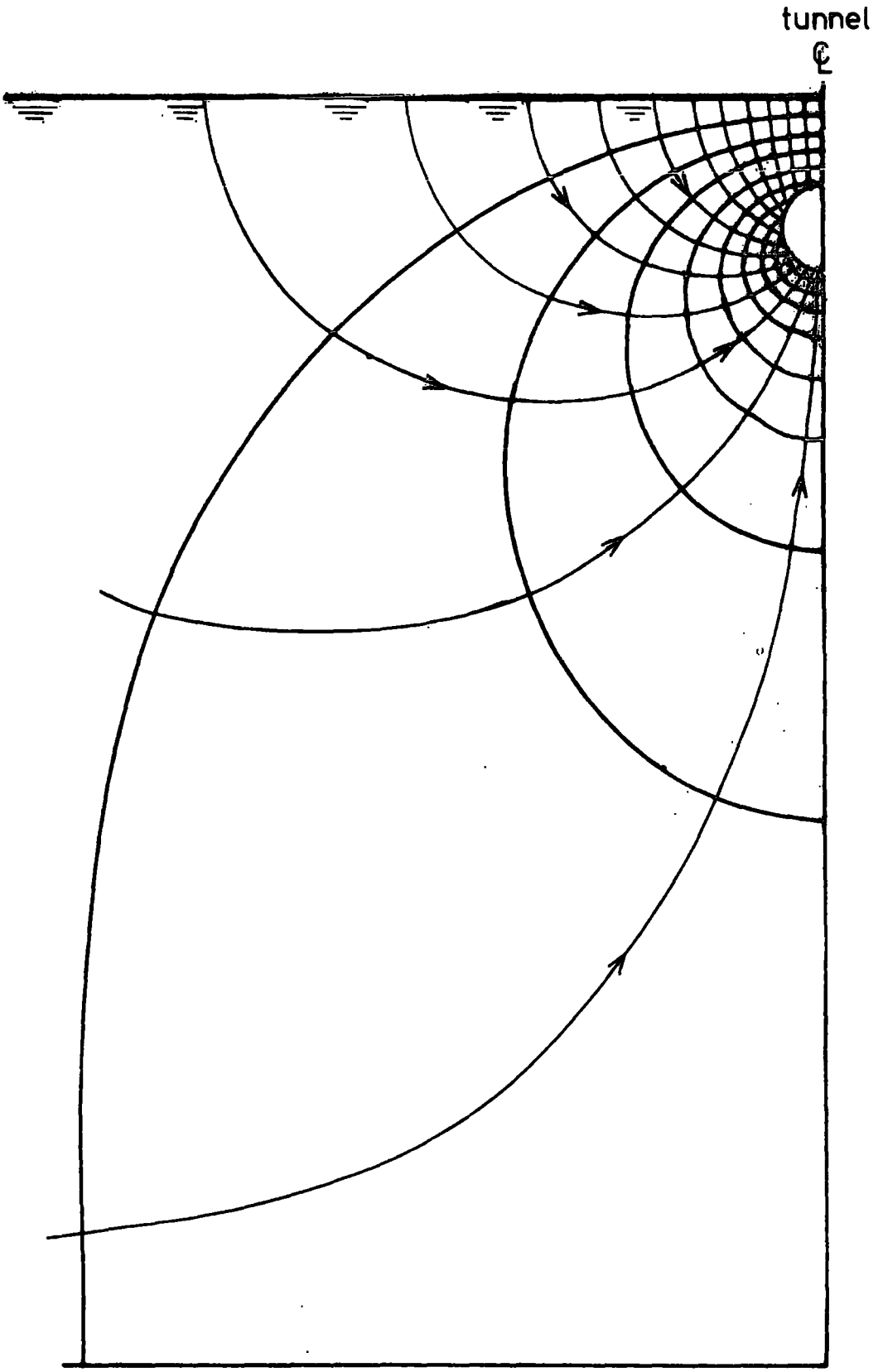

Figure 3.8

Flow net around a deep tunnel (H/D = 9.5)

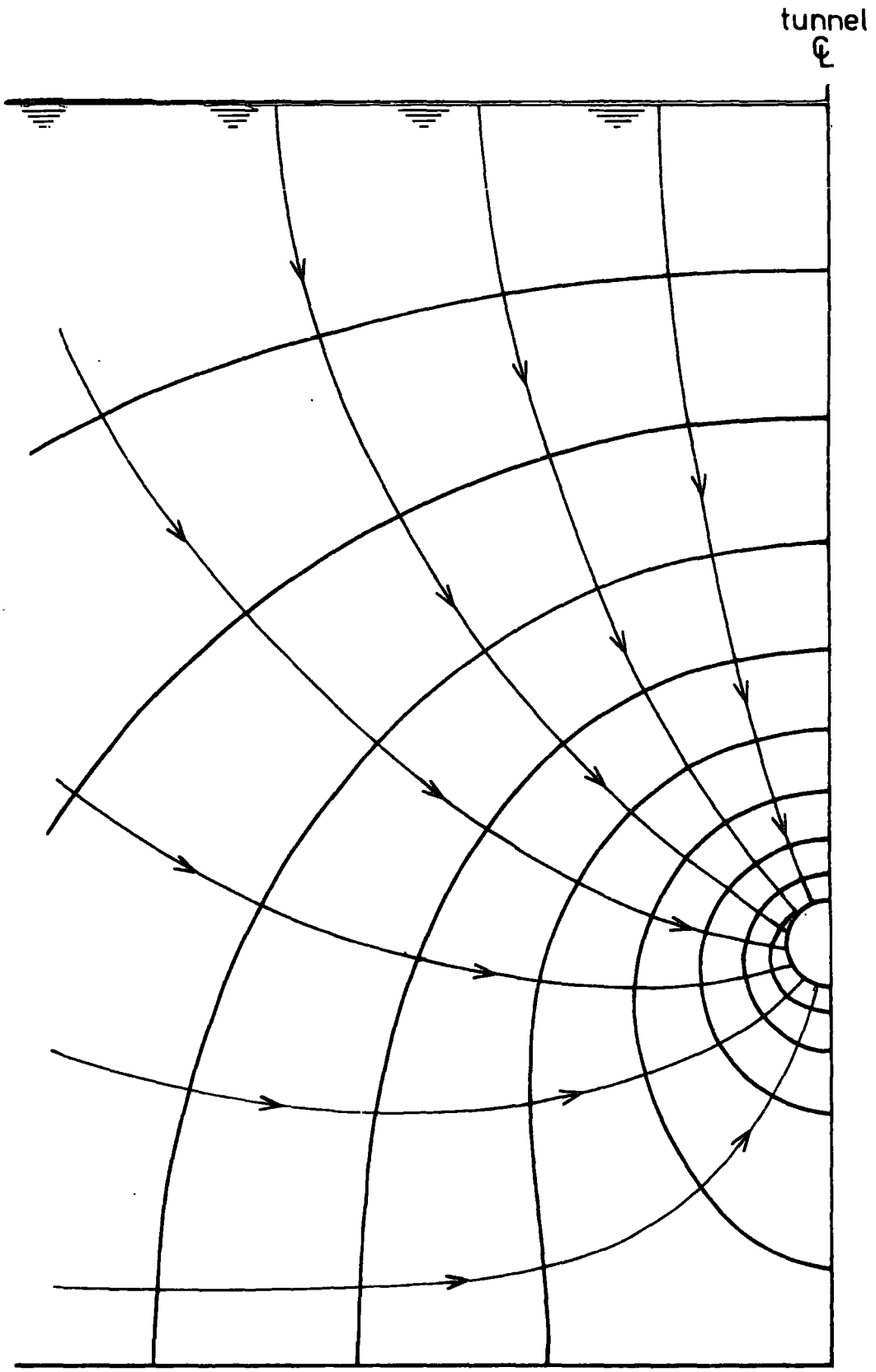

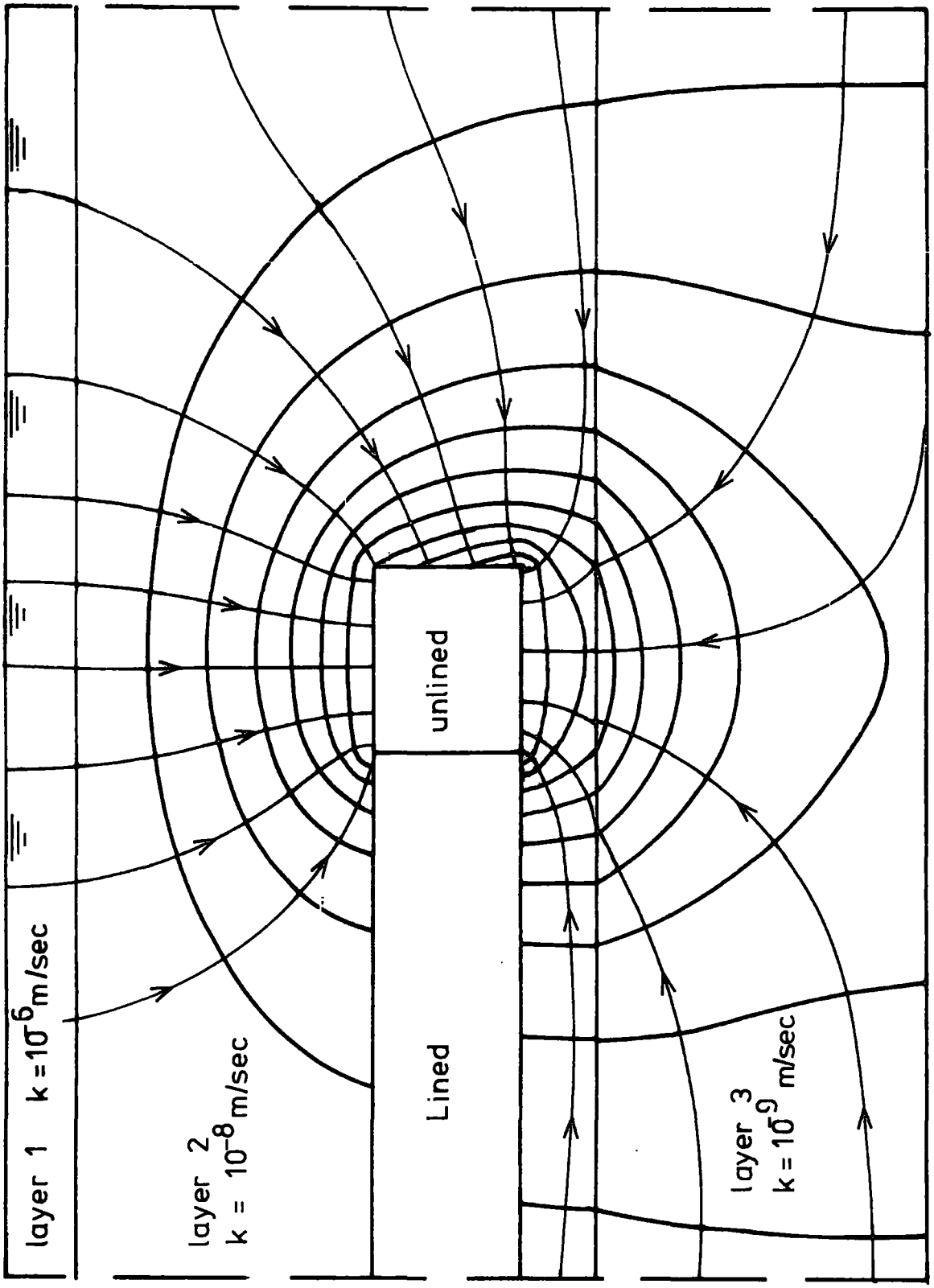

Figure 3.9
Flow net in plane of centre-line
-Willington Quay

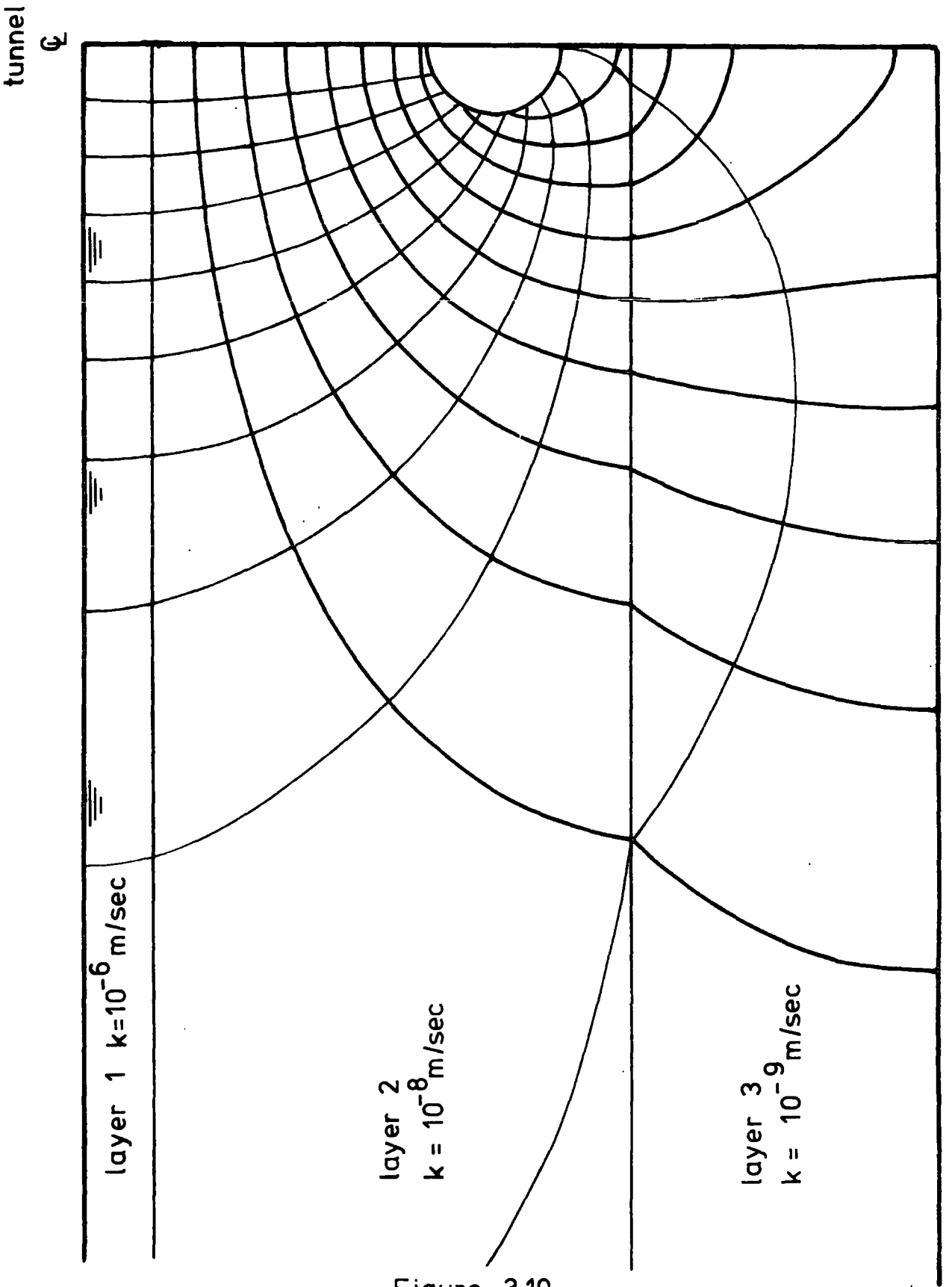

Figure 3.10

Flow net perpendicular to centre-line — Willington Quay

Chapter 4

FIELD INVESTIGATIONS

4.1) Introduction

In an attempt to clarify some of the problems described in the previous three chapters, detailed programs of field observations were carried out at three sites on Tyneside. These investigations formed a continuation and extension of those carried out at Green Park on the construction of one of the Jubilee Line running tunnels and described by Attewell and Farmer (1972; 1974).

The principal instrumentation at each site was similar and is described in detail in Appendix C. Broadly speaking, the instrumentation consisted of inclinometer tubes and magnetic settlement rings installed in boreholes set out in arrays at right angles to the tunnel centre-line, along with surface surveying monuments. The primary object of the instrumentation was to obtain a detailed view of the ground movements, around a tunnel, in three dimensions.

The results obtained from the Hebburn Site (Section 4.2) were described by Attewell et al.(1975), whilst certain aspects of the observations at Willington Quay, particularly the effects of the settlement on surface structures, were discussed by Attewell (1977b).

The three tunnels reported in this thesis were all driven in soft cohesive ground. A prior study undertaken by Durham University Engineering Geology Laboratories concerned a 4.15 m diameter shield driven tunnel at an axis depth of 30 m in the London Clay. The results from this study are discussed in Chapters 5 and 6. Of the three

tunnels described in this Chapter, one is a shield-driven tunnel in laminated clay, one is a shield-driven tunnel bored with the aid of compressed air in soft alluvial silt, and one was driven without a shield in normally-consolidated stony clay. These represent a wide variety of soft ground tunnelling conditions in materials of various properties and in tunnels of differing depths and diameters.

The locations of the sites of the three investigations are shown in Figure 1.1. All form part of the Tyneside Sewerage Scheme described in Appendix B.

4.2) Hebburn

The location of the Hebburn site is shown in Figure 1.1 and a plan of the site is given in Figure 4.1. The boreholes and surveying monuments were set out on a fairly even grassy area off Wagonway Rd., Hebburn, near the River Tyne. The instrumentation was located along a 30 m length of the Tyne South Bank Interceptor Sewer, about 20 m east of shaft D 14.

4.2.1) Site geology

The ground through which this section of the tunnel passes consists of stiff stony clay underlain by laminated clay. The log from borehole D18 is shown in Figure 4.2. Over the instrumented section of the tunnel the face was in laminated clay throughout. The boundary between it and the stony clay is shown at 6.7 m (22 ft) in borehole D18 and the instrumentation boreholes indicated that the contact lay just above the soffit throughout the instrumented length. The contact is irregular, as was seen as the tunnel approached the

instrumentation when the stony clay frequently encroached into the upper part of the face. The face passed entirely into stony clay shortly after leaving the last borehole in the array.

4.2.2) Laboratory testing

100 mm (four inch) diameter undisturbed samples were taken from each instrumentation borehole at the tunnel horizon (between 7 and 8 metres depth) and a series of laboratory tests was carried out on these by Bewick (1973). These tests included:

Quick undrained triaxial tests.

Atterberg limits.

Bulk density and S.G. determinations.

Natural moisture contents.

X-ray diffraction analyses.

Extrusion tests.

The results of these tests are summarised in Tables 4.1, 4.2 and 4.3.

The laminated clay varied in undrained shear strength from $45kN/m^2$ to $105kN/m^2$, the mean being $73.2kN/m^2$. This does not agree with the strength quoted in the site investigation report, but in view of the variability of the clay's properties this value was used in all calculations. The Atterberg limits were also quite variable and the means of these values are also presented.

Consolidation tests on the laminated clay were performed by Leach (1973), both parallel to and perpendicular to the plane of the laminations. Values of C_v (coefficient of consolidation) and M_v (coefficient of volume compressibility) were used to find the

permeability of the clay in these two directions from the formula:

$$K = C_v \cdot M_v \cdot \gamma_w$$

The results are summarised in graphical form in Figure 4.3. It can be seen from this graph that the permeability ratio at overburden stress is approximately 5. The lateral permeability is about 1.5×10^{-7} m/sec., which is sufficient to permit the clay to drain reasonably well in a horizontal direction. The vertical permeability of 7×10^{-7} m/sec seems rather high when compared with the results from the site investigation report which suggest a permeability of approximately 10^{-10} m/sec. The reason for this discrepancy is unclear, but may be due to sampling disturbance of the sandy layers.

A series of extrusion tests was carried out on the laminated clay by Bewick (1973). The principle of this test is fully described by Attewell and Boden (1971) and discussed briefly in Chapter 2. The results of these are summarised in Tables 4.2 and 4.3, and Figures 4.4 and 4.5.

4.2.3. Tunnel details

The Tyne south bank interceptor sewer at Hebburn was hand-excavated using a 2 m diameter shield. The depth to axis over the instrumented section was about 7.5 m. The shield, hydraulically operated, was approximately 2 m long, with a tailskin adding another metre to its length. The shield was similar to that illustrated schematically in Figure 1.2. In operation, a cavity was excavated for a distance of 1 or 2 rings ahead of the shield, slightly smaller in diameter than the finished tunnel, and the shield was jacked into it. Then the next lining ring (or two) was erected and the process

repeated. The face was excavated by hand with the aid of pneumatic clay spades. The resulting void behind the lining was grouted after the erection of three rings. The primary lining consisted of conventional bolted concrete segments 0.6 m in length. The cutting edge of the shield was equipped with a bead 10 mm in thickness to facilitate steering.

Two twelve hour shifts were worked on each weekday but no excavation was carried out over the weekends, when the face was normally boarded up. The face was not boarded during the weekends that face intrusion measurements were taken. An overall advance rate of 2.71 m per day was achieved including weekend stoppages, the maximum rate being 4.37 m per day (see Figure 5.2).

4.2.4) Site details

The ground surface at the Hebburn site is fairly even, sloping slightly northwards at about 2^{o} towards the river. The site is on a grassy area of public ground in front of several blocks of flats and about 20 m from the site of shaft D14 from which the tunnel was driven (see Figure 4.1).

An array of 12 boreholes was set out as shown in Figure 4.6. Six of the boreholes were located on the tunnel centre-line, the other six being set in two arrays at right-angles to the line of advance. This is the largest array of boreholes to have been used in the fieldwork. All the boreholes were drilled to a depth of about 9 m which was just below invert level. Borehole 11 contained a small diameter plastic settlement ring centre tube whilst the remainder were instrumented with inclinometer access tubes, as described in Appendix

C, installed with their keyways parallel to and normal to the tunnel centre-line. Magnetic rings around the inclinometer tubes and settlement points located in the sidewall of borehole 11 were fixed at approximate depths of 2 m, 4.5 m, and 6.5 m (soffit level) in all boreholes and at depths equivalent to axis level and invert level in selected boreholes (see Table 4.4).

The tops of the access tubes were set firmly into place with concrete. Caps were padlocked over the tops and covered by a removable wooden box (Figure 4.7). A surface levelling station (Figure 4.8) was set up adjacent to each borehole, and five more stations were set at right-angles to the tunnel centre-line as an extension of the first row of the array (Figure 4.5). Surface movements were monitored with respect to centre-punch marks on the tops of these stations. It was also necessary to protect these stations with wooden boxes.

The temporary benchmark at this site was set up some 30 m from the centre line (Figure 4.1) where no movement due to tunnel construction could be expected. Reduced levels of the vertical movements of the measurement stations and of the caps of each inclinometer tube were referred to this. Within the limits of experimental accuracy there was no discernible movement between the tubes and the adjacent levelling stations.

The measurement of lateral surface movement was complicated by the fact that the tops of the surface levelling stations were below the surface of the ground. Since it was impractical at this location to dig trenches between all the surveying points it was necessary to take measurements with the tape running along the ground and held down

onto the tops of the rods against the tape tension. In consequence, the measurement errors at this site were rather greater than at the other locations.

All the boreholes on the centre-line were taken below the level of the tunnel invert and it was therefore necessary to cut away the obstructing section of the access tube before the shield passed in order to avoid more disturbance of the tube than was necessary. When exposed at the face the tubes were pumped dry,* and then cut off about 100 mm above soffit level and their bases plugged with clay. The tubes were monitored throughout this cutting procedure, but no movement that could be attributed to the shortening operation could be detected.

The instrumentation was installed in January, 1973, and calibration was carried out during May of the same year. During June ground movements, both above and below the surface, were monitored at least once per day, the face reaching tube 3 on June 13th and passing tube 12 on June 22nd. During the following month measurements were taken less regularly until no further movement could be detected.

4.2.5) Ground anchor measurements

In addition to the instrumentation described above, it was possible to monitor sub-surface ground movement from the bottom of shaft D14 (Figure 4.1) as the tunnel approached from the west. Three 50 mm (2 inch) auger holes were drilled from the bottom of the shaft along the line of the approaching tunnel (Figure 4.9) at axis level. The auger holes were about 6 m long. Two of the holes were lined with metal tube through which ran a steel rod with a ground anchor at

*The tubes were filled with water to temperature-stabilise the inclinometer torpedo.

its far end. The ground anchor was so constructed that on emerging from the end of the lining, three spring loaded blades projected from the collar of the anchor. The anchor could be pushed into the clay, but on applying slight tension to the rod the blades were forced outwards thus keying the anchor into the ground. Where the rods projected into the access shaft they were equipped with dial gauges bearing on to a steel plate rigidly fixed to the concrete lining of the shaft. The rods were supported in the tubes by nylon bushes and the two anchors were installed at distances of 6.274 m and 6.223 m from the shaft. The dial gauges gave a direct measurement of lateral movement as the tunnel face approached.

The third tube contained a small bore plastic tube with magnetic rings around its circumference at distances of 2 m and 5 m from the shaft. The movement of the rings was monitored using a Soil Instruments reed switch assembly, similar to that used for sub-surface settlement monitoring, mounted on metal rods. It was found that when monitoring the ring at 5 m rod friction made accurate measurement impossible, and measurements on the 2 m ring were hindered both by contractors activities and by movement of the plastic centre tube.

4.2.6) In-tunnel measurements

Direct measurements of clay intrusion at the face were made using dial gauges mounted on the shield itself (Figure 4.10). The dial gauges were mounted on a system of rigid support rods running across the mouth of the shield and bore upon aluminium plates wedged into the tunnel face. Measurements were possible over 48 hour periods

each weekend when no work was being carried out at the face. Usually, during any stoppage, a tunnel face will be boarded up to prevent excessive settlement, but the stability of the soil here made it possible to leave the face unboarded. Two experiments were carried out while the face was in laminated clay, in which one dial gauge was mounted in the centre of the face and monitored over a 48 hour period. A third experiment was carried out using a modified set-up fitted with four dial gauges mounted in a horizontal row across the face (Figure 4.10). This experiment was carried out when the face had moved into stony clay, thereby giving a lower intrusion rate, but the shape of the intrusion profile (Figure 5.18) is probably also applicable to the laminated clay (see Chapter 5).

4.3) Willington Quay

Figure 1.1 shows the location of the Willington Quay site with respect to the Northumbrian Water Authority's Tyneside Sewerage Scheme, and a plan of the site is given in Figure 4.11. The boreholes and surveying stations were set up as a single array running at right-angles to the centre line of the Point Pleasant Siphon. The tunnel, 4.3 m in diameter, was constructed at an axis depth of 13.375 m.

4.3.1) Site geology

The North Bank Interceptor in the area of Willington Quay runs chiefly through stony clay. At Willington Gut, however, where the sewer passes through the Point Pleasant Siphon, it runs out of the stony clay and passes through a thick channel of silty alluvium. Borehole records (Figure 4.12) and day-to-day mapping of the tunnel

face suggest that the cross-section of the valley at this point is as shown in Figure 4.13 (Sizer, 1976).

The alluvium is underlain in places by sand and gravel beds, containing water under artesian pressure, and elsewhere by boulder clay. The boulder clay probably represents the Lower Till, since in this locality the Upper Till is only a thin bed and the channel is fairly deep (see Appendix A). The channel deposits themselves are almost certainly post-glacial. According to Sizer (1976) the channel was probably cut by meltwater deriving from the de-glaciation of the last glacial period, which also deposited the basal sands and gravels. The silty alluvium results from estuarine deposition during a subsequent rise in sea level.

4.3.2) Laboratory testing

Four inch (100 mm) diameter undisturbed samples were taken from two instrumentation boreholes at the tunnel axis level. These samples were subjected to a similar testing programme to that employed for the Hebburn samples. The results of these tests are summarised in Tables 4.5 and 4.6. The alluvium consisted of a soft, dark grey, organic silty clay with about 2.5% carbon and 40% water content (relative to dry weight). The clay contained much organic debris such as tree roots and branches. At one point a large (about 0.5 m diameter) well-preserved tree trunk was removed from the tunnel face by the contractor, a procedure which delayed construction for some time.

The undrained shear strength of the alluvium varied from 18kN/m^2 to 26kN/m^2, the mean value for Tube 1 being 25kN/m^2. This represents a very weak soil and gives an overload factor (OFS)

of 9.5 at the depth in question. Consequently, an air pressure of 90kN/m^2 (with some fluctuation) was used in the drive in an attempt to reduce the intrusion rate by decreasing the stability ratio to 5.9.

The permeability of the alluvium was ascertained from the results of consolidation tests carried out as part of the site investigation programme. An average of these tests gives a permeability of 10^{-8} m/sec.

A series of intrusion tests was carried out by the author on samples of the alluvium provided by the Northumbrian Water Authority. These tests were of a similar nature to those applied to the laminated clay from Hebburn (see Section 5.2.2) and their results are summarised in Table 4.7 and Figures 4.14 and 4.15. The results from these tests were quite variable and suggest an intrusion rate at overburden pressure of between 9.1 mm/min and 65 mm/min. This rate is extremely high and confirms the potential instability of the face without the use of compressed air.

4.3.3) Tunnel details

The section of tunnel under investigation at this site was the lower section of the Point Pleasant Siphon. This conveys the North Bank Interceptor sewer beneath the valley of Willington Gut at Willington Quay. Excavation was carried out by hand using pneumatic clay spades inside a 4.3 m diameter shield at a depth to axis level of 13.375 m. Due to the extremely rapid rate of clay intrusion into the tunnel which was anticipated from other measurement results, the bead was removed from the shield cutting edge, it being considered likely that the void behind the bead would fill up almost immediately and

consequently be of little assistance to shield steering. The shield was 2.4 m long with a 1.2 m tailskin in which the lining rings were erected. The primary lining consisted of conventional concrete pre-cast segments, 7 to a ring.

Throughout the excavation the face, although quite plastic, appeared to be firm and quite stable. Very little water was present in the tunnel, in spite of the axis being approximately 11 m below the water table, which suggests that the use of compressed air was most effective.

The tunnel was worked on a basis of two 12 hour shifts per day during the week. At weekends when no mining was done the face was boarded up with thick breastboards held in place by rams on the shield. Air pressure was maintained throughout. The tunnel was advanced at an average rate of 1.5 m/day (taking into account weekend stoppages) whilst the maximum rate achieved was 3 rings per shift, equivalent to 3.6 m/day as shown in Figure 5.21. The tunnel advance curve also shows a major hold-up for a period of two weeks at a distance of 9 m before the array. This interruption was for the installation of flameproof lighting and equipment following a report of gas seepage into the tunnel. The consequences of this break are discussed in Section 5.7.

4.3.4) Site details

The instrumentation at the Willington Quay site was set up on Gut Road, a small access road carrying heavy traffic to a factory (Figure 4.11 and Plates 4.1 and 4.2). In consequence, although the site was level and well-suited to the type of surveying in use, operations were complicated by a continuous flow of traffic.

An array of four boreholes was located at right-angles to the centre-line of the tunnel as shown in Figure 4.16. All boreholes were drilled to a depth of approximately 16 m (just below invert level) and were instrumented as described in Appendix C. Magnetic settlement rings were installed at the depths shown in Table 4.8 and piezometers were fixed 1 m above soffit level (10.075 m below the ground surface) in tube 1 and at axis level (13.375 m below the surface) in tube 2. The tops of the tubes were cut off below the surface of the road and covered with a "U4" sample tube and cap (Figure 4.17) set firmly in concrete. As at the Hebburn site, surface levelling stations were constructed alongside each borehole and as an extension to either end of the array. The locations of these stations are shown in Figure 4.11. The stations were constructed simply by driving nails into the road surface (see Appendix C) and so required no protection.

The temporary benchmark was set up some 40 m from the centre-line (Figure 4.11), well beyond the influence of the tunnel. Levels were taken to the stations and to the tops of the tubes using extension rods mounted in the tube tops (Figure 4.17). No relative movement between the tubes and the adjacent levelling stations could be observed.

Lateral surface movements were monitored as before with the tape in contact with the ground throughout its length. The uniformity of the ground surface ensured acceptable accuracy. Horizontal movement of the tube tops was checked using the levelling extension rods.

Prior to the tunnel face reaching the array it was necessary on safety grounds to grout the lower half of tube 1 to prevent any loss of air pressure from the tunnel when the tube was cut off. Possibly due to the importance of this precaution the tube was over-

filled by the contractor, leaving only the upper magnetic ring accessible. The tube was cut off when exposed in the face in a similar way to those at Hebburn. The tube was found to be in the centre of the face with the keyways parallel to, and perpendicular to the centre-line, indicating that no spiralling about the joints had occurred. Again no disturbance to the tube could be measured at the surface.

The instrumentation was installed during July, 1974. Calibration was carried out in January, 1975, and daily readings taken during February of the same year, the face passing the array on February 18th. Observations were continued at gradually lengthening intervals until no further settlement could be detected, a procedure which continued for almost 17 months. Over this considerable period of time sediments* accumulated in the bottoms of the tubes to such an extent that some of the lower magnetic rings became inaccessible. By the end of the study the inclinometer tubes were unserviceable. Sub-surface measurements were therefore discontinued before the surface surveying was completed.

4.3.5) Piezometer measurements

The piezometric head at tunnel level was measured every day whilst the tunnel face was passing the array and until any changes in head had ceased. The piezometer in borehole 2 (at axis level) provided data throughout this period. Unfortunately, the one in borehole 1 was affected by compressed air from the tunnel (presumably leaking through the grout in the borehole and thence into the instrument itself) and provided no information until the air pressure was turned off.

*Caused by heavy rainwater inwash through the road camber.

4.4) Howdon

Figure 1.1 shows the location of the Howdon site with respect to the sewerage scheme and the Howdon treatment plant. Figure 4.18 shows a plan of the site. The boreholes and settlement stations were set out on a fairly flat piece of waste ground, partly on grassy soil and partly on shale fill. The instruments were located in an array running at right-angles to a curving section of the North Bank Interceptor Sewer about 300 m north of the site of the Howdon treatment works and about 45 m north of the access shaft A/C. The area was unfenced,and being at some distance from the main road was vulnerable to a certain amount of vandalism.

4.4.1) Site geology

North of the Howdon Treatment Plant the North Bank Interceptor runs through stiff stony clay. The log from borehole C1 is shown in Figure 4.19. The tunnel face remained quite dry throughout the drive, indicating that the clay has a very low permeability.

4.4.2) Laboratory testing

Four inch (100 mm) undisturbed samples were taken from the boreholes at axis level and along with samples from the actual tunnel face these were subjected to the standard package of laboratory tests including quick undrained triaxial tests, Atterberg limits, and so on. The results of these tests are summarised in Table 4.9. The clay had an apparent cohesion of 206kN/m^2, which is rather higher than that shown from borehole C1 in the site investigation report. Using this value along with the density from Table 4.9 we obtain an overload

factor (OFS) of 1.5 approximately. This is very low and indicates that the face should be extremely stable.

Consolidation tests carried out as part of the site investigation indicate that the permeability of the clay is about 10^{-10} m/sec, that is, it is virtually impermeable. Extrusion tests were not carried out on this material, but the rate of extrusion would be expected to be similar to that for the stony clay from Hebburn (Section 5.6.7).

4.4.3) Tunnel details

The North Tyne Interceptor at Howdon has an excavated diameter of 3.675 m and a depth to axis of 14.18 m. Due to the consistency and strength of the stony clay through which it passes it was possible to construct this section of tunnel without the protection of a shield. The tunnel centre-line here negotiates a curve of 100 m radius, a procedure made easier by the absence of a shield. The excavation procedure was somewhat different from that at the other sites. A cavity was excavated to a distance of approximately 2 rings (1.2 m) ahead of the last complete lining ring. The perimeter of this cavity was trimmed by hand as smoothly and accurately as possible to be slightly larger than the outside diameter of the assembled lining. A ringwas then assembled in the cavity and the process repeated. When three rings had been assembled in this manner grout was injected into the void behind the lining. It would be possible to grout each ring separately if desired, but in deposits of this stiffness it is unlikely to be necessary.

The thickness and uniformity of the annulus behind the lining is to a large extent dependent upon the skill of the tunnellers. In

theory at least, this annulus should be smaller than that resulting from the assembly of the lining inside the tailskin of a shield. The total ground loss caused by this method of tunnelling is made up of losses at the face, which are dependent on the face area and the rate of advance, and closure of the annulus behind the lining, which itself depends on the length of time that the lining is left un-grouted.

The primary lining consists of bolted pre-cast concrete segments 0.6 m in length, 7 segments and a key being required to form a complete ring. The annulus behind the lining was grouted at fairly low pressure using a weak, sulphate resistant grout.

As in the previous two cases the tunnel was worked for two 12 hour shifts per weekday. The average rate of advance was 1.62 m per day, the maximum being 3.7 m per day (3 rings per shift).

4.4.4) Site details

Four boreholes were drilled in a line at right-angles to the tunnel centre-line at distances of 0 m, 2.5 m, 4 m, and 6 m respectively, with a fifth some 2 m further along the centre-line, as shown in Figure 4.20. All the boreholes were drilled to a depth of 17 m. They were instrumented with Soil Instruments inclinometer access tubes and magnetic settlement rings, the locations of which are shown in Table 4.10. The tops of the tubes were finished in the same way as those at Willington Quay (Figure 4.17). As at the other sites the instrumentation was installed some months before measurements began, and in an attempt to protect the tubes from vandalism during the intervening period their tops were camouflaged by covering them over with debris. Unfortunately, this proved to be somewhat counter-productive as the contractor

inadvertently bulldozed a considerable amount of soil over the top of the array. In this process the tops of the tubes were badly damaged and in one case the top section of tube was completely torn from the ground. Four of the tubes (tubes 1 to 4 in Figure 4.20) were salvaged by digging a cavity around the tube down to a depth where the tube was undamaged and fitting a new top section. This of course resulted in considerable distortion of the upper section of the tubes and was only fully successful in two cases (tubes 1 and 2). The construction of the borehole tops is shown in Figure 4.21.

After the tube tops were reclaimed, surface settlement stations were constructed adjacent to each borehole and as an extension to each end of the array (Figure 4.20). The construction of these monuments is shown in Figure 4.22. A temporary bench mark of similar construction to that at the Willington Quay site was set up in the concrete base of a lamp standard at a distance from the centre-line of about 60 m. This was well away from the zone of influence of the tunnel. A surface levelling station was also set up 3 m ahead of the array to give advance warning of the approach of the tunnel face. This also served as a check on the maximum settlement at the centre-line.

As at previous sites, levels were taken to the stations and to plugs fitted into the tops of the tubes (Figure 4.17). Again no relative movement was detected. Lateral movements were measured with the tape suspended above the ground throughout its length, so ensuring a very high degree of consistency. Since only relative movements between the stations were of interest, no attempt was made to correct for the catenary of the tape.

The bottom sections of the tubes on the centre-line were cut

off by the contractor and the disturbance to tube 1 was measured before and after this operation.

The boreholes were installed in July, 1974. Calibration was carried out during July, 1975 and measurements taken daily during the latter part of July and most of August, the face passing the array on August 8th. Measurements were continued, at lengthening intervals, until the end of October, by which time no further movement could be observed.

An associated programme of in-tunnel lining pressure and lining distortion measurements at the same location is described by El-Naga (1976).

	Instrumentation Borehole				
	1	2	9	9	12
Depth (m)	7.5	7.5	7.0	8.0	7.5
Liquid limit (%)	60.0	59.3	41.4	52.7	58.5
Plastic limit (%)	25.3	22.1	21.2	27.8	23.1
Plasticity index (%)	34.8	37.1	20.2	24.9	35.4
Liquidity index	0.19	0.16	0.31	0.09	0.13
Moisture content (%)	31.8	28.2	27.5	29.9	27.7
C_u (kN/m^2)	45 to 105 kN/m^2. Av. 73.2 kN/m^2				

Table 4.1

Laboratory test results - Hebburn

After Bewick (1973)

Sample	Depth (m)	Moisture Content (%)		OFS $\bar{\sigma}_v / c_u$	Overburden stress (kN/m^2)
1	7.5	32.32	34.74	2.3	164.97
2	7.5	30.99	36.07	3.8	276.9
4/I	7.0	27.92	37.40	1.3	96.7
4/II	8.0	29.85	42.99	1.0	73.7

Table 4.2

Moisture contents from extrusion tests and estimated stability ratios - Hebburn

After Bewick (1973)

Sample	Depth (m)	$\bar{\sigma}_f$ (kN/m^2)	$\bar{\sigma}_{ef}$ (kN/m^2)	Extrusion rate at overburden stress (mm/min x 10^{-3})	
1	7.5	167	164	3.6	3.5 (average)
2	7.5	275	265	2.9	
4/I	7.0	95	63	4.1	
4/II	8.0	76	49		

Table 4.3

Extrusion test results - Hebburn

After Bewick (1973)

Tube No.	Depth to ring (m)					Depth (m)
1.	1.94	4.42	6.57			8.5
2.	1.91	4.35	6.56	7.54		9.5
3.	1.66	3.17	6.13	7.41	8.65	9.5
4.	1.94	4.40	6.54	7.67		8.0
5.	1.92	4.39	6.26			8.5
6.	1.92	4.45	6.30			8.0
7.	1.99	4.46	6.76	7.67		8.5
8.	1.92	4.37	6.68			9.0
9.	1.94	4.36	6.70	not located	8.87	9.5
10.	1.92	4.19	-	8.12		9.0
11	2.03	4.46	6.86			9.0
12	1.90	4.39	6.22			9.5

Table 4.4

Magnetic ring locations - Hebburn

	Instrumentation Borehole					
	1a	1b	1c	2a	2b	2c
Depth (m)	11.25	13.25	14.75	13.25	14.25	15.25
Liquid limit (%)	48.5	48.5	46.5	42.6	44.5	41.8
Plastic limit (%)	28.2	28.6	25.6	28.5	28.2	27.3
Plasticity index (%)	20.3	19.8	20.9	13.1	16.3	14.6
Liquidity index	0.50	0.53	0.63	0.89	0.63	0.64
Moisture content (%)	38.3	39.1	38.8	40.2	38.5	36.6
C_u (kN/m^2)	26	25	24	18	19	21

Table 4.5

Laboratory test results - Willington Quay

After Sizer (1976)

Sample	Depth (m)	Moisture Content (%)		OFS (σ_v / c_u)	Overburden stress (kN/m^2)
		Bulk	Extruded plug		
1	4.8	50.1	60.0	4.0	83.0
2	5.7	62.4	65.4	2.6	92.8
3	7.5	50.1	68.8	7.0	130.3
4	9.4	37.9	48.5	3.0	162.0

Table 4.6

Moisture contents from extrusion tests and estimated stability ratios - Willington Quay

Sample	Depth (m)	σ_f (kN/m^2)	σ_{ef_2} (kN/m^2)	Extrusion rate at overburden stress (mm/min)
1	4.8	107.9	45.5	8.5
2	5.7	86.6	69.9	9.1
3	7.5	64.6	37.6	65.0
4	9.4	113.9	96.7	12.3

Table 4.7

Extrusion test results - Willington Quay

Borehole	Depth to ring (m)						Depth (m)
1	1.33	4.34	7.35		10.40	15.88	16.0
2	1.54	3.09	7.65	8.60	10.99	15.18	16.0
3		3.20	5.94	8.81	11.50	13.76	15.5
4		2.79	6.14	8.86	12.21		14.5

Table 4.8

Magnetic ring locations - Willington Quay

	Clay type	
	Laminated clay	Stony clay
Density kg/m^3	2029.8	2255.0
Liquid limit (%)	63.5	36.5
Plastic limit (%)	30.0	18.2
Plasticity index (%)	33.5	18.3
Liquidity index	- 0.08	- 0.33
Moisture content (%)	27.2	12.1
Cu (kN/m^2)	[illegible]	[illegible]

Table 4.9

Laboratory test results - Howdon

After El-Naga (1976)

Borehole	Depth to ring (m)			Depth (m)
1	Not used			17
2	4.8	8.1	11.6	17
3	Not used			17
4				17
5				17

Table 4.10

Magnetic ring locations - Howdon

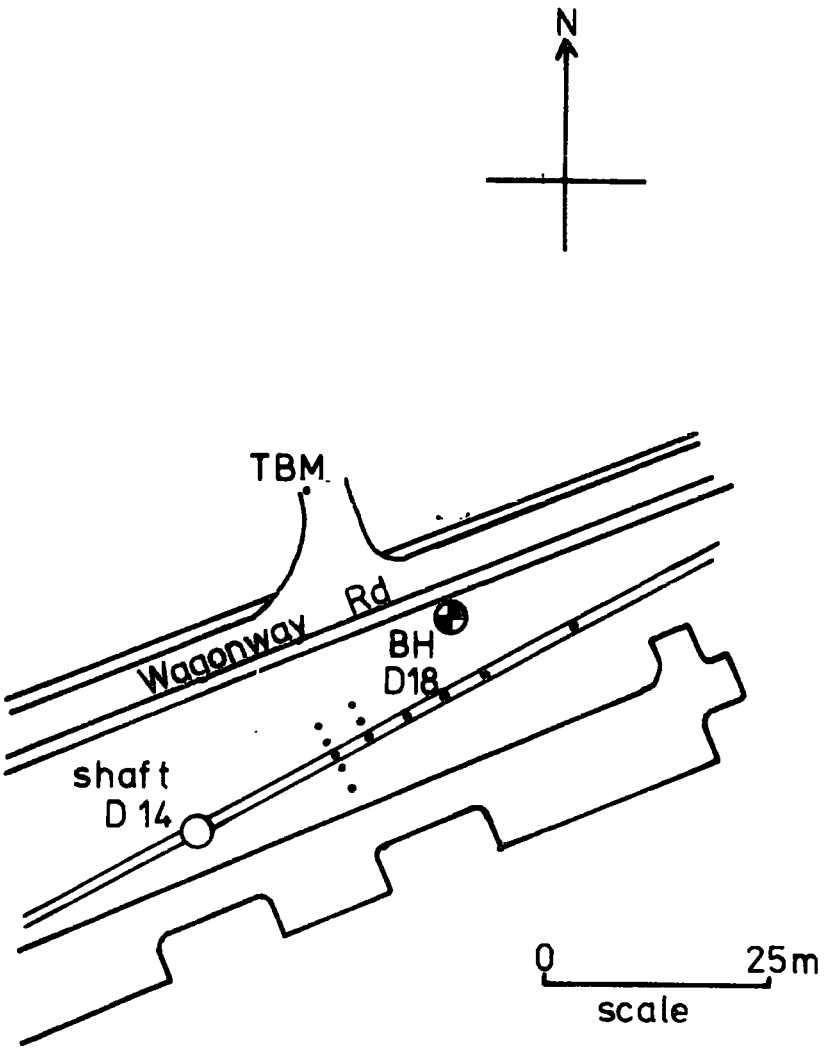

Figure 4.1
Hebburn site

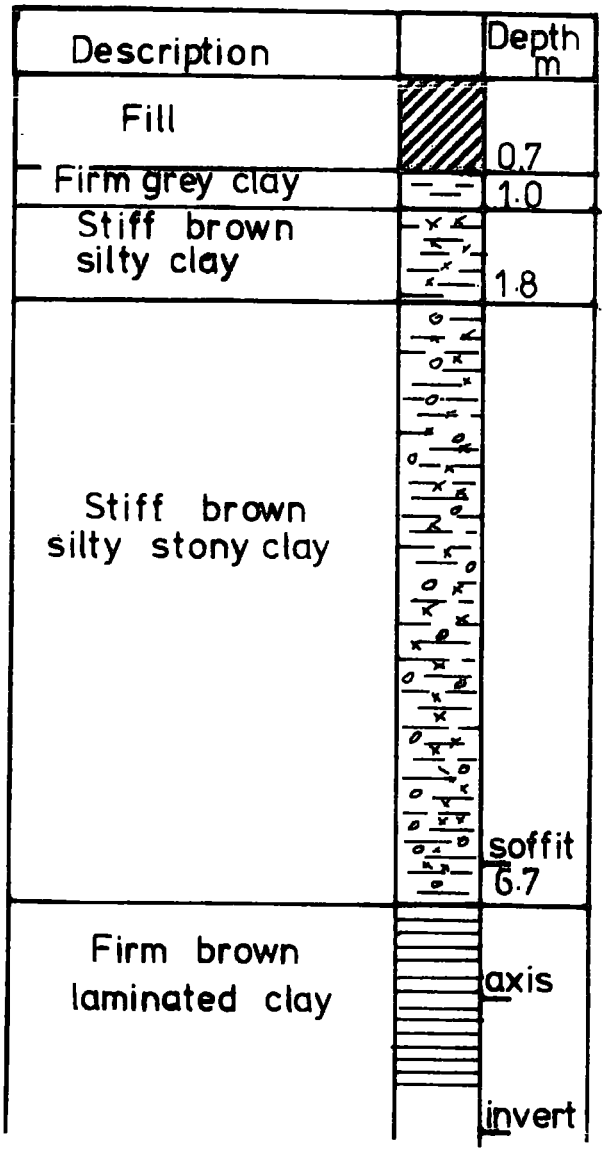

Figure 4.2
Borehole D18 - Hebburn

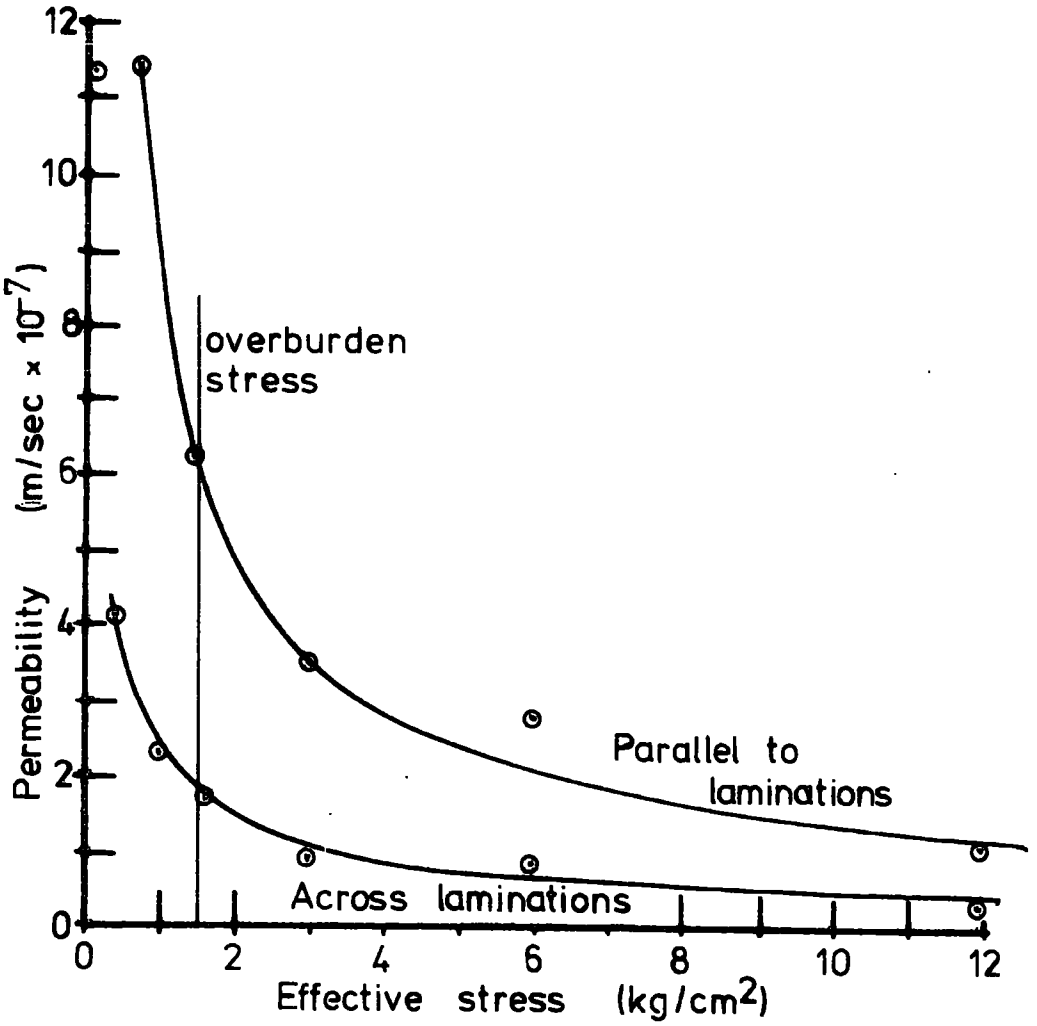

Figure 4.3
Permeability ratio - Hebburn
(after Leach 1973)

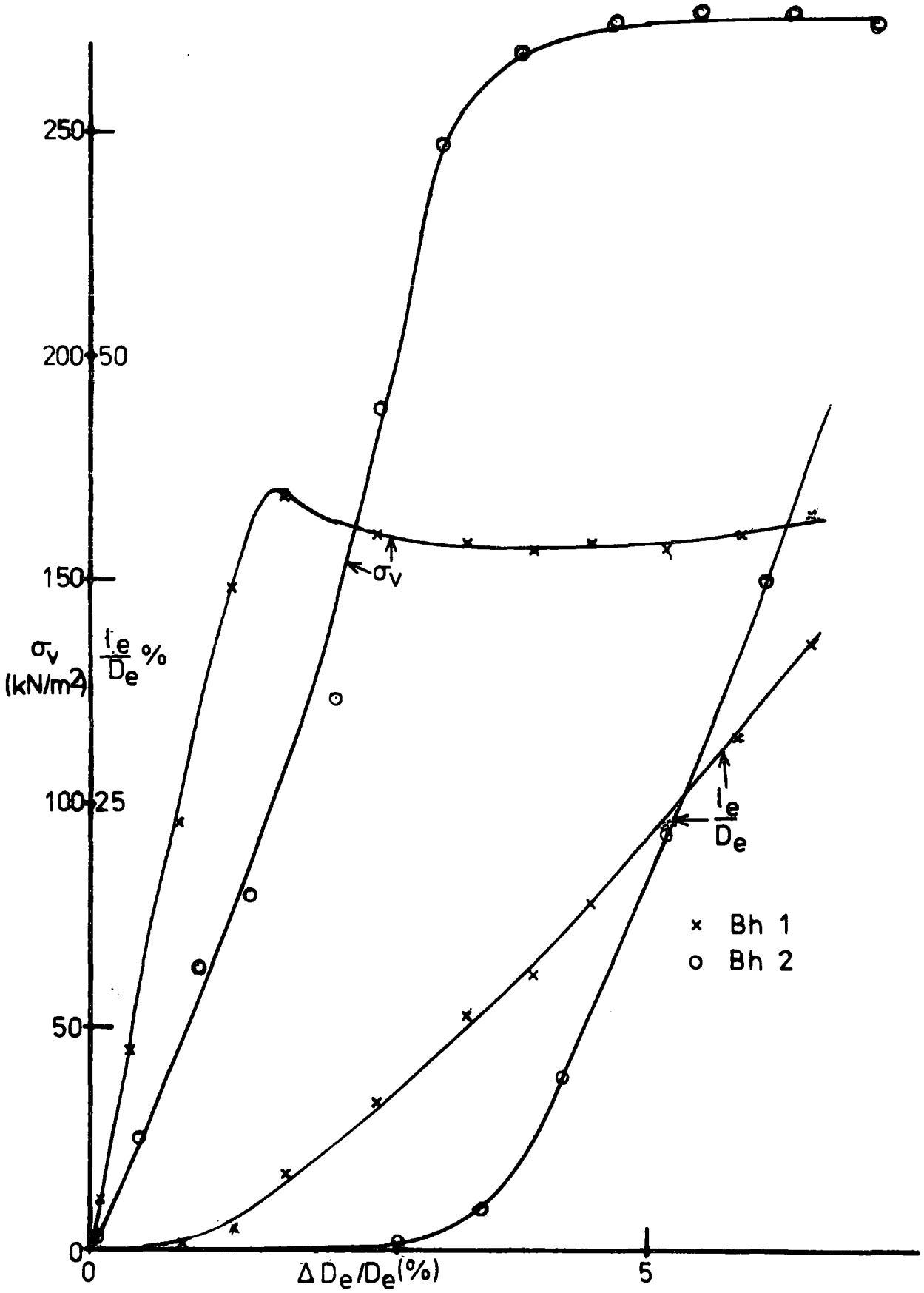

Figure 4.4
Extrusion tests (Hebburn)
(after Bewick 1973)

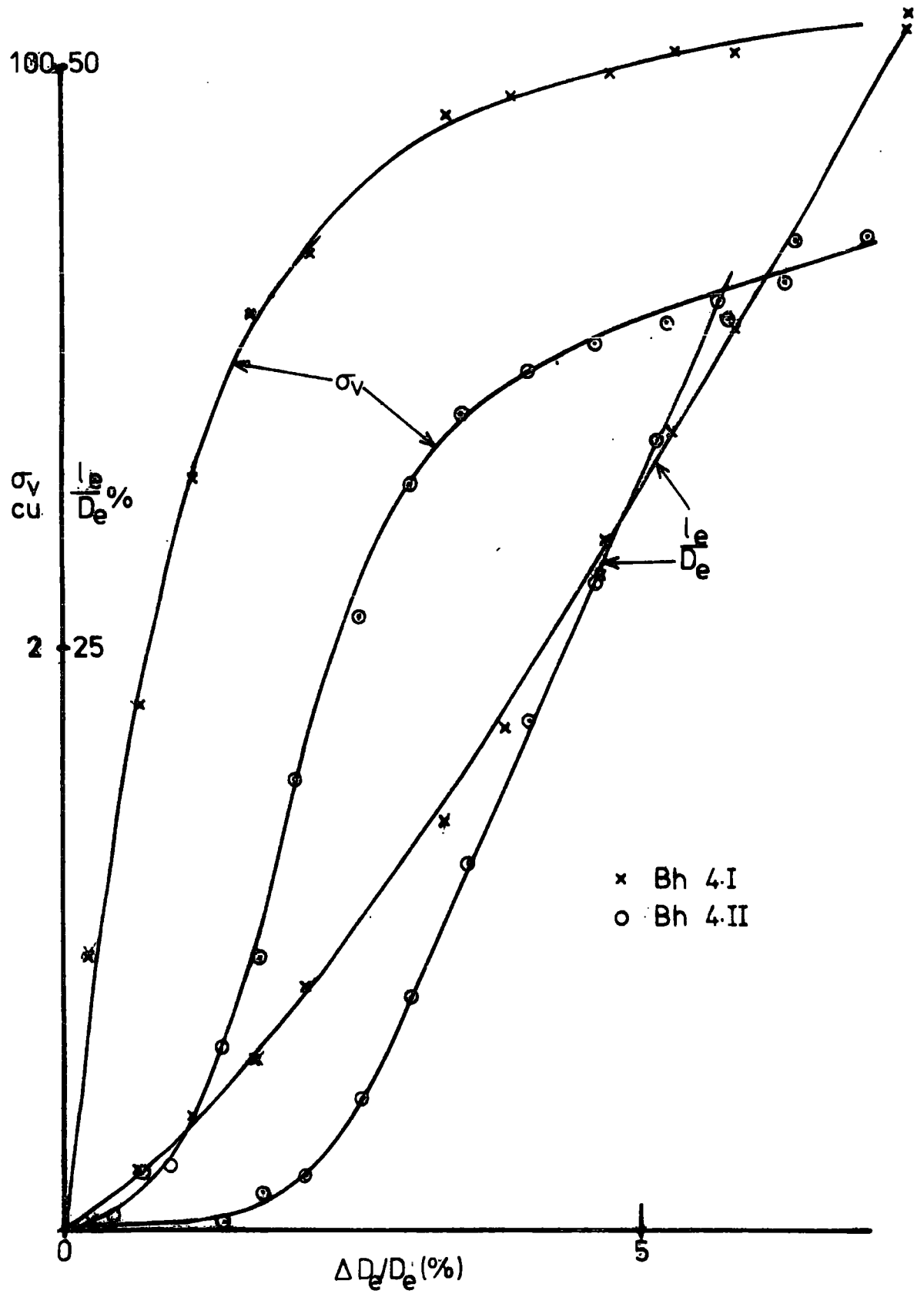

Figure 4·5
Extrusion tests (Hebburn)
(after Bewick 1973)

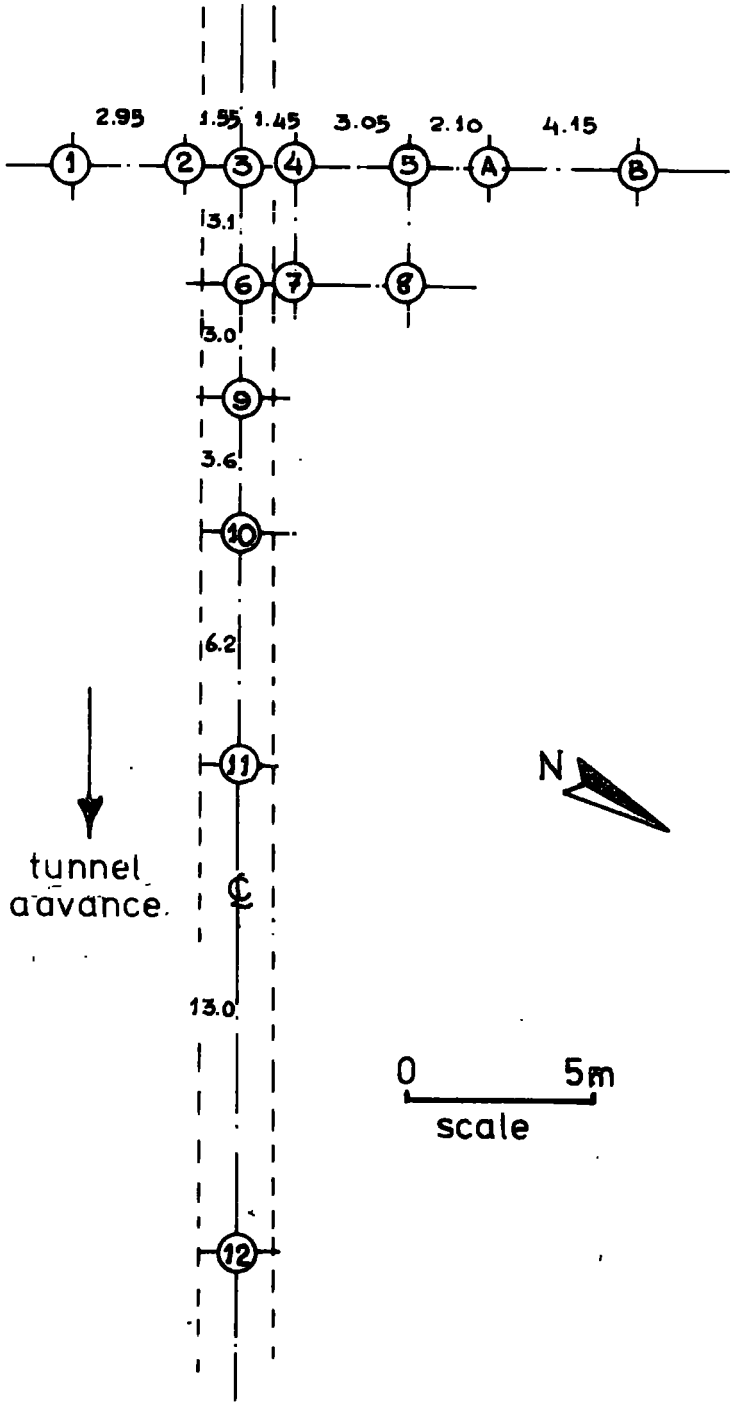

Figure 4.6

Borehole locations (Hebburn)

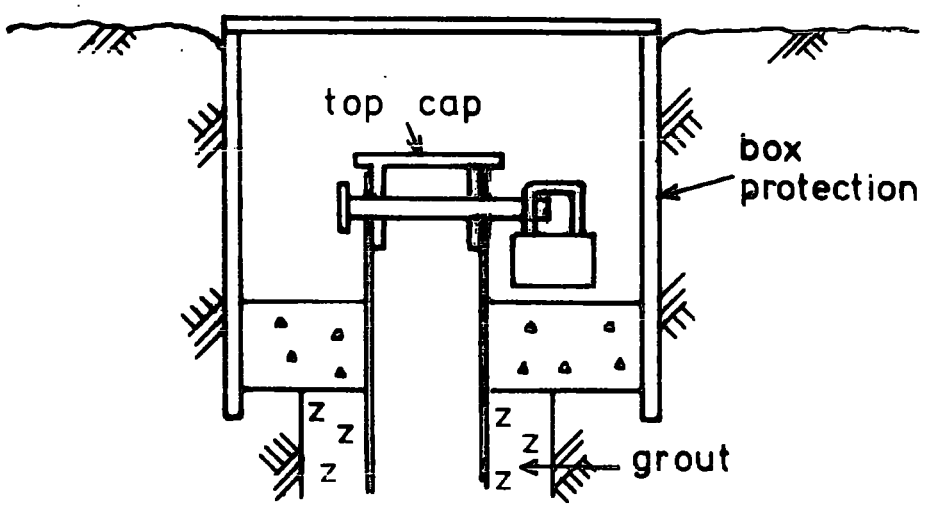

Figure 4.7
Borehole top (Hebburn)

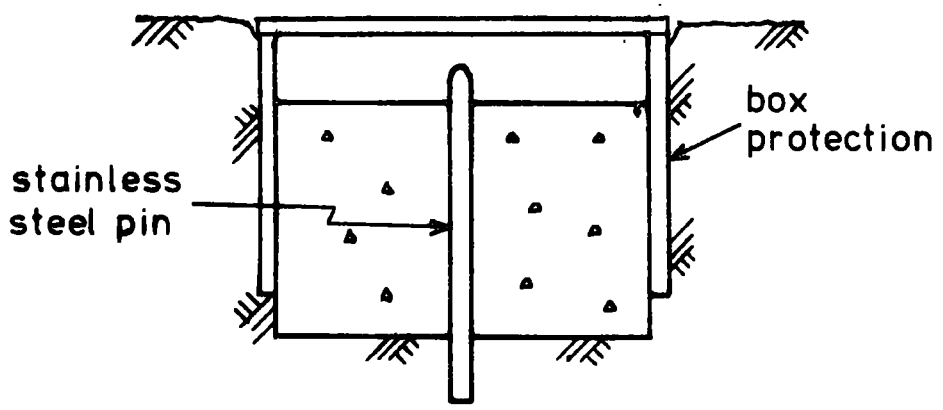

Figure 4.8
Levelling station (Hebburn)

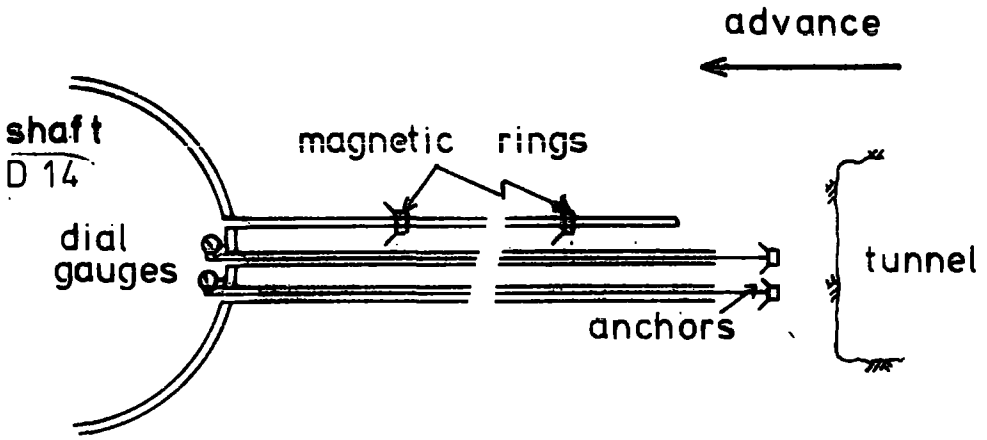

Figure 4.9
Anchor installation (Hebburn)

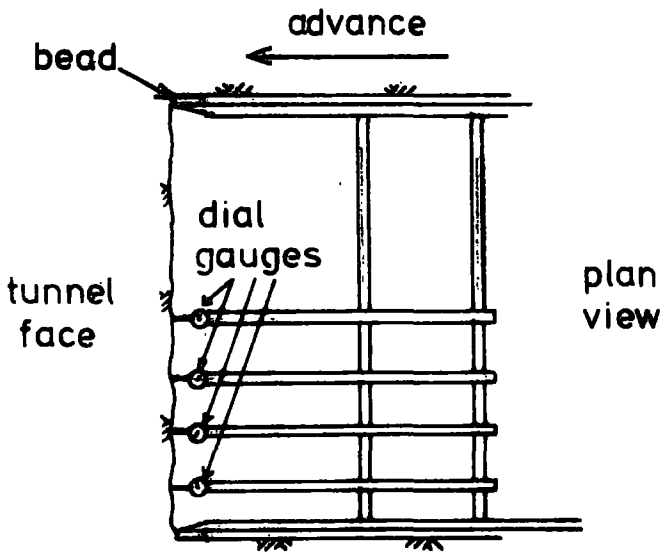

Figure 4.10
Face measurements (Hebburn)

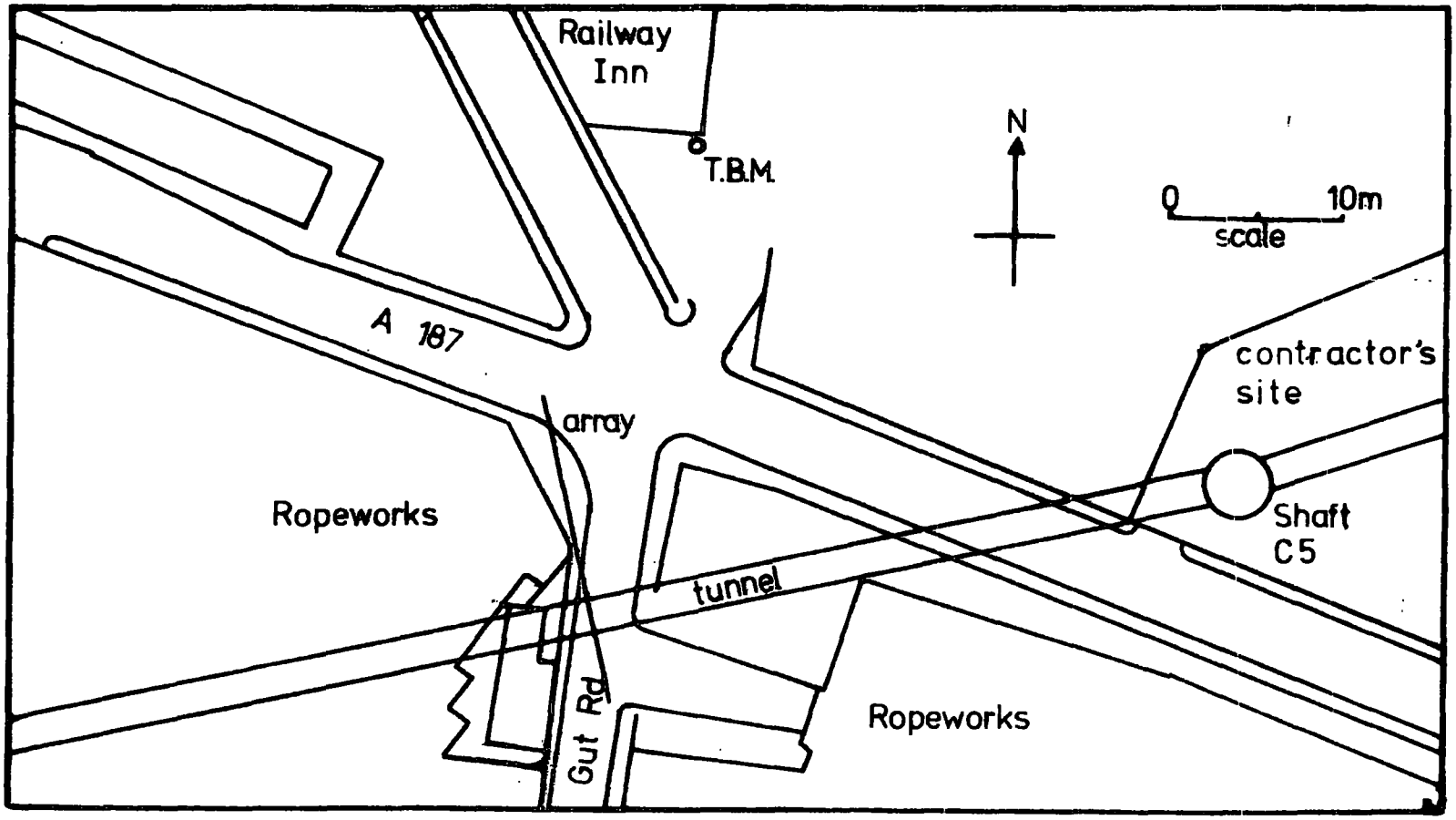

Figure 4.11
Willington Quay Site

Plate 4.1

The Willington Quay site

Plate 4.2

The Willington Quay site (close-up)

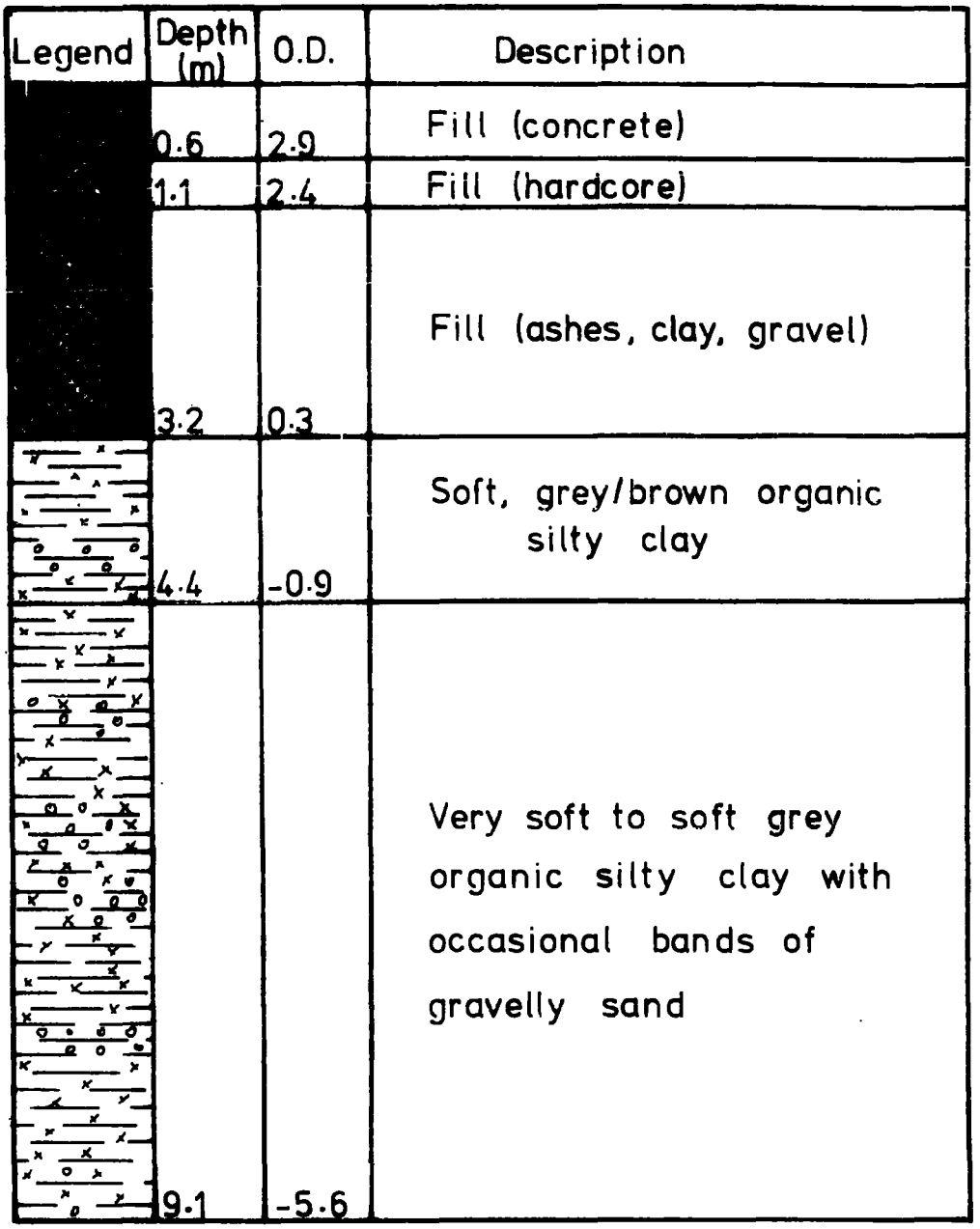

Figure 4.12

Borehole C12a - Willington Quay

150 m W of array

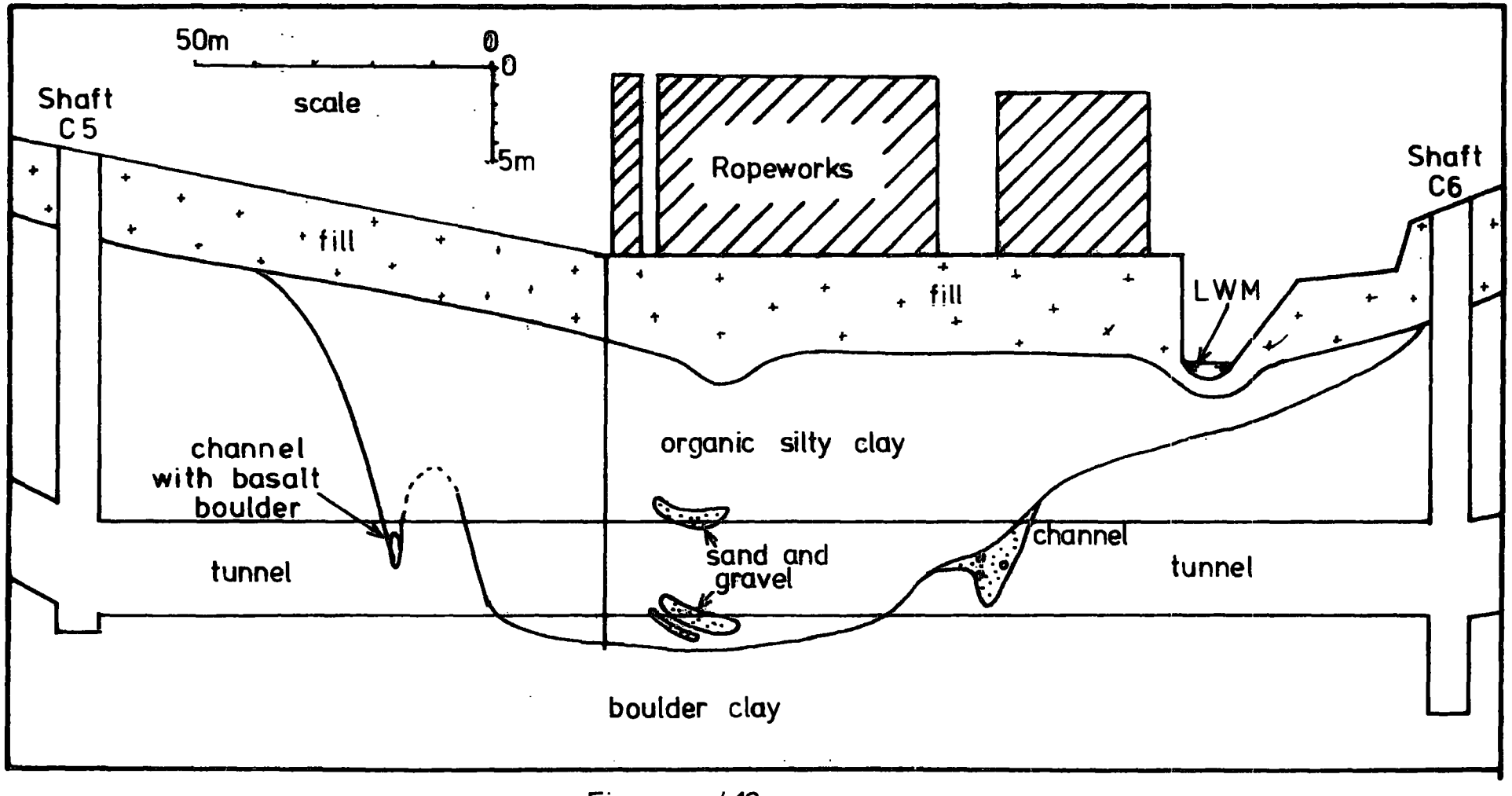

Figure 4.13
Section through buried channel

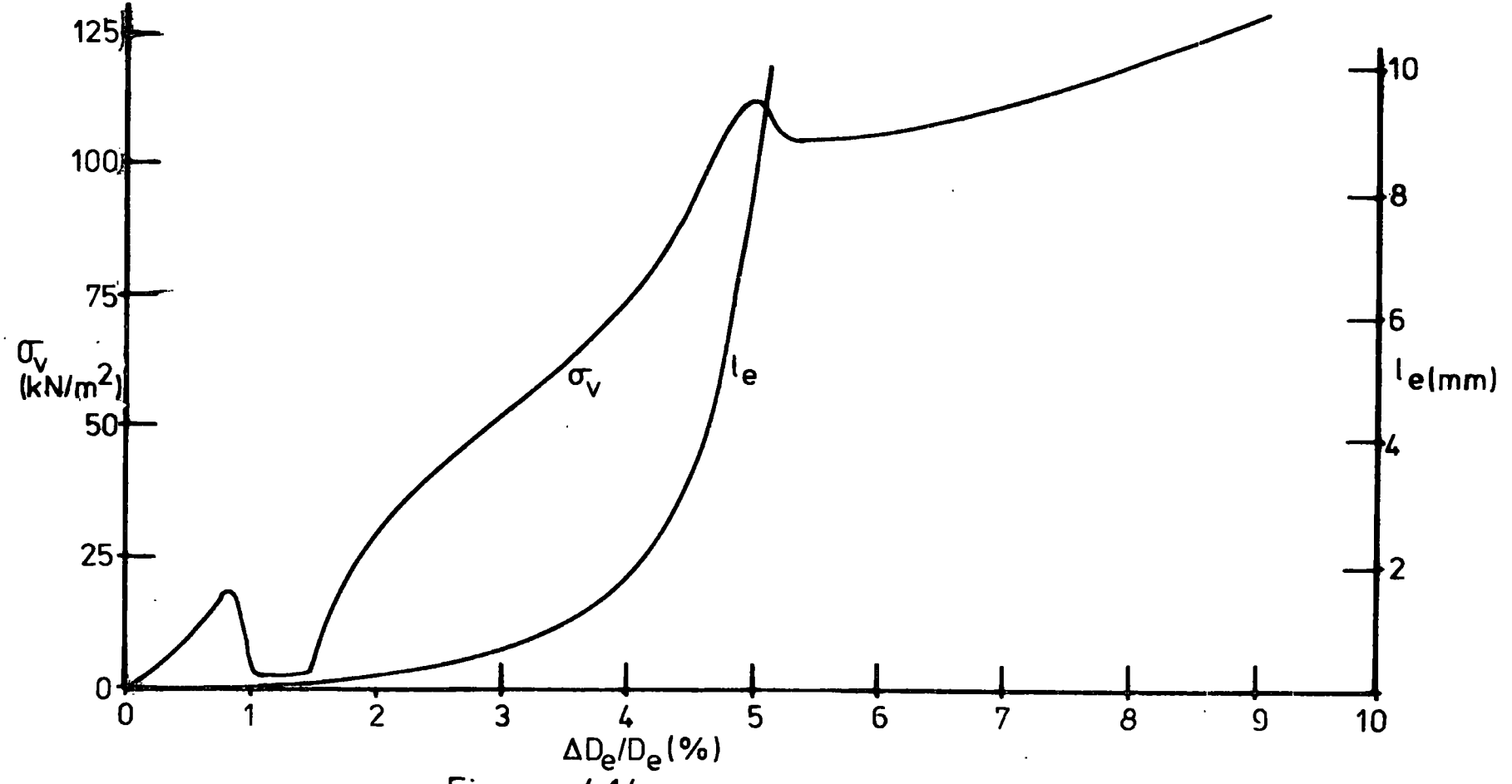

Figure 4.14

Extrusion test (Willington Quay)

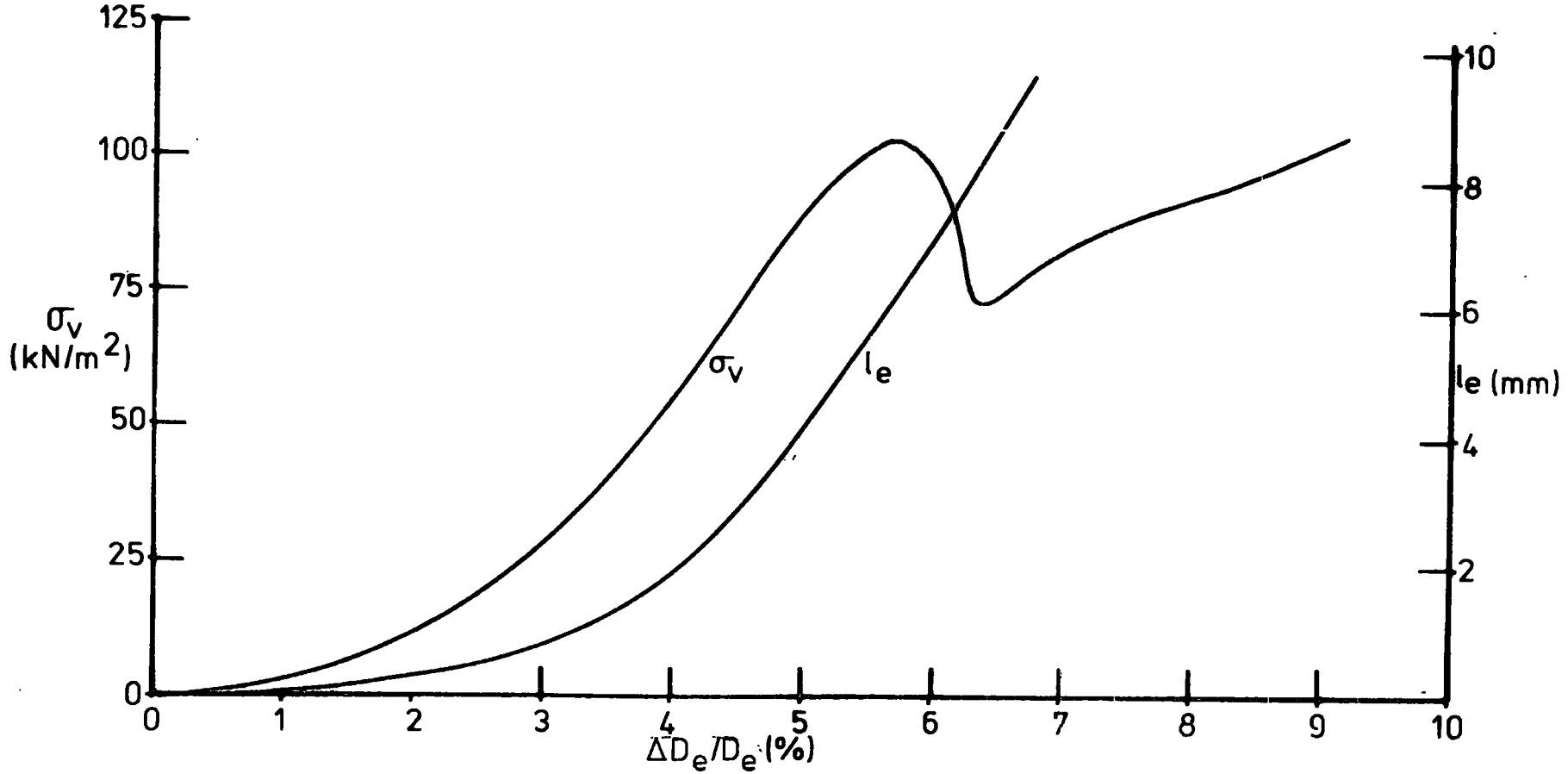

Figure 4.15
Extrusion test (Willington Quay)

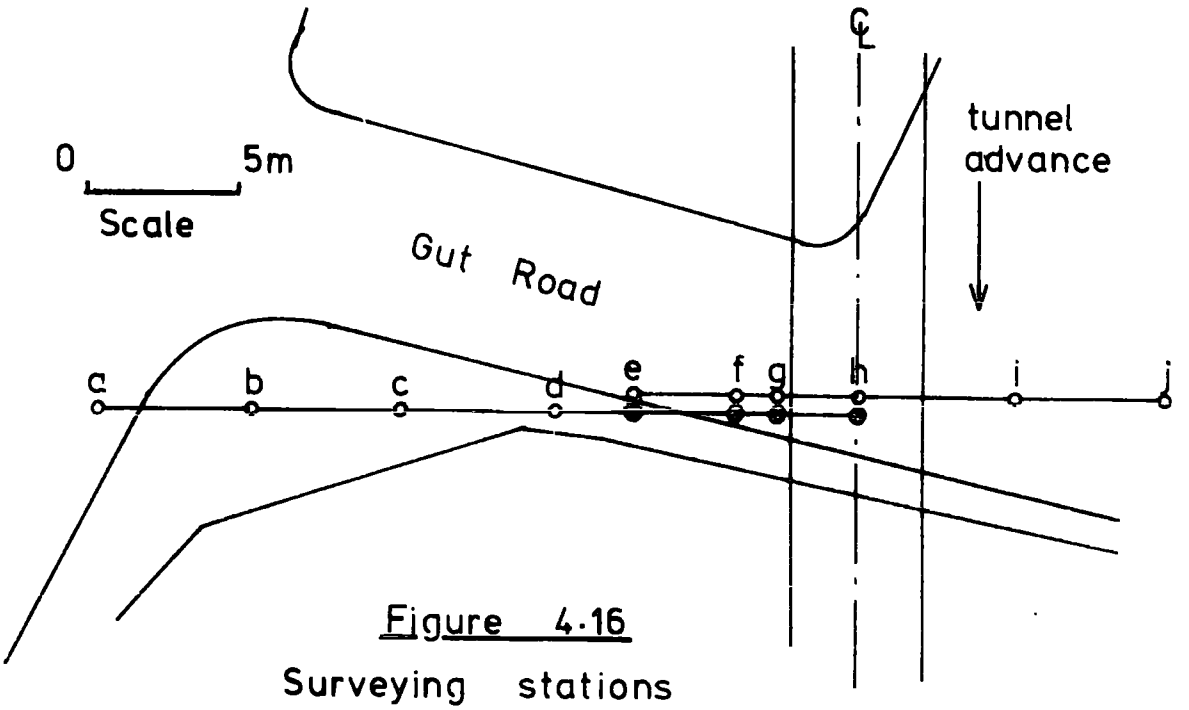

Figure 4.16
Surveying stations
Willington Quay

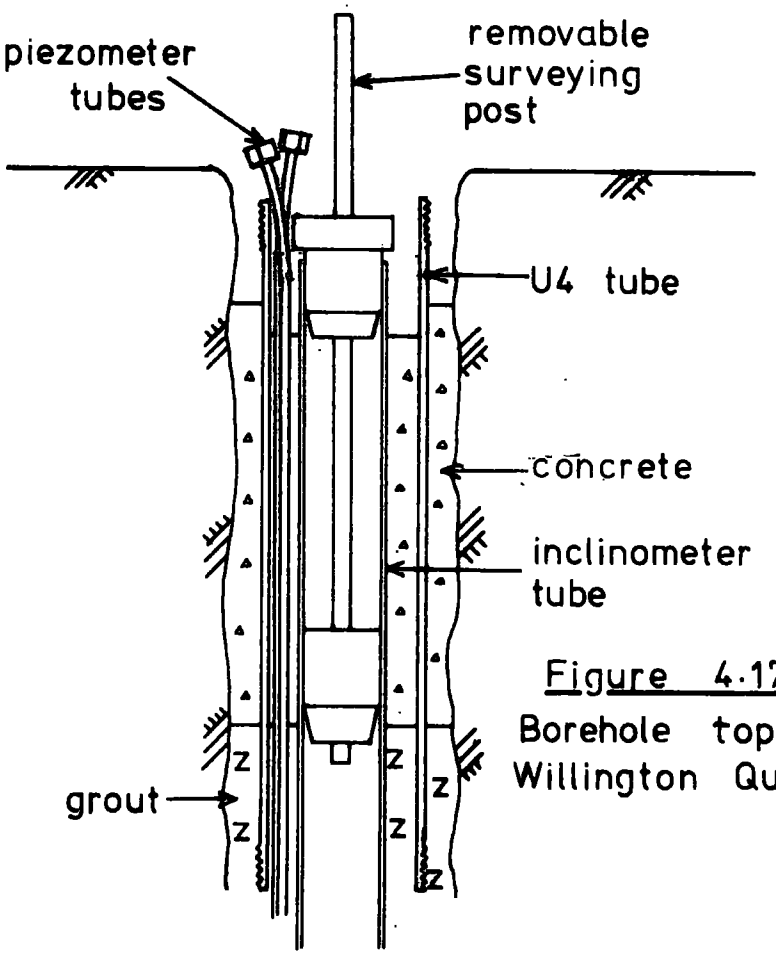

Figure 4.17
Borehole tops
Willington Quay

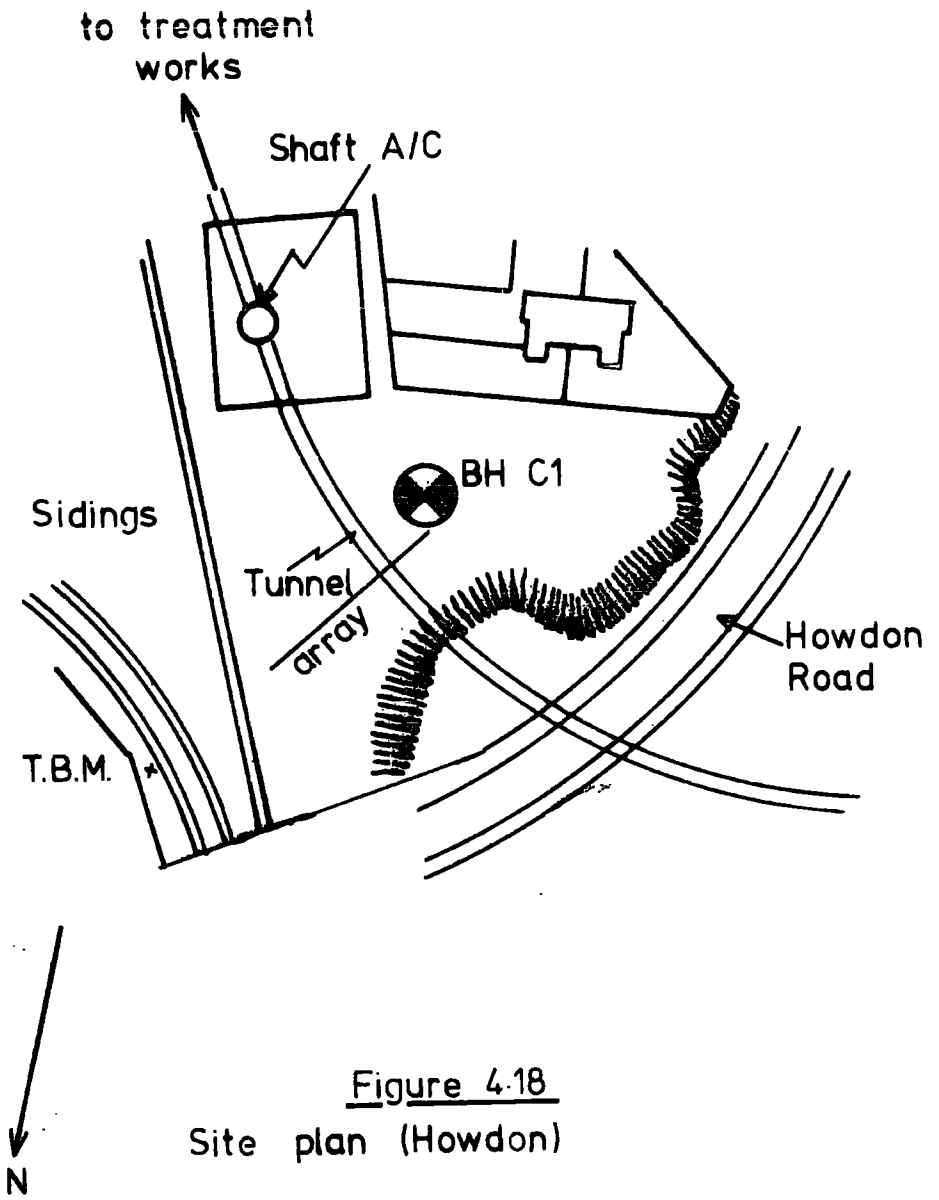

Figure 4.18
Site plan (Howdon)

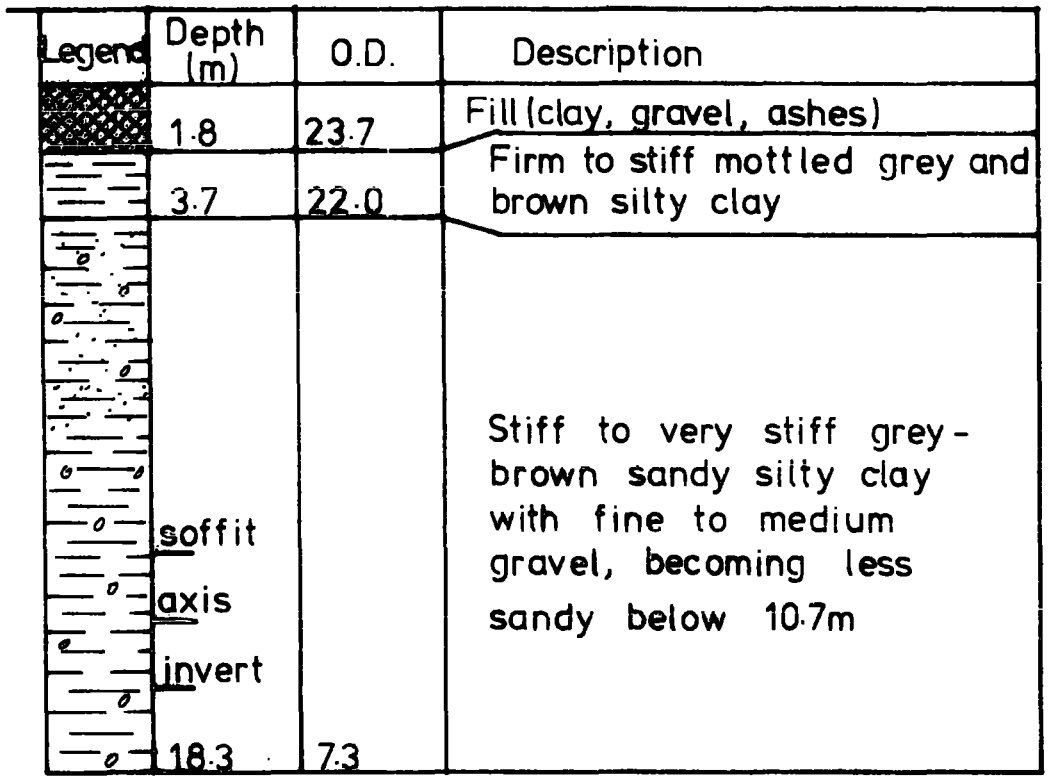

Figure 4.19
Borehole C1 (Howdon)

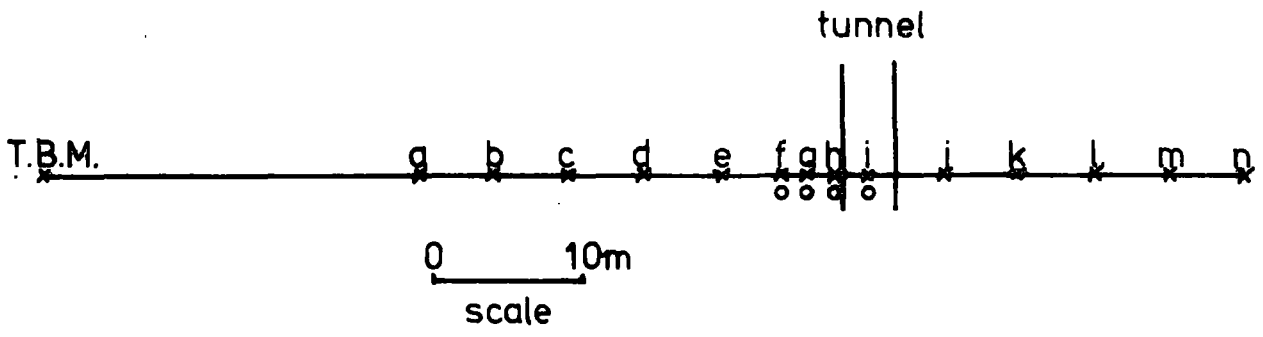

Figure 4.20
Howdon array

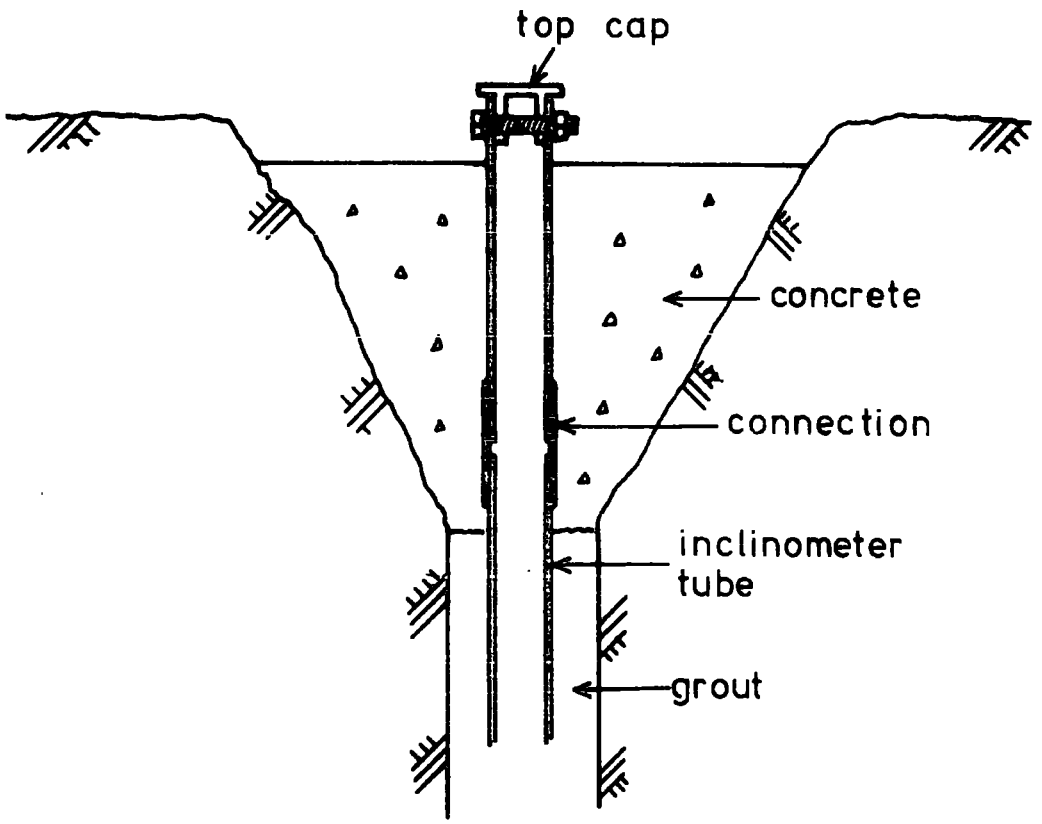

Figure 4.21
Borehole top (Howdon)

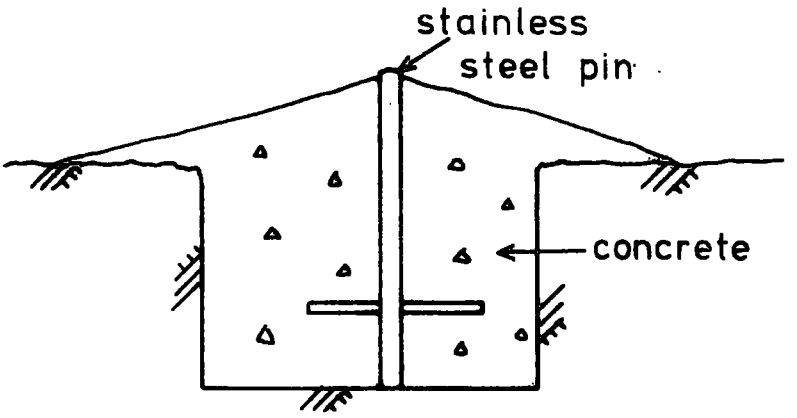

Figure 4.22
Levelling station (Howdon)

Chapter 5

PRESENTATION OF FIELD OBSERVATIONS

5.1) Introduction

In this Chapter it is intended simply to present the results of the observations described in Chapter 4. The data are presented in as simple and straightforward a manner as possible, generally in graphical form. The interpretation and discussion of these data are contained in Chapter 6.

As is clear from the description of the field instrumentation in Chapter 4 and Appendix C, the observations from each of the three sites follow the same general pattern, and have been processed in similar ways. Sections 5.2 to 5.5, which describe the data processing and presentation, apply equally to data from each site.

5.2) Plotting of data

Many of the observations presented in this chapter are time-independent; for example the ultimate settlement profile. Other data, of a more dynamic nature, may be regarded either as time-dependent or advance-dependent. The centre-line settlement development profile, for example, may be plotted with respect to time or with respect to tunnel face position. The latter is more conventional (see Attewell and Farmer, 1972) and has generally been adopted here. In some cases, however, it is clearly more rational to plot data with respect to time. The Willington Quay settlement data, for example, continues for a period of over 18 months, for most of which time the face was more than

50 m beyond the measurement array and could no longer be considered to have any direct influence. Therefore, in the case of long-term movements, it is more logical to plot time as the abscissa, and this procedure has been adopted.

5.3) The tunnel advance curve

In view of the above considerations it is necessary to convert data from the time scale, as it was collected, to the tunnel advance scale, as it is to be presented. To facilitate this procedure, a tunnel advance curve has been plotted for each tunnel. On these curves face position, tail position or grouting position are all plotted with respect to time. The data for these curves were obtained from the engineer's shift reports, and represent face position at the end of each shift. These points have been connected with straight lines, although in fact the face advance is intermittent. This "smoothing" of the curves introduces an error which may possibly be as great as 0.6 m (or the width of a lining ring). This error is unavoidable, since the face position is not recorded throughout the shift, but is considered to be sufficiently small to be acceptable. It should be noted, however, that this error should be taken into account wherever face position is considered.

By convention, the tunnel advance curves are plotted with time as the vertical axis (positive downwards) and distance horizontal. Therefore, the higher the tunnel advance rate, the smaller the gradient. Vertical sections of this curve represent stoppages, for example at weekends, holidays or disputes. A tunnel advance curve was plotted for each of the experimental sites. All values of distance to the

tunnel face were calculated from the time of observation using these graphs.

5.4) Surface measurements

As described in Chapter 4, two types of surface observation were made at all sites, these being measurements of level and of lateral displacement.

5.4.1) Presentation of surface levels

Surface levelling data are initially presented in two different ways. Firstly, centre-line level (that is, maximum settlement) is presented with respect to tunnel face position as a settlement development profile. This curve can be considered either as a graph of the development of maximum settlement with time as the tunnel face passes the measurement point, or can be said to represent a longitudinal section through the settlement trough at a given moment in time. The latter case presupposes that settlement development and maximum settlement are the same throughout the length of the tunnel, an assumption which may well be incorrect. In the case of Willington Quay a long-term settlement development profile has been plotted with respect to time (see Section 5.7.1).

Secondly, plots are produced of settlement versus distance away from the centre-line for particular points in time or values of tunnel advance, showing the shape of the settlement trough (or transverse settlement profile) at various stages in its development.

5.4.2) Presentation of lateral displacement measurements

The lateral surface displacements have been plotted on the same axes but not to the same scale as the transverse settlement profiles described above. The convention has been adopted throughout that movements towards the tunnel are plotted vertically with positive upwards. As was noted in Chapter 4 and Appendix C, the nature of the measurements is such that values of change in level (settlement) are known to a much greater degree of accuracy than those of lateral displacement. For this reason, no lateral displacement was observed at Hebburn and no displacement curves are presented, although lateral movement was indicated indirectly (see Section 5.6.4). For all the above curves the displacement scale is considerably exaggerated.

5.5) Sub-surface measurements

As in the case of surface data, sub-surface observations consist of measurements of vertical and horizontal movements. In this Chapter these measurements are presented separately. It should be noted that in both cases data have been collected over a two-dimensional grid on a vertical plane, rather than along a one dimensional array as in the case of the surface measurements. It is therefore difficult to present all the data on the same diagram, particularly when changes through time are taken into account. Various options are available, and these are explored more fully in Chapter 6. For the initial presentation of this data, the general philosophy has been to make the presentation in as simple a manner as possible.

5.5.1) Sub-surface settlement measurements

As was noted in Chapter 4, these measurements were originally

made relative to the ground surface. The data were therefore processed by adding to them the value of surface settlement observed at that position relative to the centre line at that particular time. Data for each borehole are then presented as plots of vertical settlement development with depth. These curves are presented for various moments in time (or values of tunnel advance) corresponding to the transverse settlement profiles, that is, ultimate or final settlement for Hebburn and Howdon, and several stages of settlement development in the case of Willington Quay. Vertical settlements are plotted horizontally (right positive) with depth as the vertical axis.

5.5.2) Horizontal sub-surface displacements

Measurements of sub-surface lateral displacement were taken using a Soil Instruments Digitial Inclinometer as described in Appendix C. The nature of this instrument's operation means that a certain amount of "data processing" is necessary before the results can be plotted. This procedure, along with the computer program used, is described in Appendix D. It is also necessary to correct for erroneous readings since these are not immediately apparent when actually using the instrument. These can arise due to distortions in the access tube or due to reading at joints in the tube (see Figure 5.1). The correction procedure is also described in Appendix D.

The inclinometer plots presented in the thesis consist of tracings of the computer plots for particular moments in time, with some traces corresponding as far as possible to those used for the transverse settlement profiles.

5.6) Hebburn

The data from the Hebburn site were collected over a period of about two months, between June and July, 1973. During the time that the tunnel face was within 20 m of the instrumentation array, one or two readings were taken at each station each day. Measurements were taken less frequently when the face was at a greater distance.

5.6.1) The tunnel advance curve

The tunnel advance curve is shown in Figure 5.2. The two parallel curves represent the positions of the tunnel face and the grout injection position at any moment in time. The vertical lines, numbered 3, 6 and 9 to 12, show the positions of the centre-line boreholes. The main vertical sections of the curve represent weekends, when no work was carried out, whilst the two short vertical sections at the right of the curve show lost shifts. Zero tunnel advance is taken to be at shaft D14 (see Figure 4.1).

The overall rate of advance, including all weekend stoppages, is 0.113 m/hr. The actual advance rate, calculated as the average rate during the week 11-6-73 to 15-6-73 inclusive is 0.182 m/hr. This is equivalent to about 3.6 rings per shift, the best advance achieved for a single shift being 4 rings.

5.6.2) The settlement development profiles

Six centre-line surface settlement development profiles were obtained, from levelling points by the six centre-line boreholes. These are shown superimposed in Figure 5.3. The vertical axis represents the position of the measurement points. The curves are

extrapolated from settlement-time profiles, using the tunnel advance curve (Figure 5.2). Considerable variation between the profiles is evident. The maximum settlement varies between 6 mm and 10 mm. The shape and extent of the profiles also varies, particularly in the early stages of settlement development. The location of the onset of settlement varies between 4 m and 13 m ahead of the tunnel face. Generally, the onset of settlement is quite abrupt, with between 30% and 50% of the ultimate settlement having developed by the time the tunnel face passes the measurement point. The "average" settlement development profile is shown in Figure 5.4. The main properties of this curve are listed in Table 5.1.

5.6.3) The transverse settlement profile

The transverse settlement profile for Hebburn is shown in Figure 5.5. This curve is plotted from the average of all maximum surface settlement readings and thus represents the shape of the "mean ultimate settlement trough" corresponding to Figure 5.4. Only one half of the profile is plotted, since it appears to be symmetrical. The profile is an average of data from both sides of the centre-line. The point of contraflexure (point of inflection) shown on the curve is estimated by eye. The shape of the settlement profile is discussed more fully in Chapter 6, but its main parameters are listed in Table 5.1.

5.6.4) Horizontal surface movements

Horizontal surface movements before and after the passage of the tunnel face through the array are summarised in Table 5.2. The

experimental errors incurred in these measurements are discussed in Appendix 3. As is explained there, the measurement errors in this particular location are quite large, probably in the region of 4 mm or even more. Taking this into account it must be concluded that no evidence of lateral surface movement can be deduced from Table 5.2. On the other hand the observations do not preclude the possibility of undetected movement up to 4 mm between the measuring points. It would therefore be unwise to conclude that no movement has taken place, and it is shown in Section 5.6.6 that indirect evidence suggests that movements of the order of 2 mm towards the centre-line may have occurred in places.

5.6.5) Sub-surface settlement development

Figure 5.6 shows the development of vertical settlement with depth below the surface at the tunnel centre-line and at 1.5 m and 4.5 m from the centre-line. These curves represent a combination of the magnetic ring data from all the boreholes. Whilst a certain amount of variation between the boreholes is apparent, especially over the tunnel centre-line, a clear pattern of movement can be seen. At the centre-line the settlement increases with depth to a maximum of 15 mm at crown level. This is consistent with the volume of the surface settlement trough (see Section 6.2.2). To the side of the tunnel, at 1.5 m from the centre-line the settlement can be seen to increase to a maximum of 8.25 mm at a depth of about 5 m, then decrease to zero at invert depth. At 4.5 m from the centre-line the maximum settlement of 4.5 mm is reached at a depth of about 3.5 m, decreasing to zero at about 8 m. This indicates the narrowing of the settlement

trough with depth, to be discussed in Chapter 6.

5.6.6) Horizontal sub-surface movements

Figures 5.7 to 5.10 show movements of the centre-line inclinometer tubes parallel to the line of advance of the tunnel. These curves represent measurements taken at individual boreholes at different moments in time but can be considered to show movements at different distances from the advancing face in much the same way as do the settlement development curves. However, some of the curves showing movement at a great distance behind the shield have been brought closer to the face position in order to compress the diagrams to a reasonable size. It should be noted that these curves are plotted under the assumption of zero movement at the tops of the tubes. Therefore, although their shapes may be regarded as correct, they may not, in fact, occupy the relative positions shown in the diagrams.

The general pattern of ground movement development along the centre-line as the face approaches commences with what appears to be a general movement of the ground at depth away from the tunnel face. This is considered highly unlikely. If we assume that some movement may have occurred at the tops of the tubes then a more reasonable alternative emerges, that the ground movement commences with movement of the upper part of the ground towards the face. By the time the face is 1.6 m away from the tubes about 1 mm of movement has developed at the surface and a slight "bulging" of the tubes towards the face begins to axis level. This movement reaches about 2 mm in tubes 3 and 6 at distances of 0.6 and 0.8 m respectively from the face.

Once the face has passed the array there appears to be some

movement at depth in the direction of tunnel advance, possibly due to frictional forces around the bead. This is particularly clear in the cases of tubes 9 and 12. It is difficult to estimate from these diagrams the magnitude of this "forward drag" since we have no certain datum point. The horizontal movements then appear gradually to decrease, in the cases of tubes 6 and 12 back to zero. Again it is impossible to be certain whether or not there remains a general translation of the entire cover above the tunnel after the passage of the shield, although this is regarded as unlikely.

Movements perpendicular to the tunnel line of advance are shown in Figures 5.11 to 5.15 for distances of 1.5 m and 4.5 m from the tunnel centre-line. Tubes 2, 4 and 7 show little movement until the face reaches them. Tube 2 seems to indicate movement towards the centre-line at the surface before the face arrives, but tubes 4 and 7 indicate the opposite. The reasons for this are unclear. Once the face is past the boreholes considerable displacement towards the tunnel occurs at depth, eventually reaching a maximum of about 11.5 mm in tube 7. This movement develops quite slowly in tube 2, but very rapidly in tubes 4 and 5. The movement extends upwards for about 3 m above axis level, and in tube 2 appears to extend downwards for about 2.5 m. In all 3 cases the maximum horizontal movement appears to develop somewhat below axis level. It is unclear how much movement develops at the surface. Tubes 4 and 7 seem to show very little, although tube 2 suggests a maximum towards the centre-line of about 2 mm, assuming zero movement at the base of the tube.

The movement in tubes 1 and 5, which are further from the tunnel (4.5 m from the centre-line), shows a somewhat different

pattern. The dominant feature is movement at the surface towards the centre-line, reaching a maximum of about 3 mm. Most of this movement develops after the face has passed the boreholes. Tube 5 shows evidence of a small amount of movement towards the tunnel at axis level,although this is not repeated in tube 1.

5.6.7) Intrusion rate measurements

Three experiments were carried out at Hebburn in order to determine the rate and development of clay intrusion into the tunnel face. Figure 5.16 shows ground movement versus distance to the face for the ground anchor experiments. Whilst the total amount of data is small the curves do indicate that as the face approaches the rate of ground movement accelerates.

Figure 5.17 is a plot of face intrusion against time for one of the ground anchors and the two face experiments in laminated clay. The face data refer to intrusion at the centre of the tunnel face, where the intrusion rate would be expected to be highest. The points from the three experiments are very consistent and give an excellent fit to a straight line (least squares correlation giving a correlation coefficient of 0.99). This indicates that at least over a period of 48 hours the clay at the face intrudes at a constant rate of 0.221 mm per hour. This is in very close agreement with laboratory extrusion tests carried out on the same material (see Section 4.2.2 and Bewick, 1973) which gave an extrusion rate, at this overburden pressure, of 0.218 mm per hour. The constant intrusion rate is suggestive of plastic behaviour (see Section 1.5).

The results of face measurements in the stony clay are shown

in Figure 5.18. Once again these indicate a constant rate of intrusion, this time of 0.0134 mm/hour at the centre of the face. It is to be expected that the stiffer stony clay would intrude at a lower rate than that of the laminated clay. The figure also indicates clearly the increase in intrusion rate towards the centre of the tunnel. Figure 5.18 also shows three "intrusion profiles" at 5 hour intervals illustrating the development of intrusion across the face. These profiles demonstrate that the tunnel face develops a pronounced dome-like configuration, rather than shearing around the cutting edge and intruding uniformly as a cylinder. This is quite consistent with observations made on laboratory extrusion tests, where the face "domes" until failure, at which point the clay begins to extrude as a cylindrical plug by shearing around the circumference of the aperture. There was no evidence of failure in this sense at the Hebburn tunnel face.

5.7) Willington Quay

The data from Willington Quay were collected over a period of 18 months between January, 1975 and July, 1976. During the period that the tunnel face was within 25 m of the array one set of readings was taken each day. At greater distances the readings were less frequent, culminating with readings at about 3 monthly intervals after August, 1975.

5.7.1) The tunnel advance curve

The tunnel advance curve is shown in Figure 5.19. This curve covers the period January 10 to April 20, during which time the

tunnel face progressed from 50 m ahead of the array to 122 m beyond it. As in Figure 5.2, two curves have been plotted to show the face position and the grout injection position. The array location is represented by the vertical line at zero advance. The only major stoppage, apart from weekends, occurred with the face 9 m ahead of the array, between January, 1975 and February, 1975. This stoppage resulted from a report of gas seepage into the tunnel, and the hold up was to allow flame-proof lighting and control equipment to be installed. During this period the compressed air remained in operation and the face itself was completely boarded up. This had a noticeable effect on the development of ground deformations which is discussed in the following sections.

The overall rate of advance, including weekend stoppages but excluding the hold-up referred to above, is 0.06 m/hr. The actual advance rate calculated for the period during which the face passed the array is 0.10 m/hr, which is the equivalent of 2 rings per shift.

5.7.2) The settlement development profiles

Due to the long-term nature of settlement development at this site two development profiles are presented. The first (Figure 5.20) shows settlement development relative to face position for the period January, 1975 to February, 1975. The second (Figure 5.21) shows settlement development with time over the entire observation period. Both profiles show a complex settlement history.

Figure 5.20 indicates that settlement commenced when the face was about 34 m from the boreholes. At 9 m from the measurement points an uplift of all the settlement stations occurred, coinciding

with the two-week hold up. The most plausible explanation of this uplift seems to be that the ground, being very soft, was forced upwards by the pressure of the hydraulic rams used to hold the breasting boards in place at the face.

Immediately after this stoppage settlement continued, reaching about 7 mm by the time the face was level with the array. Immediately after the face passed the array the rate of settlement decreased until the tail of the shield had passed. This is to be expected since in the absence of a bead the shield will provide support to the ground. Once the shield had passed, the rate of settlement increased once again. For the next 20 days, until the face was about 50 m past the array, settlement developed normally, having much the same form as that shown at Hebburn.

Long term settlement development is shown in Figure 5.21. At 23 days, high pressure back-grouting (at 700 kN/m^2) was carried out in the vicinity of the array, to fill any voids remaining around the lining, particularly in the soffit. This is standard practice, particularly where large settlements are expected. Surprisingly, this back-grouting coincided with a marked increase in the settlement rate. Site records show that there was no change in the air pressure during this period. The reasons for this increase in settlement rate remain unclear, and any explanation is speculative. It is suggested that the increase in settlement rate must reflect either a weakening of the soil, the opening up of further voids or the onset of consolidation due to drainage. The latter is unlikely since the air pressure remained constant. It is possible that the pressure of the back grout could cause cracking or failure in the existing grout, thus opening fresh

voids, although the mechanism by which this could occur is problematic. Alternatively the pressure could have caused local yielding in the clay around the tunnel. Associated strain-softening could cause an increase in the rate of deformation of the ground on the release of the grout pressure.

Following this acceleration the rate of settlement again gradually decreased until 66 days following the passage of the face. This marks the completion of the drive and the removal of the air pressure, corresponding with yet another increase in settlement rate. Evidence suggests that this phase of settlement represents consolidation of the ground due to drainage into the tunnel or along the zone of disturbed ground surrounding the tunnel. This phenomenon is discussed in more detail in Chapter 6.

163 days after the passage of the face a wall close to the levelling stations (shown in Figure 4.12) was demolished because of extensive settlement damage (see Plates 5.1 and 5.2). The removal of this wall coincided with extensive uplift of the settlement stations, this uplift being greatest for the stations closest to the wall. Consolidation settlement continued unabated after this uplift.

Measurements continued for a total period of 18 months, by which time settlement was virtually complete, having reached a maximum of 81.5 mm at the centre-line.

5.7.3) The transverse settlement profile

Transverse settlement profiles for Willington Quay are given in Figure 5.22. These show the shape of the trough at 0 days, 23 days, 51 days, 149 days and 504 days. Although the overall shape of the

trough is similar to that at Hebburn (see Section 5.6.3) it is notable that this trough appears to widen during the second phase of rapid settlement, between 23 days and 51 days from 30 m to 45 m (the point of inflection moves from 6.2 m to 6.8 m). During the final phase of consolidation the trough widens still further to 60 m (point of inflection at 7.6 m). The main parameters of the curves are listed in Table 5.3. It should be noted that the volume of the final settlement trough does not correspond to the volume of ground lost into the tunnel but partly to the volume decrease in the ground due to consolidation.

5.7.4) Horizontal surface movements

Four profiles of the horizontal movement of the ground surface towards the centre-line have been selected and included with the transverse profiles of the trough in Figures 5.23 to 5.26. In these figures movement towards the centre-line are shown vertically upwards, the same scale being used as for the settlement troughs. In each case it is clear that the maximum horizontal movement corresponds with the point of inflection of the transverse settlement trough, as predicted by the stochastic theory (Chapter 2). Towards the centre of the trough horizontal movements are much smaller than vertical movements (that is, total ground movements are more or less vertical) but as we move away from the centre-line the horizontal movement gradually becomes more predominant until at a distance of 13 m from the centre-line the norizontal movement exceeds the vertical. A maximum of 11.4 mm of horizontal movement develops at about 100 days. The development of lateral displacements, and the shape of the profiles, are discussed in Chapter 6.

5.7.5) Sub-surface settlement

Sub-surface settlement is shown in Figure 5.27 as settlement development with depth for each borehole at stages of settlement corresponding to those used for the transverse settlement profiles and horizontal surface movements (Figures 5.23 to 5.26). Not all the profiles run to the full depth of the boreholes for one of two reasons. Firstly, in Borehole 1, it was necessary to fill the lower part of the tube with grout to prevent air leaking from the tunnel when the tube was cut off as the tunnel face passed the array. Unfortunately, due to the importance attached to this grouting, the tube was filled to such an extent that only the upper magnetic settlement ring (at 1.33 m) was accessible. Secondly, some of the deepest magnetic rings around the bases of the other access tubes became inaccessible before settlement was completed as a result of sediment accumulation in the bottoms of the tubes over the long periods involved. In the same way the remaining settlement ring in Borehole 1 became inaccessible before any significant deviation from the surface settlement had been measured. For this reason no settlement profile has been plotted for the centre-line tube. These profiles are difficult to interpret, particularly that from tube 2.

As explained in Appendix C it is most unlikely that the settlement rings would give values of settlement greater than that which actually occurs (that is, they tend to read low) so the curves represent minimum values of settlement at a particular depth. Bearing this in mind it is suggested that the settlement rings at 7.5 m and 8.5 m depth in borehole 2 may both be giving erroneously low readings during the period 0 to 23 days, possibly due to interference with the

inclinometer tubes or because of inconsistencies in the grout around them at this depth, giving poor ring coupling with the ground. After 23 days the pattern of movements in borehole 2 is quite consistent with the other two boreholes. This is shown by the curves of Figure 5.28 which show the movement between 23 days, and 51 and 149 days. If we accept the above assumption then a consistent pattern emerges for the sub-surface settlements. Its main properties are as follows:

(a) Moving away from the tunnel centre-line the settlement at the surface and at depth decreases.

(b) Settlement increases and then decreases again with depth. This phenomenon is more pronounced close to the centre-line. In tube 2 the maximum is reached at about 7 m; in tube 3 it is reached at a depth of 6 m; and in tube 3 it is reached only 2 m below the surface.

(c) The shape of the profiles is established by 51 days. Settlement after 51 days is more or less constant at all depths.

5.7.6) Horizontal sub-surface movements

The sub-surface horizontal movements are presented as a series of inclinometer profiles taken at intervals throughout the case history and shown as Figures 5.29 to 5.35. The horizontal displacements of the tops of the tubes in the plane of the array are those measured as described in Section 5.7.4. The inclinometer profiles are plotted using these displacements as a surface datum. In the case of the profiles parallel to the centre-line it was necessary to estimate the surface displacement from the shape of the profile.

Figure 5.29 shows the development of horizontal displace-

ments in the plane of the centre-line (from tube 1) prior to the arrival of the face. Significant movement was recorded with the face some 6.7 m away. By the time the face had reached 1.8 m from the boreholes, there had developed an obvious "bulge" towards the face of 3.17 mm at axis level. Estimated surface movement had by this time developed to 1.5 mm. After this point the tube was grouted and no more measurements could be obtained. No displacement perpendicular to the centre-line was observed in borehole 1.

Figures 5.30 to 5.32 illustrate the development of movement parallel to the tunnel centre-line for the "off-centre" boreholes. Up to 66 days, that is,prior to the removal of the air pressure, these profiles show little movement. Borehole 3 seems to indicate a certain amount of movement in the direction of tunnel advance which may be repeated to a lesser extent in tube 2. This may possibly be the result of ground drag on the advancing shield. Surface movements are also in the direction of advance, towards the centre of the buried valley. After the air pressure was removed, at 66 days, much larger movements, again towards the centre of the buried valley (see Figure 4.14),can be seen to develop. The cause of this late development of horizontal displacement, and its connection with long-term consolidation processes, are discussed in Chapter 6.

Figures 5.35 to 5.37 show the development of lateral subsurface movement in a plane perpendicular to the tunnel centre-line. During the first 66 days, prior to the removal of the air pressure, all boreholes show the development of movement towards the centre-line. This movement generally increases with depth, forming a "bulge" towards the tunnel, this being most pronounced in borehole 2, closest to the

tunnel. Generally, the movements grow less with distance from the centre-line. After the air pressure is removed, the profile for tube 4, 7.5 m from the centre-line, remains fairly steady for some time. However, between 51 and 72 days tube 2 shows a marked reversal in movement at depth. This is considered to be the result of high-pressure back-grouting at 700 kN/m^2 which was carried out in the location of the array at 71 days. This may have actually forced the alluvium away from the tunnel at depth. This type of movement is not apparent at tube 3, although the development of a "bulge" in the profile towards the tunnel at 4 m depth may be in some way connected with the same process.

A further phase of movement away from the tunnel at depth occurs between 150 and 176 days. This corresponds both with the demolition of the wall at the surface (see Section 5.7.2) and a significant increase in the height of the water table (Section 5.7.7), and may reflect the re-establishment of higher piezometric pressure around the tunnel after caulking. This is discussed further in Section 5.7.7 and by Sizer (1976).

Minor distortion of the top section of tube 2 is evident from -5 days onwards. This may have been caused during the process of taking lateral surface displacement measurements (see Appendix C).

5.7.7) Pore-pressure measurements

The effect of the tunnel passing the piezometer in borehole 2 is shown with respect to tunnel-face position in Figure 5.36. The pore pressures before the array was reached were 108.5 kN/m^2 in borehole 2 and 77.9 kN/m^2 in borehole 1, indicating a water table

about 2.3 m below the ground surface, assuming that there is no aquiclude between the piezometers and the surface. In borehole 1, air from the tunnel penetrated the grout above the soffit and leaked through the piezometer, so making accurate readings impossible until the air pressure was released. In borehole 2 the piezometric pressure increased to 120.5 kN/m^2 as the tunnel passed, equivalent to a water table 1 m below the ground surface, that is,a rise in head of 12 kN/m^2, or 1.3 m of water. This compares with an air pressure in the tunnel of 90 kN/m^2. This pressure, at the soffit of the tunnel,is sufficient to raise the water table to 2 m below the ground surface. It is suggested, therefore, that the rise in pressure measured at the piezometers must be due to the driving of the shield itself increasing the stress level in the ground and hence at least temporarily raising the pore pressure close to the tunnel.

Long term changes in piezometric head are shown in Figure 5.37. When the compressed air was released the tunnel was able to act as a drain to the surrounding alluvium. This drainage facility resulted in a lowering of the pore pressure in both piezometers until at 119 days the piezometric head was down to 3.5 m below the surface. Varying weather conditions tend to make the results somewhat erratic.

Between 119 days and 176 days a significant rise in the pore pressure takes place. This may be attributed to a reduction of the water inflow into the tunnel due to caulking of the tunnel along with a period of high rainfall. It is significant that this increase is associated with the uplift at 162 days, as noted in Sections 5.7.2 and 5.7.5.

5.8) Howdon

Measurements were taken at the Howdon site between July, 1975 and September, 1975. A complete set of all readings was taken each day during the period that the tunnel face was within 20 m of the instrumentation array. As is described in Appendix C, due to vandalism it only proved possible to monitor movements in two of the original 5 boreholes. Neither of the piezometers was operational for the same reason.

5.8.1) The tunnel advance curve

Figure 5.38 shows the tunnel advance curve for Howdon during the measurement period July 14th to September 30th. As for the previous case histories, the two curves represent the face position and the grout injection position. These curves are close together due to the fact that no shield was used in this drive. Tunnel advance is shown relative to shaft A/C (Figure 4.18). As at Hebburn and Willington Quay, the short vertical sections of the curve represent weekend stoppages. Unfortunately at Howdon, one of these stoppages occurred with the face only 1.5 m past the array. This may have had some effect on the shape of the settlement development profile (Section 5.8.2).

The average rate of advance over the entire 120 m shown in Figure 5.40 is 0.068 m per hour. The actual advance rate over the week August 4th to August 8th was 0.155 m/hr, equivalent to 3 rings per shift.

5.8.2) The settlement development profiles

Two centre-line settlement development profiles are shown in

Figure 5.39, for stations o and i. These indicate that settlement commenced about 18 m ahead of the face. By the time the face was level with the array, 4.6 mm of settlement had developed, and by the time the face was 70m past the array settlement was virtually complete. The form of the profile appears much the same as that of Hebburn (see Section 6.2). The profiles appear to steepen very slightly during the weekend stoppage 1.5 m from the boreholes, although only about $\frac{1}{2}$ mm of settlement is indicated over this period. The major properties of the settlement development profile are listed in Table 5.4.

5.8.3) The transverse settlement profile

The development of the transverse settlement profile is shown in Figure 5.40. It is clear that the trough does not have a symmetrical shape, the points of inflection being at 6.02 m on the east and 7.75 m on the west. This is thought to be due to the curvature of the tunnel centre-line at this point. Once the face is past the measurement array the trough appears to retain a constant width throughout its development. Fluctuations in the level of stations l, m, n are due to their location at some distance from the TBM and therefore being less accurately levelled.

Figure 5.41 illustrates the ultimate settlement trough along with the lateral movement profile. This settlement trough is the mean of the measurements at either side of the centre-line. A maximum of 11.2 mm of settlement is developed. The shape of this profile and its comparison with the other case histories is discussed in Chapter 6, but its main properties are listed in Table 5.4.

5.8.4) Horizontal surface movements

The profile of the ultimate horizontal surface displacement is shown in Figure 5.41 along with the surface settlement trough. As in the case of Willington Quay, maximum horizontal movement is developed at the point of inflection of the settlement trough. A maximum displacement of 5 mm is observed at this point. At about 11 m from the centre-line horizontal and vertical movements are equal, and beyond this point horizontal movement predominates.

5.8.5) Sub-surface settlement

Due to problems with vandalism at this site (see Appendix C) it only proved possible to obtain a steady set of datum values for tube 2, at 2.5 m from the centre-line. The development of settlement with depth for this tube is shown in Figure 5.42. This diagram shows the ultimate settlement which was developed. It can be seen that settlement does not increase uniformly with depth. The unexpectedly high settlement at ring 1 (4.8 m deep) may possibly be caused by disturbance of the upper section of the tube due to the several modifications and repairs which became necessary during the course of the measurement programme. The lower sections of the tube show settlement increasing with depth, reaching 19 mm at a depth of 11.6 m.

5.8.6) Horizontal sub-surface movements

Inclinometer profiles parallel to, and perpendicular to, the centre-line are shown in Figures 5.43 and 5.44. As at Willington Quay, the movement was measured relative to the tops of the tubes and the movement of the tops measured independently and superimposed on the

final profiles. As previously discussed, it only proved possible to monitor movements in two boreholes. Many of the sets of readings obtained from these proved to be highly erratic, probably because of instability of the upper sections of the inclinometer tubes, which had been replaced prior to the measurement programme. The more unreliable of these sets of readings have been discarded.

Figures 5.43 shows movement at the centre-line parallel to the tunnel line of advance. Once the shield has passed the array the boreholes can be seen to be distorted at their bases in the direction of tunnel advance, due most probably to the "dragging" effect of the shield. Above this the tubes appear to remain more-or-less vertical.

Movements perpendicular to the tunnel line of advance are shown for borehole 2, at a distance of 2 m from the centre-line. The final shape of the inclinometer profile, with the tunnel face 38 m beyond the array, would appear to indicate movement towards the centre-line at the surface of 3.4 mm, increasing to a maximum of 11.3 mm at a depth of 10 m, 2.3 m above soffit level. This is reasonably consistent with the observations from the other sites, although there is no indication of the "bulge" inwards towards the tunnel which was clearly observed at Hebburn (Figures 5.11 to 5.13).

Maximum settlement (avg)	=	7.9 mm
Maximum rate of settlement (avg)	=	0.65 mm/m advance
	=	0.13 mm/hr
Onset of settlement at 9 m ahead of face		
Completion of settlement at 17.5 m behind face		
Settlement above face	=	40% of total
Settlement trough width	=	22 m
Maximum gradient of trough	=	1.2 mm/m
Maximum gradient occurs at 2 m from centre-line.		

Table 5.1

Settlement parameters - Hebburn

	Pre-Settlement			Post-Settlement		
	Mean Measured Length (m)	Correction Factor	Corrected Length (m)	Mean Measured Length (m)	Correction Factor	Corrected Length (m)
1 - A	11.961	-0.003	11.961	11.961	-0.0005	11.961
1 - B	15.073	-0.0006	15.072	15.069	-0.0007	15.068
1 - C	18.114	-0.0006	18.113	18.111	-0.0009	18.110
1 - D	21.130	-0.001	21.129	21.126	-0.0014	21.125
D - 2	18.144	-0.0006	18.143	18.142	-0.0008	18.141
D - 3	16.666	-0.0006	16.665	16.666	-0.0007	16.665
D - 4	15.210	-0.0006	15.209	15.211	-0.0007	15.210
D - 5	12.203	-0.0003	12.203	12.204	-0.0005	12.203
3 - 10	9.670	-0.0003	9.670	9.671	-0.0004	9.671
12 - 10	19.321	-0.0007	19.320	19.323	-0.0009	19.322
12 - 9	23.004	-0.0008	23.003	23.006	-0.0011	23.005
12 - 6	25.921	-0.0009	25.920	25.923	-0.0012	25.922
6 - 11	15.940	-0.0007	15.940	15.941	-0.0009	15.940

Coefficient of expansion of tape = $12 \times 10^{-6}/^{\circ}C$

Calibration temperature = $20^{\circ}C$

Table 5.2

Horizontal surface movements - Hebburn

Maximum settlement	=	81 mm
Maximum rate of settlement	=	1.2 mm/m advance
	=	0.09 mm/hr
Onset of settlement at 36 m ahead of face		
Completion of settlement at approximately 450 days after start.		
Settlement above face	=	8% of total
Settlement trough width	=	50 m
Maximum gradient of trough	=	4.1 mm/m
Maximum gradient occurs at 9 m from centre-line.		
Maximum lateral displacement	=	12 mm
Maximum lateral displacement occurs at 7.5 m from centre-line.		

All values for ultimate, post-consolidation settlement trough.

Table 5.3

Settlement parameters - Willington Quay

Maximum settlement	=	11 mm
Maximum rate of settlement	=	0.49 mm/m advance
	=	0.03 mm/hr
Onset of settlement at 20 m ahead of face		
Completion of settlement at 80 m behind face		
Settlement above face	=	41% of total
Settlement trough width	=	40 m
Maximum gradient of trough	=	1.2 mm/m
Maximum gradient occurs at 6 m from centre-line.		
Maximum lateral displacement	=	5 mm
Maximum lateral displacement occurs at 7 m from centre-line.		

Table 5.4

Settlement parameters - Howdon

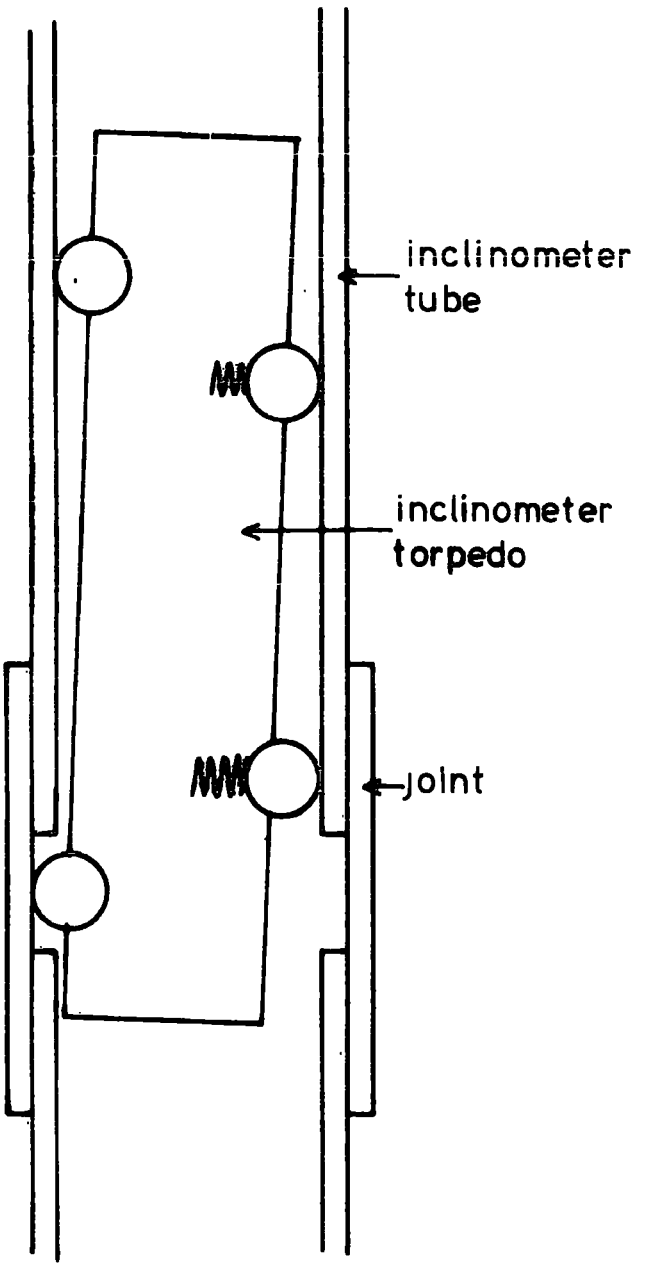

Figure 5.1
Erroneous inclinometer
reading

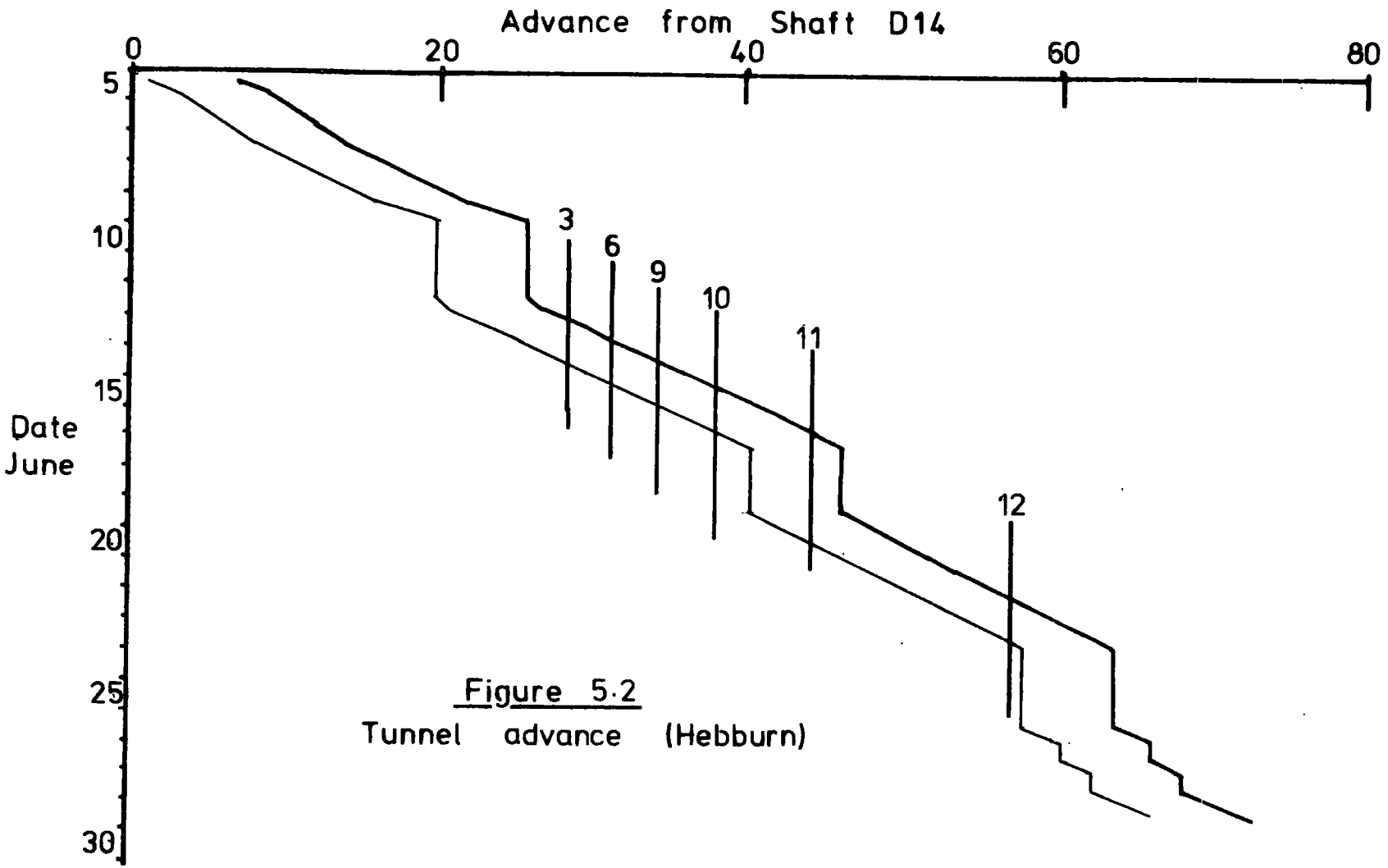

Figure 5·2
Tunnel advance (Hebburn)

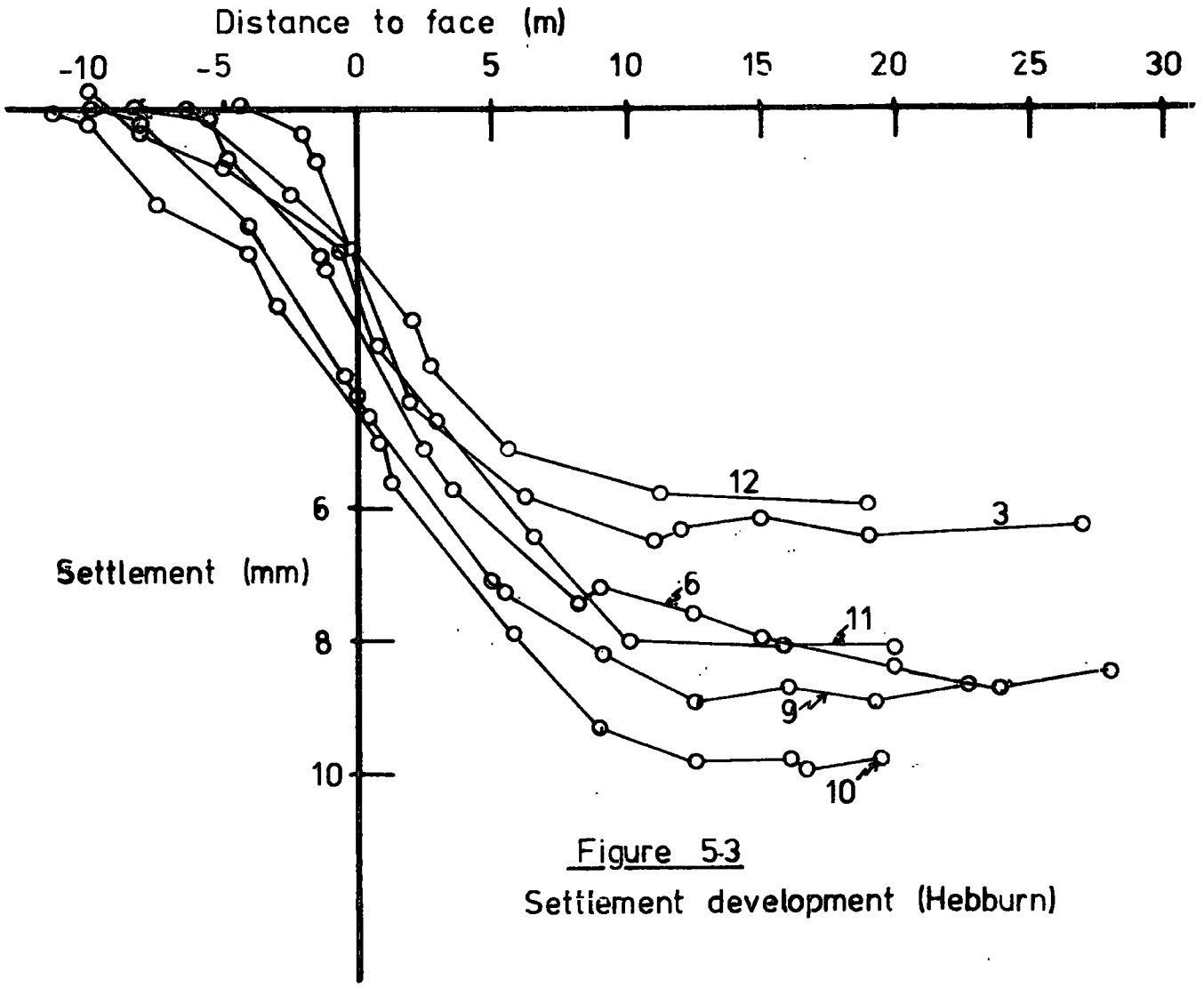

Figure 5-3

Settlement development (Hebburn)

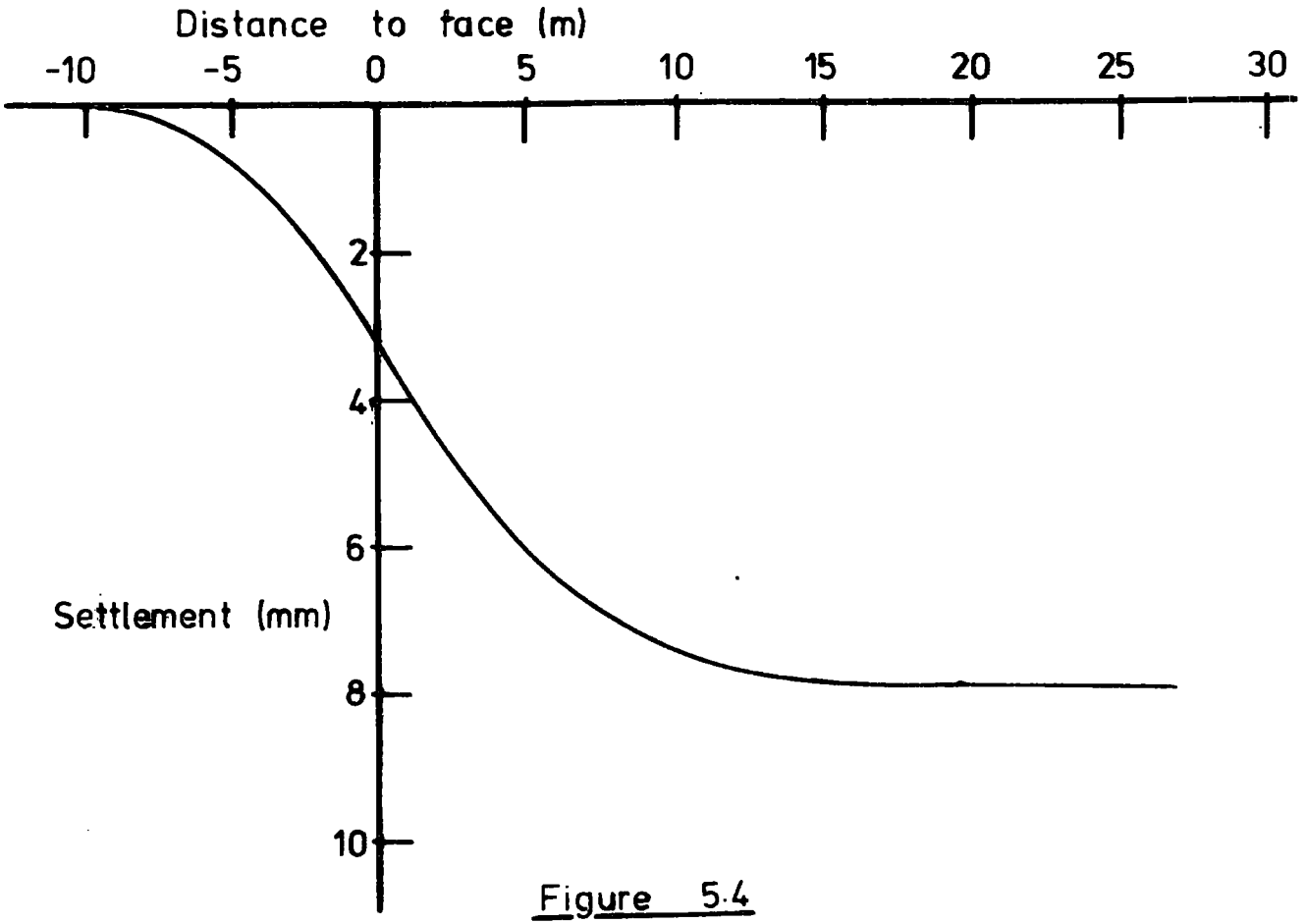

Figure 5.4

Average settlement development (Hebburn)

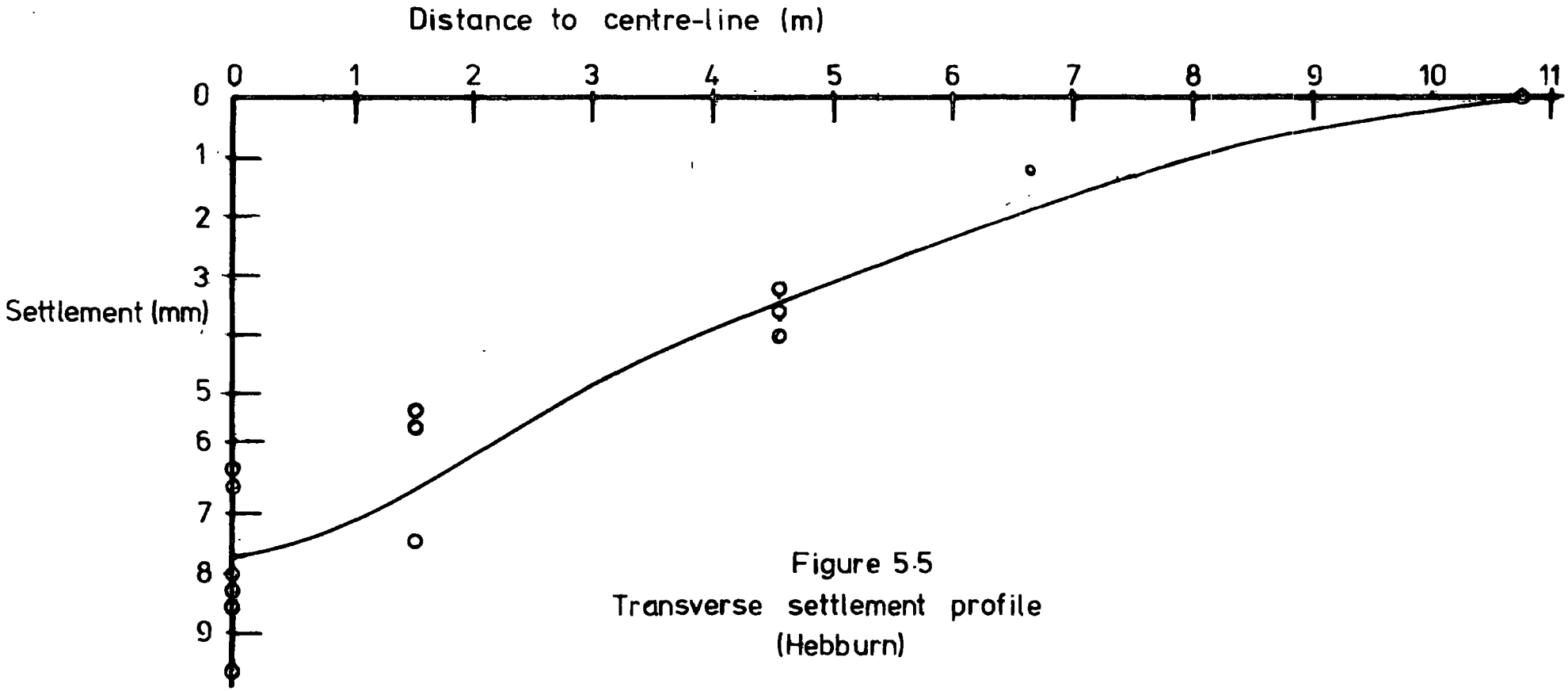

Figure 5.5
Transverse settlement profile
(Hebburn)

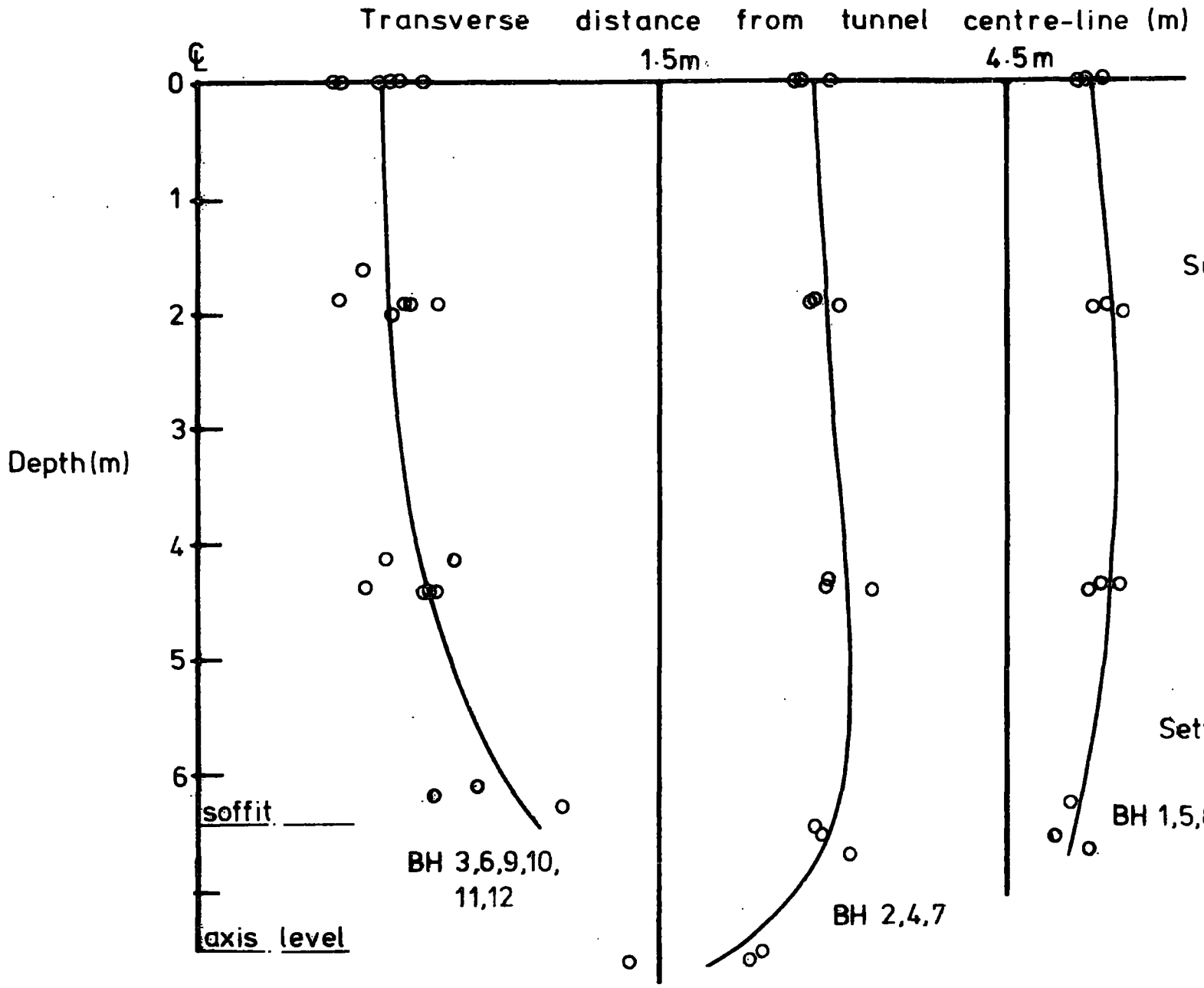

Figure 5·6

Sub-surface settlement
(Hebburn)

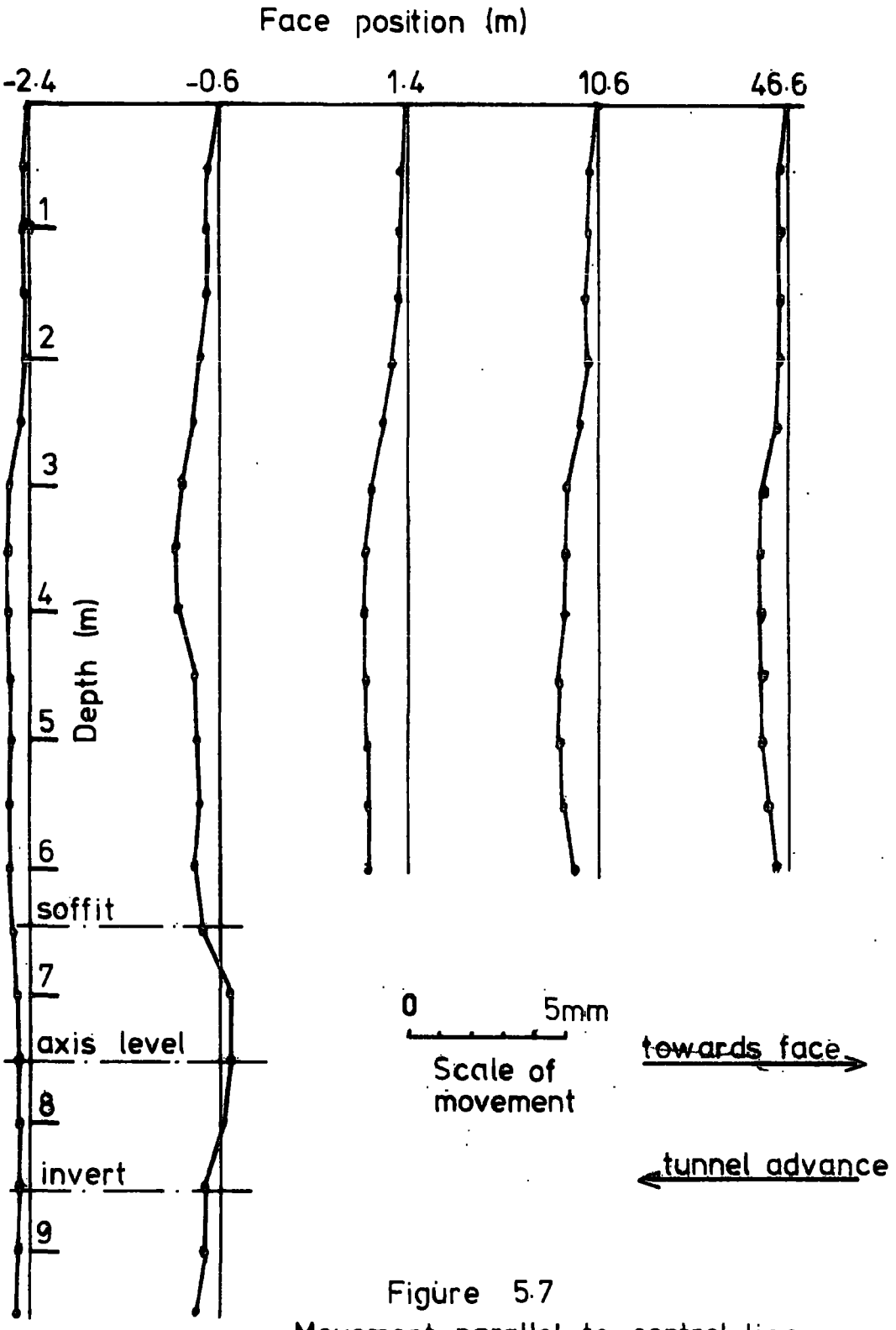

Figure 5.7
Movement parallel to centrel line
B.H. 3 (Hebburn)

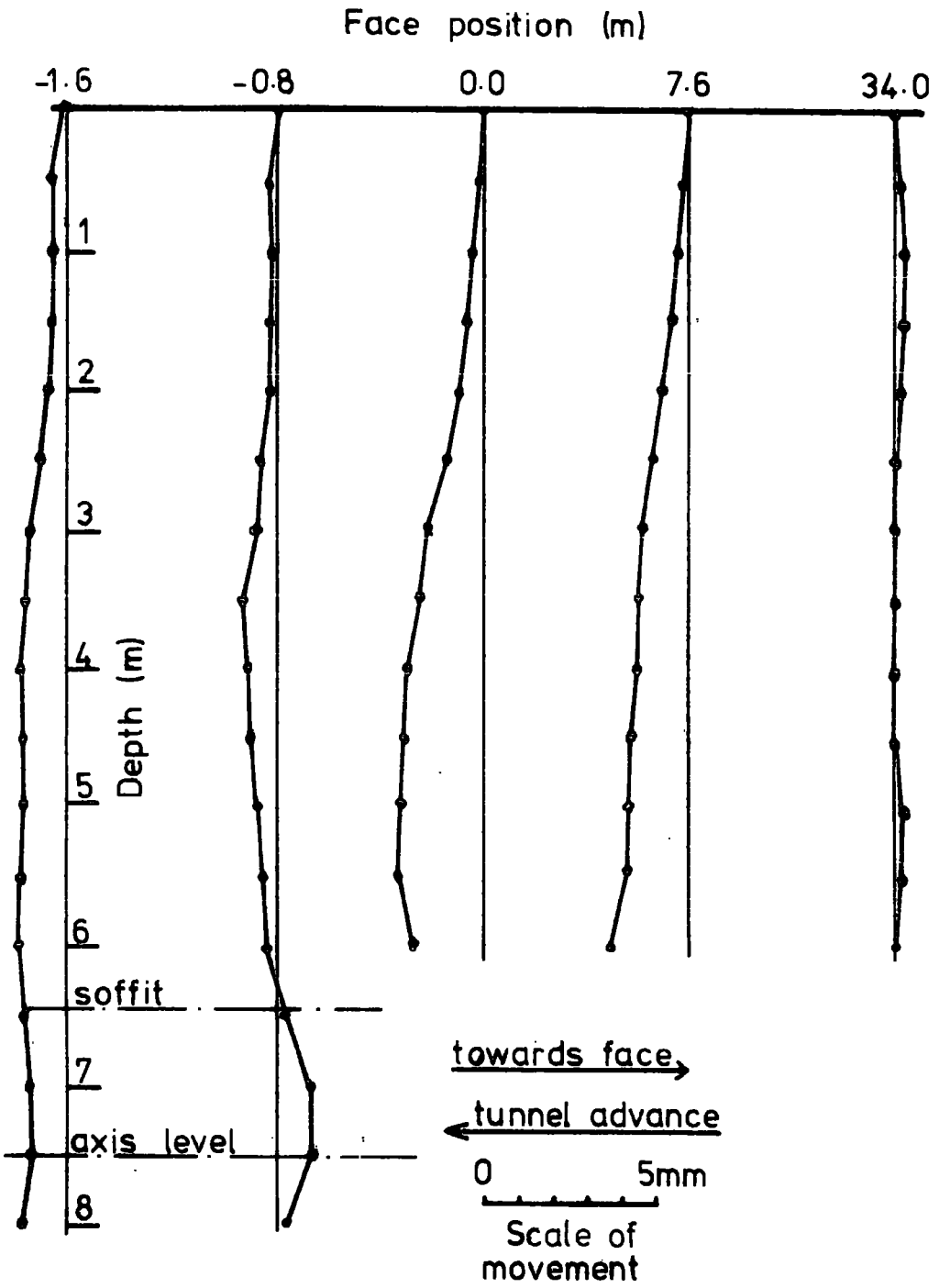

Figure 5.8
Movement parallel to centre-line
B.H. 6 (Hebburn)

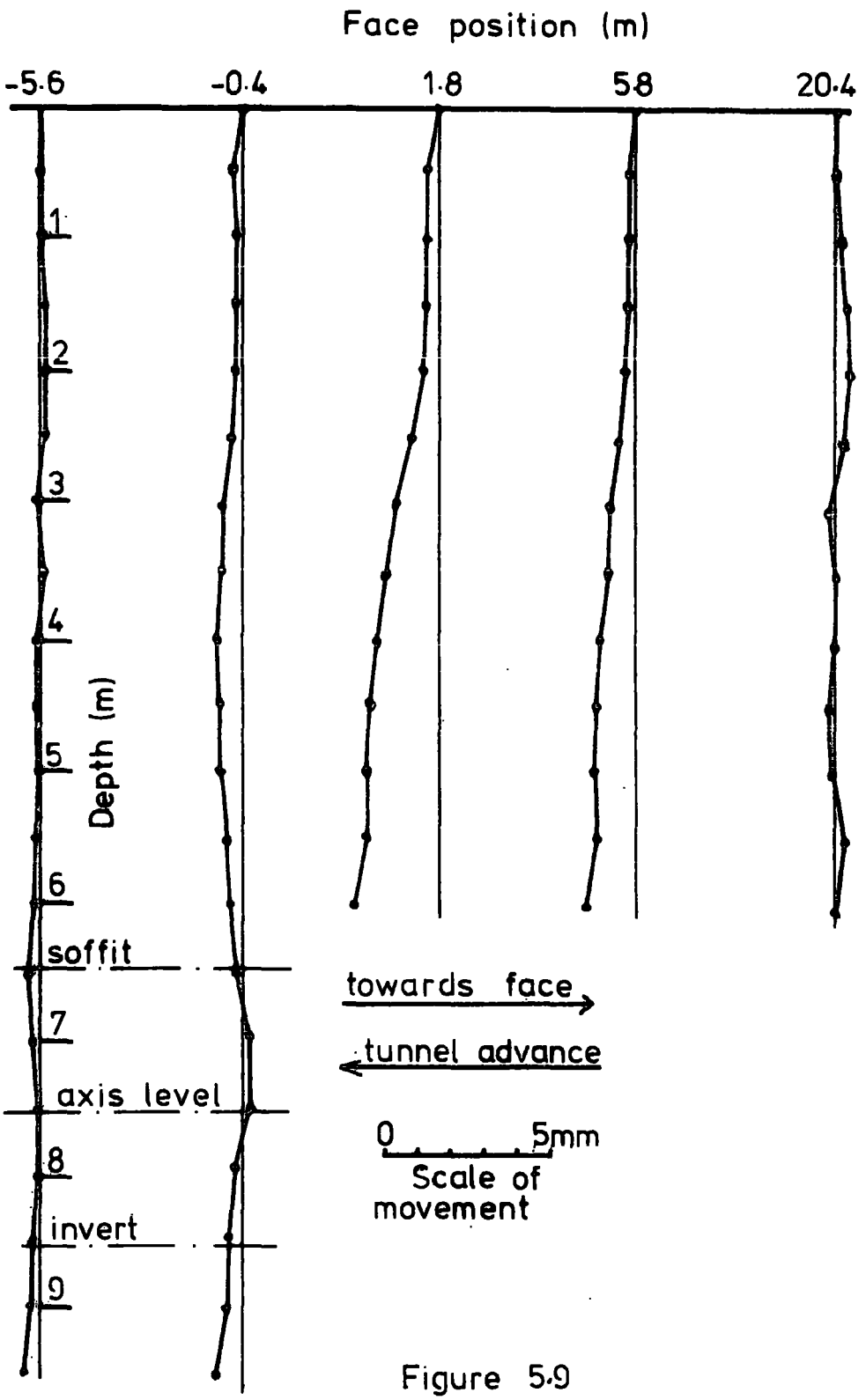

Figure 5·9

Movement parallel to centre-line BH 9 (Hebburn)

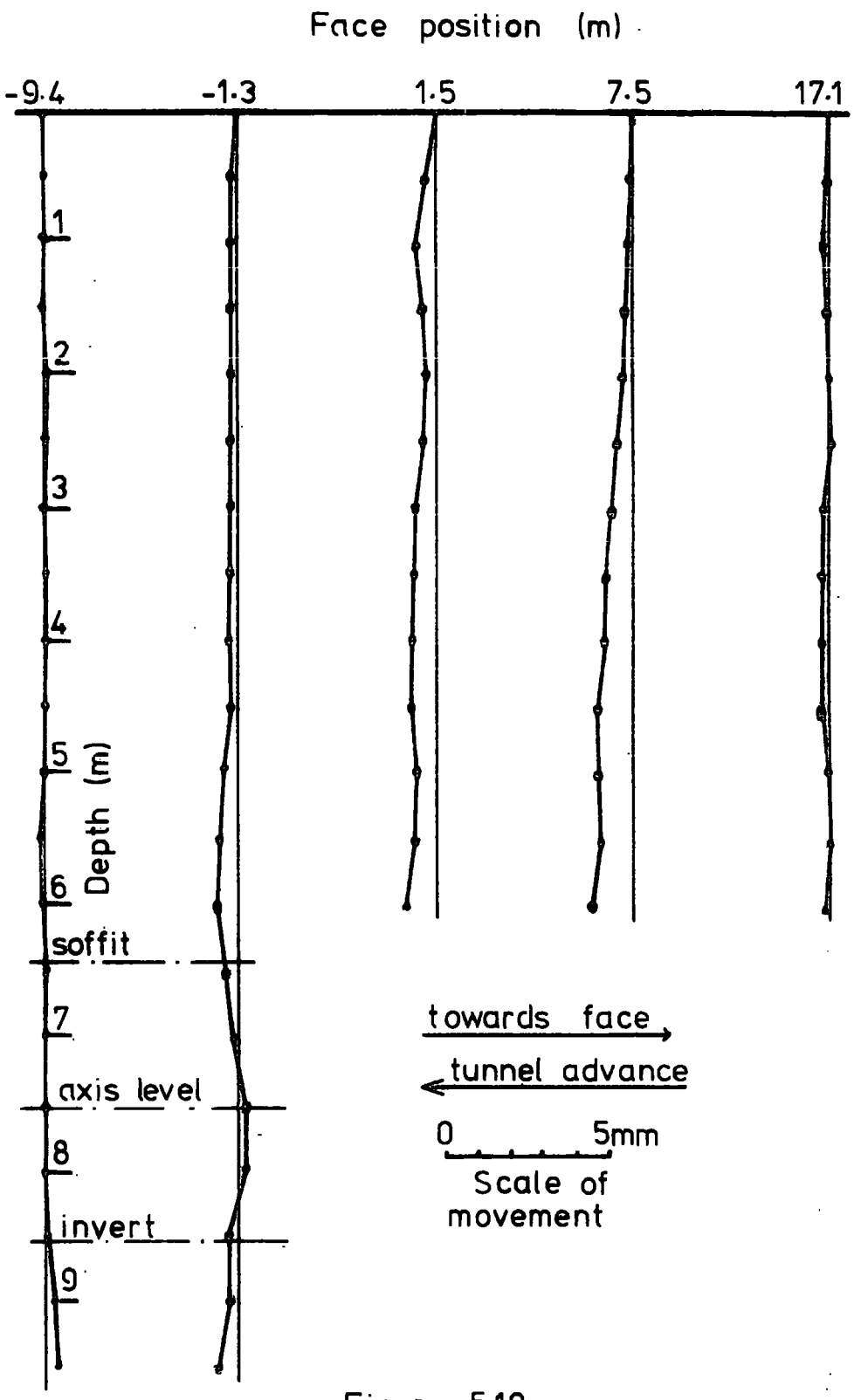

Figure 5.10

Movement parallel to centre-line
B H 12 (Hebburn)

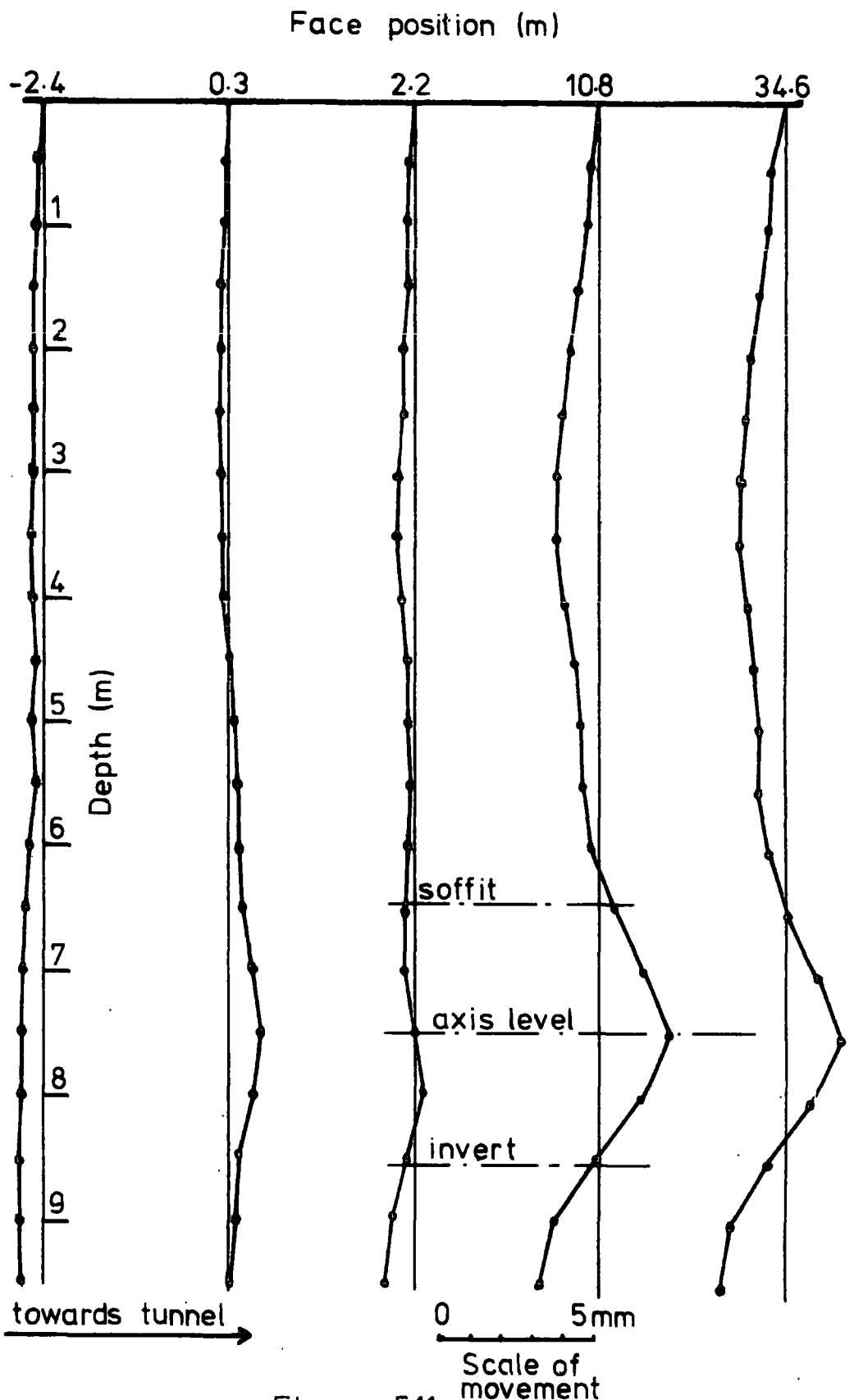

Figure 5.11
Movement perpendicular to centre-line
BH 2 (Hebburn)
1·5m from tunnel centre-line

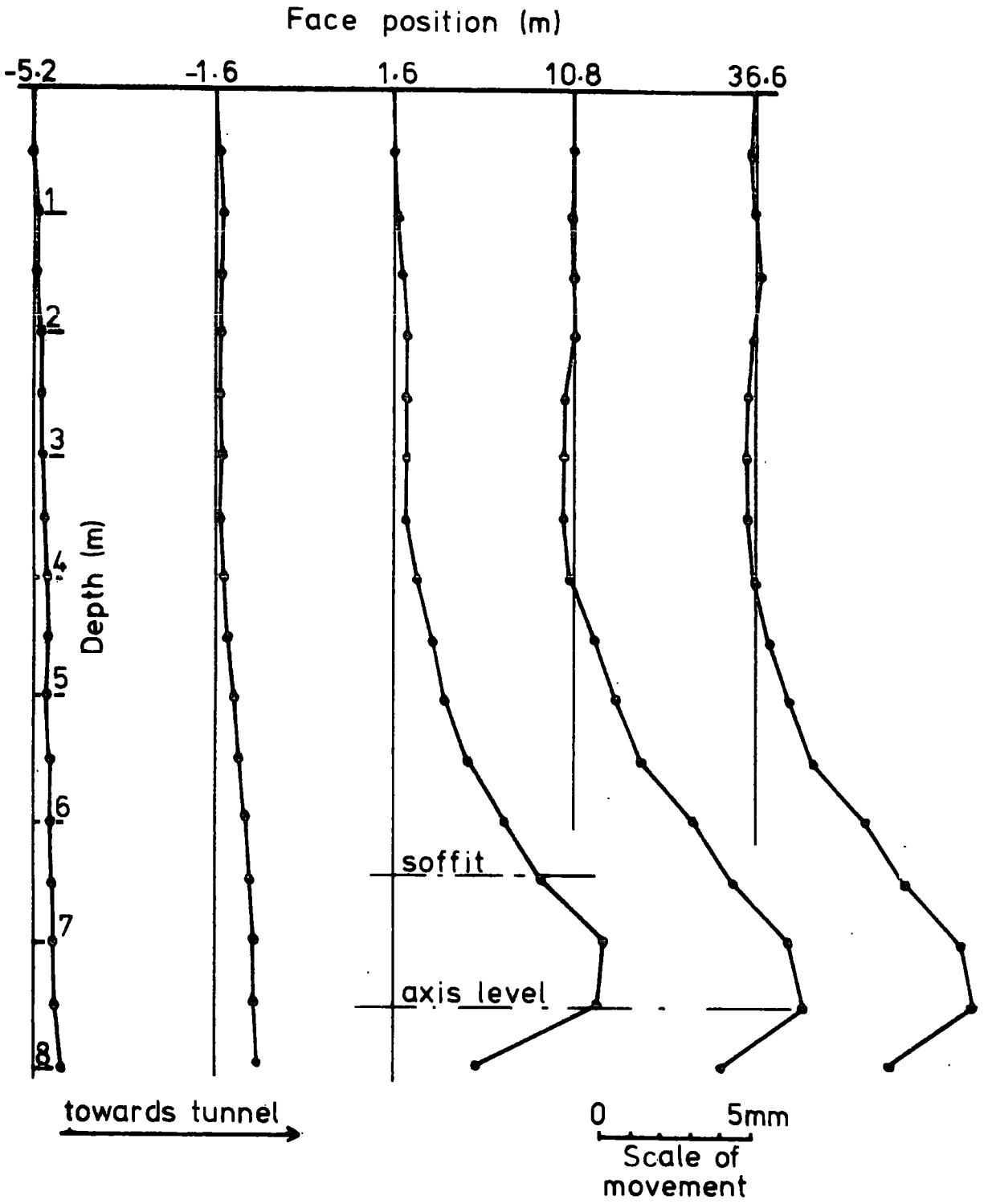

Figure 5.12

Movement perpendicular to centre-line

B H 4 (Hebburn)

1.5 m from tunnel centre-line

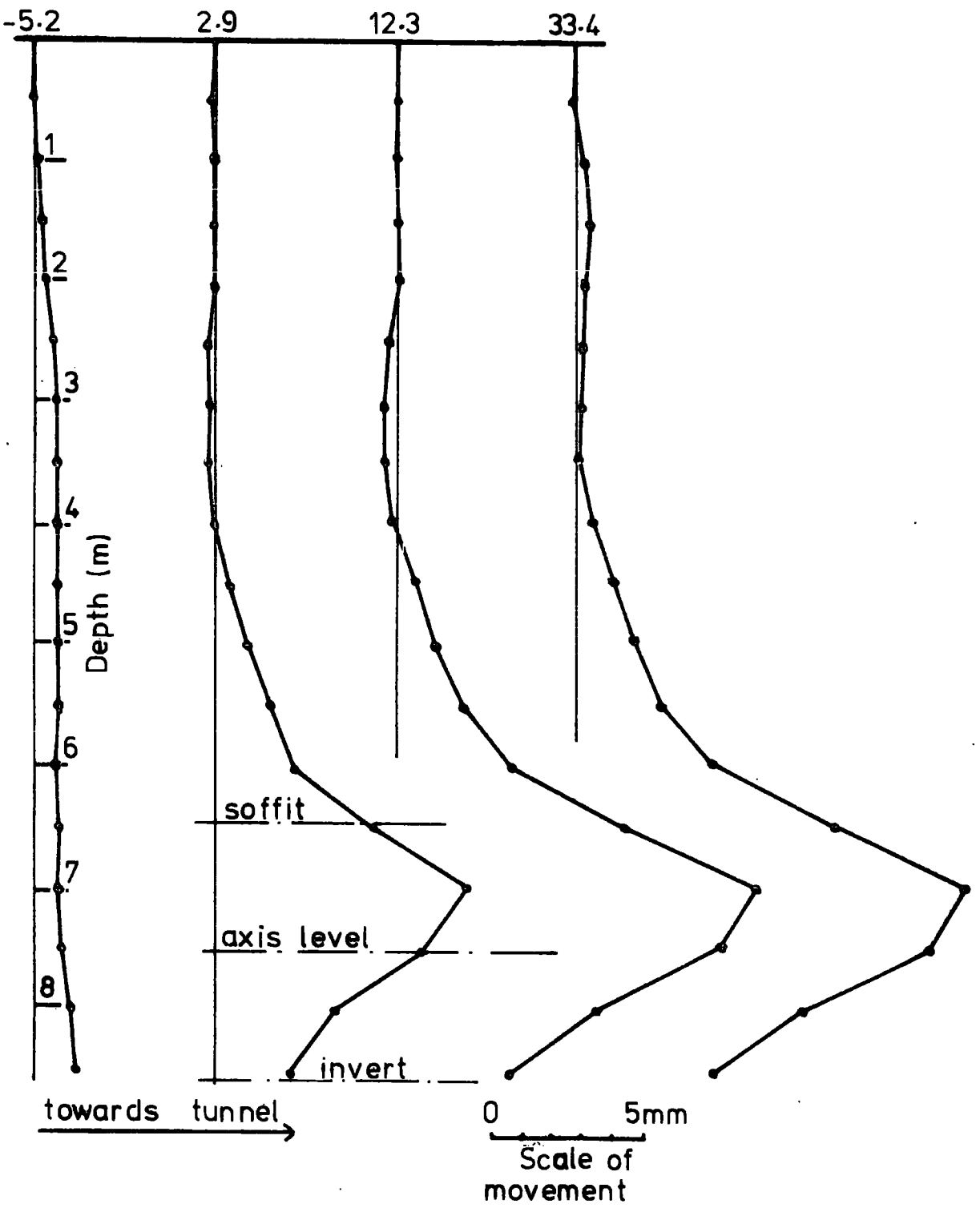

Figure 5·13

Movement perpendicular to centre-line

BH 7 (Hebburn)

1·5m from tunnel centre-line

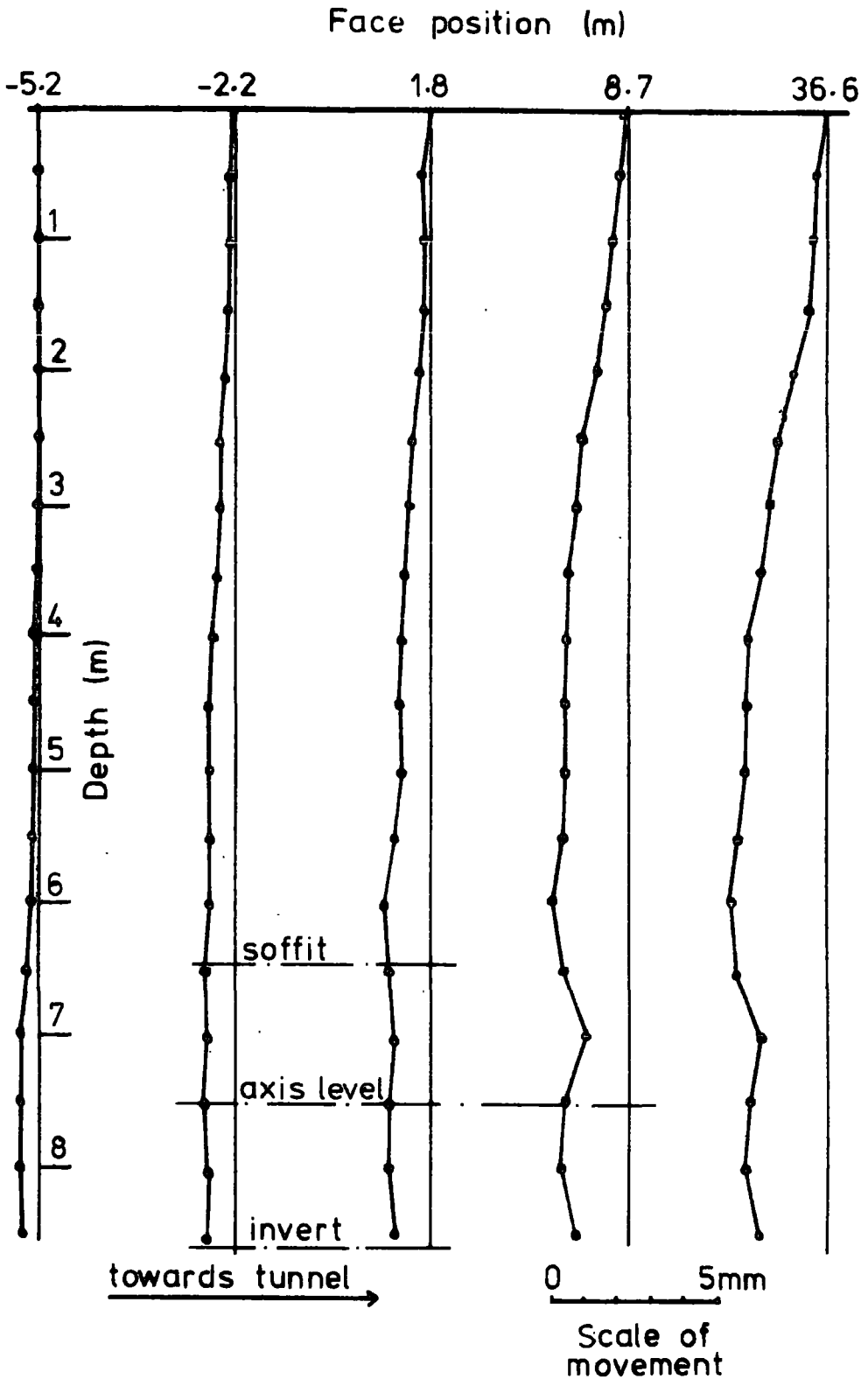

Figure 5.14

Movement perpendicular to centre-line

BH 1 (Hebburn)

4.5m from tunnel centre-line

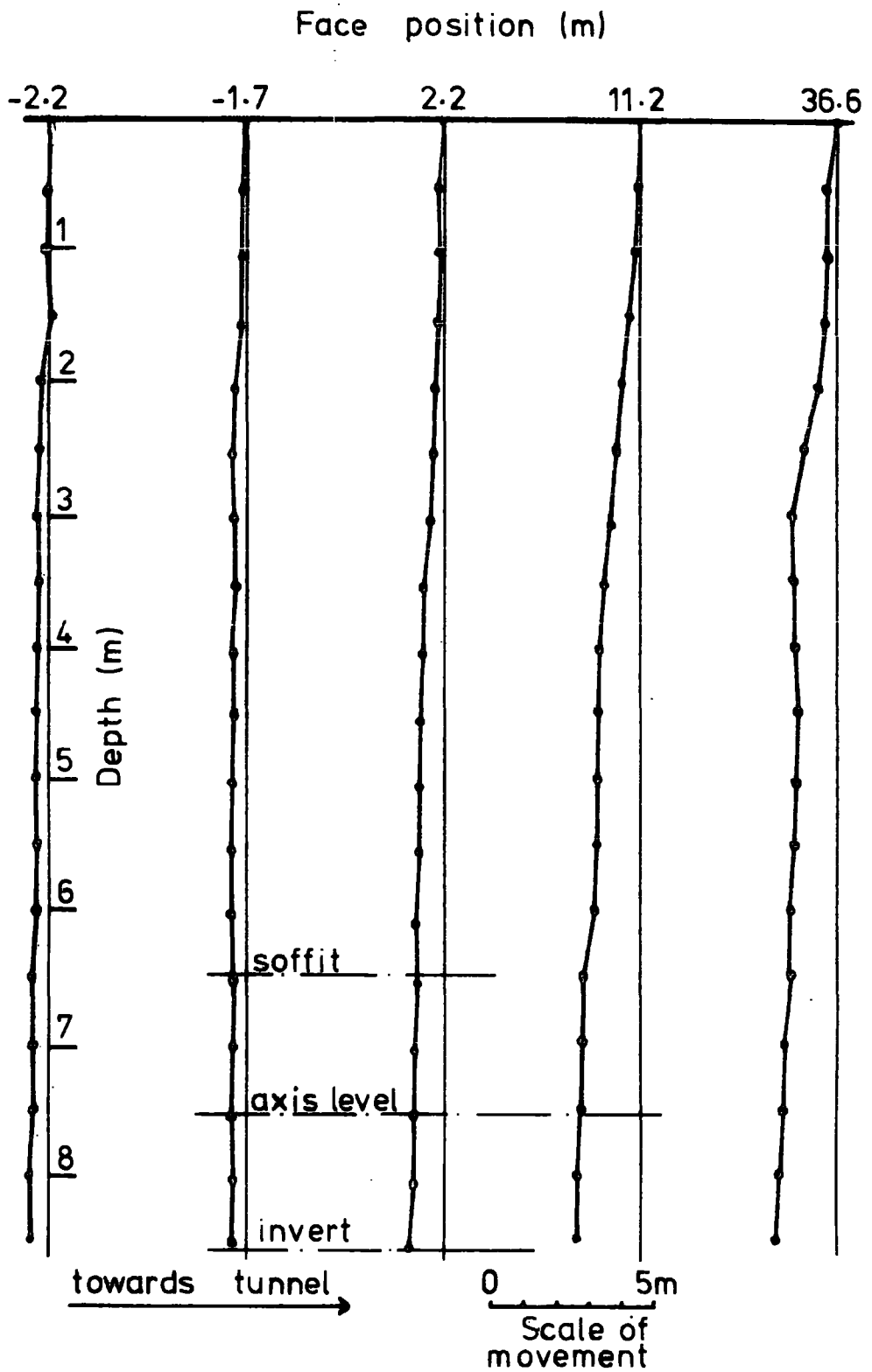

Figure 5·15

Movement perpendicular to centre-line

BH 5 (Hebburn)

4·5 m from tunnel centre-line

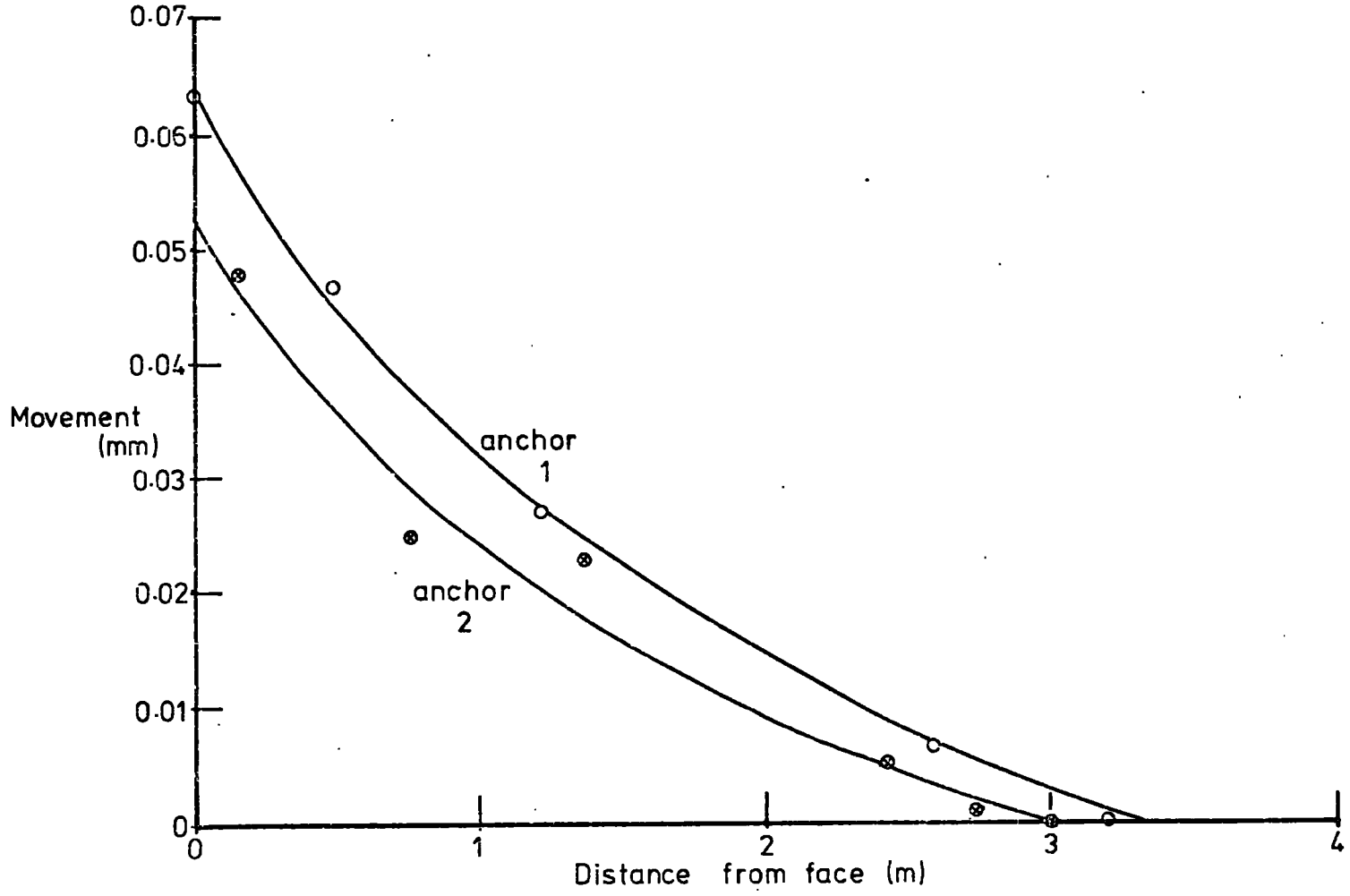

Figure 5.16

Ground anchor movements
Hebburn

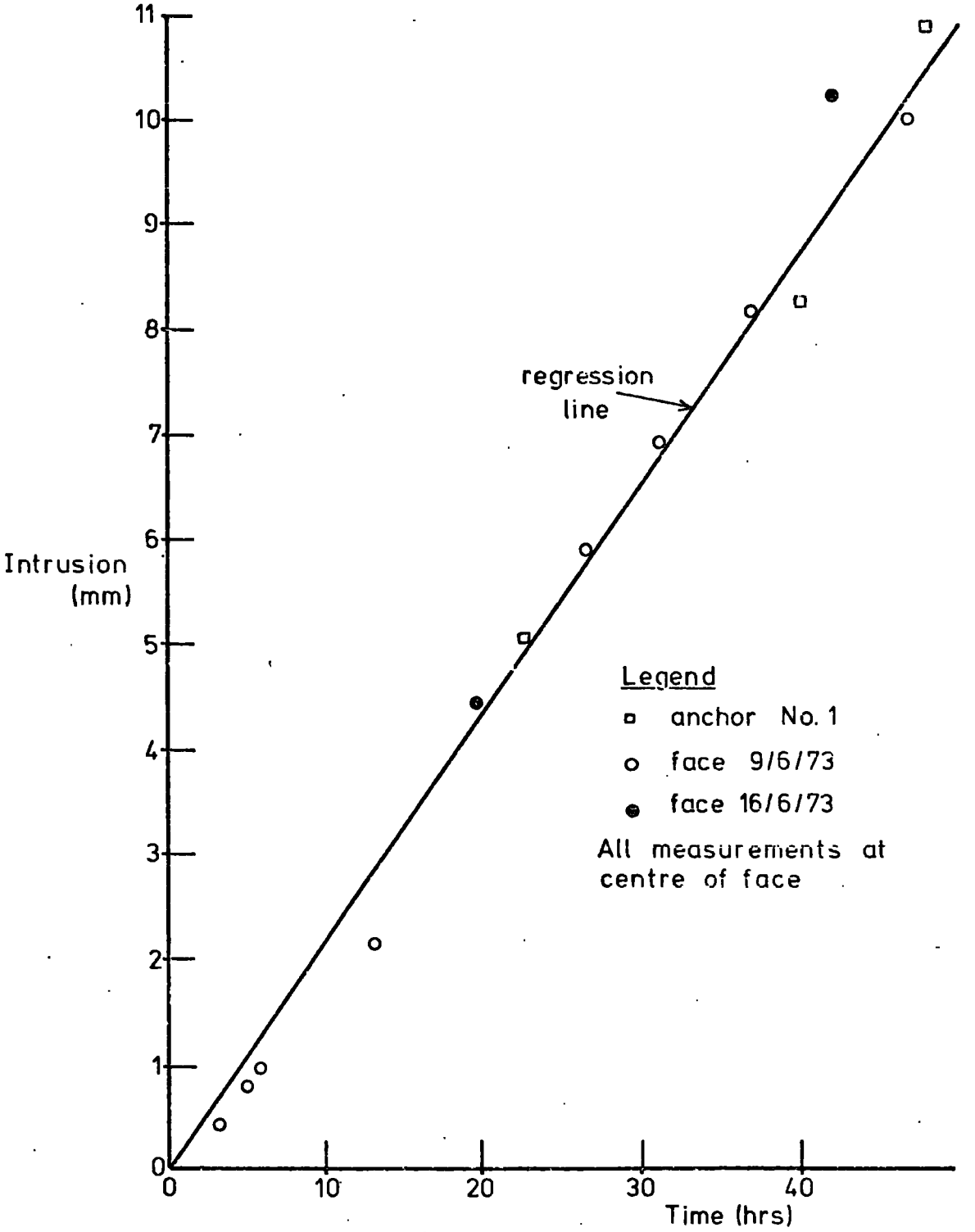

Figure 5.17
Face intrusion (laminated clay) Hebburn

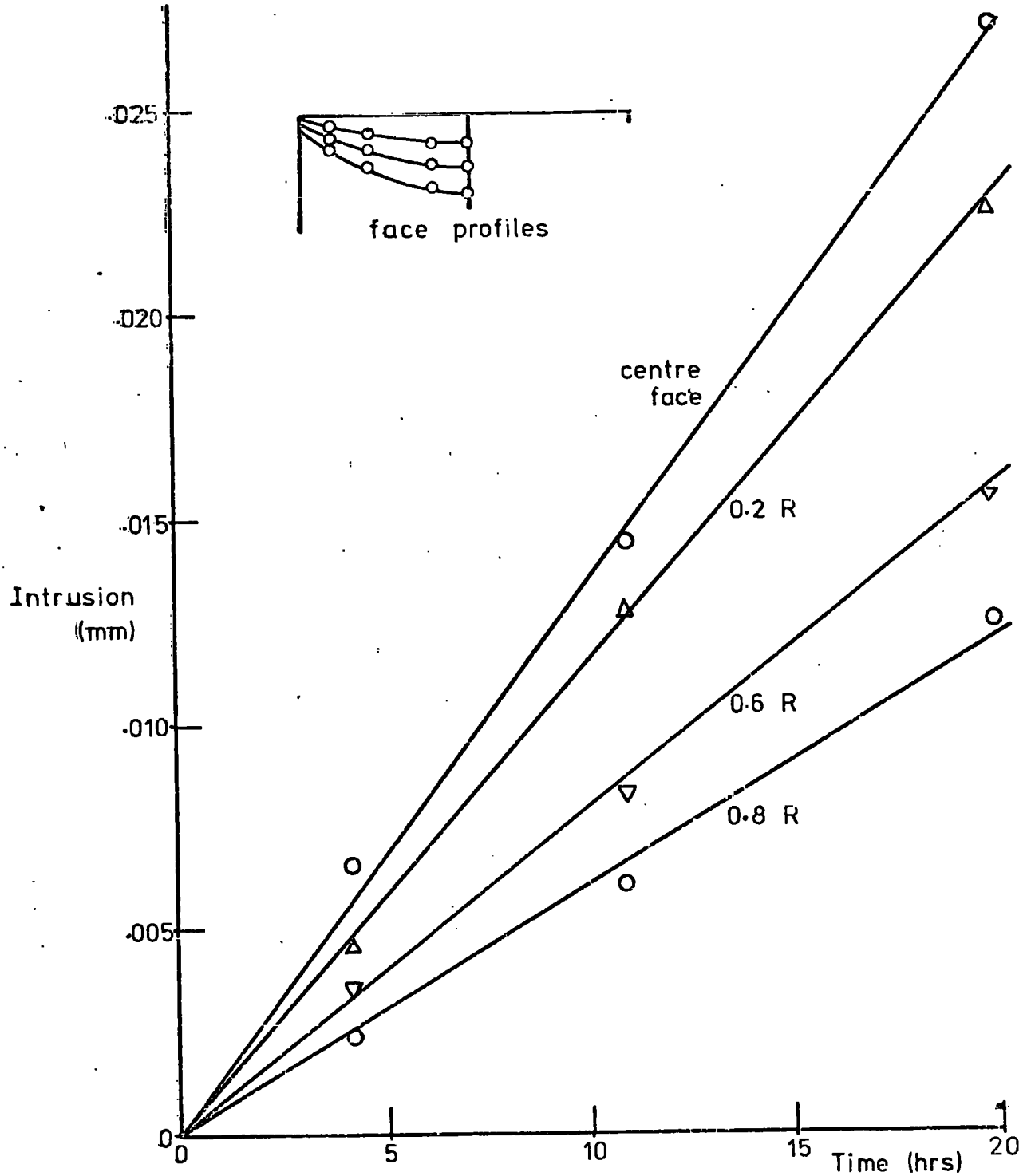

Figure 5·18

Face intrusion (stony clay)
Hebburn

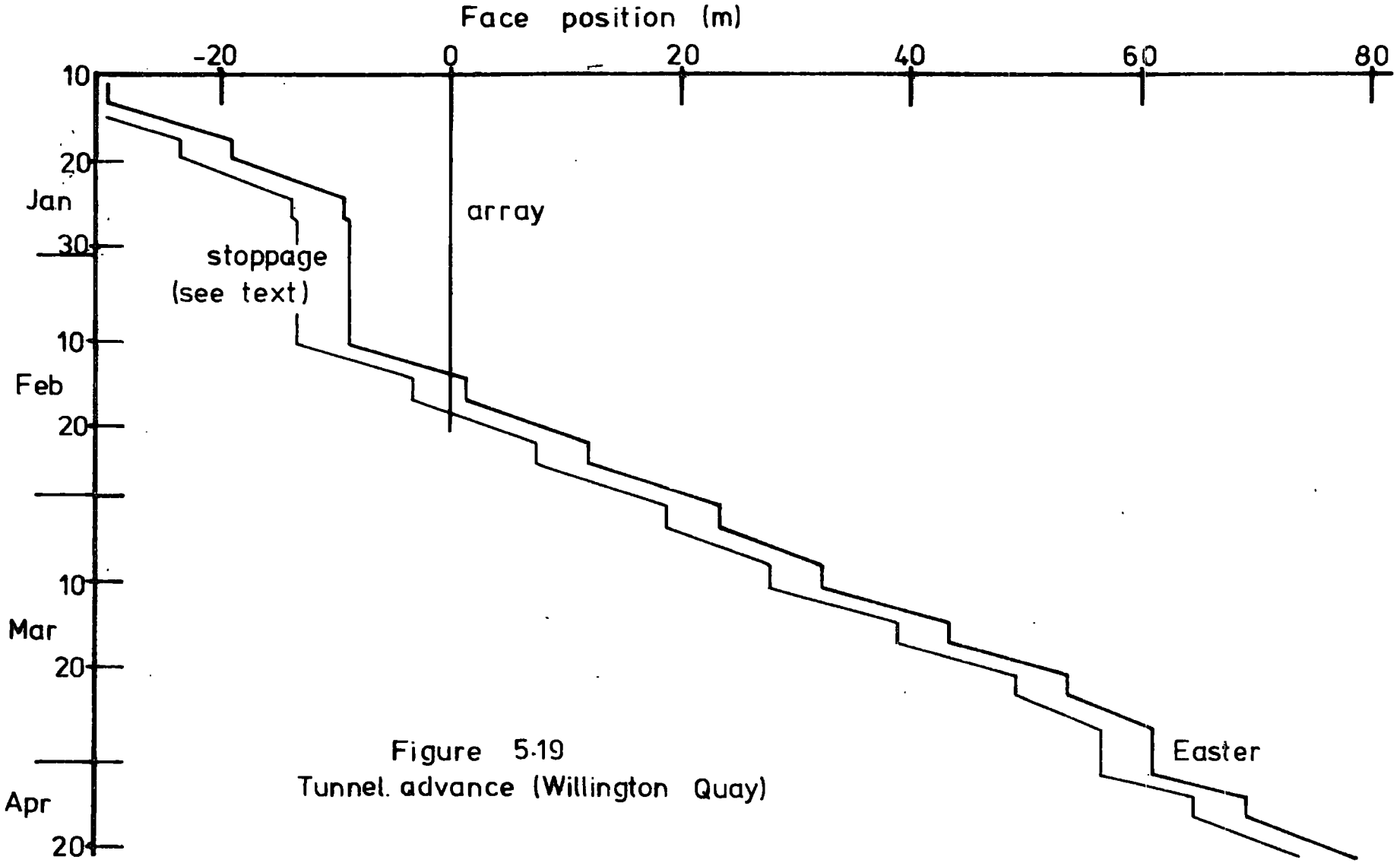

Figure 5.19
Tunnel advance (Willington Quay)

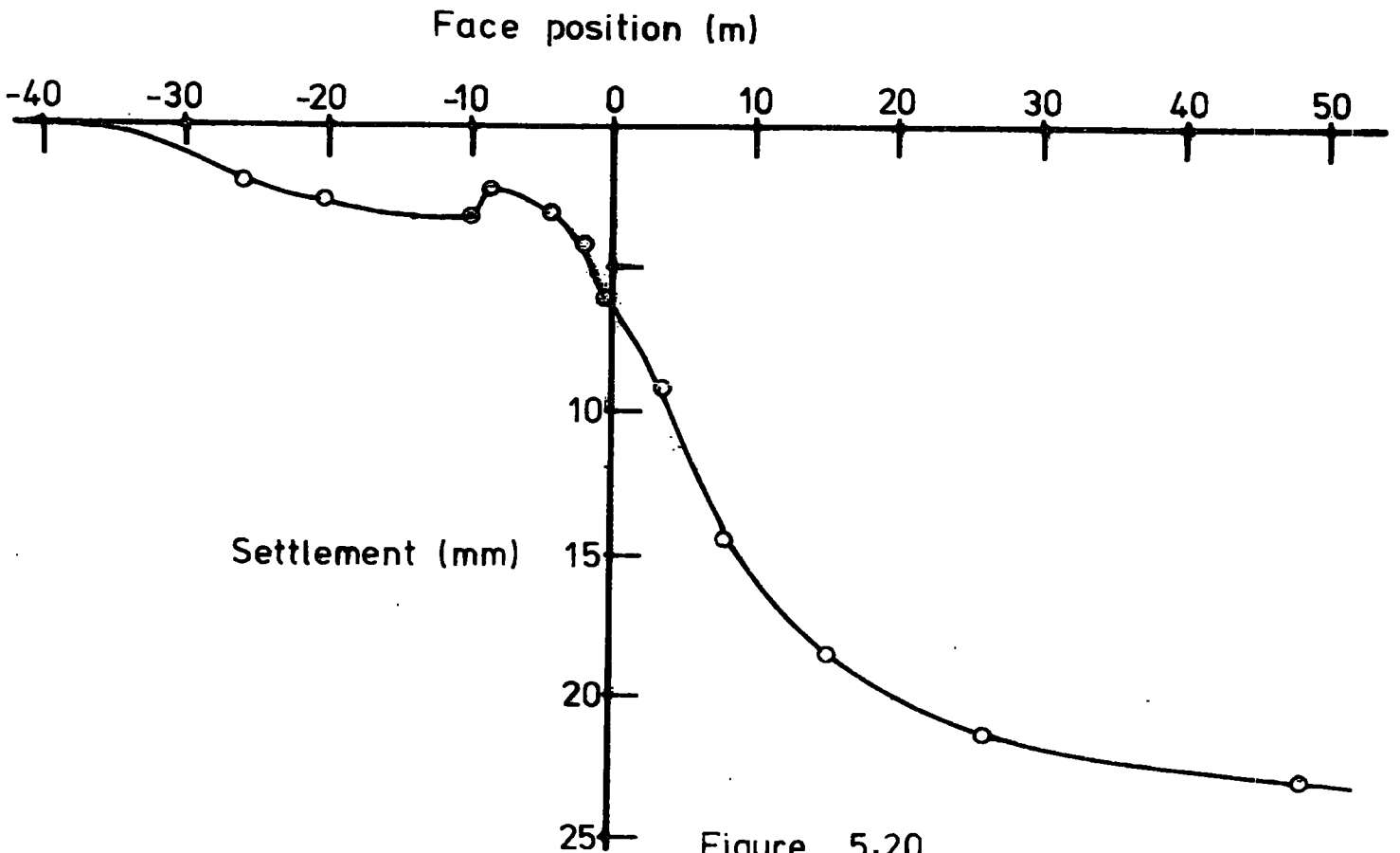

Figure 5.20

Short-term settlement development
(Willington Quay)

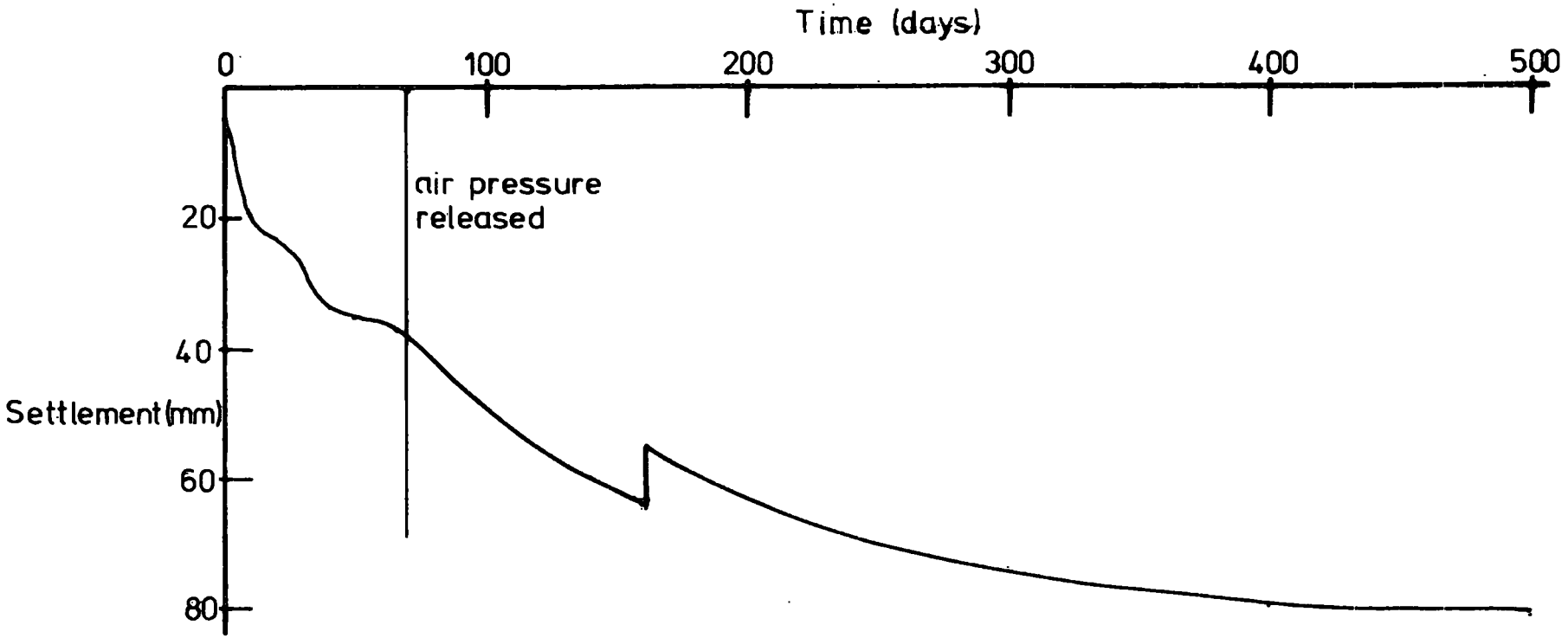

Figure 5.21

Long-term settlement development
(Willington Quay)

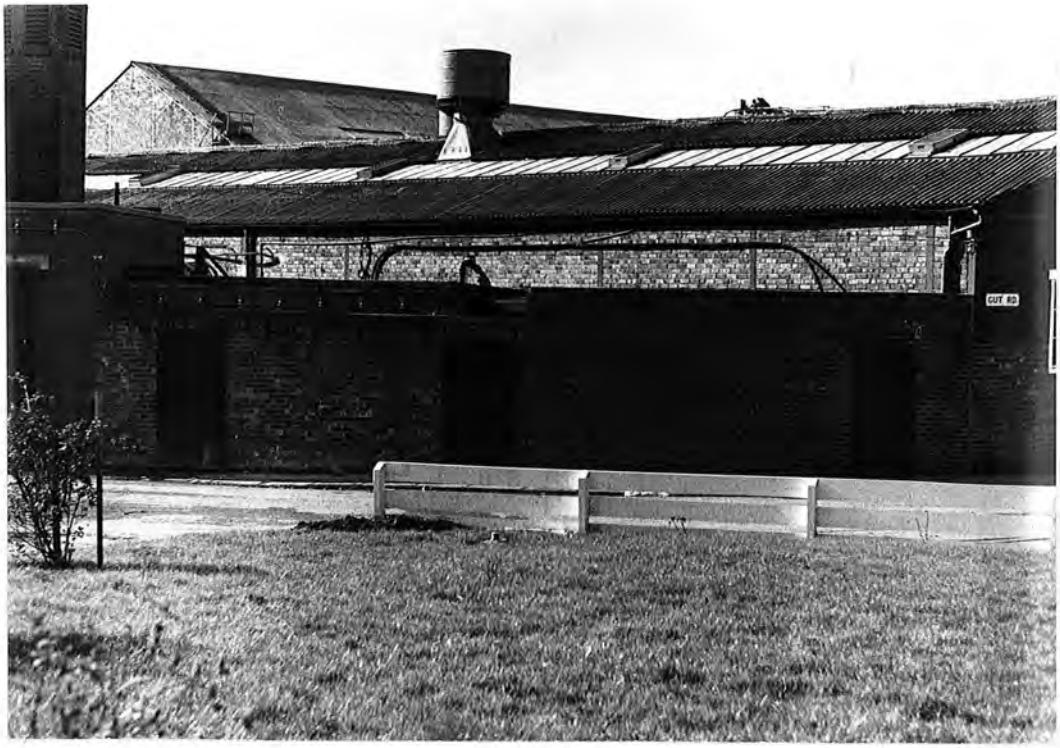

Plate 5.1

Damage to wall at Willington Quay

Plate 5.2

Damage to wall at Willington Quay

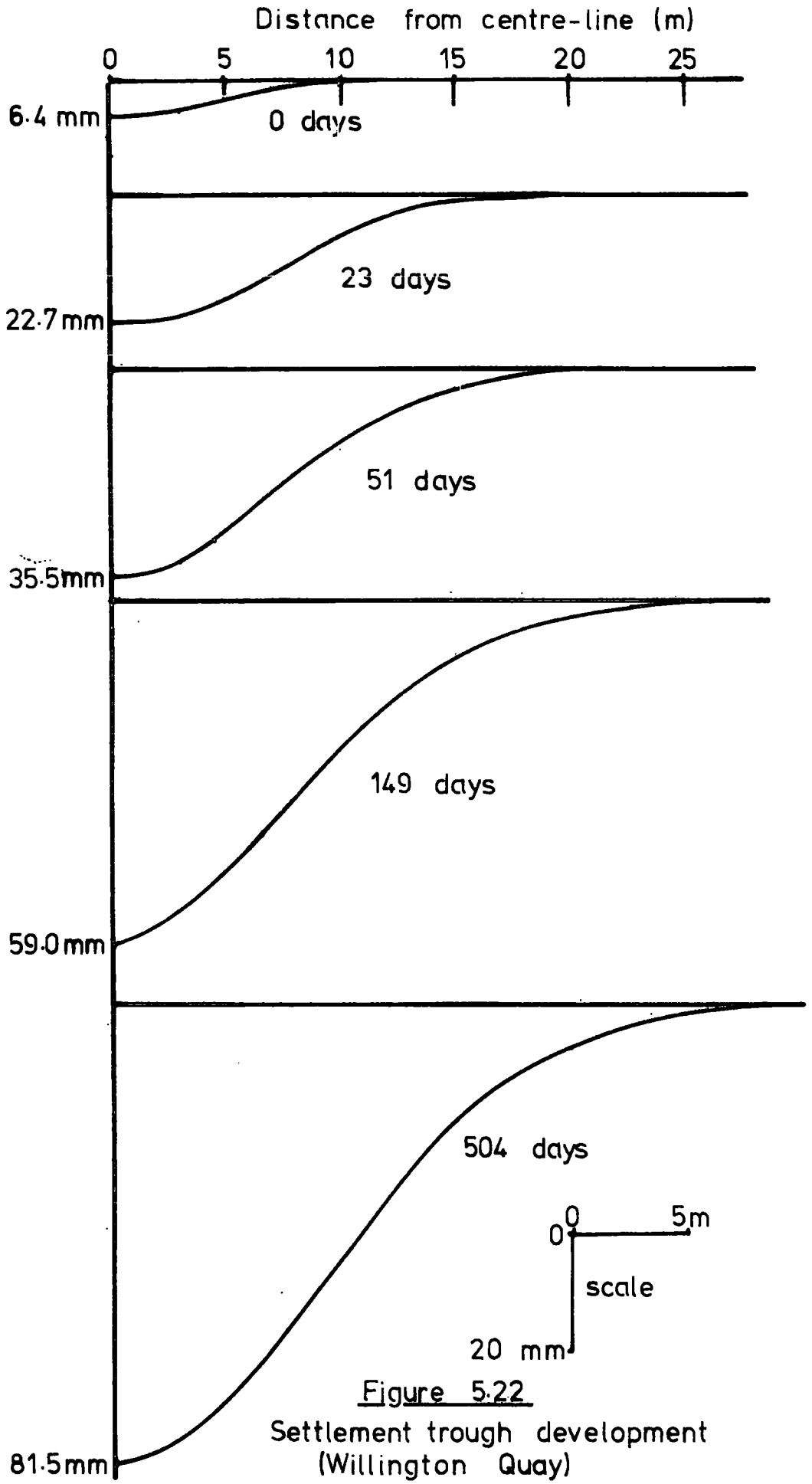

Figure 5.22

Settlement trough development (Willington Quay)

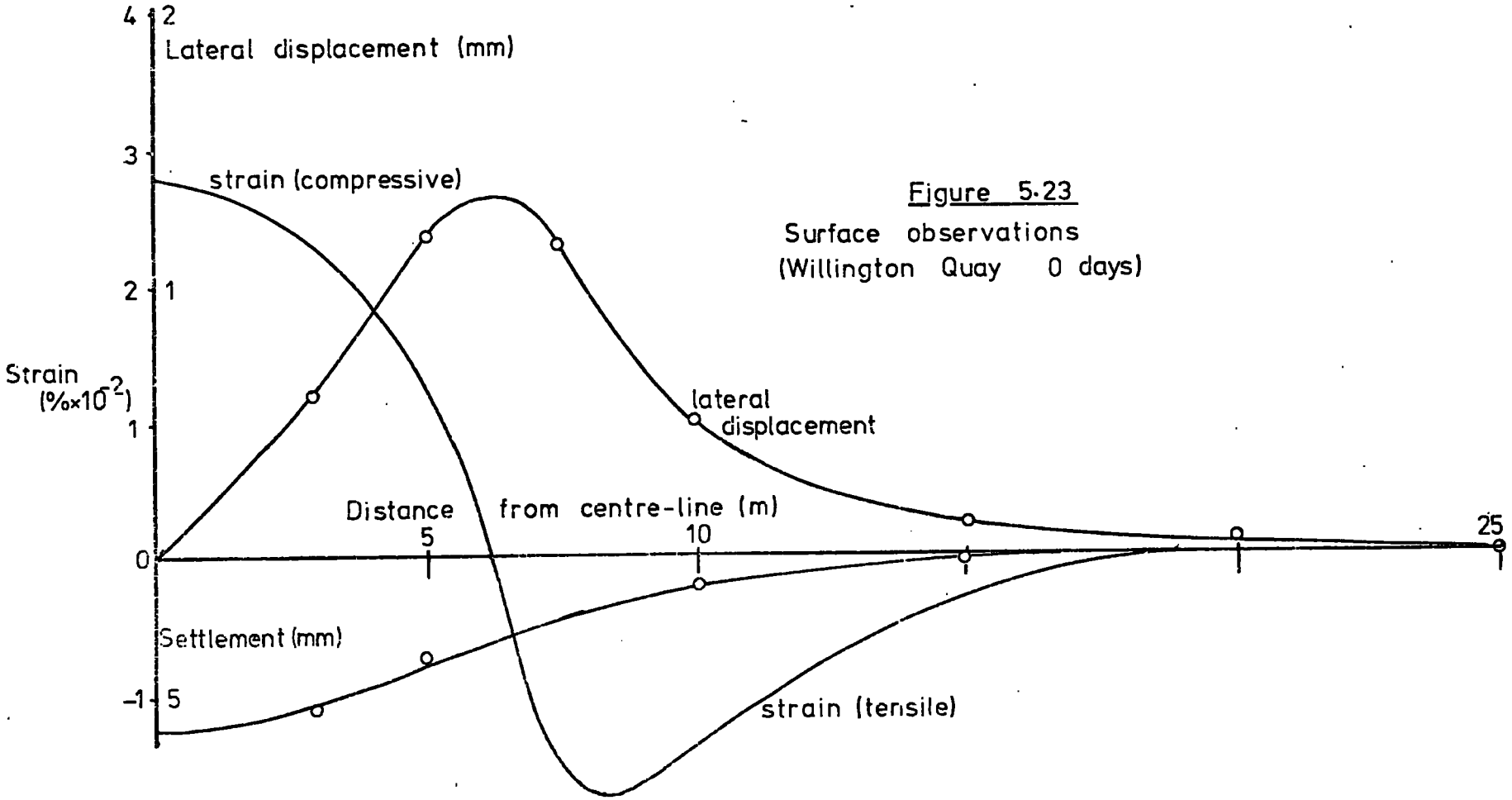

Figure 5.23

Surface observations
(Willington Quay 0 days)

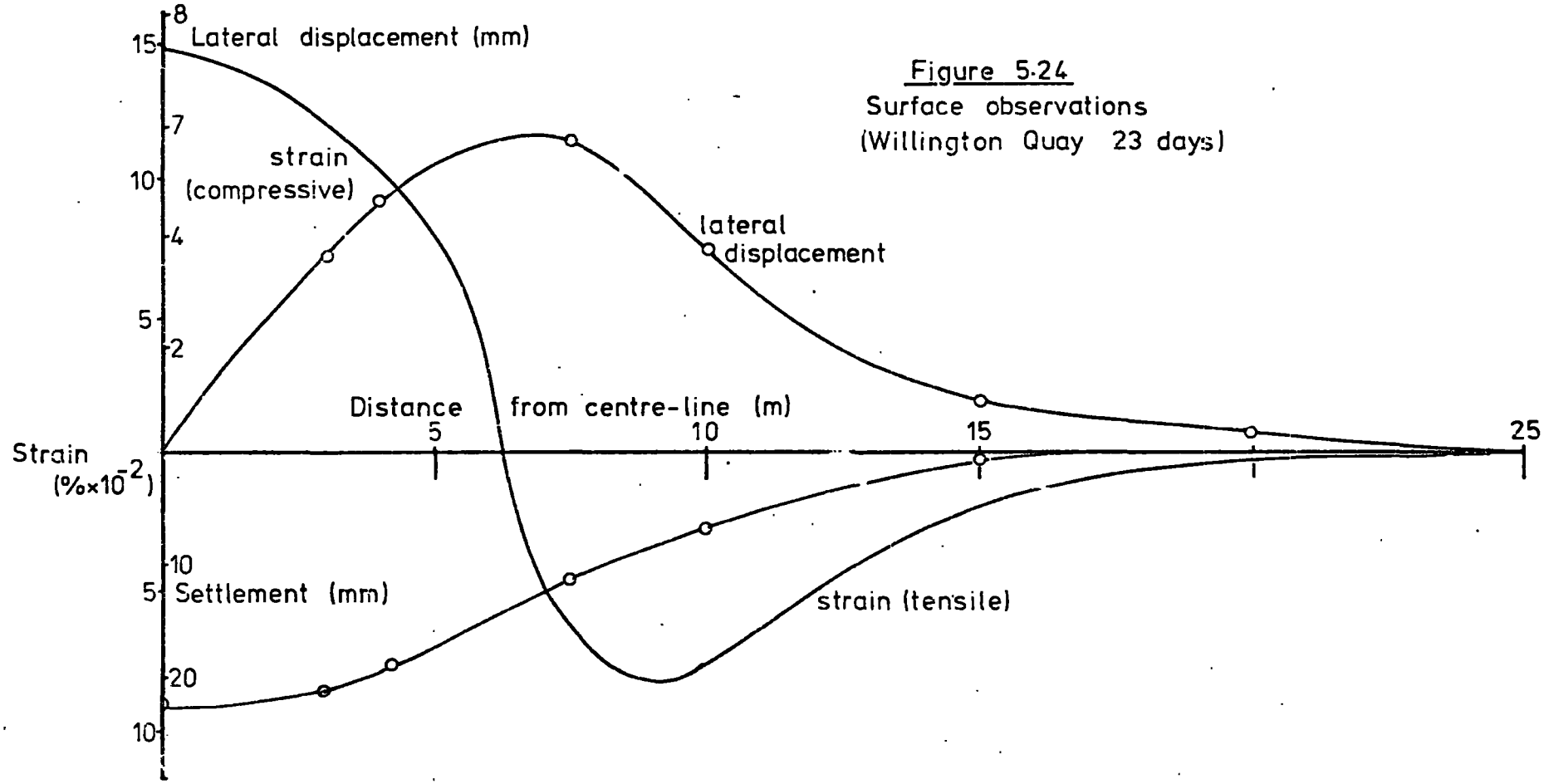

Figure 5.24
Surface observations
(Willington Quay 23 days)

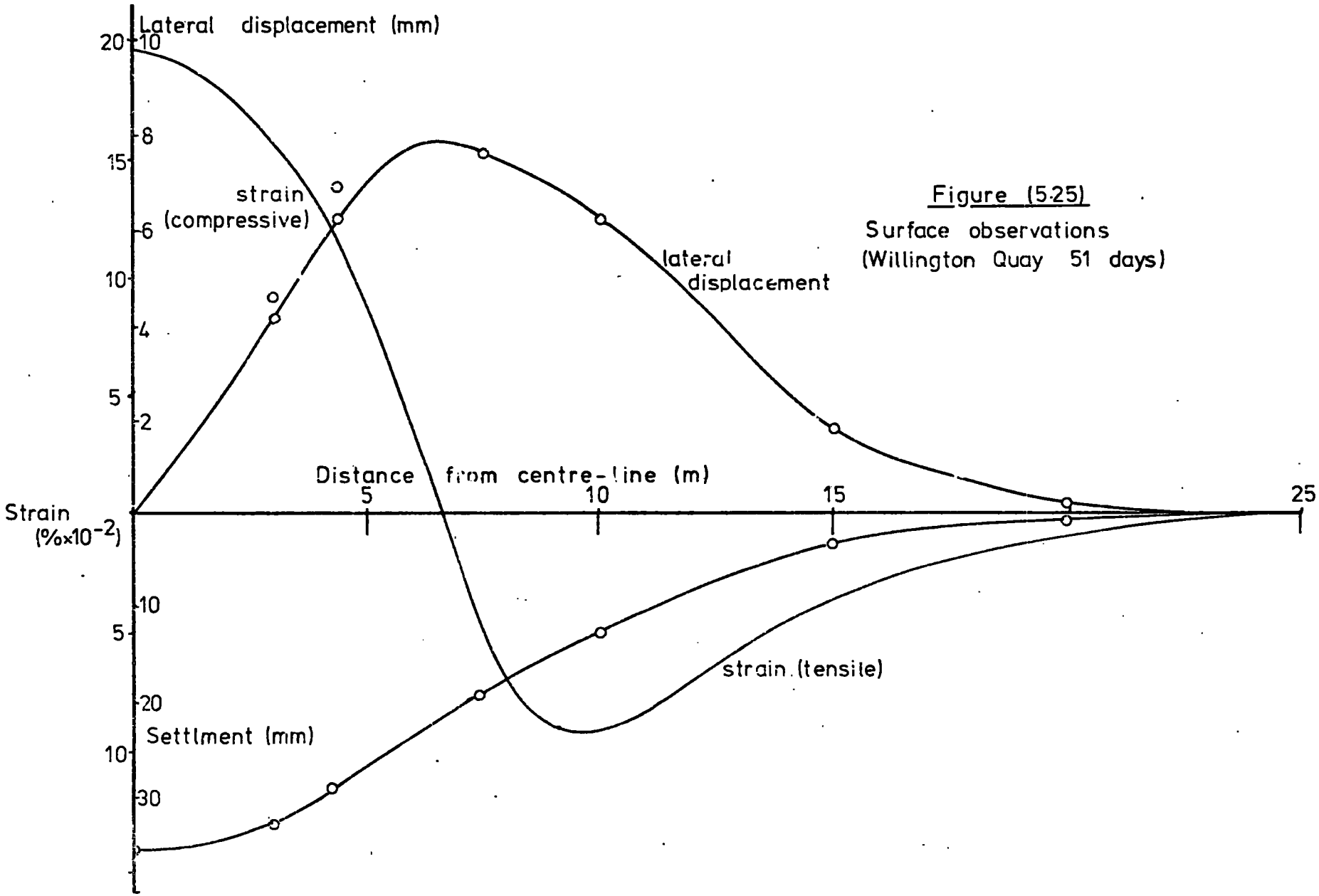

Figure (5.25)

Surface observations
(Willington Quay 51 days)

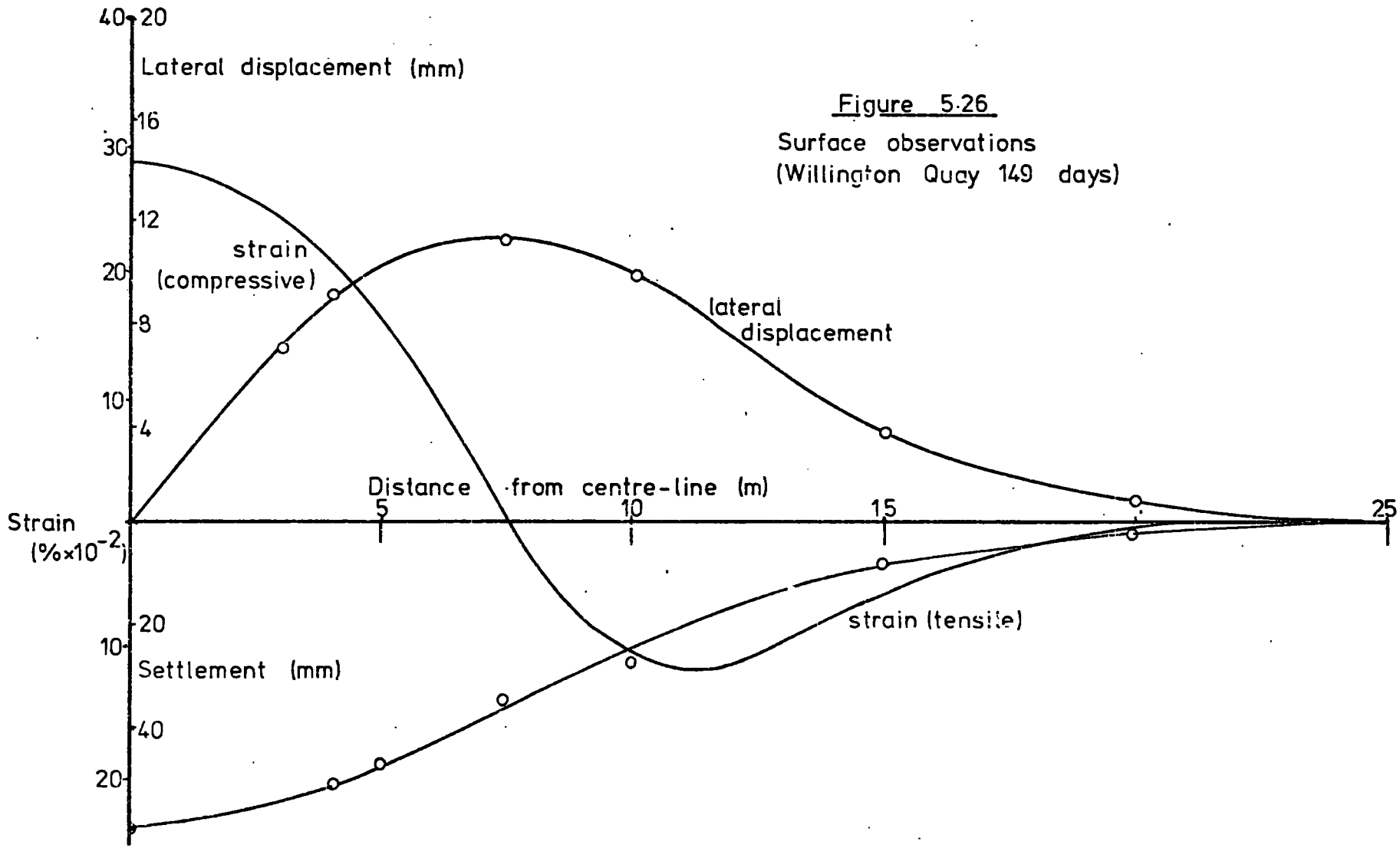

Figure 5.26

Surface observations
(Willington Quay 149 days)

Figure 5.27

Sub-surface settlement (Willington Quay)

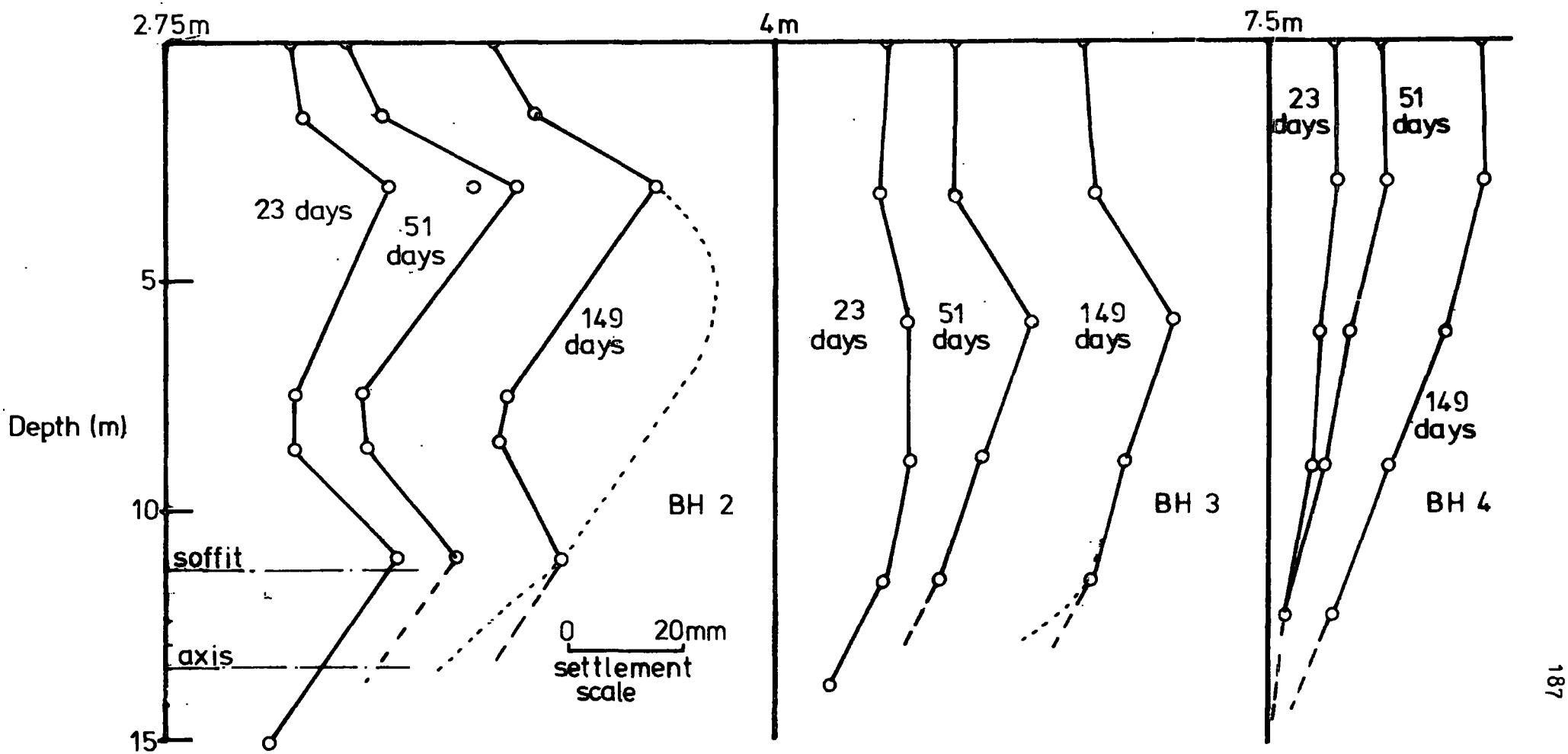

Figure 5.28

Long-term sub-surface settlement

(Willington Quay)

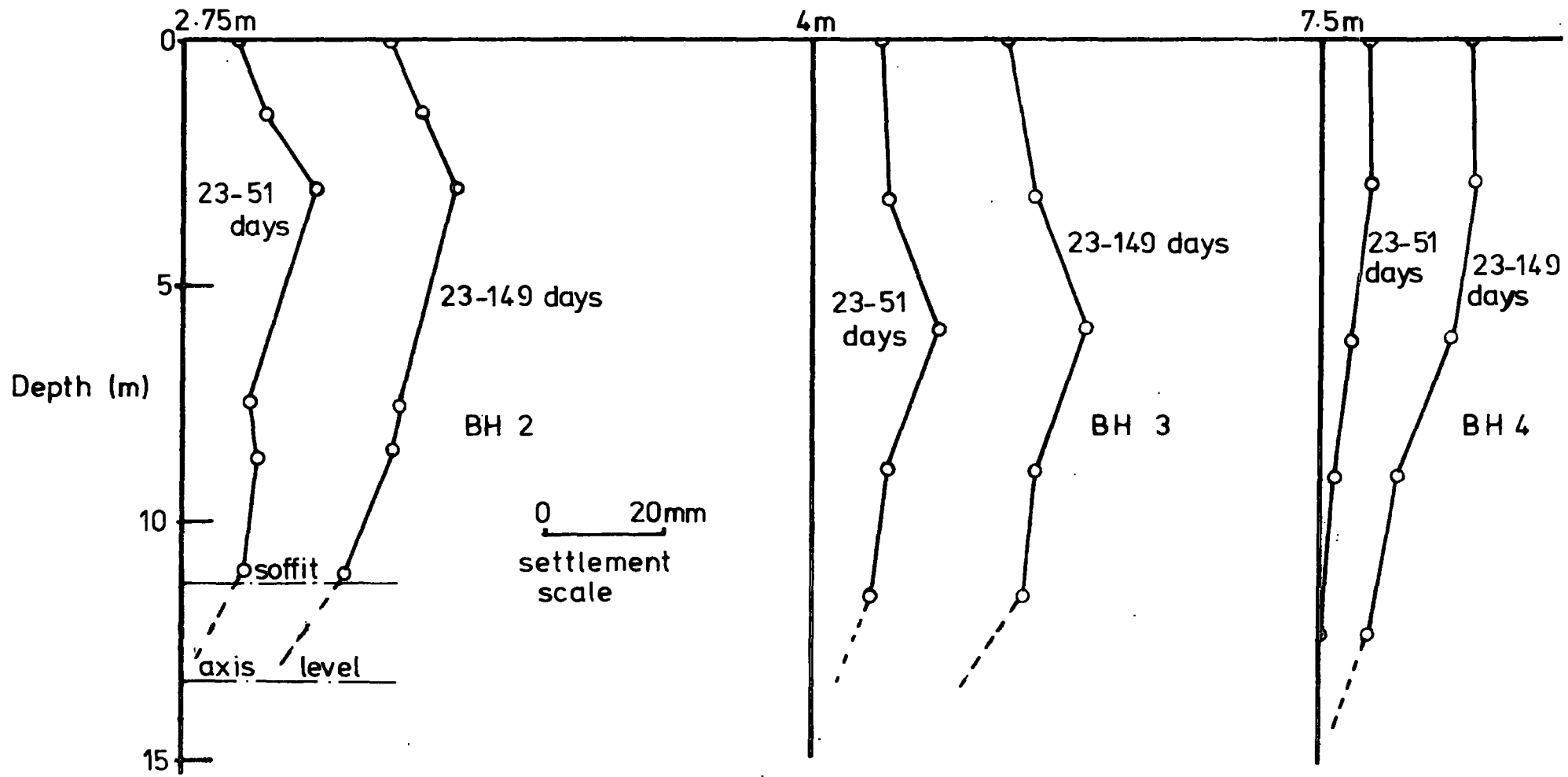

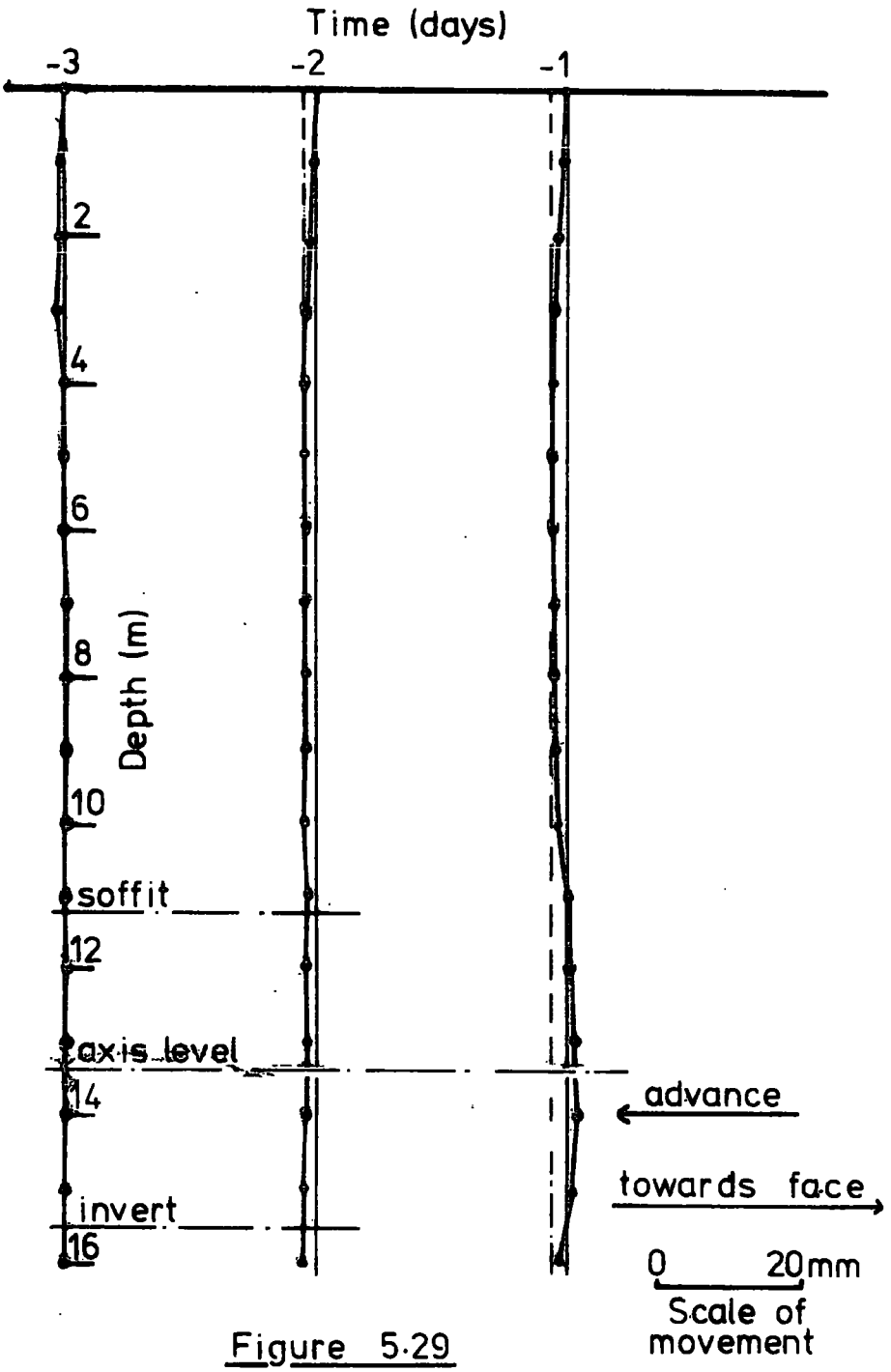

Figure 5.29

Movement parallel to centre-line BH 1 (Willington Quay)

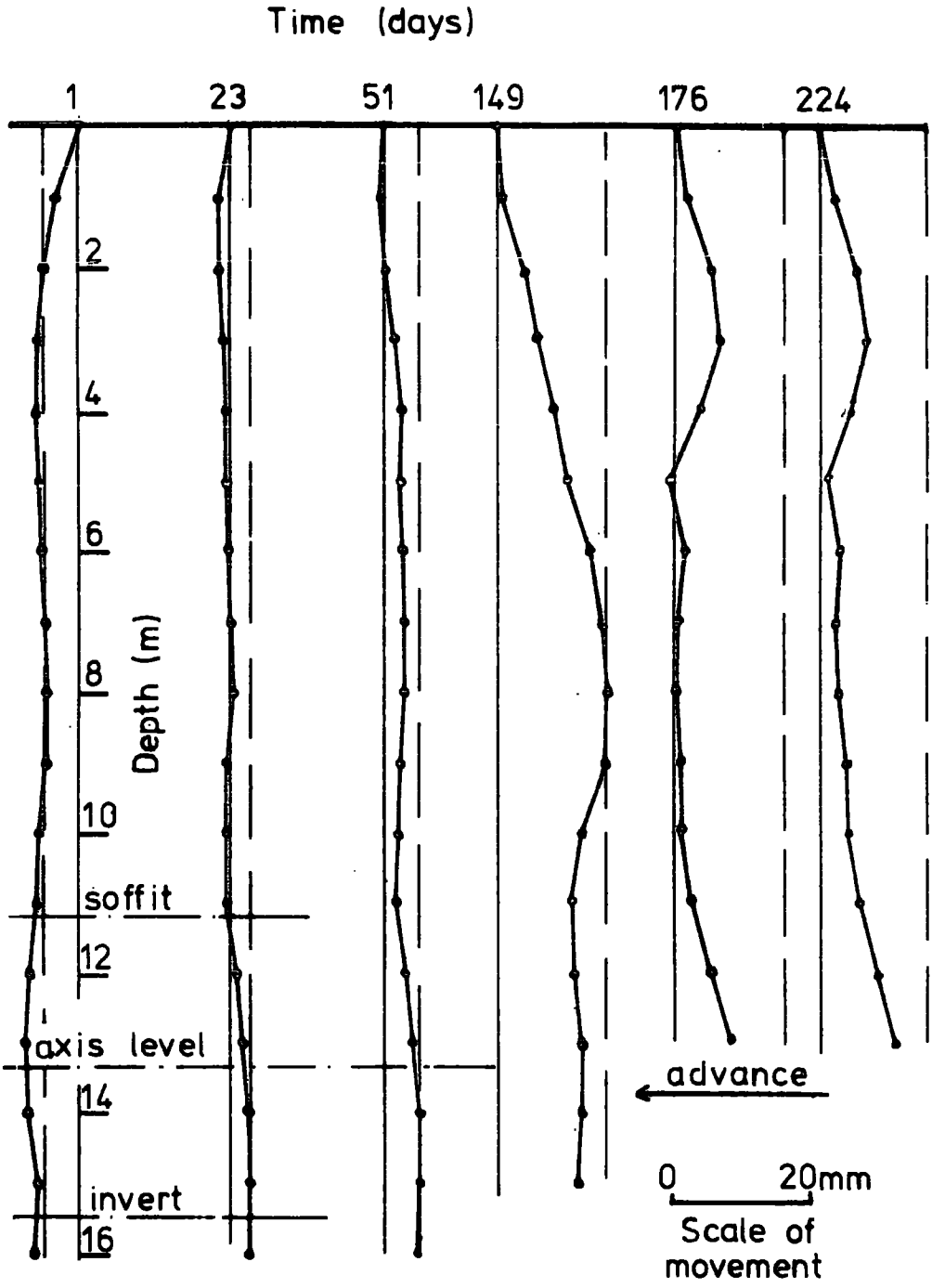

Figure 5.30

Movement parallel to centre-line

BH 2 (Willington Quay)

2.75m from tunnel centre-line

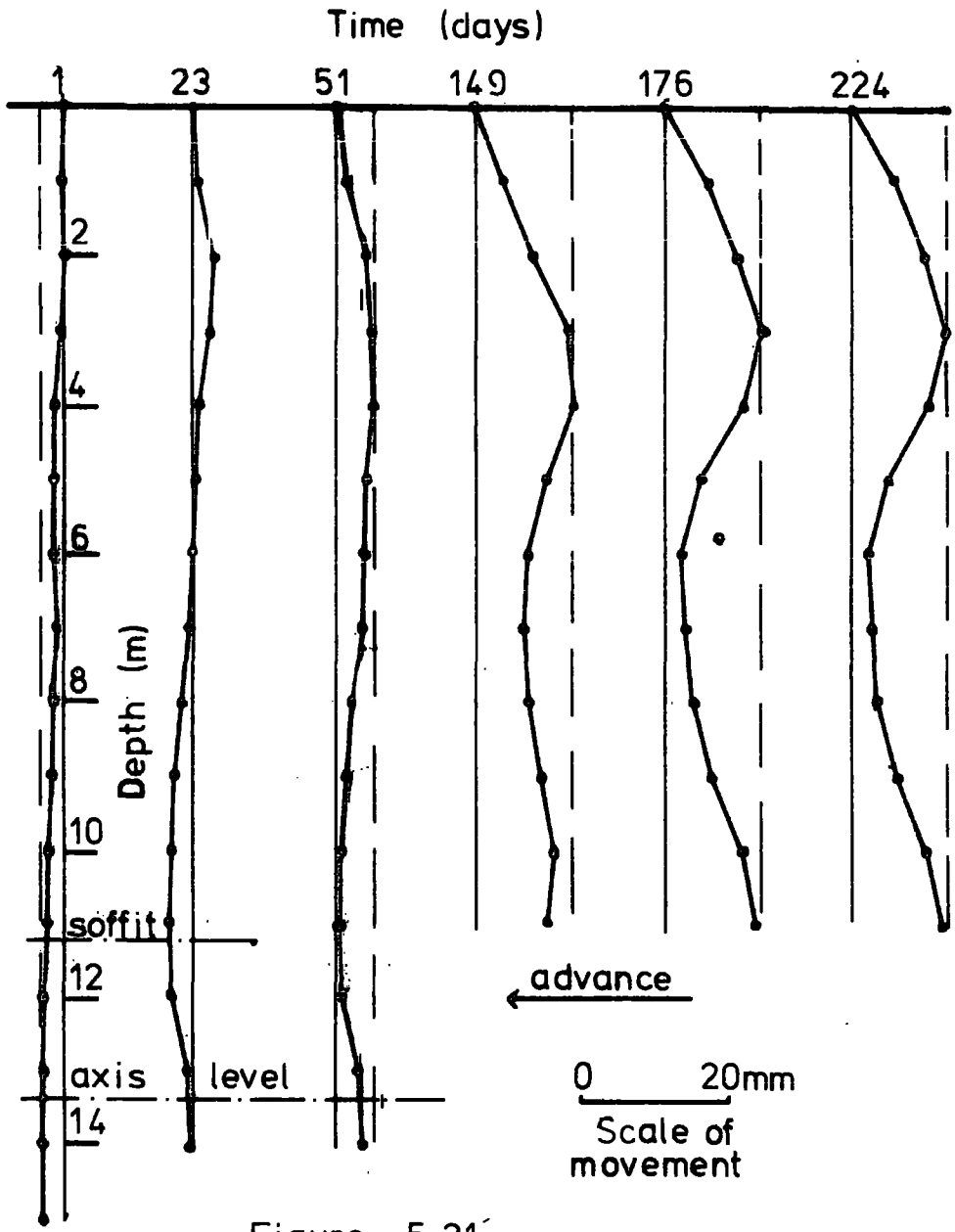

Figure 5·31

Movement parallel to centre-line

BH 3 (Willington Quay)

4m from tunnel centre-line

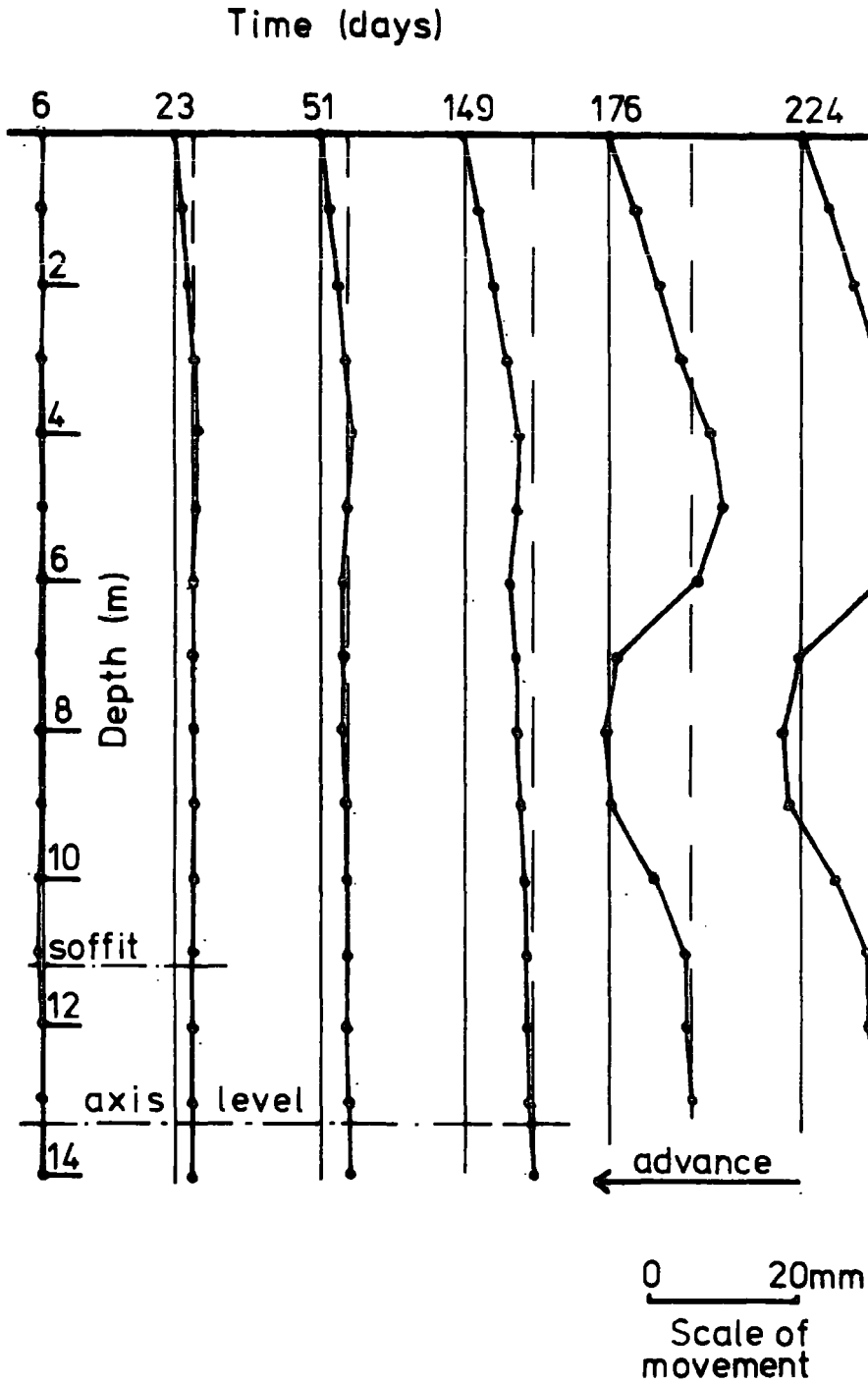

Figure 5.32

Movement parallel to centre-line

BH 4 (Willington Quay)

7.5m from tunnel centre-line

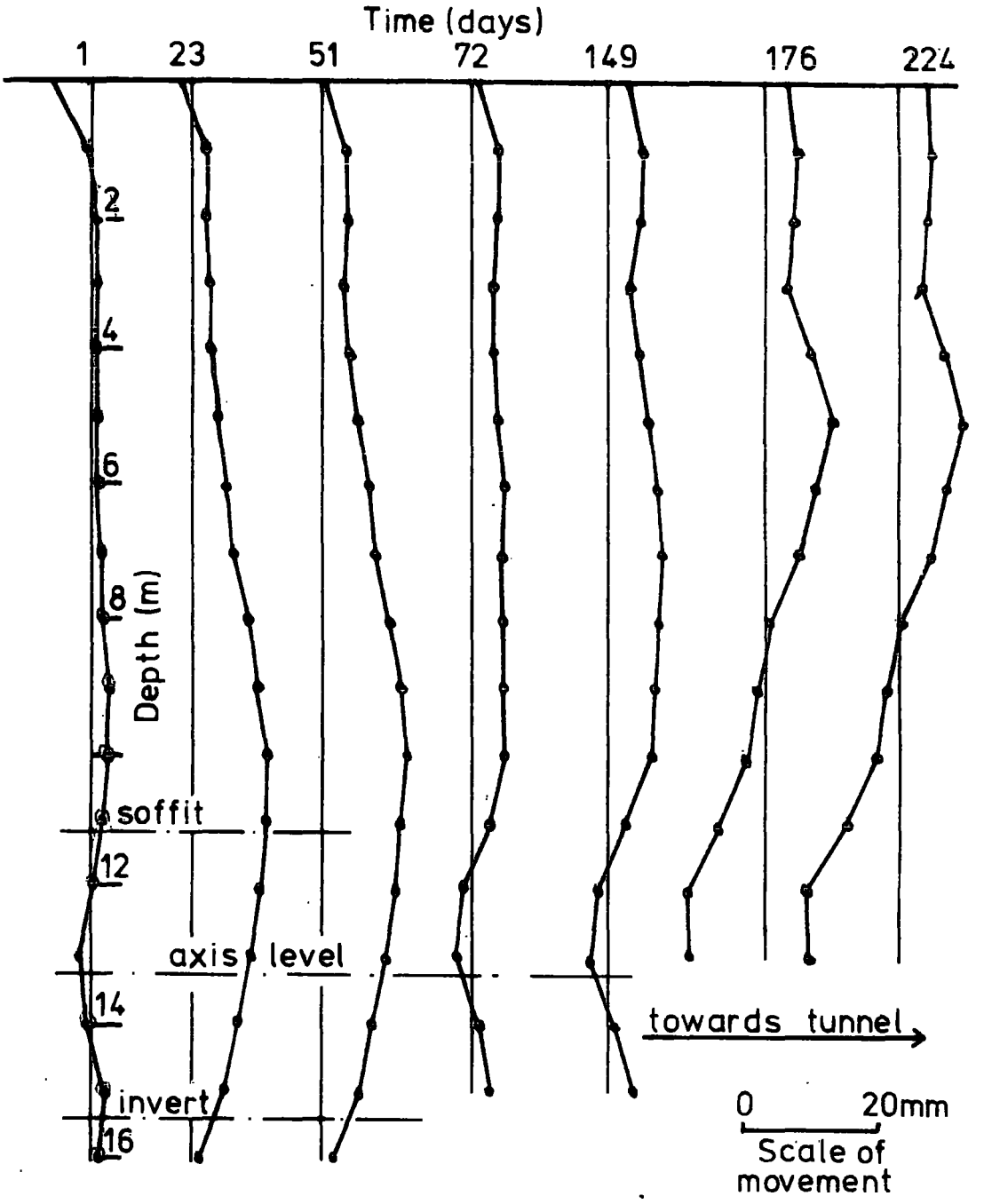

Figure 5.33

Movement perpendicular to centre-line

BH 2. (Willington Quay)

2.75m from tunnel centre-line

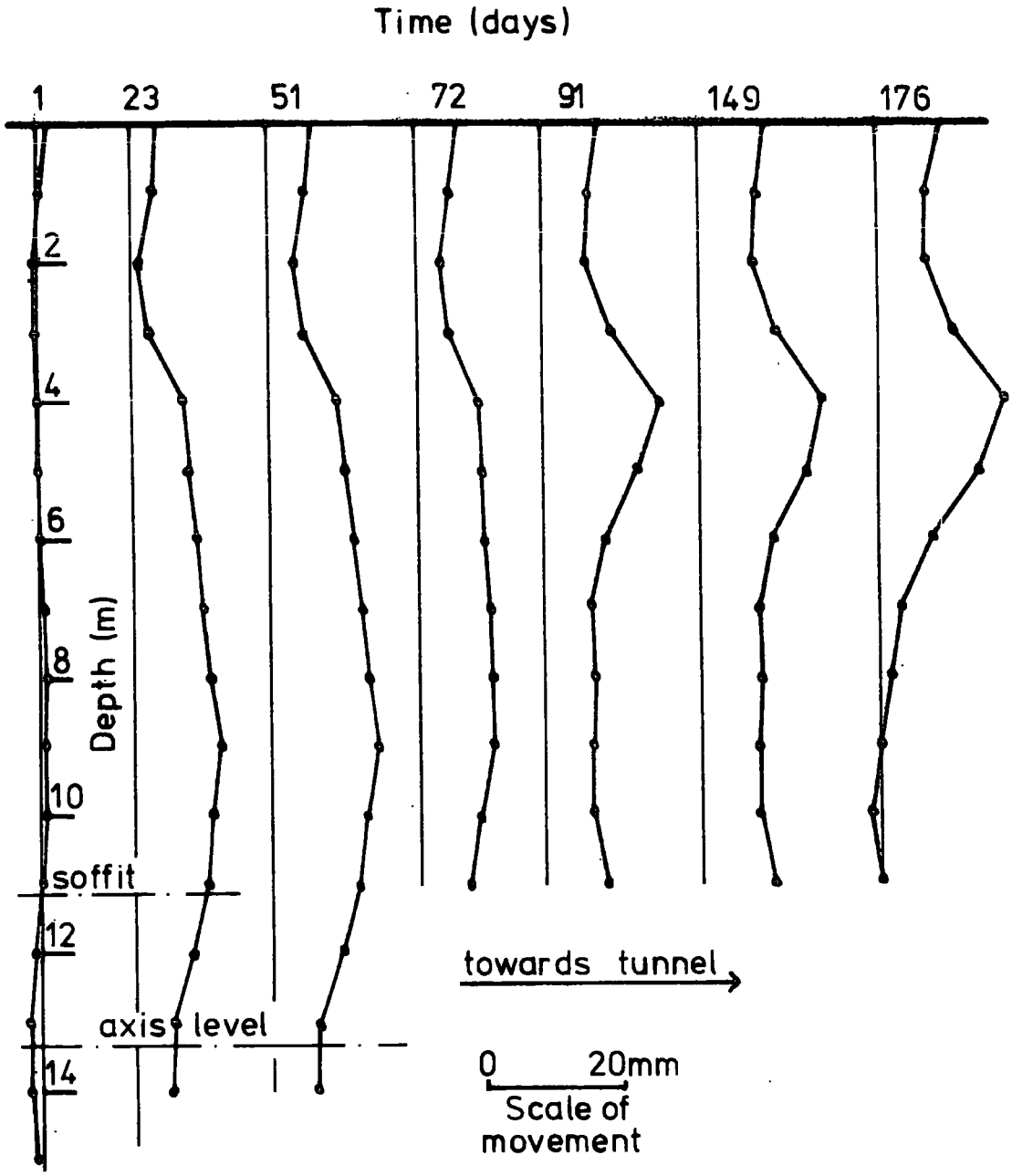

Figure 5.34

Movement perpendicular to centre-line

BH 3 (Willington Quay)

4m from tunnel centre-line

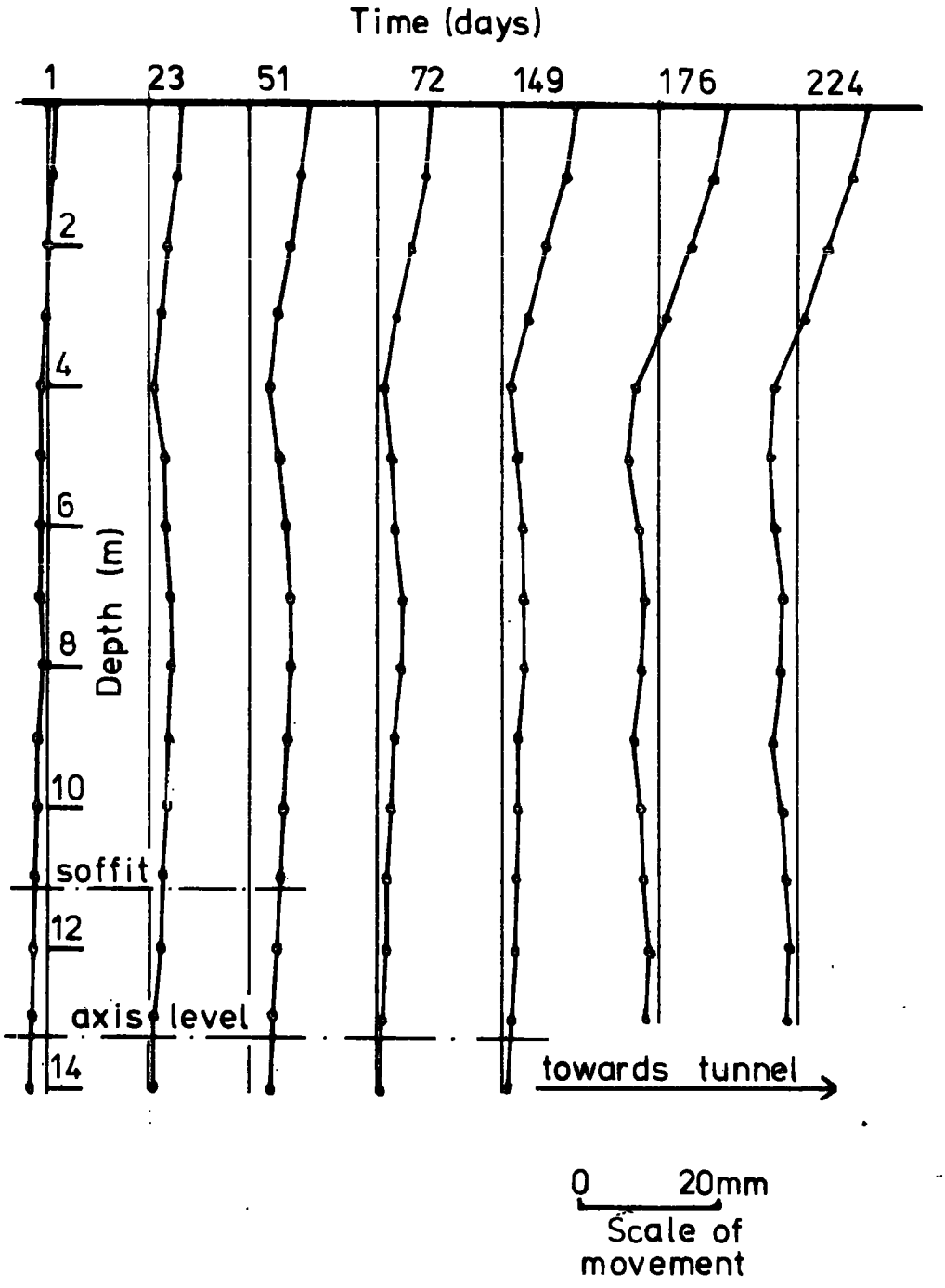

Figure 5.35

Movement perpendicular to centre-line

BH 4 (Willington Quay)

7.5m from tunnel centre-line

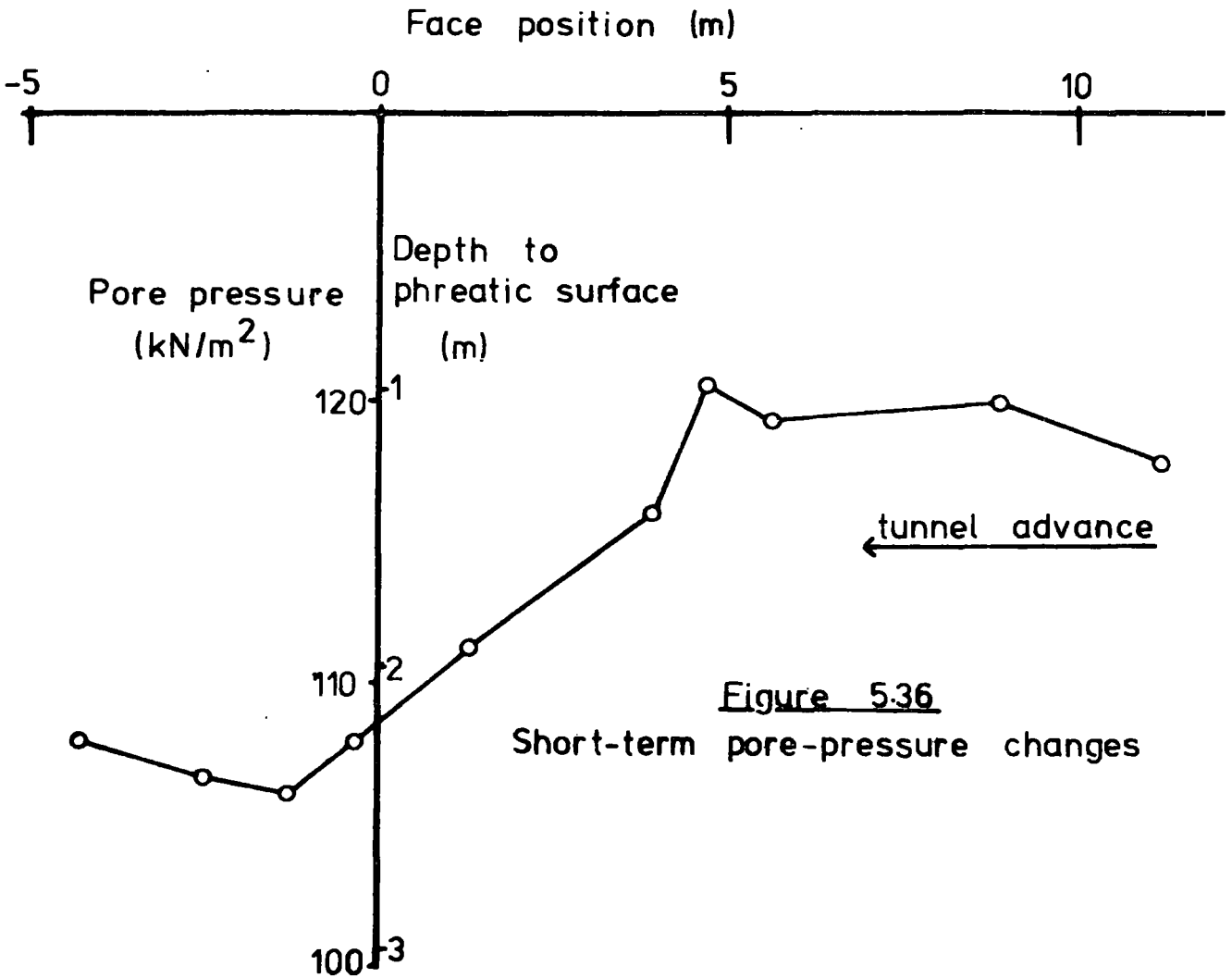

Figure 5.36
Short-term pore-pressure changes

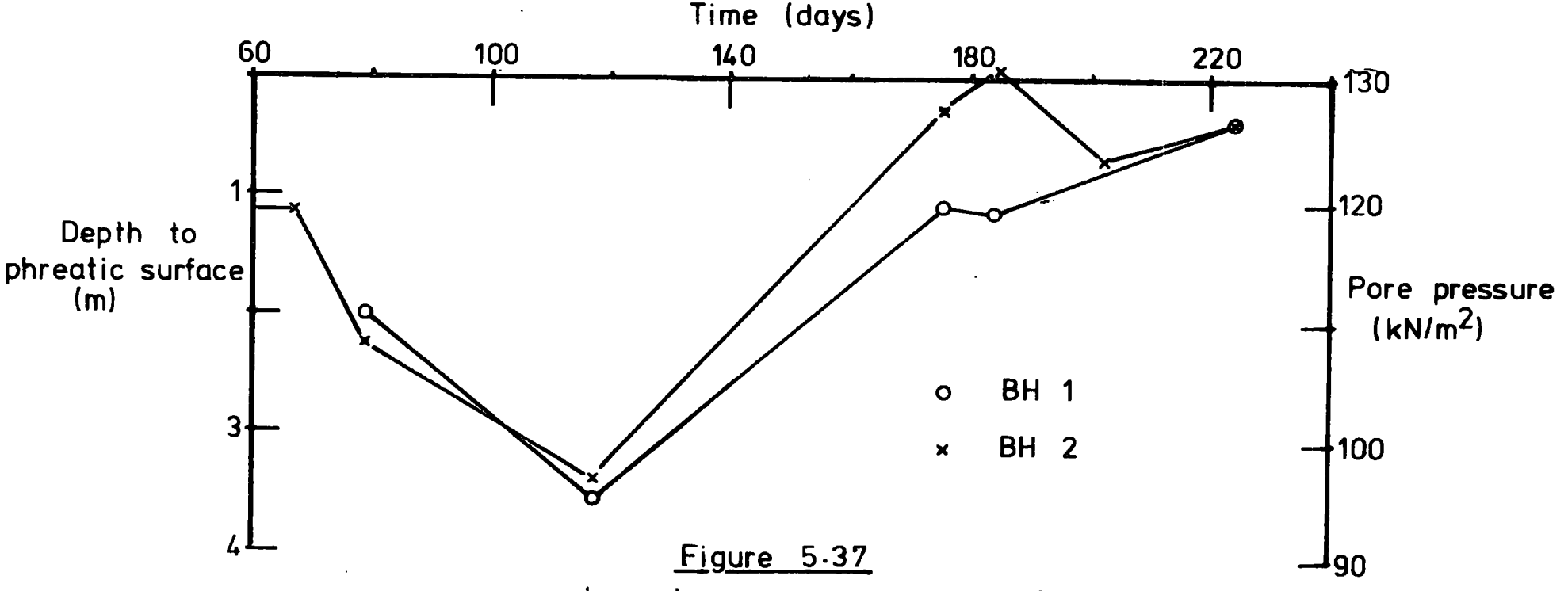

Figure 5.37
Long-term pore-pressure changes

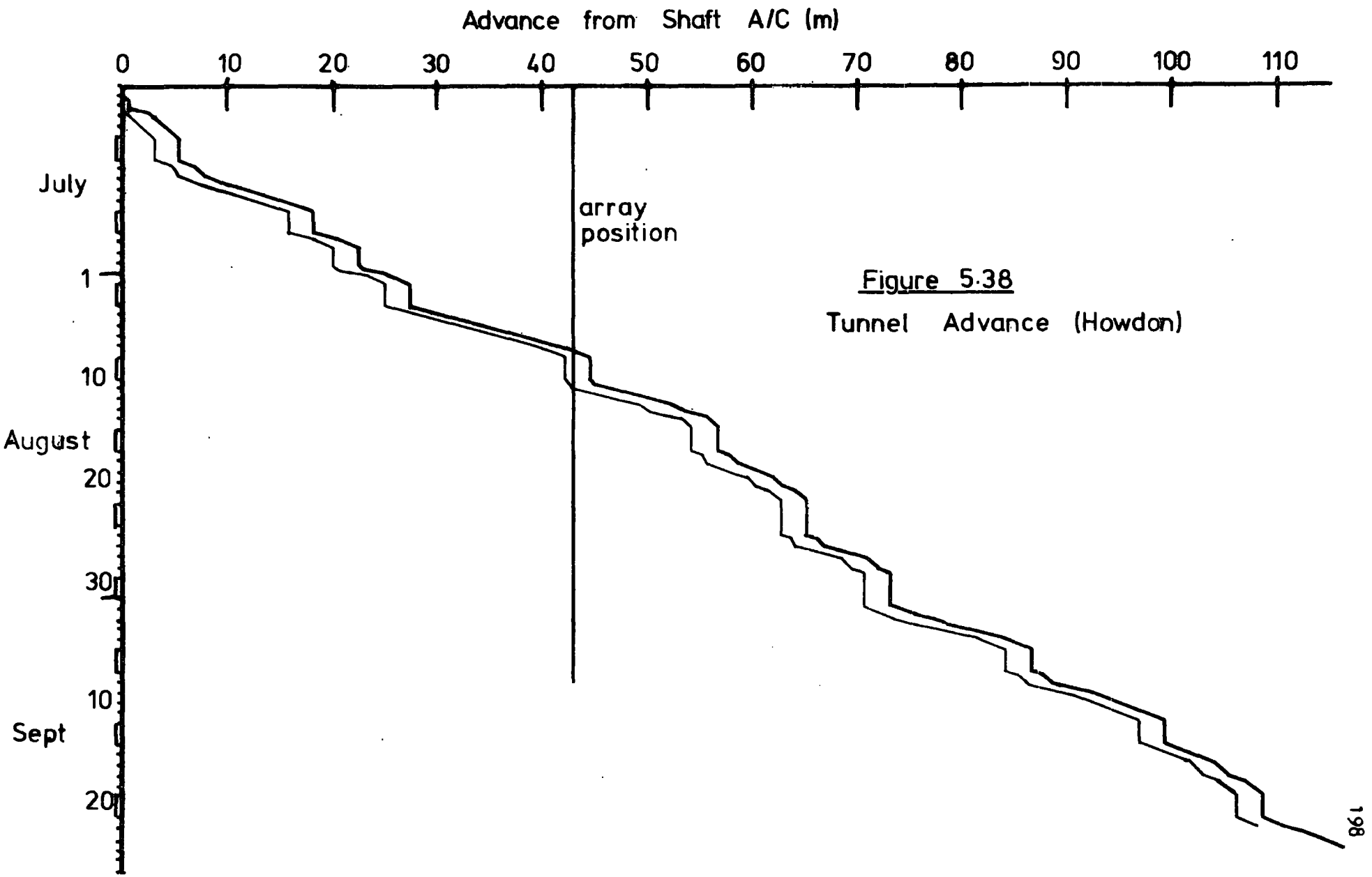

Figure 5.38

Tunnel Advance (Howdon)

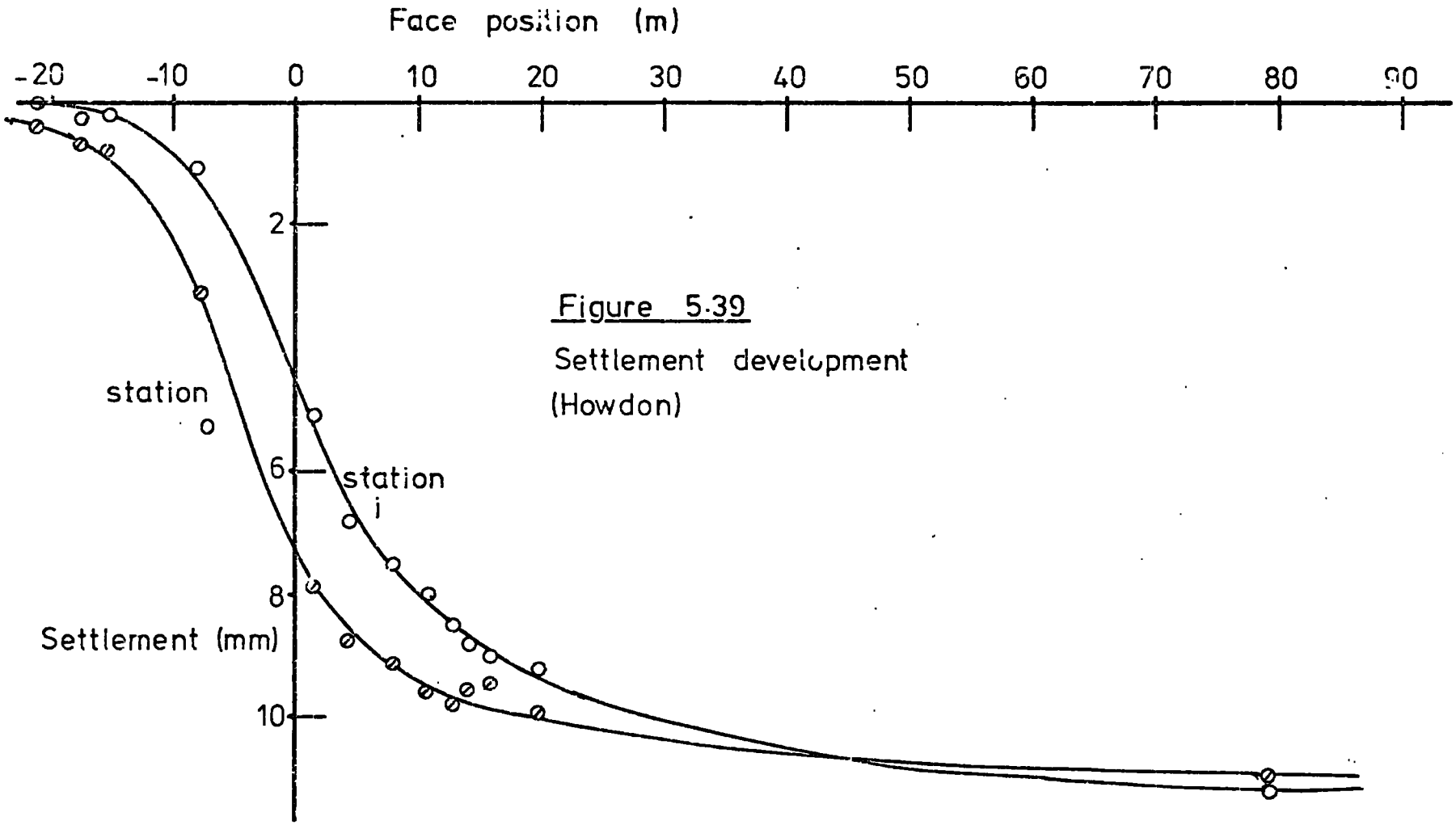

Figure 5.39

Settlement development (Howdon)

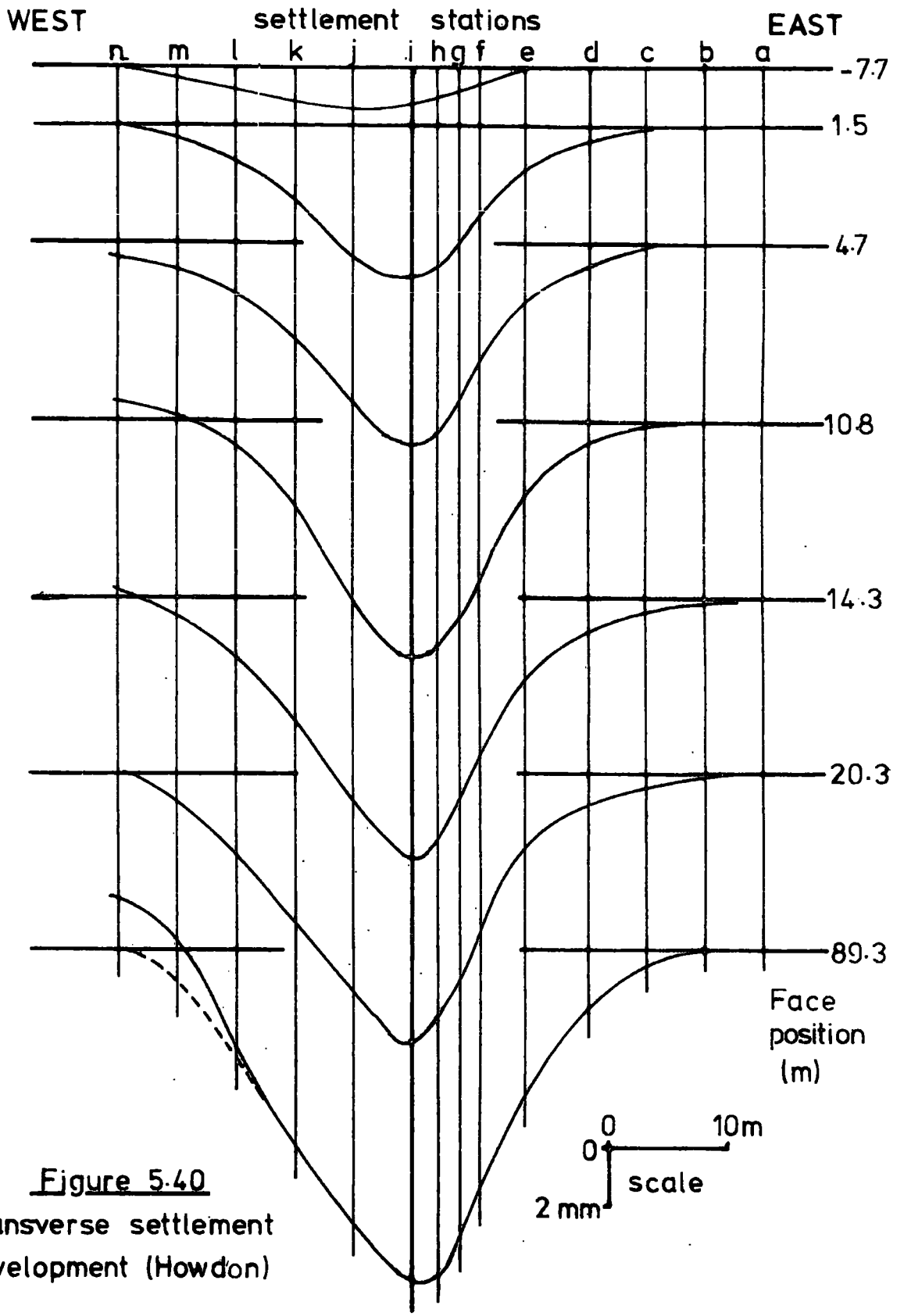

Figure 5.40
Transverse settlement development (Howdon)

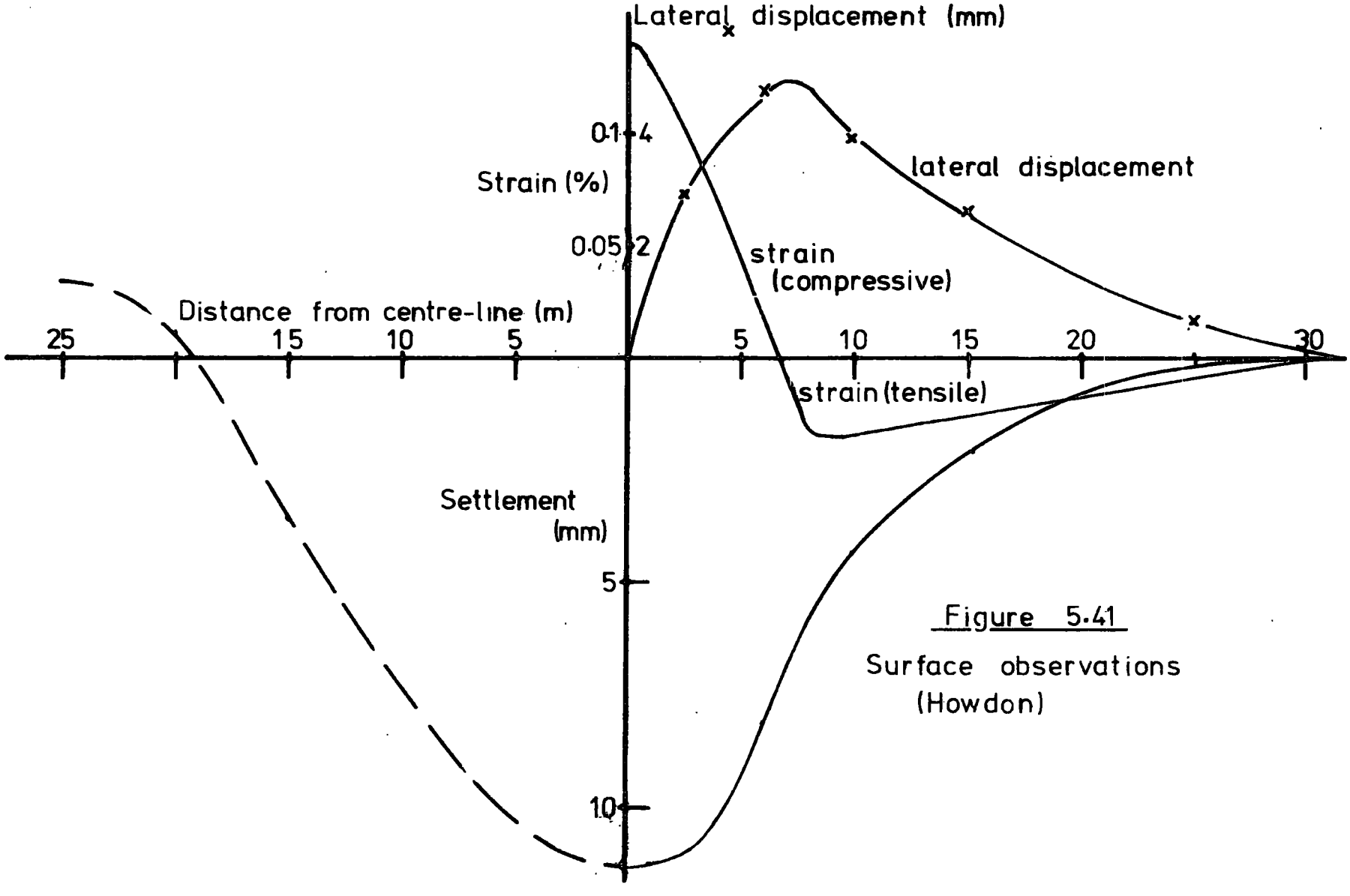

Figure 5.41

Surface observations
(Howdon)

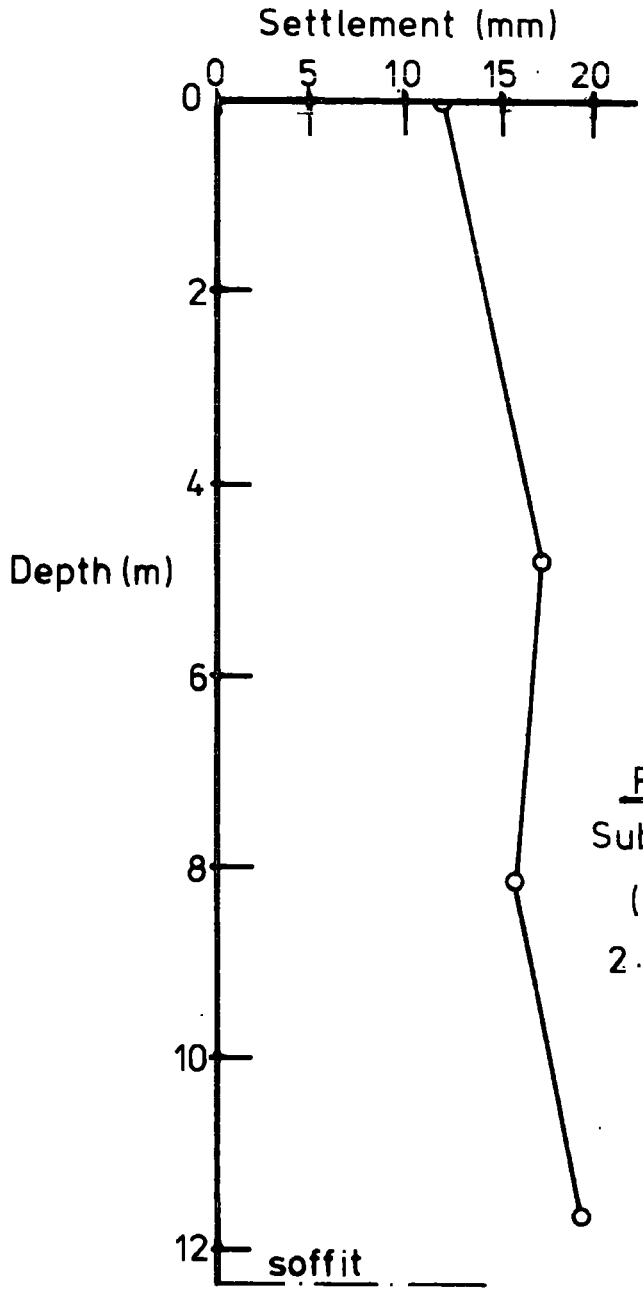

Figure 5.42
Sub-surface settlement
(Howdon) BH 2
2.5m from centre-line

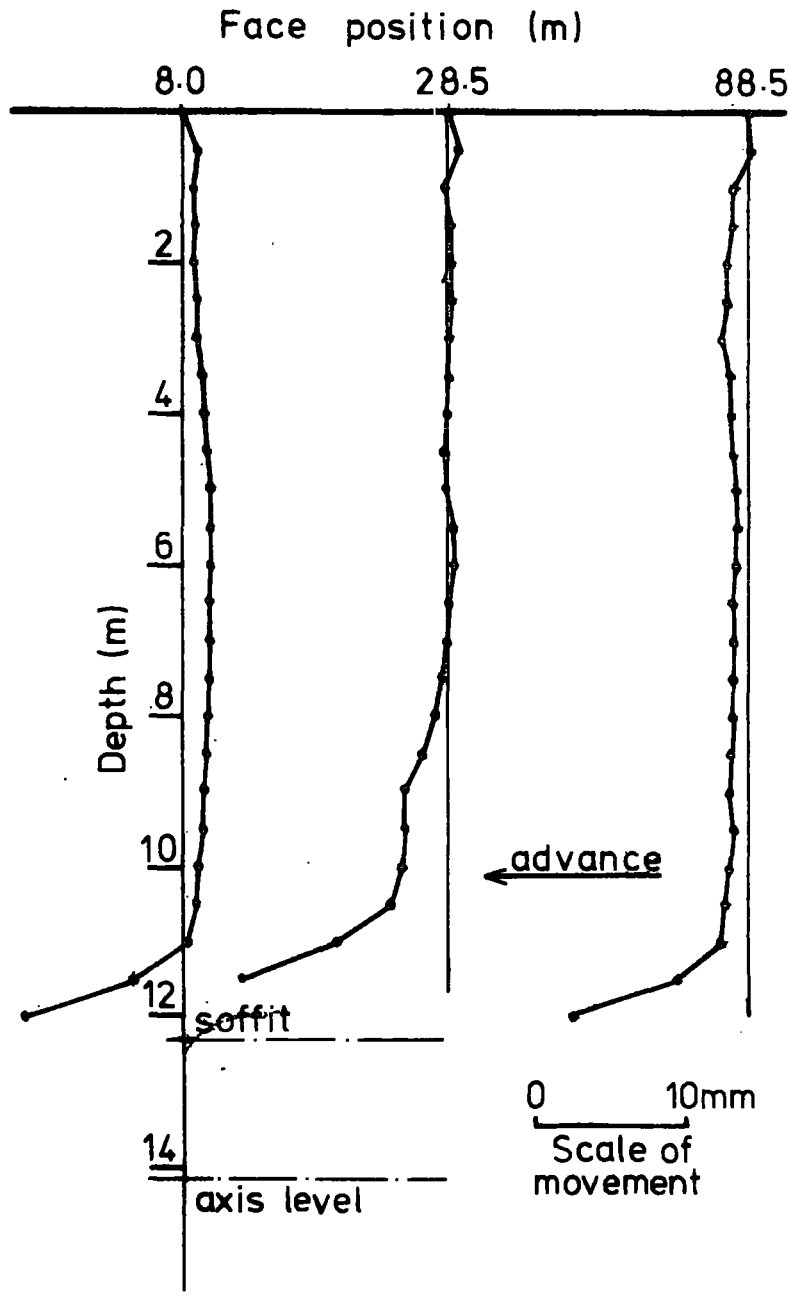

Figure 5·43

Movement parallel to centre-line

BH 1 (Howdon)

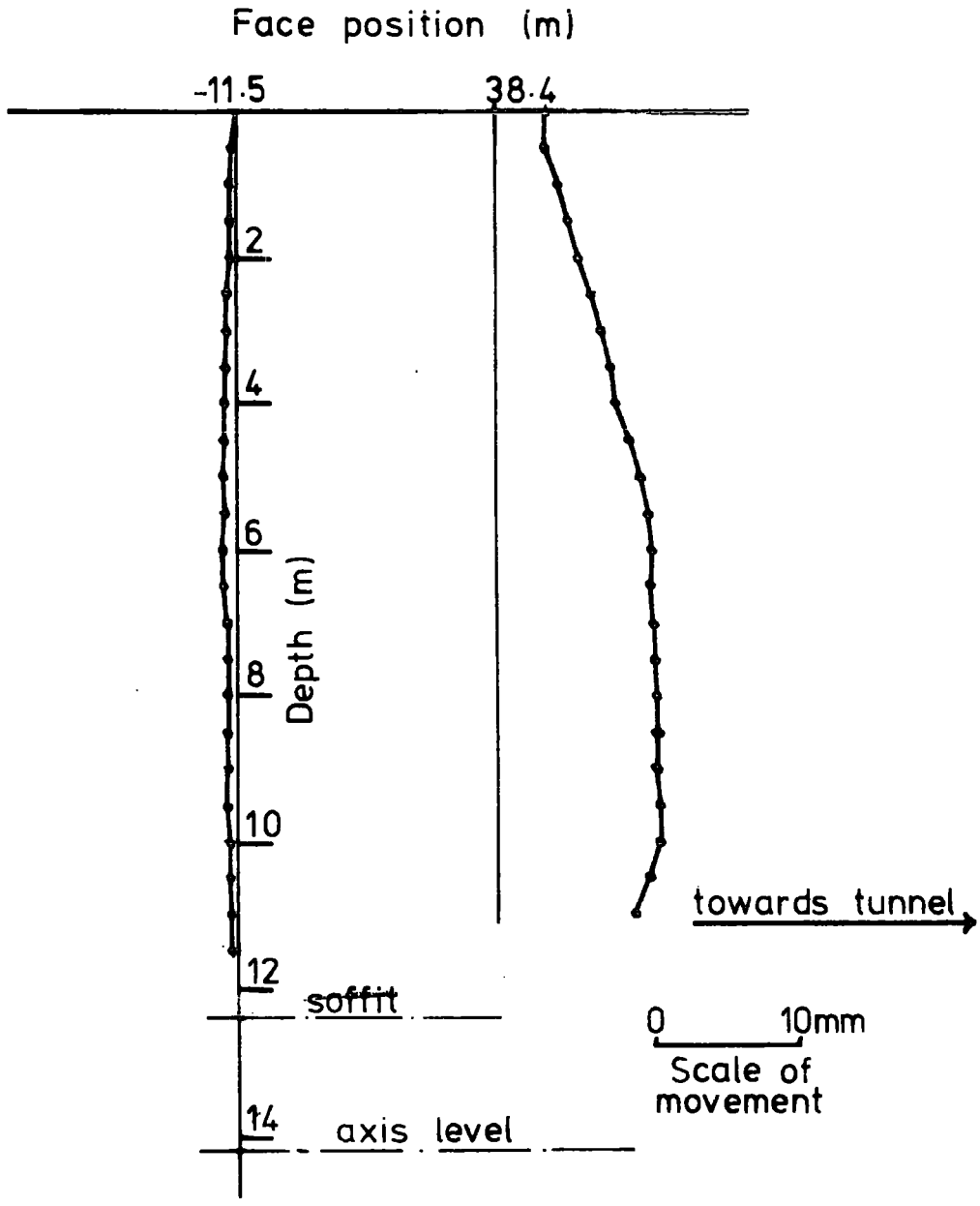

Figure 5.44

Movement perpendicular to centre-line

BH 2 (Howdon)

2.5m from tunnel centre-line

Chapter 6

DISCUSSION AND COMPARISON OF EXPERIMENTAL OBSERVATIONS AND THE STOCHASTIC MODEL

6.1) Introduction

To facilitate a comparison between the three case histories, the principal results from each site are summarised in Tables 6.1 to 6.3. The results from a previous case history carried out by the University of Durham Engineering Geology Laboratories under the supervision of Dr. P.B. Attewell are summarised in Table 6.4. This table refers to measurements carried out during the construction of one of the tunnels for the London Underground Jubilee line (then called the Fleetline) at Green Park. These measurements were carried out principally by Mr. A. Gowland but the author was concerned extensively with the processing and interpretation of the results.

The four case histories comprise a variety of geometries and ground conditions and include excavations both with and without a shield. As was pointed out in Chapter 2, in order to predict settlement effects over a tunnel it is necessary first to estimate the likely volume loss. It is possible to calculate this approximately from a knowledge of the rate of intrusion of the soil and the dimensions and rate of advance of the tunnel, or empirically, as will be shown in Section 6.2.2. However, to make use of this information we must first show that the predicted shape of the settlement trough corresponds with that observed in the field.

6.2) Comparison of the stochastic model with surface measurements

Figure 6.1 shows all four settlement troughs from the four field investigations plotted to the same scale. Superimposed on these profiles are profiles predicted using the stochastic model as described in Chapter 2. The curves were calculated numerically for an annular source of ground loss using the program listed in Appendix E. The settlement trough volume, one of the initial parameters fed into the program, was set equal to the measured volume of the observed settlement troughs. It is immediately clear that,provided the settlement volume can be estimated correctly,the stochastic model provides an excellent fit to the experimental curves. The profile for Willington Quay, although quite acceptable as a predicted settlement trough, shows the greatest discrepancy, the measured trough being narrower and deeper than the calculated profile. This profile shows settlement after 23 days, before the second, pure consolidation phase of settlement had begun. However, it is quite possible that even at this stage a certain amount of consolidation may have occurred, which of course is not accounted for by the stochastic model. It should also be noted that whilst the other three profiles are for tunnels in purely cohesive materials, the overburden at Willington Gut was of a more frictional nature, being alluvial silt with sand lenses, and this also may have the effect of narrowing the settlement trough. The trough from Howdon appears to be shallower and slightly wider than the predicted trough but this is considered to be due largely to the asymmetrical shape of the trough, itself possibly caused by the curvature of the centre-line.

Figure 6.1 also shows predicted lateral displacement profiles (from equation 2.18) for all four sites, along with measured profiles

from Willington Quay and Howdon, no lateral displacements having been measured at Green Park or at Hebburn. Once again the agreement between the predicted and measured profiles is considered to be quite good, taking account of the error inherent in the measurement method (Appendix C). Movements at Willington Quay are smaller than predicted, which tends to support the theory that some consolidation is involved, since consolidation settlement would not be expected to induce lateral movements. Lateral movements at Howdon are slightly greater than predicted, again possibly due to the curvature of the centre-line. It should be noted, however, that the discrepancies between the measured and calculated lateral displacement profiles are not much greater than the estimated measurement errors and may, therefore, be even less than shown in Figure 6.1.

Figure 6.2 shows profiles of measured and calculated surface tilt and calculated lateral strain for all four sites. The Willington Quay and Howdon profiles also show "measured" lateral strain. Tilt was measured directly from the observed transverse settlement profiles. Lateral strain was measured indirectly as the gradient of the lateral displacement profiles. As might be expected, these graphical procedures incur further errors and in consequence the discrepancies between the measured and theoretical curves are greater than for settlement or displacement. This is particularly obvious in the Willington Quay tilt profile and in the Howdon strain profile, in both cases the theoretical curves underestimating the measurements. Also, the observed maximum tilt at Howdon is closer to the centre line than is predicted by the stochastic model, a direct consequence of the asymmetry of the settlement profile.

In the case of strain and tilt, therefore, the stochastic model would appear to be a less satisfactory predictor, although one should bear in mind that the errors in the observed profiles may be quite great. Nevertheless, on the basis of these case histories, the model does provide a rough estimate of the magnitudes of these parameters, and seems to predict their distributions reasonably well.

6.2.1) The settlement trough geometry

As is shown above, the stochastic model, as developed in Chapter 2, fits quite well with the data from the four case histories so far observed by the author. This model uses the extremely simple relation between the depth to the source of ground loss and the point of inflection (i) of the resulting settlement trough:

$$Z = 2i \qquad (6.1$$

This relation takes no account of the size or diameter of the opening since it strictly applies to the "source function" describing settlement above an infinitesimally small source of ground loss. Numerical methods can be simply applied to take account of the shape of the opening, although in many cases it is reasonable to regard the tunnel itself as a point source. Schmidt (1969) and Peck (1972) have proposed the more general relation:

$$\frac{2i}{D} = \left(\frac{Z}{D}\right)^{n} \qquad (6.2$$

where D = tunnel diameter,

and n = empirical constant

They have suggested the value of 0.8 for the value of n based on empirical studies of several case histories. This relation is

considered by the author to be unsatisfactory from a theoretical point of view (see Section 2.9).

Attewell (1977) presents data from 30 case histories in his state of the art review. These data are reproduced in Table 6.5. Using these data along with that from the three sites described above, a plot of the point of inflection (i) against axis depth (Z) was drawn (Figure 6.3). Although these data do show a certain amount of scatter, the best straight line through it is fairly close to the theoretical relation. The data obtained by the author, and that from Green Park fit the theoretical relation (equation 6.1) almost perfectly. The most divergent data is that collected during the construction of the Washington, D.C. metro and the one data point from the TRRL tunnelling trials in the Chalk at Chinnor. Table 6.5 shows the ground conditions encountered for each data point. It is clear from this table that many of the Washington, D.C. metro measurements, which give narrower troughs than would be expected, were taken over tunnels constructed in sands or gravels. As was discussed in Sections 2.3.2 and 2.4.4 there is some theoretical basis, as well as evidence from physical models, that narrow troughs may occur above tunnels in frictional materials.

On the other hand, the TRRL tunnelling trials at Chinnor, carried out primarily to test tunnelling machine performance in Chalk for the ill-fated Channel tunnel, indicate the formation of a settlement trough considerably wider than would be predicted by the stochastic model. It would, perhaps, be unreasonable to expect a good fit with this data from what is in fact a rock tunnel.

Disregarding the above data we obtain the third straight line of Figure 6.3 from regression analysis. As can be seen, this line

is quite close to the predicted relation of Equation 6.1. To test the data in more detail, and to compare its fit with the two relations in equations 6.1 and 6.2, the data was analysed using the Michigan Interactive Data Analysis System (MIDAS), a comprehensive statistical package supported by NUMAC. This package provides a flexible and simple-to-use statistical testing facility, considerably enhanced by its capability for interactive data manipulation and processing.

Figure 6.4 produced using MIDAS shows the data of Table 6.5 plotted as 2i/D against Z/D. This figure uses all of the data from Table 6.5 and therefore includes frictional as well as cohesive soils. The two straight lines show the theoretical relation of equation 6.1 and the best straight line fit to the data points from regression analysis. The two lines are very close together. Least squares regression analysis gives a multiple r of 0.90 indicating the high degree of correlation between the two variables. The equation of the least squares regression line is:

$$\frac{Z}{D} = 0.03 + 1.09 \left(\frac{2i}{D}\right) \qquad (6.3$$

This evidence confirms that at least for these case histories, the stochastic model with its simple linear relation between tunnel depth and trough width gives a good correspondence with reality. In order to test the "goodness" of the Peck-Schmidt relation (equation 6.2) it is necessary to apply a logarithmic transformation to both variables (Z/D and 2i/D) in order to enable a straight line to be fitted to the data by regression. The relation of Equation 6.2 then becomes:

$$\text{Log}_e(Z/D) = 0.8 \ \text{Log}_e(2i/D) \qquad (6.4$$

This transformation was carried out using MIDAS and the resulting scatter plot is shown in Figure 6.5. As in Figure 6.4, this

plot uses all of the data from Table 6.1, including that from the Chinnor trials and the Washington metro. Once again, a straight line fits the transposed data quite well. The three straight lines shown on Figure 6.5 show Peck's relation (equation 6.2), the relation derived from the stochastic model (equation 6.1) and the best straight line fit derived by least squares regression analysis. It is clear that the regression line fits best with the stochastic relation. This is confirmed by the equation of the regression line, which is:

$$\text{Log}_e\ (Z/D) = 0.23 + 0.93\ \log_e(2i/D) \qquad (6.5$$

$$\text{or} \quad \frac{Z}{D} = 1.26\ \left(\frac{2i}{D}\right)^{0.93}$$

Although the above analysis indicates that both Peck's model and that developed in this thesis both fit the data reasonably well, it appears that the simple relation of equation 6.3 provides the best straight line fit. This is sufficiently close to equation 6.1 to provide at least limited confirmation of the validity of the stochastic model as proposed in Chapter 2.

6.2.2) The prediction of settlement trough volume

As was discussed in Chapter 1 (Section 1.13) it is feasible to calculate the volume of ground lost into a tunnel from a knowledge of its geometry and rate of advance, along with an estimate of the intrusion rate of the soil. At present, however, the latter is difficult to estimate with any accuracy, although further development of the intrusion test (Attewell and Boden, 1971) may prove valuable in this respect. The accuracy of this approach also depends on the assumption that there is no volumetric strain in the ground during settlement (or at least that the degree and distribution of volumetric strain is known).

This assumption is discussed in Section 6.5.

In the absence of an analytical method of estimating volume loss, an alternative approach is to attempt to find an empirical relation between the observed volumes of settlement troughs and some other easily measurable or calculable parameter. It is reasonable to expect that the volume of ground loss will be a function of the size of the tunnel and its stability, and therefore, as a first approximation, an attempt was made to relate these factors by relating percentage volume loss ($V_S\%$) to the Stability Ratio. A plot of percentage volume loss against OFS (from the data in Table 6.5) is shown in Figure 6.6. A reasonably good straight line fit is obtained to this data, in spite of the highly simplified model used. Regression analysis of this data gives the equation:

$$V_S\% = -1.14 + 1.33 \text{ OFS} \qquad (6.6$$

Although this implies negative volume loss at small values of OFS, the fit for values of OFS greater than 1.3 is quite good, giving an r statistic of 0.89 (that is, 80%) of the variance in $V_S\%$ is explained by equation 6.6). It is probable that the straight line relation ceases to hold for small values of OFS, but, as a rough guide, it may be assumed that equation 6.6 holds down to an OFS of 1.3, below which zero settlement occurs (the effects of this assumption are unlikely to be of great importance since for such stable faces settlement is unlikely to be a problem in any case). Equation 6.6 can be used to determine the likely volume loss over any tunnel, and this factor can be inserted into the stochastic equations (2.18 to 2.22) in order to predict settlement. Figure 6.7 shows settlement troughs predicted in this way for the tunnels described in Chapter 4 along with that at

Green Park. Although their agreement with the measured profiles is not as good as that shown in Figure 6.1, it is nonetheless adequate as a prediction.

It should be noted that equation 6.6 takes no direct account of such factors as ground intrusion rate, tunnel advance rate or tunnel geometry and so on, factors which were shown in Chapter 1 to have a direct bearing on the volume of ground which would be expected to be lost into the tunnel. In view of this, the degree of correlation shown between volume loss and OFS is quite surprising. Whilst the tunnel geometry is partially included in the volume term, since percentage volume loss is used, and intrusion rate is presumably related to OFS, it remains true that settlement volume would be expected to be directly related to tunnel advance rate. The validity of equation 6.6 may be partly due to the fact that tunnel advance rates are fairly uniform in most tunnels. However, variations in tunnelling rate may account for much of the scatter of the points in Figure 6.6.

In view of the above limitations an attempt has been made to construct a more sophisticated model taking into account all the known variables. From equations 1.1 and 1.2 (Chapter 1) we derive:

$$V_s = \frac{\pi D^2}{4} \frac{R_i}{R_a} + D R_i T_g \qquad (6.7$$

using the nomenclature described earlier. The standing time of the ground (T_g) is equal to the average distance between the face and the point of grout injection (L) divided by the tunnel advance rate (R_a), giving:

$$V_s = \frac{\pi D^2}{4} \frac{R_i}{R_a} + D \frac{R_i}{R_a} L$$

$$= \frac{\pi D^2}{4} \frac{R_i}{R_a} \left(1 + \frac{4L}{D}\right) \qquad (6.8$$

If we assume that the intrusion rate (R_i) is a function of the OFS, then:

$$V_s = F \frac{OFS}{R_a} \frac{\pi D^2}{4} \left(1 + \frac{4L}{D}\right)$$

$$V_s\% = F \frac{OFS}{R_a} \left(1 + \frac{4L}{D}\right) \qquad (6.9$$

In Figure 6.8 $V_s\%$ is plotted against OFS/R_a $(1 + 4L/D)$ for the four case histories described in Tables 6.1 to 6.4. A curve has been drawn "by eye" through the four points and the origin. It can be seen that an excellent fit is obtained using a smooth, first-order curve. However, the sparseness of data used to plot this curve makes the relation very tenuous, and in practice it is probably better to use equation 6.6 for predicting volume loss.

It should be noted that the empirical nature of equation 6.6 implies that it predicts the "average" settlement to be expected over a shield driven tunnel using "normal" construction methods. Any unusual features in the construction of the tunnel may alter this volume of ground loss. In particular, it is to be expected that any factors causing a delay in the grouting up of the rings will result in significantly greater ground loss, and conversely it may be possible to reduce the settlement volume by grouting earlier than is normal practice.

6.3) Ground movement vectors

As discussed in Section 6.2 it would appear that the stochastic model will adequately predict movements at the ground surface, particularly settlement, from a knowledge of the volume of lost ground. No consideration has yet been given to the nature of the sub-surface movement, as described by the inclinometer and magnetic settlement ring data.

Inclinometer data in a direction parallel to the tunnel centre-line indicates that as the face approaches, the ground directly ahead of the face moves inwards towards the tunnel. Only slight movements are noted above or to the sides of the tunnel. By the time settlement is complete, little movement parallel to the centre-line is visible except very close to the tunnel itself where movement is generally apparent in the direction of tunnel advance. It is considered, therefore, that apart from in the distorted zone directly around the tunnel, movements parallel with the centre-line may reasonably be ignored in any consideration of the ultimate, or final, state of the ground around the tunnel (that is, it would appear that ground loss into the tunnel face, parallel to the centre-line, is ultimately translated into movement in a plane perpendicular to the centre-line). This assumption has commonly been made in the literature (Schmidt, 1967; Peck, 1972; Attewell, 1977) and plane strain conditions have been assumed in the development of the stochastic model in Chapter 2.

In order to clarify the general nature of the movements in the plane perpendicular to the centre-line, vector diagrams have been drawn for the data from Green Park (Figure 6.9), Hebburn (Figure 6.10) and Willington Quay (Figures 6.11 and 6.12). No vector diagrams have been shown for Howdon, due to the lack of adequate sub-surface data. It should be noted that the vectors shown in Figures 6.9 to 6.12 do not represent actual observations, but rather a combination of interpolations from the inclinometer profiles and the settlement ring measurements. This operation enables a regular grid of vectors to be produced, both clarifying the diagrams and simplifying the subsequent construction of contour diagrams (Section 6.3.2). Whilst in this form

the data are not very amenable to quantitative analysis, the vector diagrams do provide a convenient and clear visual impression of the nature of the overall ground movements around these tunnels.

The vector diagrams show movement generally downwards and inwards, towards the tunnel, as would be expected. Both at Hebburn and at Willington Quay (23 days) vertical and horizontal movements are of the same order of magnitude with vertical movements predominating, particularly towards the ground surface. At Green Park horizontal movements appear to be much smaller than vertical settlements. It should be noted however that in this case the horizontal displacements, being extrapolated from inclinometer profiles, are therefore relative to datum points at the ground surface. If any inward surface movement occurred at Green Park, and was not detected, then the resulting inclinometer profiles would underestimate the horizontal displacements, causing the vectors apparently to tend to the vertical.

The Willington Quay 149 day vectors tend to be more vertical than those at 23 days, particularly close to the tunnel. This would tend to confirm the notion that consolidation has taken place. It is to be expected that ground movements due to consolidation would be primarily vertical, and that these movements would occur in the drained zone around the tunnel (Chapter 3). The transmission of this movement to the surface would be expected to result in both vertical and lateral movements, in a similar way to those caused by normal ground loss, these movements developing above the consolidating zone.

Just above the "shoulders" of the tunnel the displacement vector can be seen to be directed slightly outwards (Figure 6.12). The

vertical extent of this outward movement is shown more clearly in the inclinometer profile (Figure 5.35). This movement was explained in Chapter 5 as resulting from high-pressure back-grouting of the lining (Section 5.7). The vector diagram shows that this outward movement is still accompanied by downward settlement. Sizer (1975) using the same data produced a series of vector diagrams for various stages in the development of movement around the Willington Quay tunnel. These diagrams indicate that at the time of back-grouting the movement is predominantly outwards, with vertical, consolidation settlement occurring immediately before and immediately afterwards.

It would appear from Figures 6.9 to 6.12 that there is a small amount of downward and inward movement below the level of the tunnel invert. The cause of this movement is unclear. However, its magnitude is small and it is quite possible that it is,in fact,a consequence of the extrapolation procedure, no measurements of settlement having been obtained from this depth.

6.4) Sub-surface ground movement contours

As an alternative method of presenting the data of Section 6.4, contour diagrams of sub-surface movements and strains are presented in Figures 6.13 to 6.25. For each of the four cases (Green Park, Hebburn and Willington Quay 23 days and 149 days) contours of vertical movement, horizontal movement, and total movement have been plotted. Two sets of vertical movement curves are shown for Green Park, since there was a small amount of uplift observed at this site. The contour diagrams of vertical and horizontal movement were extrapolated from the settlement ring data and the inclinometer data by

producing a series of "sections" through the ground along a regular grid in both the horizontal and vertical directions and locating the positions of the intersections of the contour lines with this grid. The same "sections" were also used for the production of the vector diagrams (Section 6.3). In all cases contours have been shown below the level of the tunnel and at distances from the centre-line well beyond the positions of the boreholes. In these areas, where of course there was no observational data, it was necessary to extrapolate the sections by eye, assuming that the displacements in these areas would be tending towards zero. Whilst this procedure is regarded as providing a reasonable estimate of the ground movements, the contour lines in these areas should be regarded as approximate.

6.4.1) Contours of vertical displacement

Contours of vertical displacement for the three sites are shown in Figures 6.13 to 6.17. There is a reasonably close similarity between all of these figures, indicating the same general distribution of vertical displacement in each case. In all cases settlement increases with depth over the centre-line but decreases with depth at distances from the centre-line greater than about 0.3 of the depth to axis. In all cases a small amount of downward movement is indicated below the level of the tunnel invert, this movement reaching a maximum at about 1.5 times the tunnel radius from the centre-line (see Section 6.3). At Willington Quay 23 days (Figure 6.16), the contours just beneath the surface in the vicinity of the centre-line turn more or less horizontal and are fairly close together, indicating a rapid increase in settlement with depth in this area. This phenomenon

is reflected in the ground strain contours and is discussed in Section 6.5.1. The contours for Willington Quay at 149 days (Figure 6.17) indicate clearly the widening of the trough during long term consolidation, and also show that there is no apparent increase in settlement below invert level, where little consolidation would be expected to take place.

6.4.2) Contours of horizontal displacement

Contours of horizontal sub-surface displacement are also shown in Figures 6.14 to 6.17. The contours for Green Park, Hebburn and Willington Quay 23 days (Figures 6.14 to 6.16) all show a characteristic pattern which can perhaps best be described as being similar to a large ear emerging from either side of the tunnel. This indicates the zone of maximum lateral movement, starting approximately at the spring-line of the tunnel and moving outwards and upwards towards the surface. As noted in Chapter 5, the maximum lateral movement at the surface coincides with the point of inflection of the settlement profile. If this is also the case below the surface then the contours would appear to show that the width of the trough, as indicated by the point of inflection, does not decrease linearly with depth, as is predicted by the simple stochastic model. This is confirmed by the contours of vertical movement. It may be partly due to the effect of shape of the tunnel (that is, the distribution of ground loss) close to the tunnel itself, and may also indicate that below the surface the maximum lateral movement does not correspond with the point of inflection of the settlement trough. This evidence does suggest that the stochastic model is inadequate to predict sub-surface

movements, in spite of its effectiveness at the surface.

At Green Park the zone of maximum lateral movement appears to rise almost vertically from about invert level, which would imply that at the surface the point of maximum lateral movement falls well inside the point of inflection. As noted in Section 6.2 this is probably due to the underestimation of lateral movements from the inclinometer profiles.

The Willington Quay contours for 23 days (Figure 6.16) show that the maximum lateral movement occurs at some distance above and to the side of the tunnel itself. This may indicate a reduction in lateral movement due to slight "squatting" of the lining or possibly may indicate a slight amount of consolidation close to the tunnel which would tend, of course, to be in a vertical direction.

In all three of these cases, lateral movement appears to extend well below the tunnel invert, this being particularly noticeable at Hebburn (Figure 6.15). The movement appears to extend to a lower level than the vertical displacements, although once again the contours are of a somewhat speculative nature. This movement bdow invert level would tend to confirm that around the tunnel the stochastic model is unable to explain or predict the actual ground behaviour.

The Willington Quay contours for 149 days (Figure 6.17) show the movement away from the tunnel already noted in Section 6.3. Beyond this small zone of outward movement there is only a small amount of lateral displacement, movement below invert level having virtually disappeared. The zone of maximum lateral displacement appears to have migrated upwards towards the ground surface. This general reduction in inward movement at depth may be a response to the high-pressure back-grouting discussed in Section 6.3, the continuing settlement being due

entirely to consolidation processes. Conversely, the increase in lateral movement at depths down to about 8 m indicates a normal settlement response in this zone. Volumetric strain contours (Section 6.6.2) tend to confirm this view.

6.4.3) Contours of total displacement

The contours of total ground displacement, shown in Figures 6.18 to 6.21, are somewhat more difficult to interpret than those of settlement or lateral displacement. At Green Park, Hebburn and Willington Quay 23 days maximum movement occurs in the crown and around the "shoulders" of the tunnel, decreasing towards the invert as would be expected. The Willington Quay contours for 149 days (Figure 6.21) show maximum movement occurring at a depth of 4 m, well above the tunnel soffit. This is due to the consolidation of the deeper ground around the tunnel. The widening of the zone of influence between 23 days and 149 days is very apparent from these contours.

The total displacement contours can be considered to delineate the "zone of influence" of the tunnel. This zone can be seen at Hebburn to be quite wide at axis level, in comparison with the other cases. It is indicative of the anisotropic nature of the laminated clay in which the tunnel was excavated.

6.5) Sub-surface strain contours

Contours of vertical strain can be calculated by differentiating settlement along the vertical direction and similarly those of horizontal strain by differentiating lateral strain horizontally. This procedure was carried out graphically on the same "sections" used to

produce the displacement contours, since strain was not measured directly. This method of estimating strain must inevitably introduce further errors, as the contour plots should only be regarded as an approximate guide to the actual ground strain. Volumetric strain is calculated by summing the vertical and horizontal strains.

6.5.1) Contours of horizontal and vertical strain

Contours of vertical and horizontal strains are shown in Figures 6.22 to 6.25. Both sides of the diagram, vertical and horizontal strain for each site, should be considered in conjunction. As was discussed in Chapter 2, the "inward" nature of the lateral movement implies that the ground within the inflection points of the settlement profile should be laterally compressed, whilst that outside the inflection points should be in tension in the horizontal sense. This appears approximately to be the case at Green Park, Hebburn and Willington Quay 23 days (Figures 6.22 to 6.35). The narrowness of the compressive zone above the Green Park tunnel would be explained by the underestimation of lateral movements. At Hebburn (Figure 6.26) there appears to be a compressive zone beneath the tunnel. It may be in some way related to the anisotropic nature of the laminated clay encouraging lateral movement even beneath the tunnel, or may, on the other hand, simply be an error caused by extrapolation of the data below the bases of the boreholes.

The tensile, or expansive nature of the vertical strain at the tunnel at Green Park and Hebburn (Figures 6.22 and 6.23) is a result of increasing settlement with depth, the compressive zones at either side indicating the reverse. The contours of vertical displacement at Willington Quay (23 days) (Figure 6.24) are rather more complex. As in the above two cases, the ground dilates vertically above the tunnel

as is to be expected. The tensile zone directly below the surface above the centre-line may possibly be due to a certain degree of "arching" of the pavement structure beneath which these measurements were taken. The reason for the compressive zone approximately midway between the surface and the tunnel is unclear. It could result from an anomalously low reading from one of the centre-line settlement rings, which would be quite feasible if coupling between the ring and the ground were poor.

Figure 6.25 shows lateral and vertical strain contours for Willington Quay at 149 days. Contours of lateral strain indicate a compressive zone around the sides of the tunnel, presumably due to the high pressure back-grouting carried out at 71 days (Chapter 5). Zones of high compressive and tensile strain can be seen at a depth of around 4 m. In this area vertical strains are quite low. The relation between the tensile and compressive zones at this point indicates a localised inward movement of the ground towards the centre-line. This localisation suggests the possibility of an erroneous measurement of lateral displacement at this point, possibly caused by distortion of the inclinometer tube. Conversely, at the level of the lower part of the tunnel a zone of positive vertical strain can be seen stretching about 2 tunnel diameters away from the centre-line. This is thought to delineate the area in which consolidation has occurred. The dilating zone just beneath the surface is still visible, although the maximum strains are lower, so indicating some breakdown of the arching effect of the road surface.

6.5.2) Contours of volumetric strain

Contours of volumetric strain for the three locations are shown along with total displacement contours in Figures 6.18 to 6.21. These diagrams were constructed by summing the contours for horizontal and vertical strain. In these diagrams positive strains represent compression of the ground whilst negative strains show dilation. In the cases where no consolidation is expected (Figures 6.18 6.18 to 6.20) these strains are fairly low, reaching a maximum of 0.8% at Willington Quay (Figure 6.20), 0.4% at Hebburn (Figure 6.19) and only 0.2% at Green Park (Figure 6.18). Nevertheless, this does indicate that a small degree of volumetric change does occur above these tunnels, contrary to the assumptions in the stochastic theory. At Green Park there appears to be compression directly above the tunnel, up to about 8 m below the surface, dilation above and to the sides of this, and another zone of compression beyond the dilational zone. These contours are, of course, influenced by the measurements of lateral displacement. If these measurements were erroneously low (Section 5.4) we would then expect the true contours of volumetric strain to be displaced laterally, away from the tunnel centre-line, relative to those shown in Figure 6.18, resulting in a wider zone of compression above the tunnel, and possibly removing the outer compressive zone altogether.

At Hebburn (Figure 6.19) the contours indicate a compressive zone above the tunnel, extending up to the surface, another compressive zone below, and to the sides of the tunnel, with a dilation zone outside these. Above axis level this corresponds with the pattern proposed for Green Park. The compressive zones at either side of the tunnel are due primarily to the vertical strains noted in Section 6.5.1. In both cases,

volumetric strain at, and close to, the ground surface is extremely low, reaching a maximum of approximately 0.05% at Hebburn, and indicating that the stochastic relationships proposed in Chapter 2 hold good in this zone.

At Willington Quay (Figures 6.20 and 6.21), where consolidation is thought to have taken place, the picture is rather more complicated. At 23 days (Figure 6.20) the strains are quite low in magnitude. The tensile zone directly beneath the centre-line at the surface, noted in Section 6.5.1 is still visible, along with a dilation zone directly above the tunnel, presumably caused by continuing ground collapse into voids around the tunnel due to the extremely weak nature of the soil. Apart from the dominantly vertical strains around the centre-line, strains at the surface are once again very low.

The contours at 149 days (Figure 6.21) show the zone of compressive strain to either side of the tunnel where consolidation is presumed to have taken place, a maximum volumetric strain of 2.4% occurring. The zones of high strain at 4 m below the surface probably represent an erroneous measurement of lateral displacement (see Section 5.4). Disregarding this localised disturbance, the rest of the ground at depth is generally in compression, as would be expected if consolidation has taken place. As can be seen by a comparison between Figures 6.25 and 6.21, this strain is principally in the vertical direction.

6.6) Consolidation at Willington Quay

As was discussed in Section 6.5.2 the zones of high volumetric strain at the sides of the tunnel observed at Willington Quay (Figure

6.21) may well represent consolidation of the silt, a notion supported to some extent by the very long-term nature of the settlement. In Figure 6.26 centre-line surface settlement is plotted against log time. It is quite clear that on removal of the air pressure from the tunnel the curve steepens and becomes approximately linear if allowance is made for the uplift at 160 days. This is very similar to the form of curve obtained from a standard consolidation test.

It is possible to calculate the amount of consolidation settlement to be expected at Willington Quay using equation 3.14 of Chapter 3. We assume a compression index of 0.3 and a void ratio of 1 for the silt, and calculate the compression of a layer of silt 5 m thick (approximately the thickness of the zone of high volumetric strain). The piezometer at axis level indicated a fall in pressure due to the removal of the compressed air of approximately 22 kN/m^2. If we regard this as equivalent to the increase in effective stress, then:

$$S = \frac{5 \times 0.3}{2} \log_{10} \frac{(205 + 22)}{205}$$

$$= 33 \text{ mm}$$

The observed consolidation settlement is approximately 50 mm. Taking into account the approximate nature of the assumptions involved in the above calculation the agreement is considered to be quite reasonable. The fact that the predicted value is lower than the measured settlement may be partly due to the fact that some degree of consolidation occurred outside the zone of high volumetric strain and that not all of the 60 mm long-term settlement was due to consolidation.

Depth to axis (Z)	=	7.5 m
Diameter (D)	=	2.014 m
Z/D	=	3.72
Maximum settlement (S max)	=	7.9 mm
Point of inflection (i)	=	3.9 m
Settlement volume (V_s)	=	0.077 mm/m advance
	=	2.42%
Maximum lateral surface movement (S_h max)	=	3 mm (estimated)
Maximum lateral surface strain (E max)	=	unmeasurable
Maximum surface tilt (T max)	=	0.13%
Maximum settlement rate (ds/dt)	=	0.13 mm/hr
Maximum intrusion rate (de/dt)	=	0.221 mm/hr
C_u of laminated clay	=	73.2 kN/m^2
Bulk density of stony clay	=	2.1 Mg/m^3
Bulk density of laminated clay	=	1.9 Mg/m^3
Overburden stress at axis level	=	148 kN/m^2
Stability ratio (OFS)	=	2.02
Advance rate - average	=	0.11 m/hr
Advance rate - maximum	=	0.18 m/hr

Table 6.1.

Summary of observations - Hebburn

Depth to axis (Z)	=	13.375 m
Diameter (D)	=	4.25 m
Z/D	=	3.15
Maximum settlement (S max)	=	23.5 mm (23 days)
	=	81.5 mm (ultimate)
Point of inflaction (i)	=	6.1 m - 8.5 m
Settlement volume (V_s)	=	0.365 m^3/m } 23 days
	=	2.57% }
	=	1.74 m^3/m } ultimate
	=	12.27% }
Maximum lateral surface movement (S_h max)	=	12 mm
Maximum lateral surface strain (E max)	=	0.23%
Maximum surface tilt (T max)	=	0.55%
Maximum rate of settlement (ds/dt)	=	0.095 mm/hr
Average intrusion rate (from lab tests) (de/df)		30 mm/hr
C_u of silt	=	25.4 kN/m^2
Bulk density of silt	=	1.82 Mg/m^3
Overburden stress at axis level	=	239 kN/m^2
Air pressure	=	90 kN/m^2
Stability ratio (OFS) without air pressure	=	9.5
with air pressure	=	5.95
Advance rate - average	=	0.06 m/hr
- maximum	=	0.1 m/hr

Table 6.2

Summary of observations - Willington Quay

Depth to axis (Z)	=	14.18 m
Diameter (D)	=	3.625 m
Z/D	=	3.91
Maximum settlement (S max)	=	11.2 mm
Point of inflection (i)	=	6.9 m
Settlement volume (V_s)	=	0.21 m^3/m advance
	=	2.07%
Maximum lateral surface movement (S_h max)	=	5 mm
Maximum lateral surface strain (E max)	=	0.14%
Maximum surface tilt (T max)	=	0.098%
Maximum rate of settlement (ds/dt)	=	0.03 mm/hr
Maximum intrusion rate (estimated) (de/dt)	=	0.06 mm/hr
C_u of stony clay	=	100 kN/m^2
Bulk density of stony clay	=	2.1 Mg/m^3
Overburden stress at axis level	=	292 kN/m^2
Stability ratio (OFS)	=	2.92
Advance rate - average	=	0.068 m/hr
Advance rate - maximum	=	0.15 m/hr

Table 6.3

Summary of observations - Howdon

Depth to axis (Z)	=	30 m
Diameter (D)	=	4.15 m
Z/D	=	7.23
Maximum settlement (S max)	=	6 mm
Point of inflection (i)	=	15 m
Settlement volume (V_s)	=	0.23 m^3/m
	=	1.7%
Maximum lateral surface movement (S_h max)	=	Unmeasured
Maximum lateral surface strain (E max)	=	Unmeasured
Maximum surface tilt (T max)	=	0.033%
Maximum rate of settlement (ds/dt)	=	0.042 mm/hr
Average intrusion rate (estimated) (de/dt)	=	0.0055 mm/hr
C_u of London Clay	=	214.6 kN/m^2
Bulk density of London Clay	=	1.92 Mg/m^3
Overburden stress at axis level	=	565 kN/m^2
Stability ratio (OFS)	=	2.6
Advance rate - average	=	0.116 m/hr
Advance rate - maximum	=	0.148 m/hr

Table 6.4

Summary of observations - Green Park

Tunnel	Tunnel Data			Settlement			Settlement Trough									
	Axis Depth z, m	Dia. 2a, m	z/2a	Surface δ_{vmax}, mm	Crown δ_{vmax}, mm	Volume V_s, m^3/m	i, m	i/z	m 2.51, m	Slope of surface Transverse	Forward	Surface strain Transverse Comp.	Transverse Tens.	Forward Comp.	Forward Tens.	Horiz. displ. δ_{hmax} mm
A. London Transport Fleet Line, Green Pk (Attewell & Farmer, 1974, a,b).	29.3	4.15	7.06	6.17	17	0.19 (1.6%)	12.6	6.1	32 (β=46°)	1:5000 av. 1:4000 max	1:5000 av.					
B. N.W.A.Sewerage Scheme Tyneside, Hebburn. (Attewell et al, 1975)	7.5	2.01	3.7	7.86	12	0.077 (2.4%)	3.9	3.7	4.75 (β=50°)	1:1600 av. 1:757 max.	1:1200 av.					
C. N.W.A.Sewerage Scheme Tyneside, Willington Quay Siphon, Contract 52. (Attewell & Farmer 1976).	13.375	4.25	3.15	81.5		1.86 (13.4%)	9.1	4.28	22.7 (β=57°)	1:182 max.		0.23%	0.15%			12
D. N.W.A.Sewerage Scheme, Tyneside, Howdon. (Glossop, 1976)	14.18	3.625	3.91	11.2		0.194 (1.4%)	6.9	3.8	17.25 (β=47°)	1:1020 max.	1:1750 max	0.1%				5
E. London Transport Fleet Line, Regent's Pk. Northbound Tunnel (Barratt & Tyler, 1976)	20	4.15	4.7	7	16	0.48 (1.3%)	10.3	4.96	25.75 (β=50°)	1:5000 av. 1:2325 max.						
F. London Transport Fleet Line, Regent's Pk. Southbound tunnel (Barratt & Tyler, 1976)	34	4.15	8.2	5	11	0.13 (1.4%)	15.2	7.32	36.0 (β=47°)	1:5000 av. 1:3571 max.						
G. London Transport Experimental tunnel, New Cross (Bodon & McCaul, 1976).	10	4.15	2.4	21.5	21		5	1.52	12.5 (β=66°)		1:1.5 max.					
H. TRRL Tunnelling trials Chinnor. (McCaul et al, 1976).	8	5	1.6	8	22.3		7	1	17.5 (β=?)	1:826 max.	1:1076 max.					
I. Washington D.C.Metro Lafayette Square (Butler & Hampton, 1975)	11.6	6.4	2.25	114.8	335-410	1.21 (1.8%)	4.5	1.4	11.25 (β=35°)							
J. Washington D.C.Metro Project A-2 1st tunnel																
C line	14.6	6.4	2.3	152	365	1.7	4.5	1.4	11.25 (β=28°)	1:75 av. 1:50 max.	1:50	1:75	1:150			
B line	14.6	6.4	2.3	134		1.5	4.2	1.3	11	1:75 av. 1:50 max.	1:60					
A line (Ranseire, 1975)	14.6	6.4	2.3	76		1.0 (1.5%)	3.4	1.7	14 (β= 36°)	1:180 av 1:160 max.	1:200					
K. Washington D.C.Metro Treasury Yard (Ranseire, 1975)	11.6	6.4	1.8	280	350	1.4 (4.3%)	1.3	0.6	5 (β=0°)	1:18 av. 1:15 max.						
L. Washington D.C.Metro 1st tunnel Section a	20.9	6.4	3.3	6	14	0.1	5.1	1.6	12 (β=23°)	1:2000 av.	1:2000 1:1400					
Section b (MacPherson, 1975)	23	6.4	3.6	3	52	<0.1 (0.3%)										
M. Frankfurt Shield, Fohrgasse (T-9) (Chambosse, 1972; Sauer & Lame, "?"; Breth & Chambosse, 1972).	12.1	6.5	1.9	70	140	0.86 (2.6%)	4.9	1.5	12 (β=35°)	1:172 av. 1:60 max.	1:100					
N. Frankfurt Shield, Domplatz (authors as in M)	15	6.5	2.3	21	52	0.24 (1.2%)	6.0	2.1	17 (β=42°)	1:700 av. 1:500 max.						
O. Frankfurt Shield, Dominikanergasse (authors as in M)	10.5	6.5	1.6	140	-	1.46 (4.1%)	3.9	1.2	10 (β=33°)	1:70 av. 1:30 max.						
P. Frankfurt,no shield, Baulos 17 (authors as in M)	15.3	6.5	2.1	13	17	0.25 (0.7%)	7.1	2.2	18 (β=48°)							
Q. Frankfurt,no shield, Baulos 16a, Tunnel 13 (Authors as in M)	15.3	6.5	2.5	10	18	0.18 (0.5%)	7.1	2.2	18 (β=43°)	1:800 av.						
R. Heathrow Cargo Tunnel (Wood & Gibb, 1971; Smyth-Osbourne, 1971).	13.3	10.9	1.2	12	14	0.19 (0.2%)	6.5	1.2	16 (β=38°)	1:1000av.						
S. Boa Vista, Sao Paulo. (Costa et al, 1974)	11.8	5.5	2.2	70	74	1.2 (5%)	6.9	2.5	17 (β=50°)	1: 210 av.						
T. Brussels Metro (Vinzel & Herman 1969)	16	10	1.6	150	-	2.0 (2.5%)	5.5	1.1	13 (β=21°)							
U. Mexico City, Siphon II, Manuel Gonzales. (Tinajero & Vieites, 1971).	11.7	2.9	4	105	170	2.1 (5%)	7.8	5.4	20 (β=58°)	1:150 av.						
V. Lower Market St., B.A.R.T., San Francisco (Kuesel, 1972)	19	5.5	3.4	36	-	0.64 (2.7%)	6.9	2.5	17 (β=37°)	1:500 av.	1:300 - 1:500					
W. Washington, D.C. Metro, F2a-1 route tunnels. (Cording et al, 1976).																
1 IB	20.3	5.5	3.7	5	30	0.12 (0.5%)										
5 IB	20.3	5.5	3.7	3	23	0.07 (0.3%)										
9 IB	22.5	5.5	4.1	8	53	0.2 (0.8%)	8.52	3.1	21 (β=39°)	1:2500 av.	1:2500					
10 IB	21.4	5.5	3.9	13	-	0.32 (1.3%)			26	1:1500 av.						
11 IB	22.0	5.5	4.0	10	18	0.23 (1.0%)	9.90	3.6	25 (β=45°)	1:2500 av.	1:1800					

Table 6.5 (continued overleaf)

after Attewell (1977)

Tunnel	Diameter 2a metres	Depth z metres	Ground Description	Geotechnical Properties	Construction Method and Lining
A. London Transport Fleet Line Green Pk. (Attewell and Farmer, 1974 a,b).	4.15	29.3	Stiff, fissured, overconsolidated London Clay. Tunnel horizon blue clay overlain by weathered brown clay.	c_u = 270 kN/m^2 $\frac{z}{c_u}$ = 2.1	Shield construction. Cast iron lining. 7 segments per ring, erected in shield tail. Annulus behind rings contact grouted after every shove.
B. N.W.A. Sewerage Scheme, Tyneside, Hebburn (Attewell et al., 1975)	2.01	7.5	Laminated clay overlain by stony clay.	c_u = 75 kN/m^2 $\frac{z}{c_u}$ = 2.02	Shield construction. 5 segment precast concrete lining per ring erected in shield tail. Annulus behind rings contact grouted every three rings.
C. N.W.A. Sewerage Scheme Tyneside, Willington Quay Siphon, Contract 32 (Attewell & Farmer, 1967).	4.25	13.375	Silty alluvium/alluvial clay with sand and gravel lenses containing water at artesian pressure.	c_u = 33 kN/m^2 $\frac{z}{c_u}$ = 9.4; $\frac{z - \sigma_i}{c_u}$ = 5.9	Shield construction. Compressed air pressure 90 kN/m^2. 7 segment pre-cast concrete lining per ring erected in shield tail. Annulus behind rings contact grouted every three rings.
D. N.W.A. Sewerage Scheme, Tyneside, Howdon (Glossop, 1977)	3.625	14.18	Boulder/stony clay.	c_u = 100 kN/m^2 $\frac{z}{c_u}$ = 2.92	Shieldless construction. 5 segment pre-cast concrete lining per ring erected up to the face. Annulus behind rings contact grouted every three rings.
E. London Transport Fleet Line Regent's Park Northbound tunnel (Barratt & Tyler, 1976)	4.15	20	Stiff, fissured, overconsolidated London Clay.	c_u = 230 kN/m^2 $\frac{z}{c_u}$ = 1.70	Shield construction. Expanded concrete segmental lining.
F. London Transport Fleet Line Regent's Park Southbound tunnel (Barratt and Tyler, 1976).	4.15	34	Stiff, fissured overconsolidated London Clay.	c_u = 230 kN/m^2 $\frac{z}{c_u}$ = 1.70	Shield construction. Expanded concrete segmental lining.
G. London Transport Experimental tunnel, New Cross (Bodem and McCaul, 1974)	4.15	40	Sandy gravel.	-	Slurry (bentonite) shield.
H. T.R.R.L. Tunnelling trials at Chinner (Bignell & Bodem, 1976; McCaul et al., 1976).	5	8	Highly discontinuous Lower Chalk formation.	-	Full face tunnelling machine, cruciform head with drag picks jacking against a two-section reaction ring. Lining comprised mining arches at 1 metre spacing.
I. Washington D.C. Metro, Lafayette Square (Butler and Hampton, 1975).	6.4	11.6	Sand and gravel with interbedded silty sand, sand and clay.	c = 48-96 kN/m^2 ϕ = 25°-36° $\frac{z}{c_u}$ = 3.3 (estimated)	Shield construction with bucket digger. Primary liner of steel ribs and hardwood lagging boards expanded during and after the shove. Sand-cement-bentonite grout injected originally through liner but later through crown of shield at the front.
J. Washington D.C. Metro Project A-2. C line, B line A line (Hanamire, 1975)	6.4	14.6	Medium dense silty sand and gravel, interbedded with sandy, silty clays.	c_u = 75 kN/m^2 $\frac{z}{c_u}$ = 4	Shield construction with bucket digger. Primary liner of steel ribs and timber lagging expanded during and after the shove. Partial de-watering with wells 60m apart on centre line.
K. Washington D.C. Metro, Treasury Yard (Hanamire, 1975)	6.4	11.6	Medium dense silty sand and gravel interbedded with sandy silty clays.	c_u = 75 kN/m^2 $\frac{z}{c_u}$ = 3	Shield construction with ripper bucket digger. Primary liner of steel ribs (four-section) placed on 4ft centres with full timber lagging. Lining expansion during and after shove.
L. Washington D.C. Metro, 1st tunnel Section a Section b (MacPherson, 1975)	 6.4 6.4	 20.9 23	Dense sand and gravel, very dense, slightly cemented sand.	-	Articulated shield with bucket digger. Steel segments erected in tailskin and grouted before shove.
M. Frankfurt Shield, Fahrgasse (T-9) (Chambosse, 1972; Sauer & Lamm, 1973; Breth and Chambosse, 1972).	6.5	12.4	Sand with some limestone and clay marl lenses.	-	Shield construction. Bolted concrete segments.
N. Frankfurt Shield, Doeplatz (authors as in M)	6.5	15	Frankfurt clay marl with some limestone and sand lenses.	c_u = 130-550kN/m^2 $\frac{z}{c_u}$ = 0.6 - 2.5	Shield construction. Bolted concrete segments.
O. Frankfurt Shield, Dominikanergasse (authors as in M)	6.5	103	Sand with some limestone and clay marl lenses.	-	Shield construction. Bolted concrete segments.
P. Frankfurt, no shield, Baulos 17 (authors as in M)	6.5	13.3	Frankfurt clay marl with some limestone and sand lenses.	c_u = 130-550kN/m^2 $\frac{z}{c_u}$ = 0.6-2.5	Shieldless construction: heading and bench. Soil anchors: shotcrete and light steel ribs for support.
Q. Frankfurt, no shield, Baulos 16a Tunnel 1; (authors as in M)	6.5	16	Frankfurt clay marl with some limestone and sand lenses.	c_u = 130-550kN/m^2 $\frac{z}{c_u}$ = 0.6-2.5	Shieldless construction: heading and bench. Soil anchors: shotcrete and light steel ribs for support.
R. Heathrow Cargo Tunnel (Wood and Gibb, 1971; Smyth-Osbourne, 1971)	10.9	13.3	Upper section of London Clay with 3.5m of clay cover under wet gravel.	c_u = 72-275kN/m^2 $\frac{z}{c_u}$ = 1 to 4	Shield construction and hand excavated. No tail to the shield - concrete segmental lining expanded behind shield.
S. Boa Vista, São Paulo (Costa et al., 1974)	5.5	11.8	Sand and clay lenses.	-	Shield construction with compressed air.
T. Brussels Metro (Vannel and Herman, 1969)	10	16	Upper half of tunnel - uniform, cohesionless sand; lower half of tunnel - clayey sand.	-	Shield construction, hand excavated. Lining segments built in tail.
U. Mexico City Siphon II Manuel Gonzales (Tinajero & Violtes, 1971)	2.9	11.7	Plastic lacustrine clay.	c_u = 40 kN/m^2 $\frac{z}{c_u}$ = 5	Shield with oscillating cutters. Steel lining. Lining grouted 8m behind shield. Cutters offer support to three-quarters of face. Ground de-watering before tunnelling.
V. Lower Market St., B.A.R.T., San Francisco (Enzel, 1972)	5.5	19	Soft plastic clay.	c_u = 40 kN/m^2 $\frac{z}{c_u}$ = 14 (estimated)	Shield, with a rotating cutter wheel. Compressed air support. Grouted segmental lining.
W. Washington D.C. Metro F2a-1 route tunnels (Cording et al., 1976) 1 I B 3 I B 9 I B 10 I B 11 I B	 5.5 5.5 5.5 5.5 5.5	 20.3 20.3 22.5 21.4 22.0	Very variable. Medium stiff-to-hard clays: clayey sands - sandy clays: coarse sand and gravel.	-	Articulated (3 segment) shield construction. Excavation by large, half-moon shaped, hydraulically-operated digger spade. Tunnelling below the water table, but ground de-watered by deep well pumping in advance of tunnel construction. Segmented steel lining erected in tail of shield. Serves as both a primary and secondary, or permanent, support.

Table 6.5 (continued) after Attewell (1977)

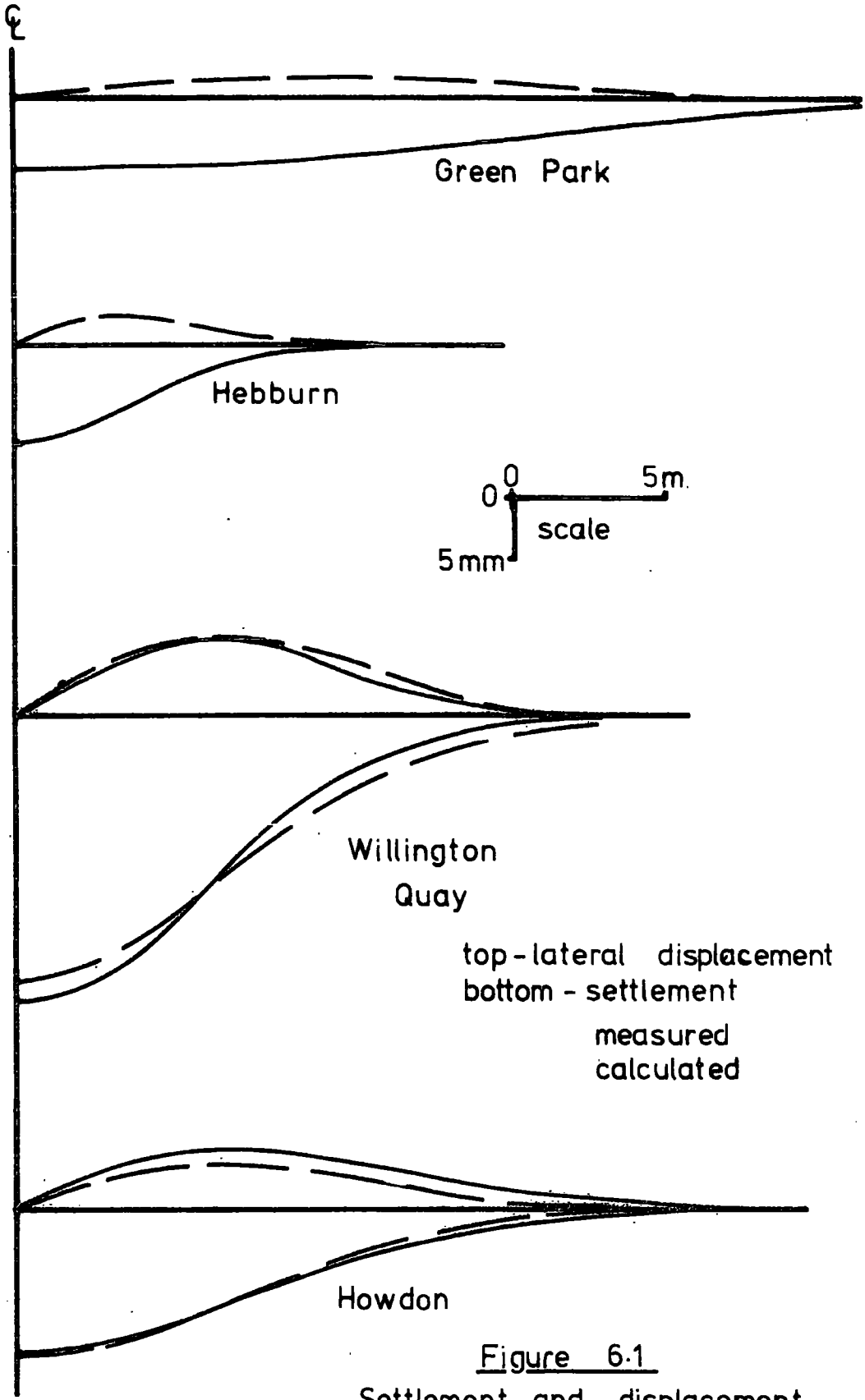

Figure 6.1
Settlement and displacement

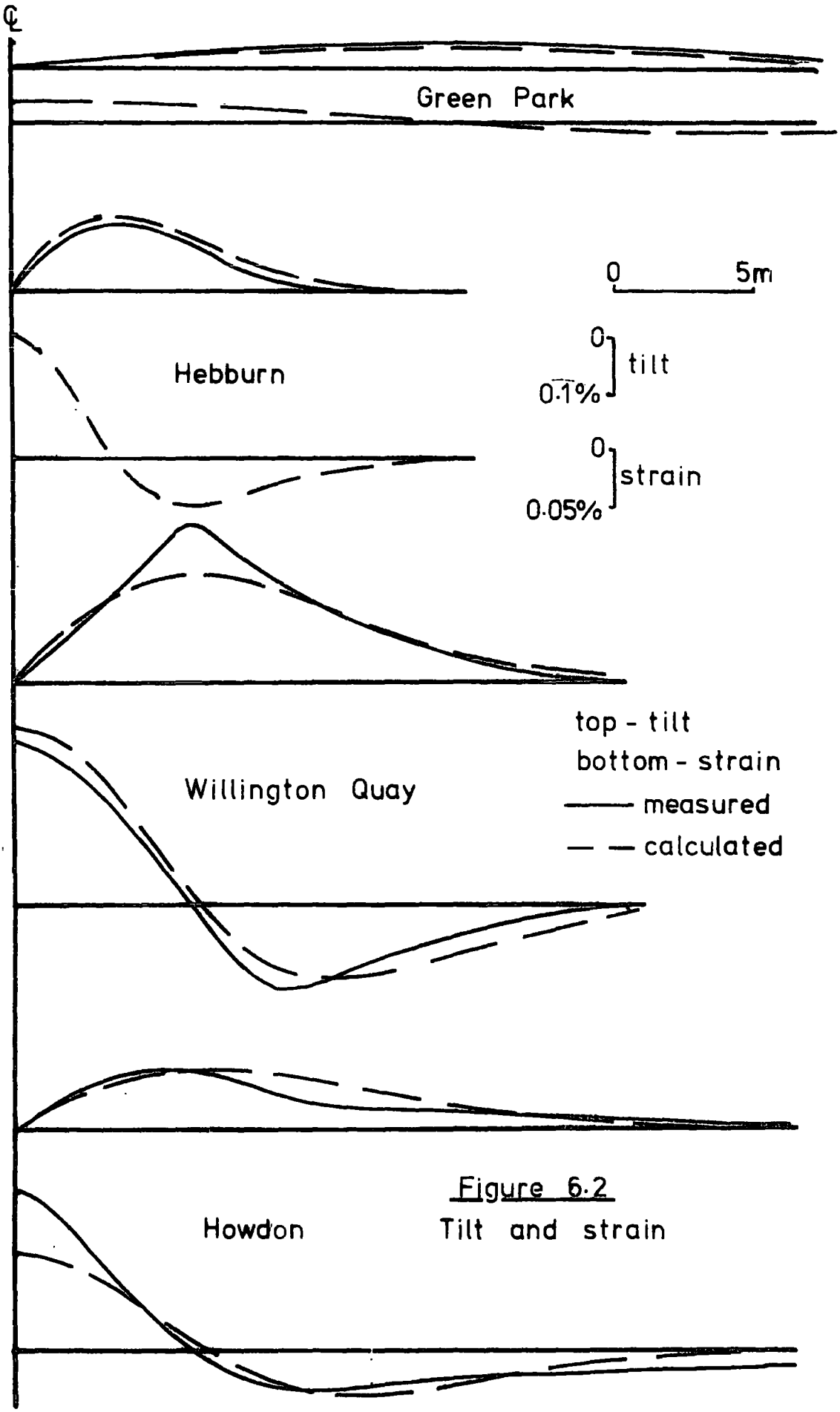

Figure 6·2
Tilt and strain

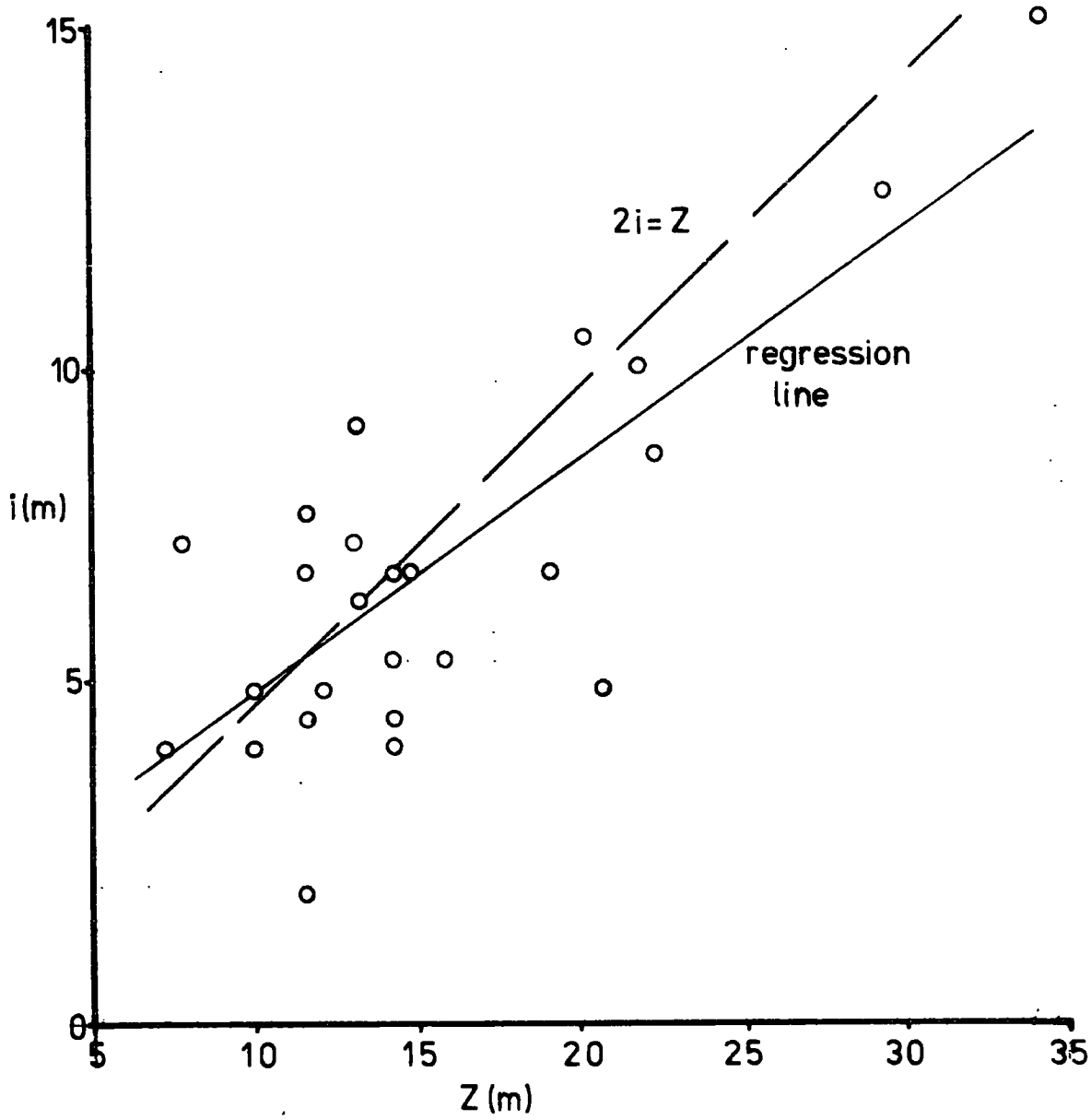

Figure 6.3
i Vs Z

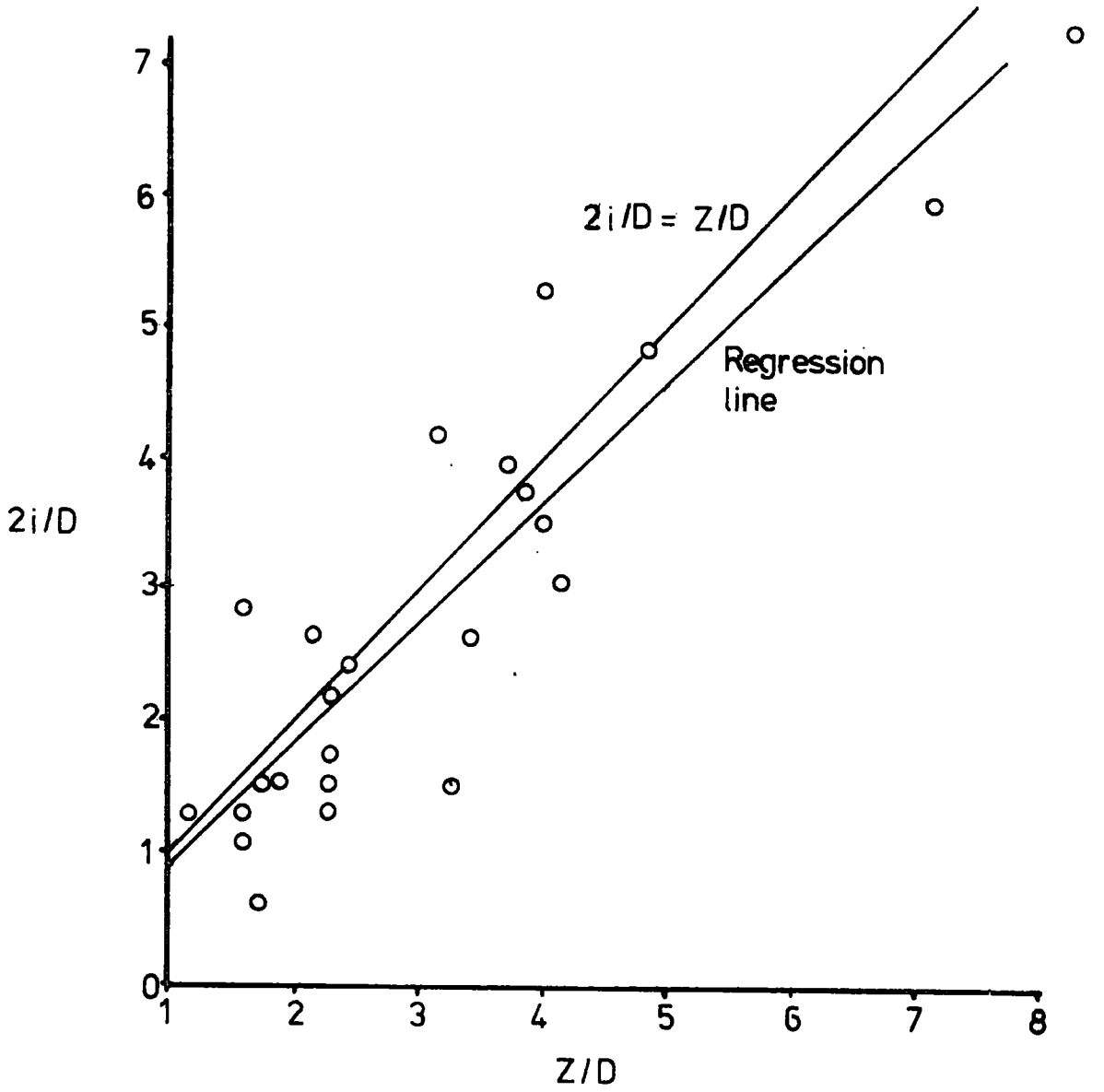

Figure 6.4
2i/D Vs Z/D

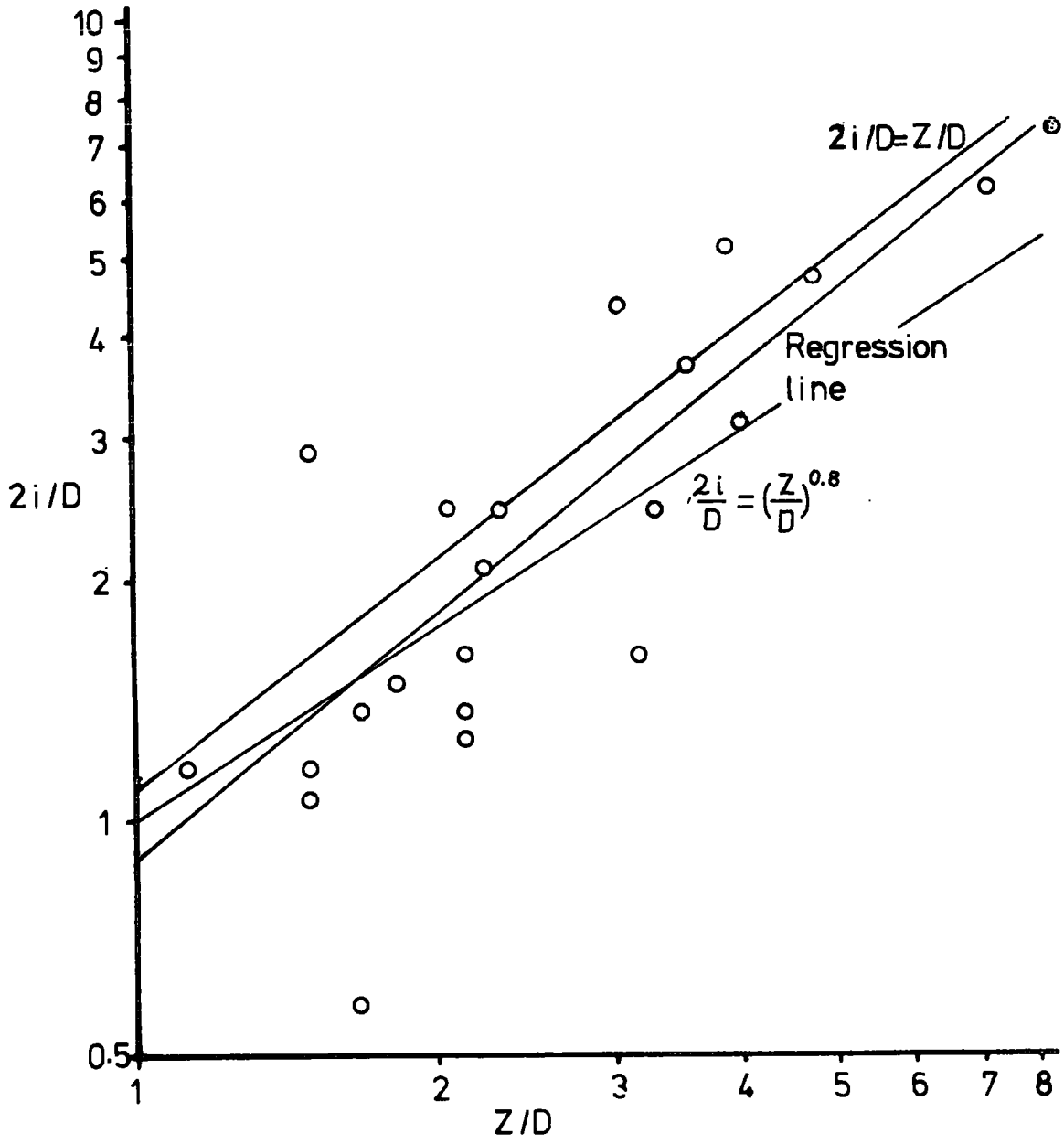

Figure 6.5
Log 2i/D Vs Z/D

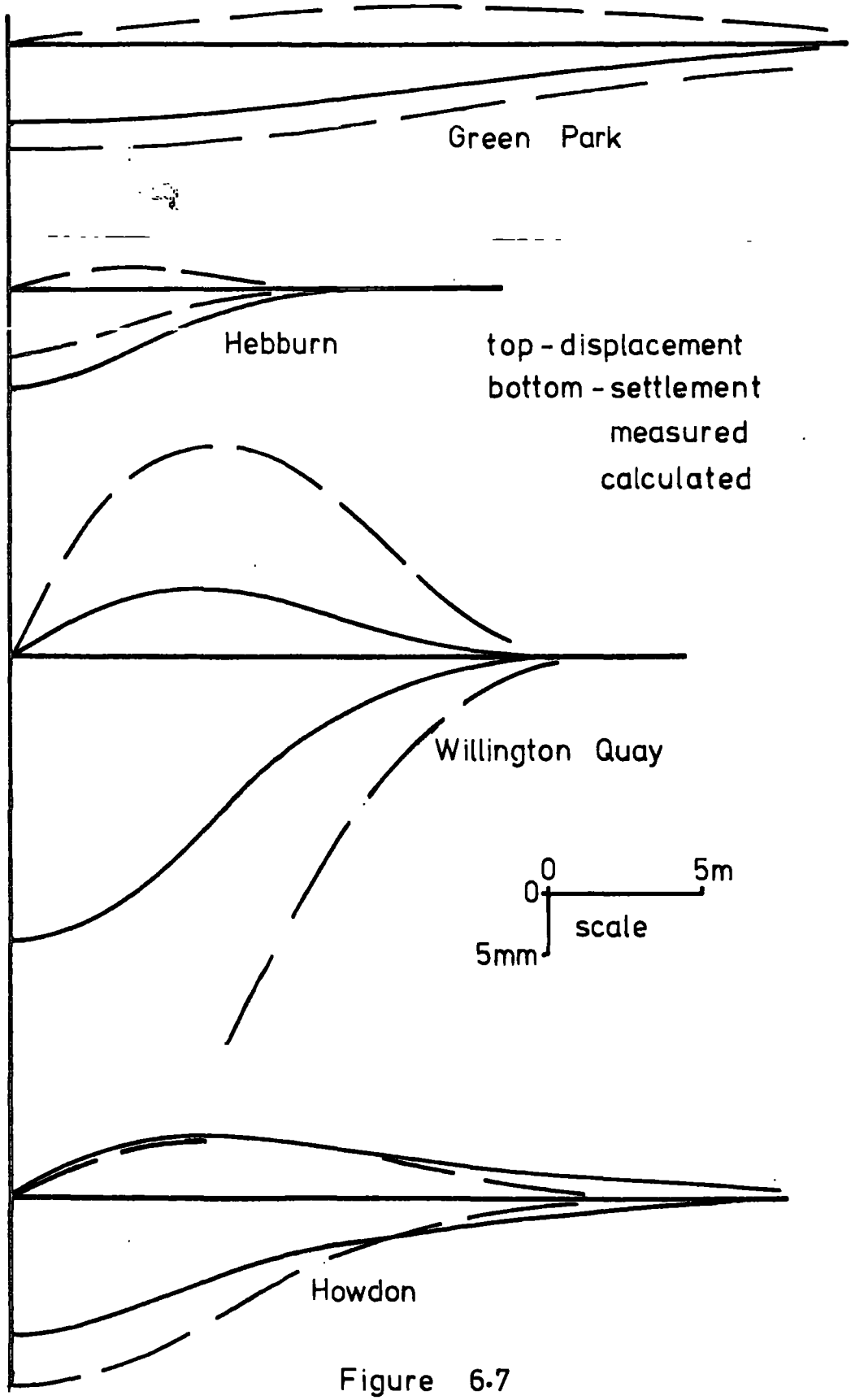

Figure 6.7
Settlement and displacement (2)

Figure 6.8

V_s versus $\frac{OFS}{R_a}(1+\frac{4L}{D})$

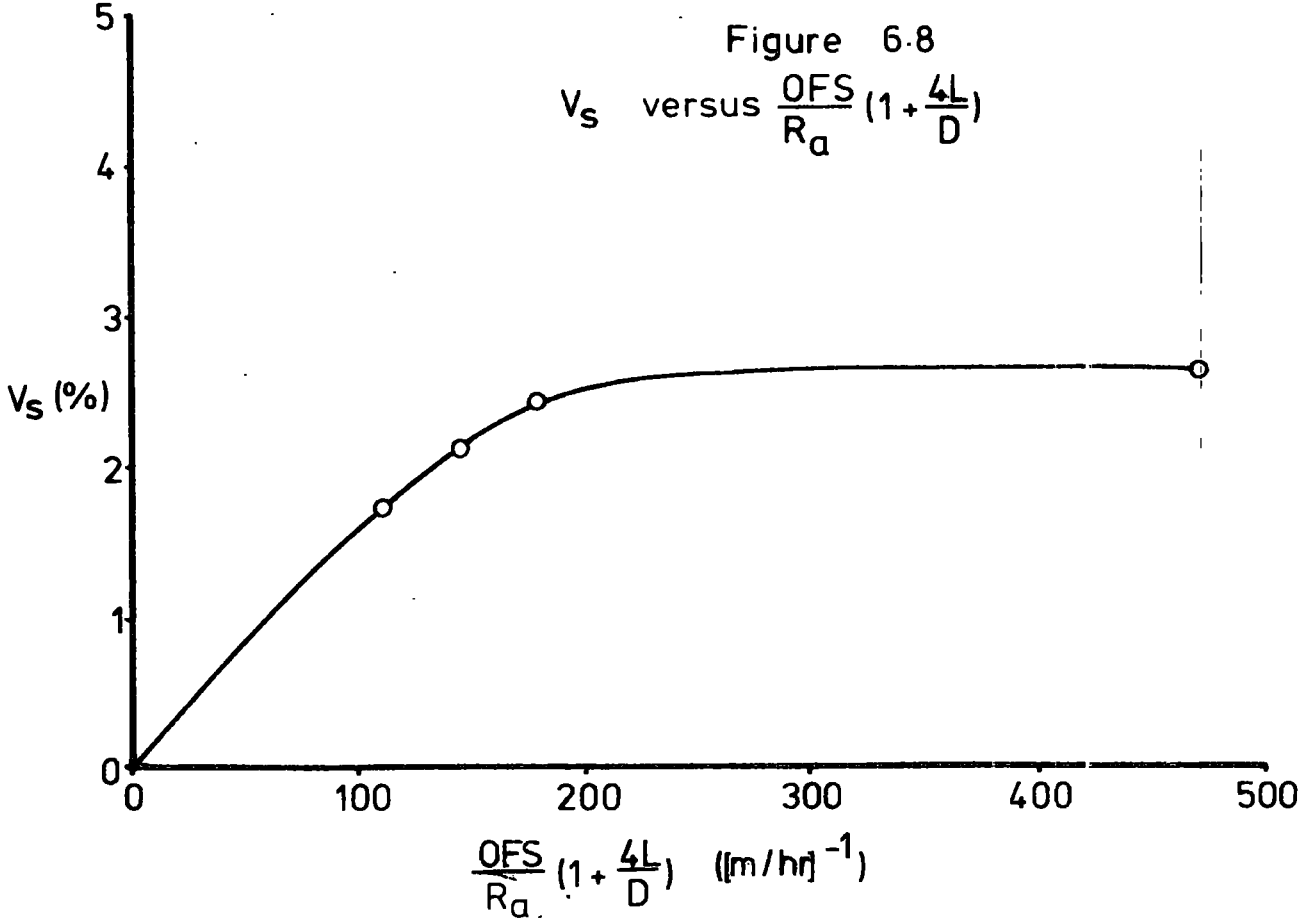

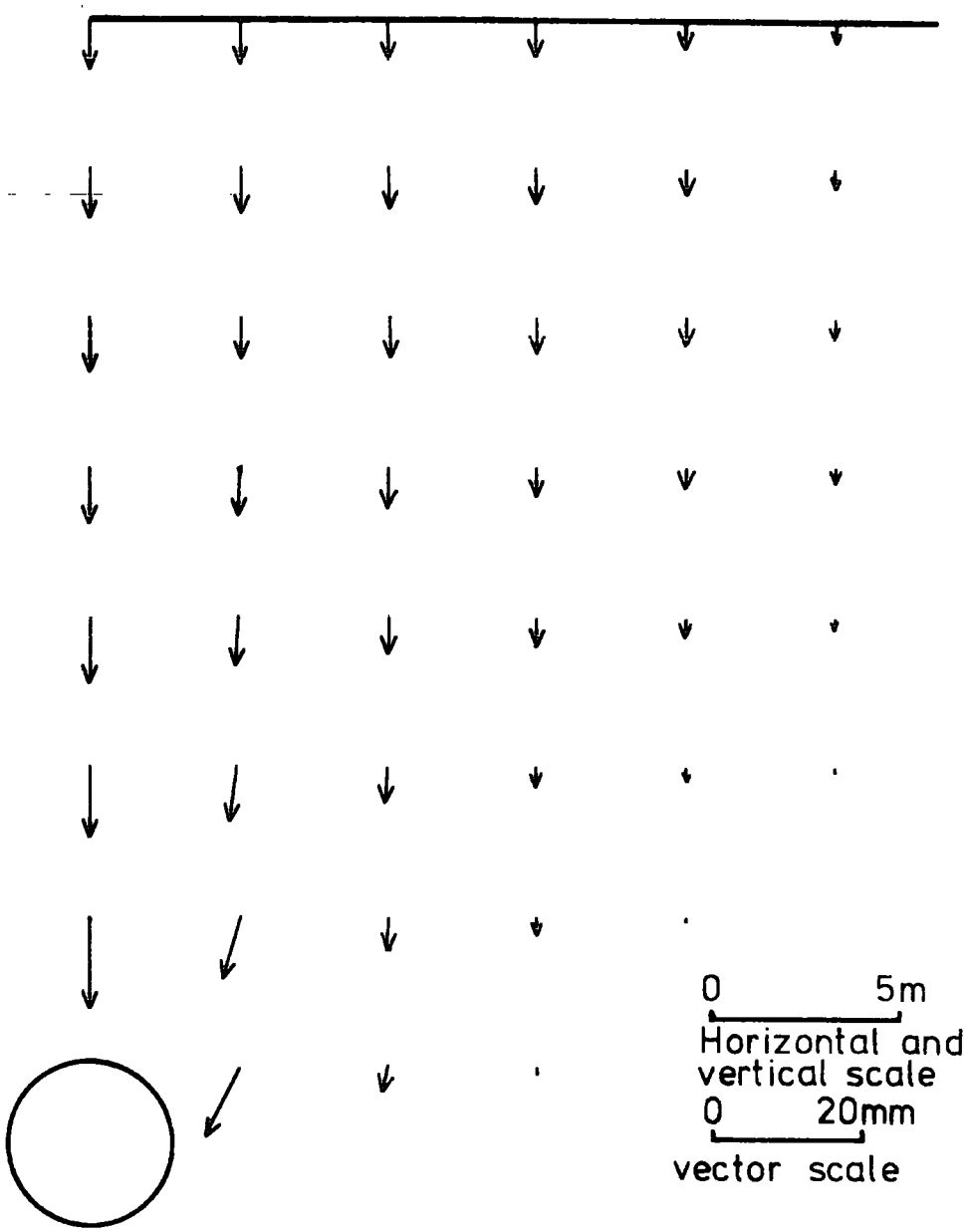

Figure 6.9
Displacement vectors
Green Park

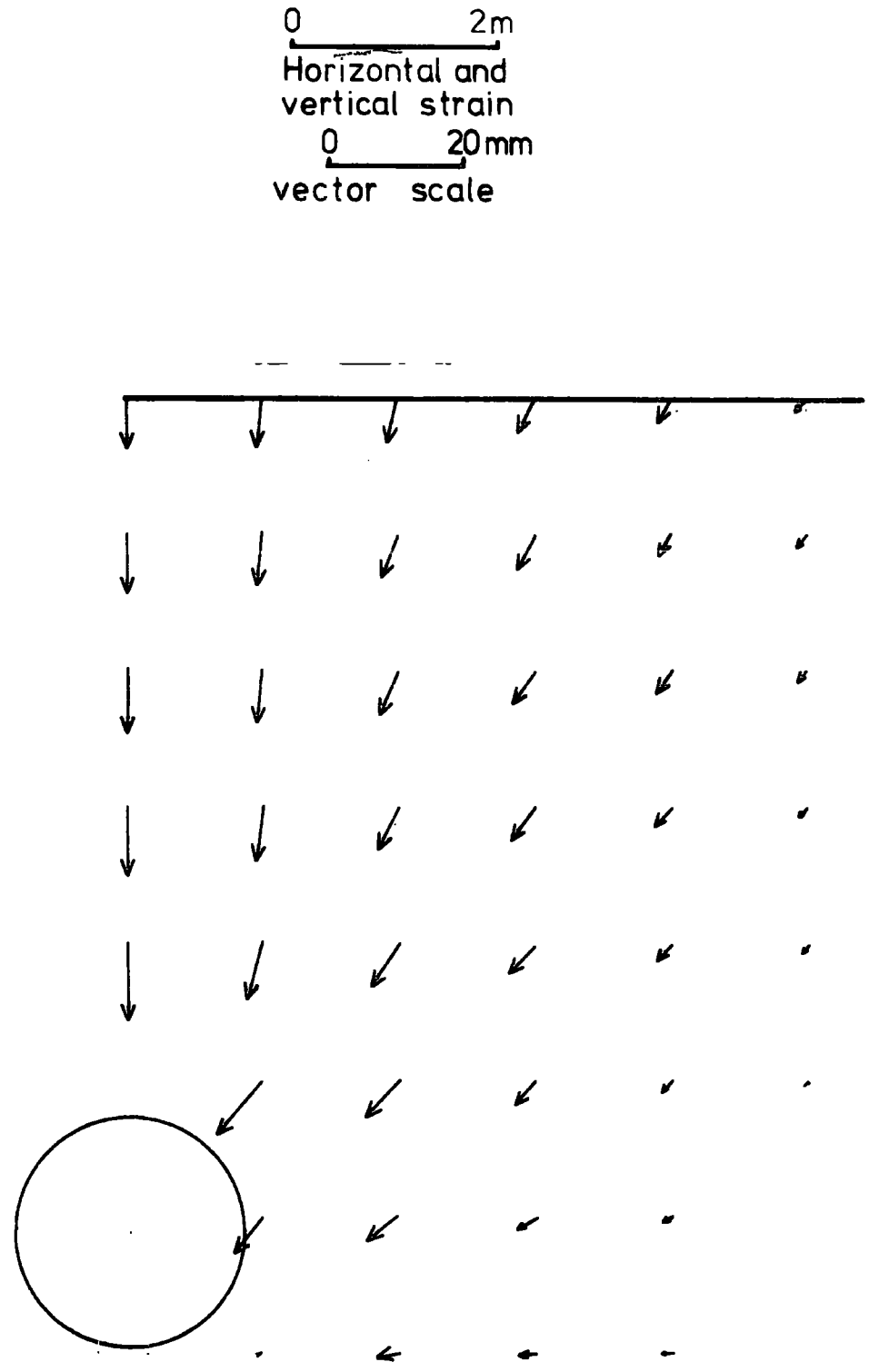

Figure 6.10

Displacement vectors
Hebburn

0 2m
Horizontal and vertical scale

0 50mm
vector scale

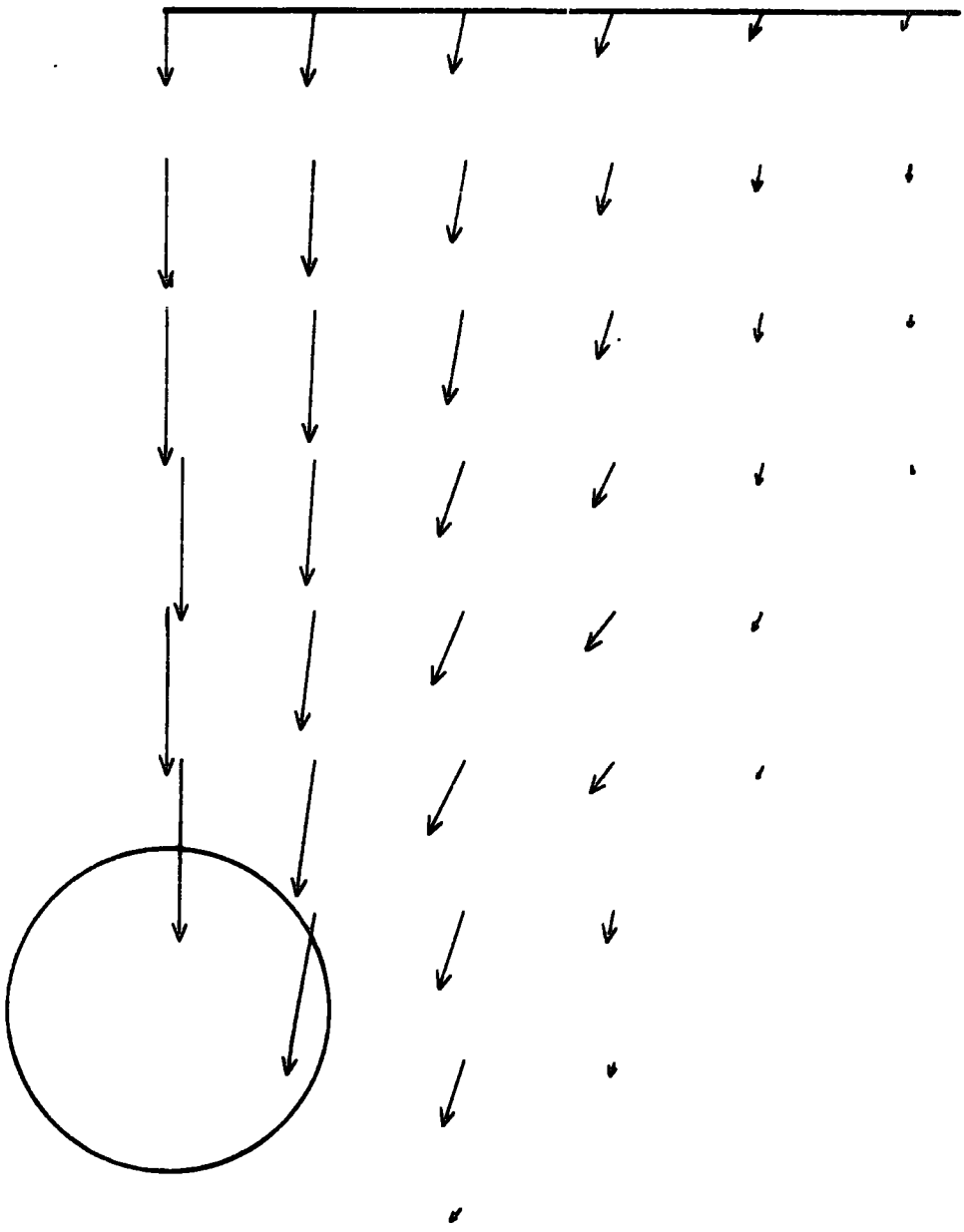

Figure 6.11
Displacement vectors
Willington Quay 23 days

0 2m
Horizontal and vertical scale
0 100mm
vector scale

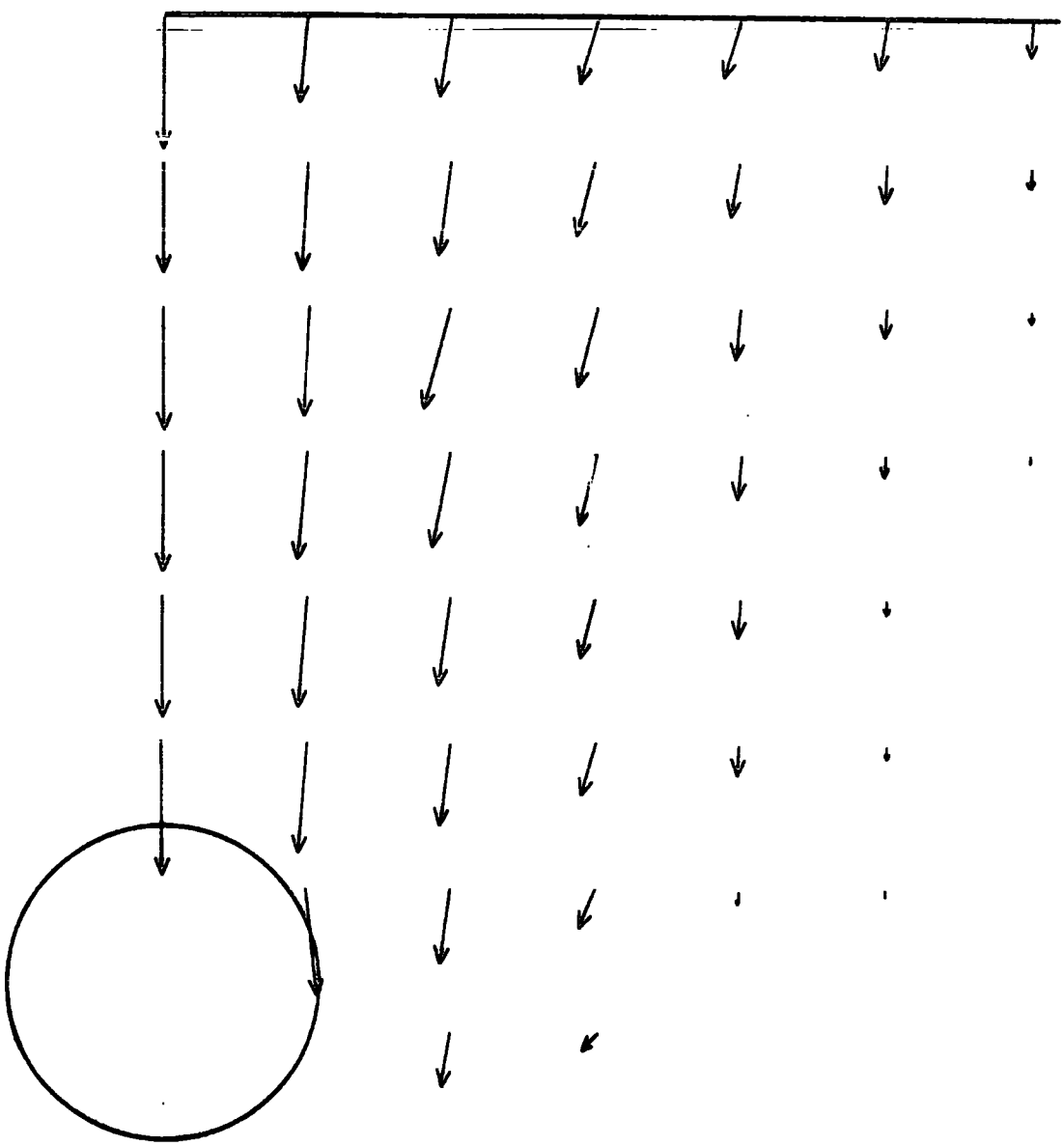

Figure 6.12
Displacement vectors
Willington Quay 149 days

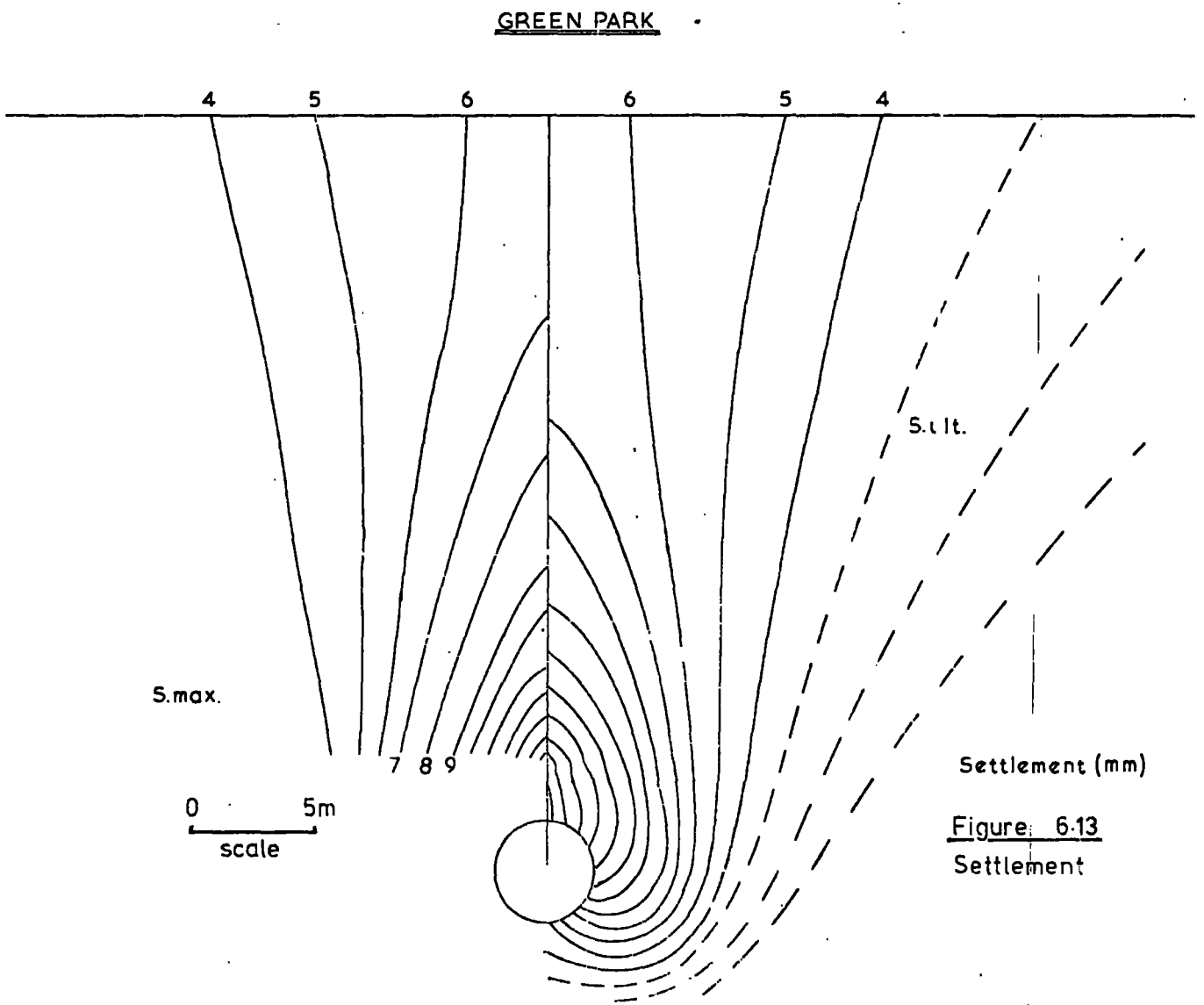

Figure 6.13
Settlement

Green Park

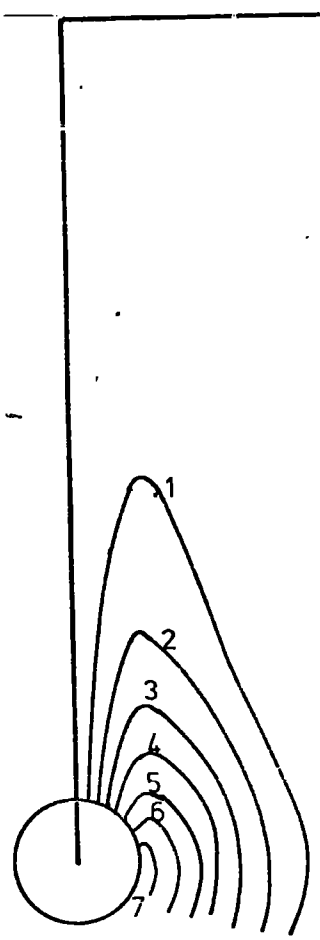

Lateral
displacement
(mm)

Figure 6·14

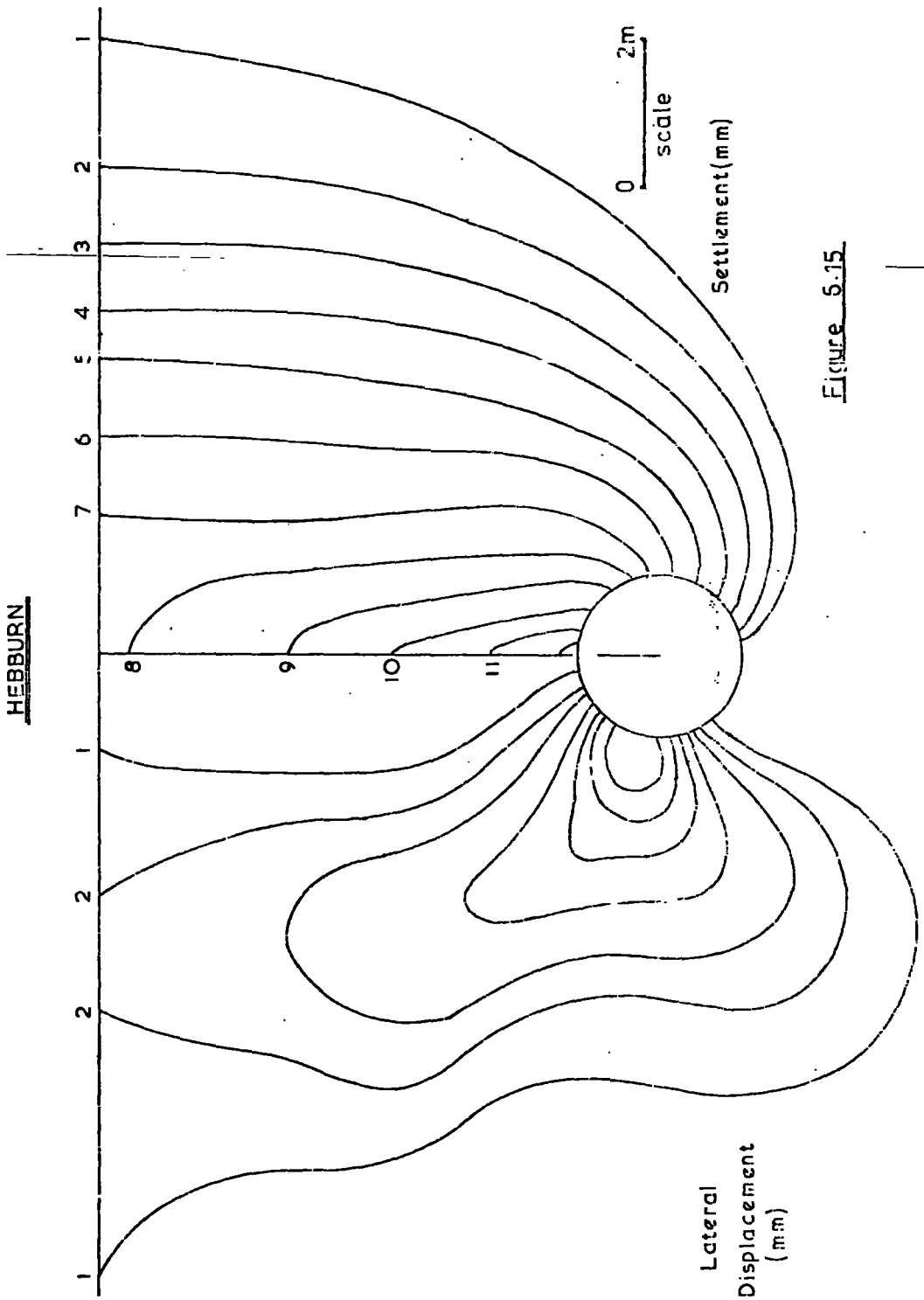
HEBBURN
1
2
3
4
5
6
7
8
9
10
11
0
2m
scale
Settlement(mm)
Lateral
Displacement
(mm)

Figure 5.15

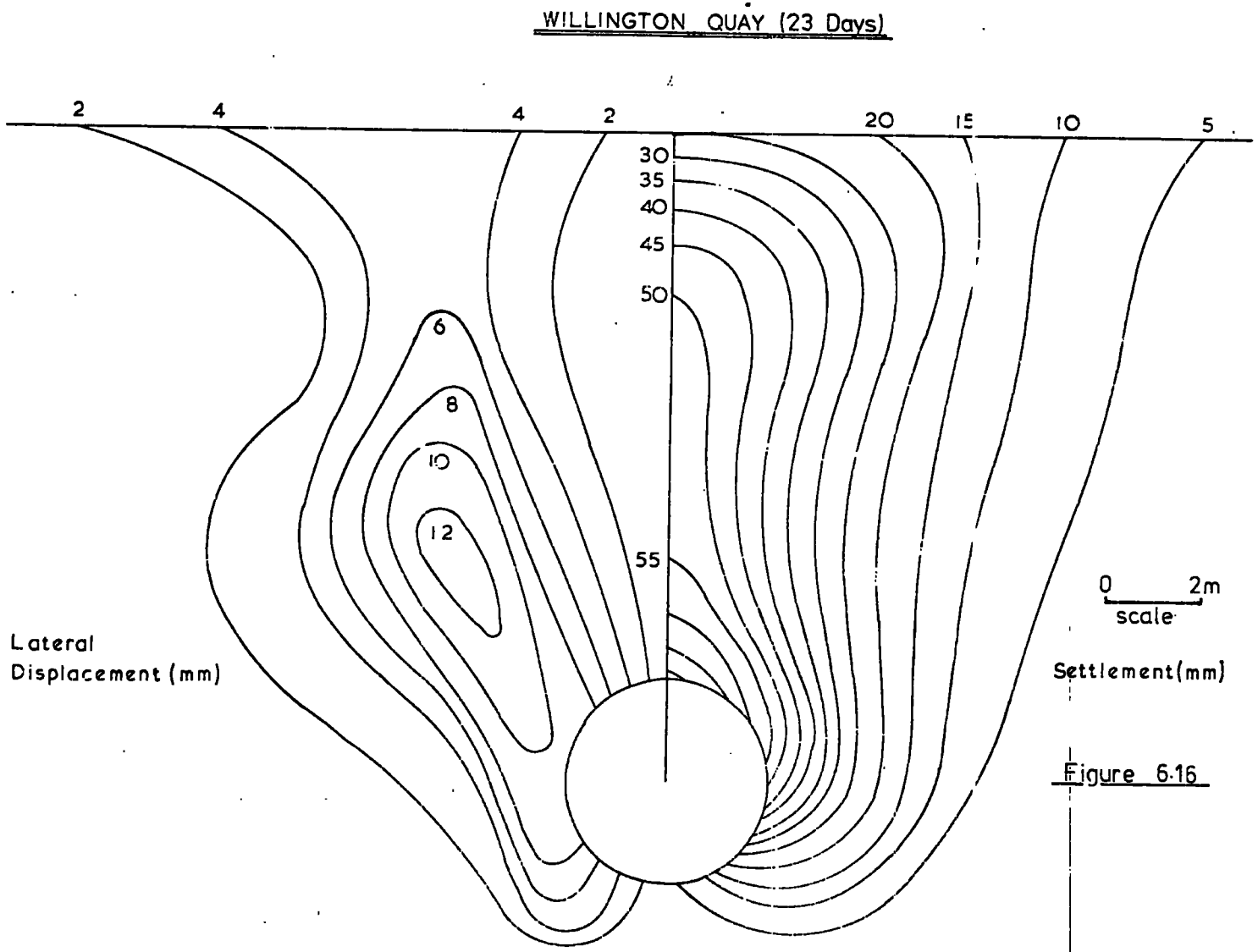
WILLINGTON QUAY (23 Days)
2
4
4
2
20
15
10
5
30
35
40
45
50
6
8
10
12
55
0
2m
scale
Lateral
Displacement (mm)
Settlement(mm)

Figure 6.16

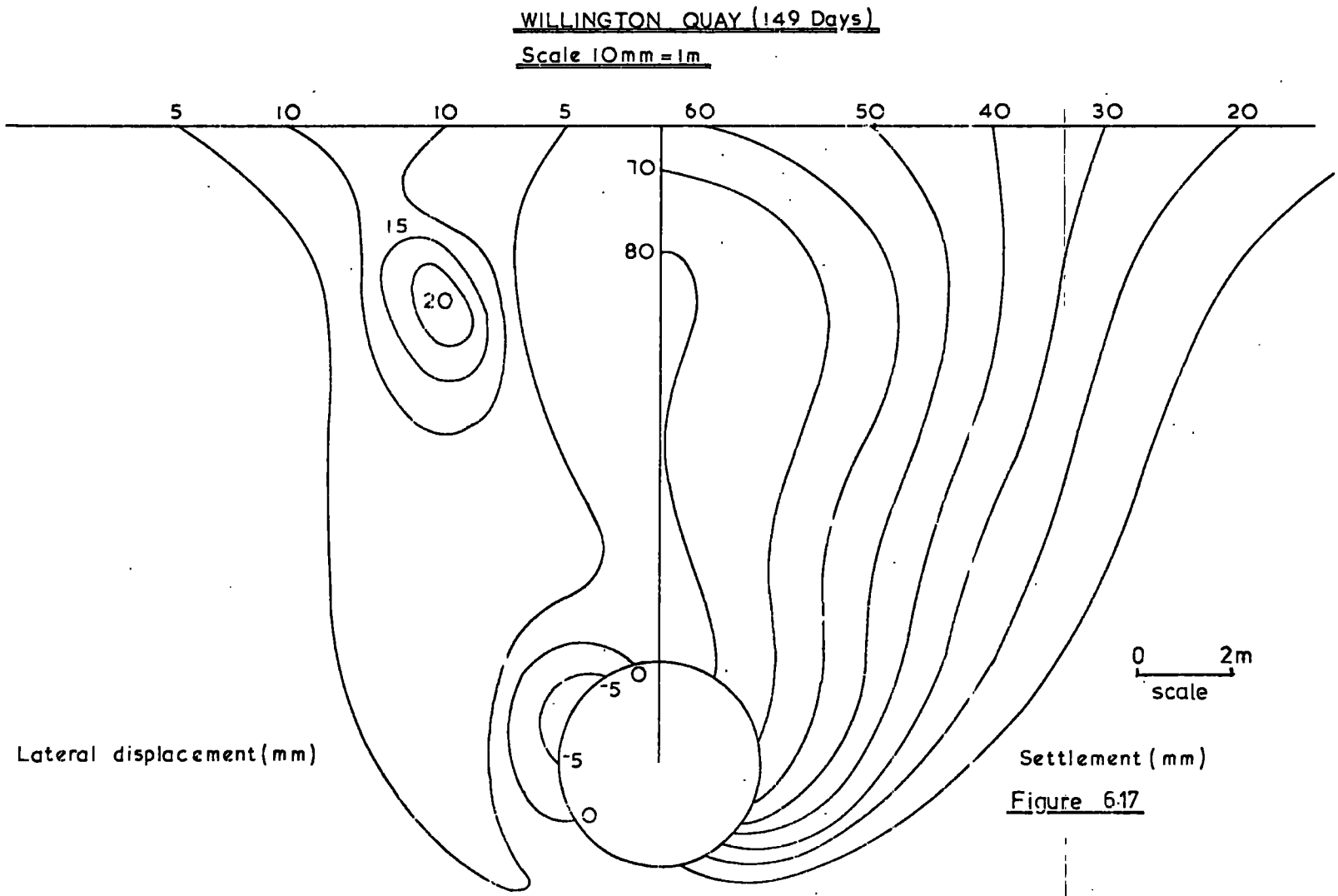
WILLINGTON QUAY (149 Days)
Scale 10mm = 1m
5
10
10
5
60
50
40
30
20
70
80
15
20
0
-5
-5
0
0
2m
scale
Lateral displacement (mm)
Settlement (mm)

Figure 6.17

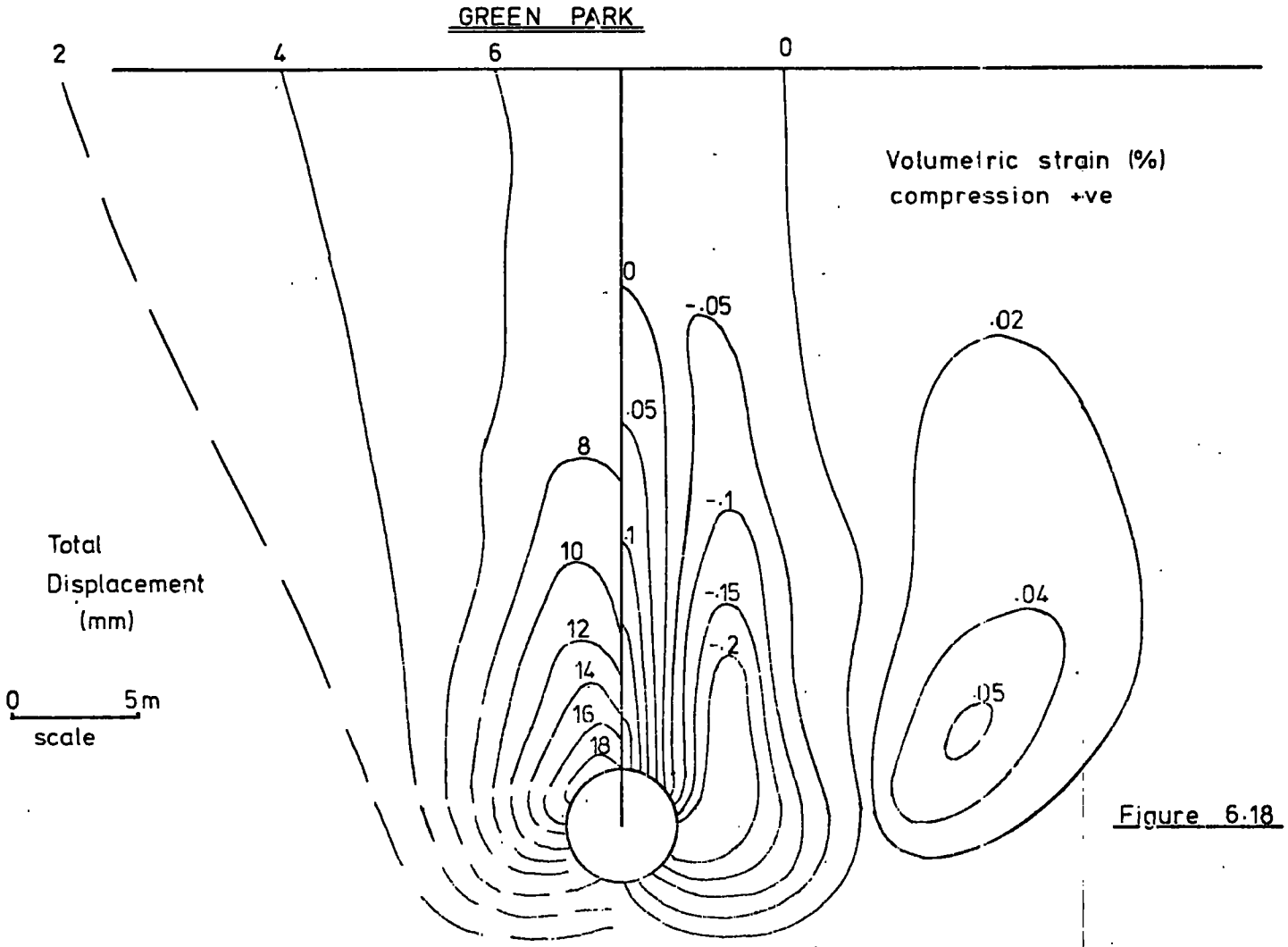
GREEN PARK
2
4
6
0
Volumetric strain (%)
compression +ve
0
-.05
.02
.05
8
-.1
.1
10
-.15
.04
12
-.2
14
.05
16
18
Total
Displacement
(mm)
0
5m
scale

Figure 6.18

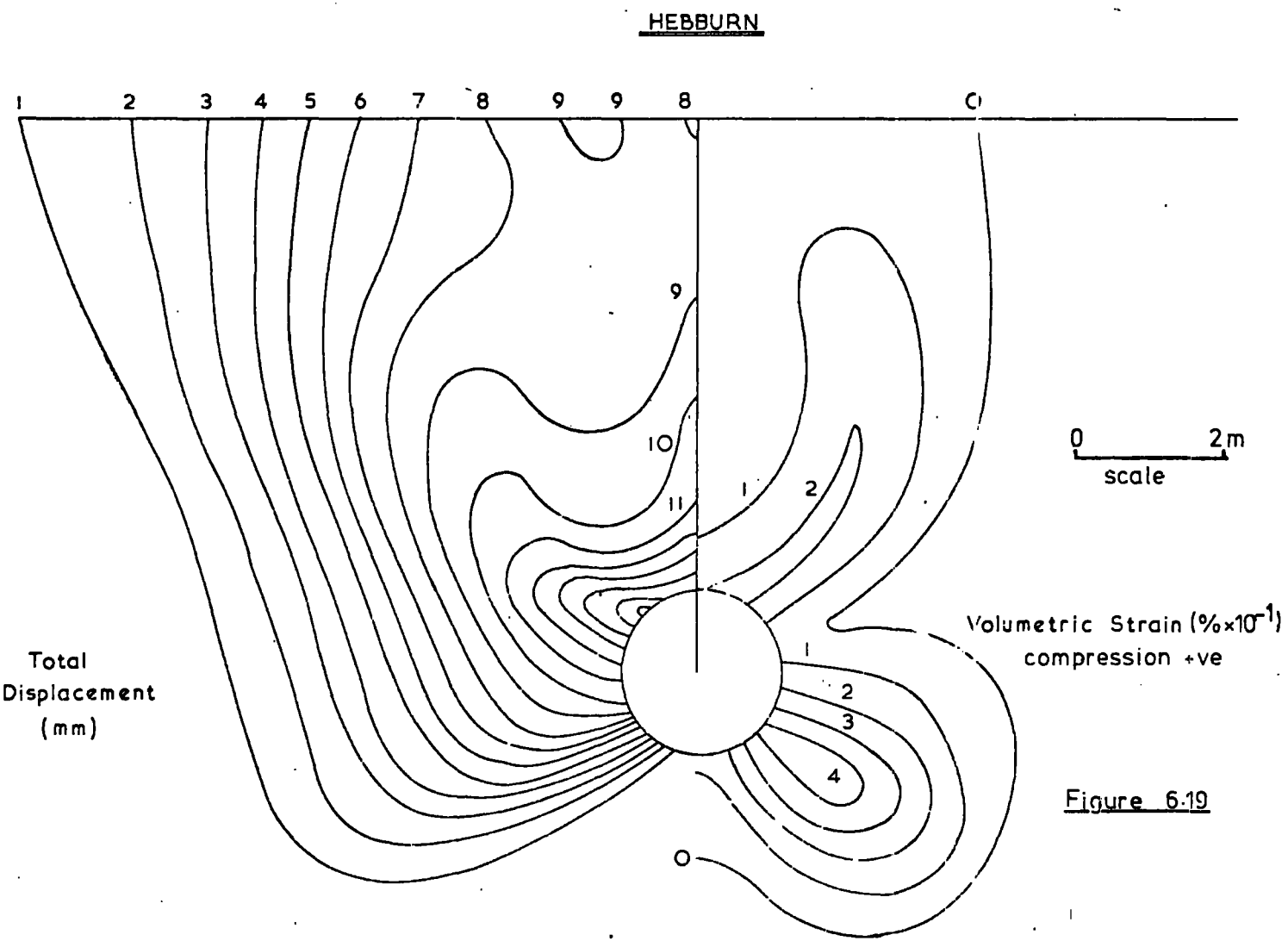
HEBBURN
1 2 3 4 5 6 7 8 9 9 8 0
9
10
11
1 2
0 2m
scale
Total
Displacement
(mm)
Volumetric Strain (%×10⁻¹)
compression +ve
1
2
3
4
0

Figure 6.19

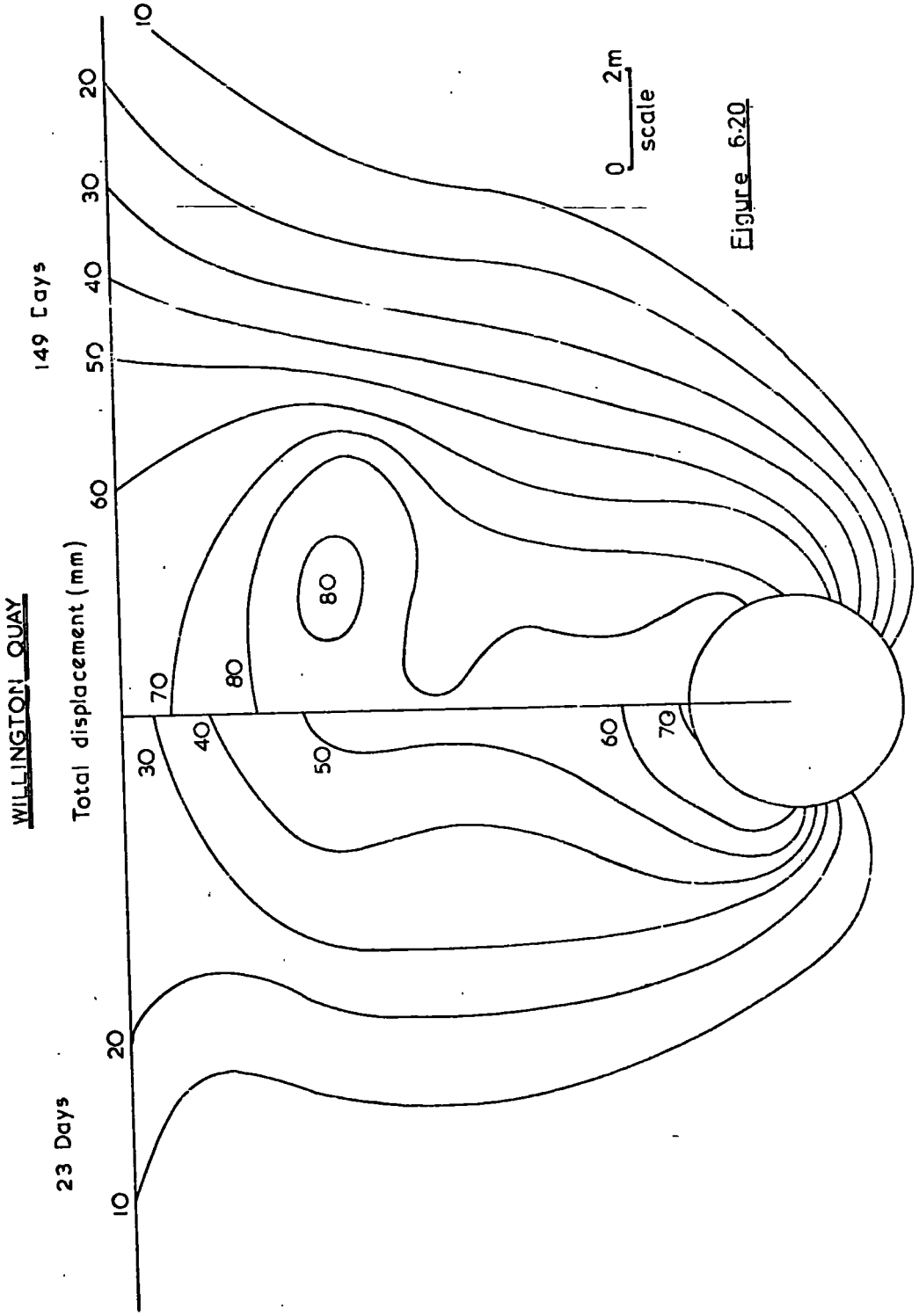
WILLINGTON QUAY
Total displacement (mm)
149 Days
23 Days
10
20
30
40
50
60
70
80
0
2m
scale

Figure 6.20

WILLINGTON QUAY

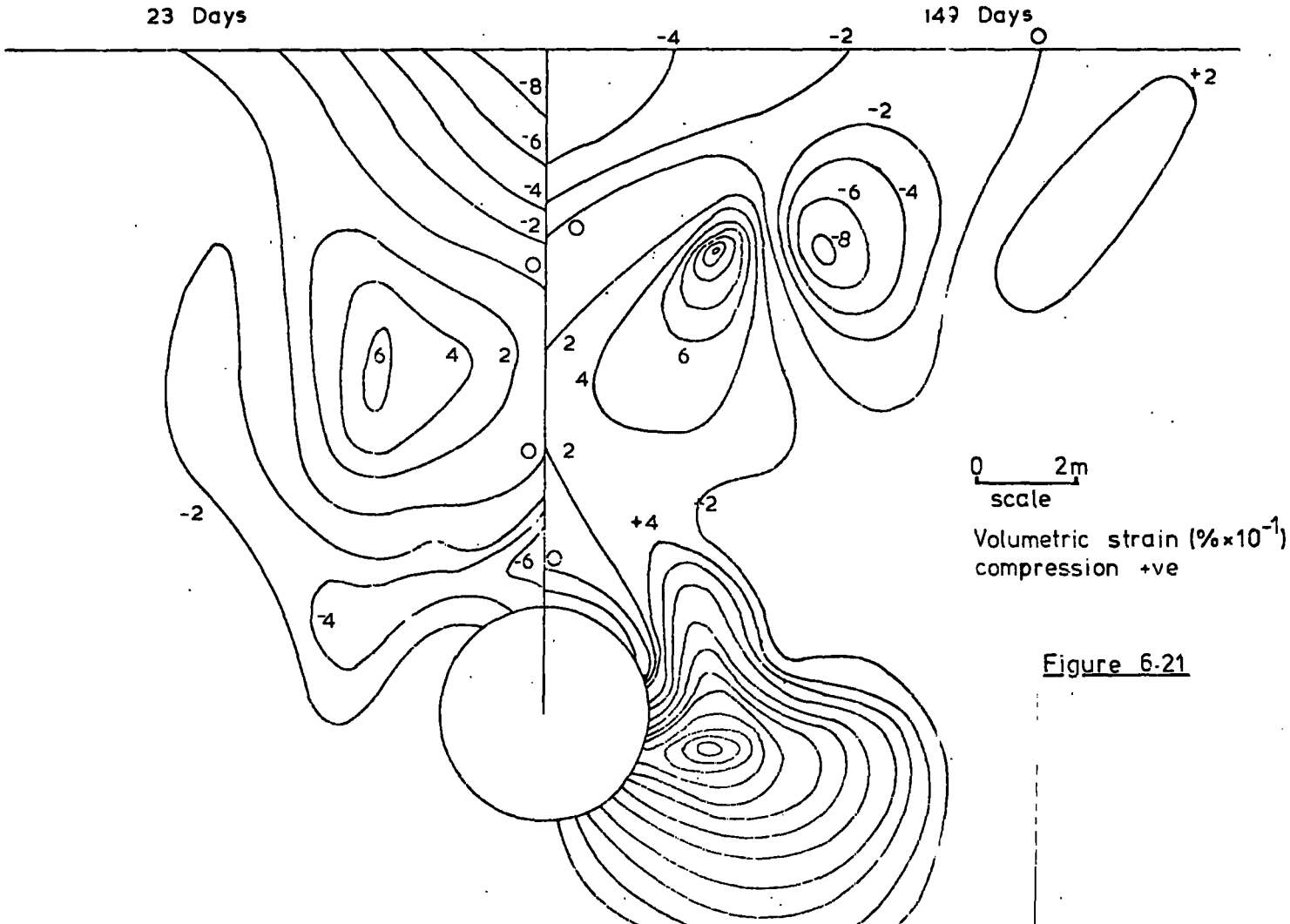

Figure 6.21

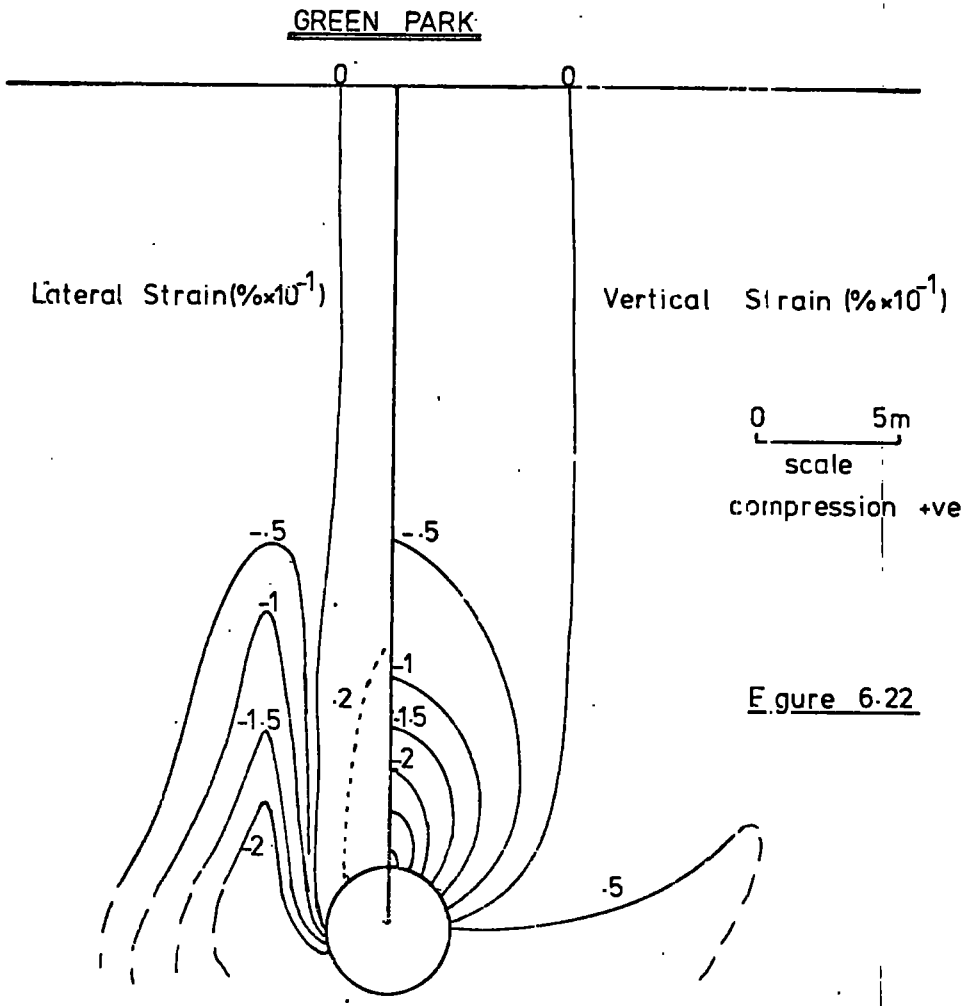
GREEN PARK
0
0
Lateral Strain(%×10⁻¹)
Vertical Strain (%×10⁻¹)
0 5m
scale
compression +ve
-.5
-1
-1.5
-2
-.5
-1
-1.5
-2
-.5

Figure 6.22

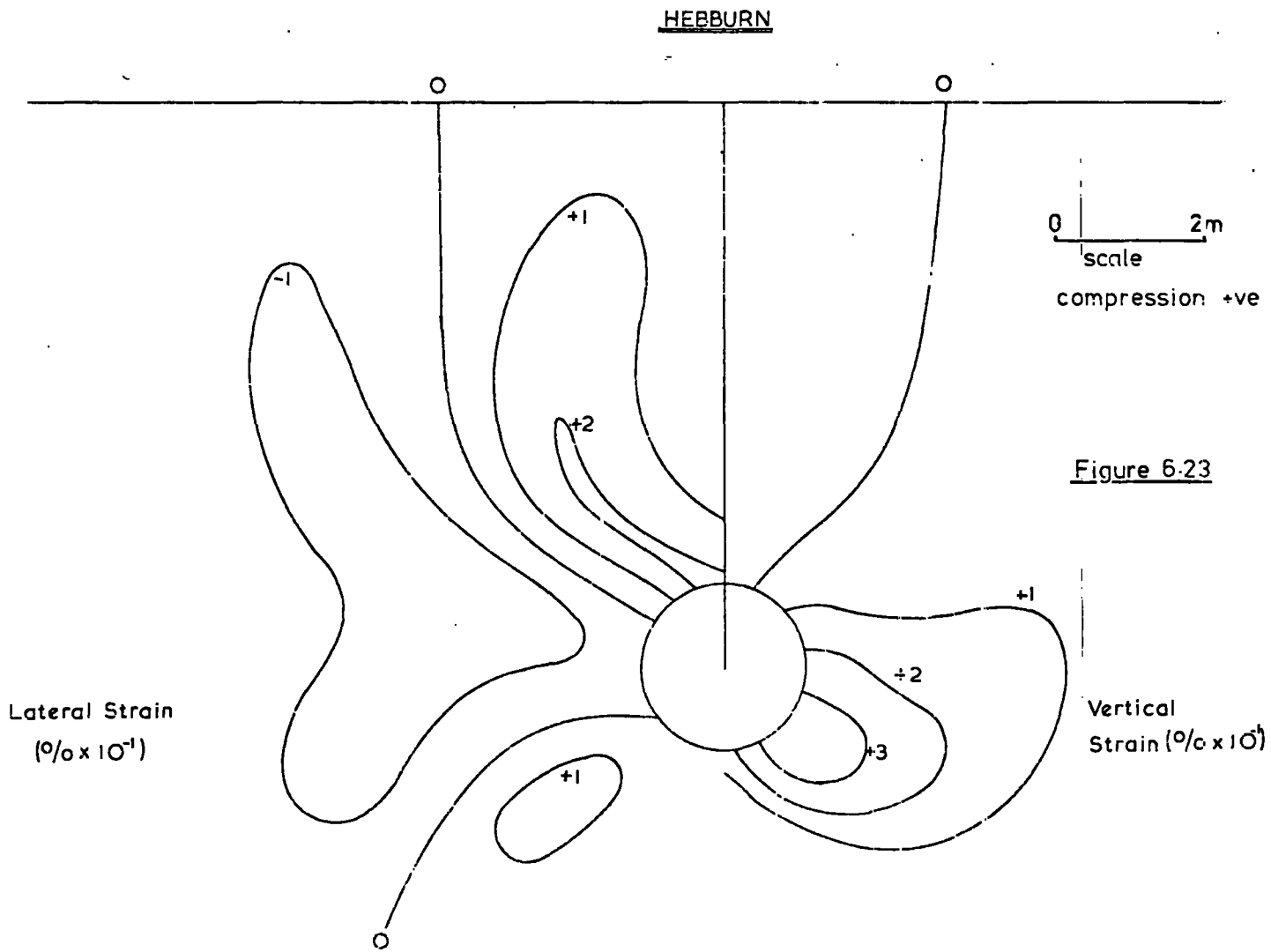
HEBBURN
0
2m
scale
compression +ve
+1
-1
+2
+1
+2
+3
+1
Lateral Strain
(0/00 x 10-1)
Vertical
Strain (0/00 x 10-1)

Figure 6.23

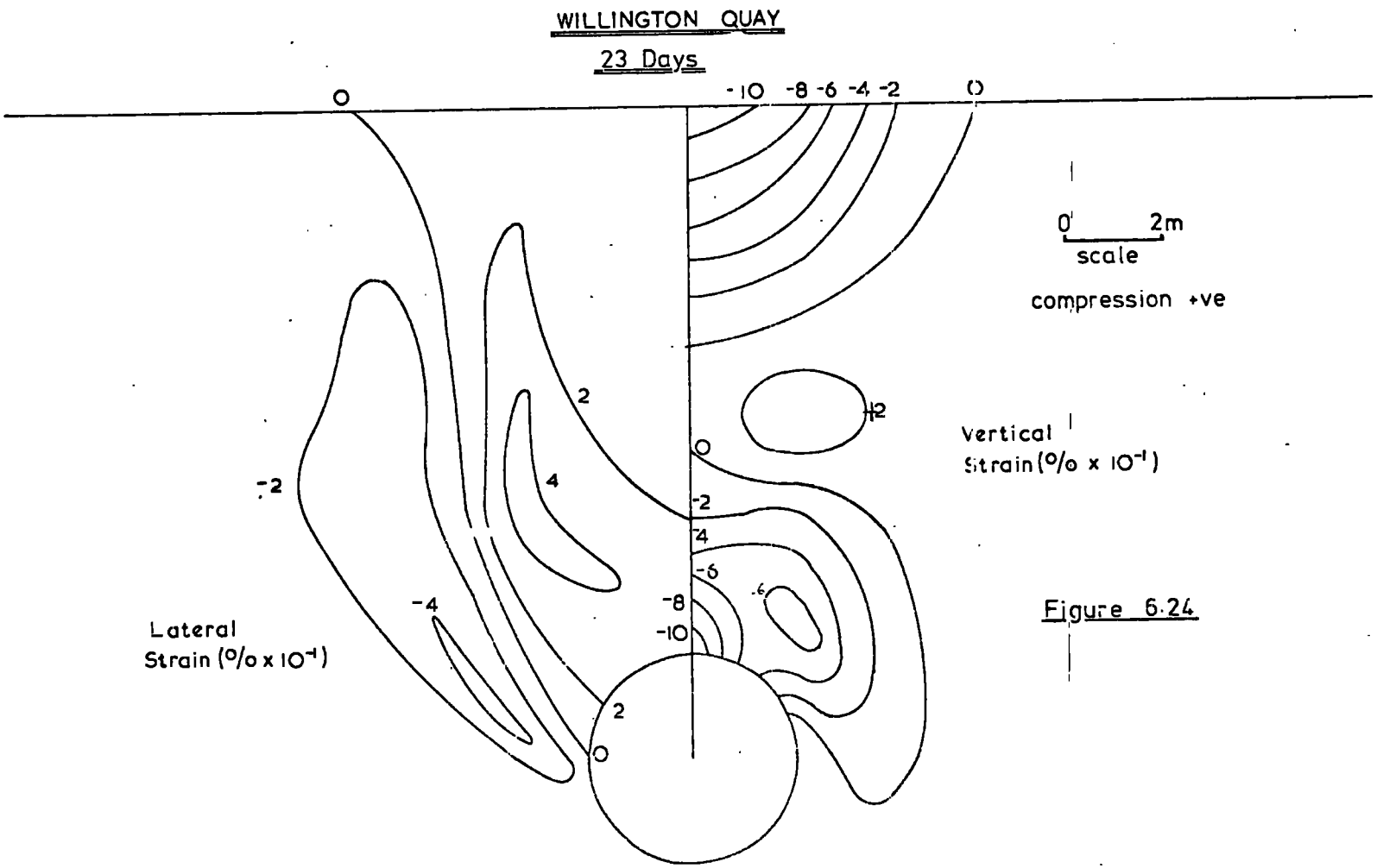
WILLINGTON QUAY
23 Days
0
-10 -8 -6 -4 -2
0
0 2m
scale
compression +ve
Vertical
Strain (% x 10⁻¹)
Lateral
Strain (% x 10⁻¹)
2
4
-2
-4
2
0
-2
-4
-6
-8
-10
2
0

Figure 6.24

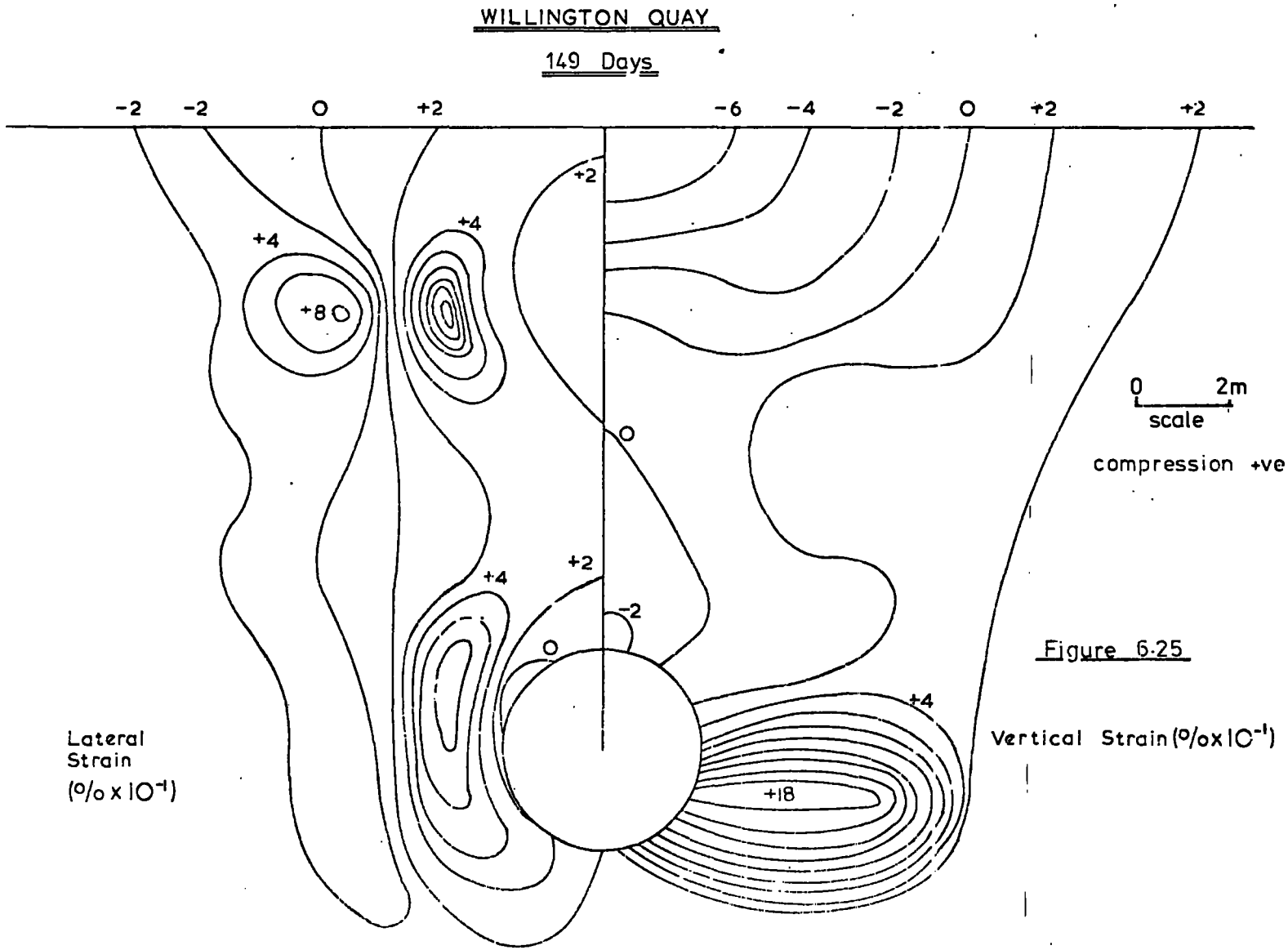
WILLINGTON QUAY
149 Days
-2
-2
0
+2
-6
-4
-2
0
+2
+2
+4
+4
+8 0
+2
0
+4
+2
-2
0
+4
+18
0
2m
scale
compression +ve
Lateral Strain (o/o x 10⁻¹)
Vertical Strain (o/ox 10⁻¹)

Figure 6.25

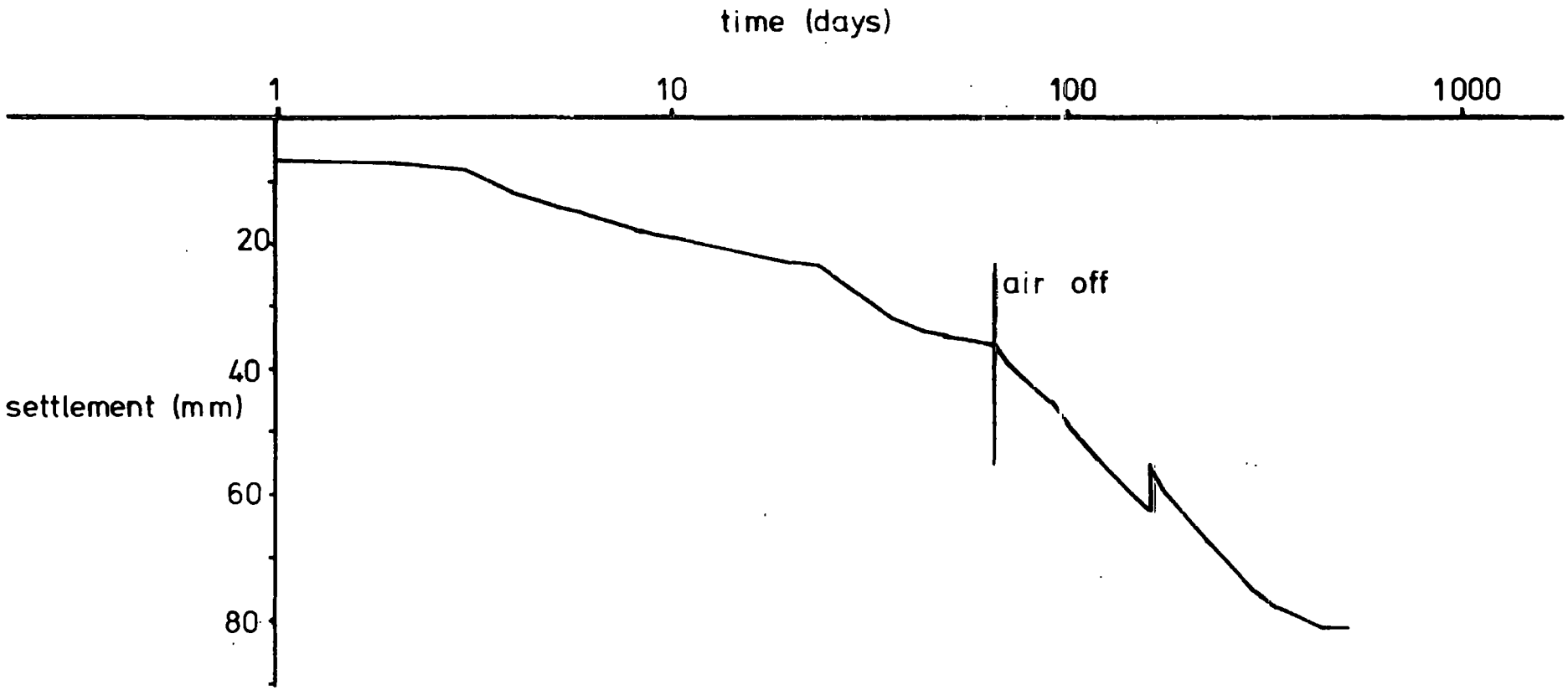

Figure 6.26

Settlement Vs log time - Willington Quay

CONCLUSIONS

1. Published studies, although providing information on the character of ground movements caused by tunnelling in soft ground, offer only limited insight into the actual mechanisms generating these deformations. Observations made in the body of the thesis indicate that further research into this subject is necessary. In particular, research into the nature of ground movements close to the tunnel excavation itself is required, with the object of delineating the mode, and extent, of "failure" of the soil, and to provide a better estimate of volume losses into the tunnel.

2. Two distinct types of settlement phenomena have been identified. First, settlement may be caused by "ground loss," both into the excavation and into the annulus around the lining. This type of settlement results directly from the nature of the excavation itself, and therefore its development depends upon both the depth of the tunnel and the rate of tunnel advance. It can be regarded as an undrained, constant-volume process.

Second, settlement may be caused by long-term volume changes in the ground. It is caused in clay soils by consolidation which results from drainage into, or around, the lined tunnel. This type of settlement occurs with the release of compressed air, when this type of ground restraint has been used.

Although these two effects may take place concurrently, they can be regarded as entirely distinct, with their development and distributions superimposed. When compressed air has been used, consolidation settlement may develop some time after volume loss settlement is complete.

3. Settlement (S), lateral displacement (S_h) and lateral strain (ε_h) at a transverse distance x from the tunnel centre-line, and caused by volume losses into the tunnel, can be predicted using stochastic or probabilistic methods, provided that the magnitude of the volume loss is known, and assumed to be equal to the volume of the settlement trough (V_s). The following relations have been developed for a point source of ground loss at a depth Z in cohesive soil:

$$\text{Surface settlement } (S) = 2V_s/(\sqrt{2\pi}Z) \exp(-2x^2/Z^2)$$

$$\text{Lateral surface displacement } (S_h) = (x/Z)\, S$$

$$\text{Lateral surface strain } (\varepsilon_h) = (1 - 4x^2/Z^2)\, S/Z)$$

The model settlement trough takes the form of a Gaussian distribution and is validated empirically by previously published case history data. On the settlement curve there are two points of inflection ($\pm$ i) at a distance of Z/2 either side of the tunnel centre-line. The above relations should strictly be regarded as "source functions", although for depth-to-diameter ratios greater than 2 they can be used to determine surface settlement, lateral displacement and lateral strain directly. For points less than about two diameters from the centre of the tunnel, the "source functions" must be combined numerically to provide an accurate

estimate of the above parameters.

4. The volume of the surface settlement trough ($V_s\%$), expressed as a percentage of tunnel volume, is related empirically to the ground stability ratio (OFS) by the expression:

$$V_s\% = -1.14 + 1.33\ OFS$$

This relation must be regarded as tentative and temporary, being based on case history evidence available at the time of writing.

5. Results from the three sites can be summarised as follows:

	Hebburn	Howdon	Willington Quay (23 days)	Willington Quay Long-term
Depth to axis (m)	7.5	14.18	13.375	13.375
Diameter (m)	2.014	3.625	4.25	4.25
Advance rate (m/hr)	0.11	0.068	0.06	0.06
C_u of soil kN/m^2	73.2	100.0	25.4	25.4
OFS	2.02	2.92	5.95	(9.5)
S max (mm)	7.9	11.2	23.5	81.5
S_h max (mm)	3 *	5.0	6.0	12.0
ε_h max (%)	-	0.14	0.15	0.23
i (m)	3.9	6.9	6.1	8.5
$V_s\%$	2.42	2.07	2.57	12.27

Results from Hebburn and Howdon correspond reasonably well with predictions using the stochastic model and would appear to

*estimated

reflect undrained, volume-loss settlement. The early stages of settlement at Willington Quay, up to 23 days after passage of the shield, also agree with the stochastic model. In the long-term, however, the settlement trough deepens and widens whilst lateral displacement and strain do not increase to a corresponding extent. This long-term settlement, developing after release of the compressed air from the tunnel, is considered to be caused by consolidation due to drainage into the tunnel.

6. Seepage forces, as estimated from flow nets, would seem to have an appreciable effect on tunnel face stability. These, however, would be largely counteracted by the use of compressed air. They should therefore be taken into consideration in those cases where a tunnel beneath the water table would otherwise appear to be sufficiently stable to excavate in free air.

7. As was evident at Willington Quay, settlement caused by consolidation may be greater in magnitude than that attributable to volume loss. Where compressed air is not used, consolidation may commence a short distance ahead of the face, and its onset will be concurrent with volume-loss settlement. It may then be difficult to distinguish between the two phenomena. More commonly, consolidation will occur on the release of air pressure, and can be regarded as a distinct and separate phase of settlement.

The geometry of the consolidation settlement trough is difficult to predict. It will depend on the extent of the drained

area around the tunnel and would be expected to be wider than that due to volume loss, particularly in soils of anisotropic permeability which may drain horizontally for some distance from the tunnel.

The effectiveness of caulking in reducing consolidation settlement depends on the relation between the permeability of the caulked lining and that of the surrounding soil. In clays, caulking will have little or no effect, although consolidation in this case will be extremely slow to develop, whereas in coarse silts the effect of caulking may be considerable.

At the present time, the effects and mechanism of consolidation around tunnels are not well understood. Only an estimate of expected consolidation settlement can be made with the aid of flow-nets. It is considered that further research in this area would prove invaluable, especially in view of the large contribution that consolidation may make to the total settlement. In particular, more quantitative information is required on changes in the pore-pressure regime around tunnels, both during construction and after the release of any compressed air.

8. This thesis has shown how case-history evidence can be used to support a theory of ground movement caused by tunnelling. It must be recognised, however, that the resulting empirical relations between fixed design variables and geotechnical variables do not in any way cater for the effects of either inadequate workmanship or unexpected and poor ground conditions at the tunnel face. Ground - and especially surface - movement prediction may proceed only with a concomitant awareness that local anomalous deformations may invalidate such predictions.

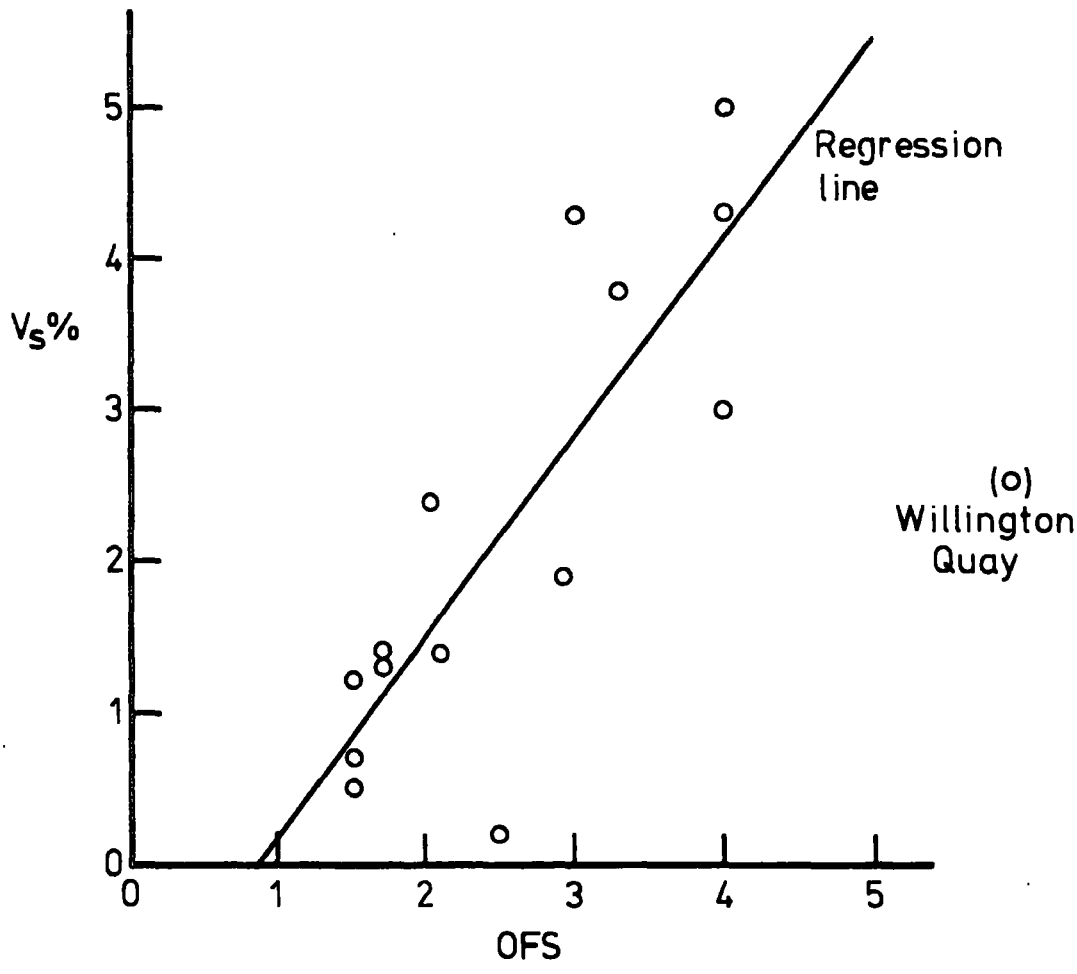

Figure 6.6

Settlement volume Vs OFS

REFERENCES

Abbot, M.B., Ashamalia, A.F. and Rodenhuis, G.S. - On the numerical computation of stratified ground-water flow, Hydrol. Sci. Bull. 17 (1972) 177-182.

Anderson, E.R. and McCusker, T.G. - Chemical consolidation in a mixed face tunnel, Proc. N.A. Rapid Exc. and Tunn. Conf., A.I.M.E. 1 (1972) 315-330.

Atkinson, J.H., Cairncross, A.M. and James, R.G. - Model tests on shallow tunnels in sand and clay, Tunnels and Tunnelling 6 (1974) 28-32.

Attewell, P.B. - Ground movements caused by tunnelling in soil, Proc. I. Struct. E./U.W.I.S.T. Conf. on Large Ground Movements and Structures, University of Wales Institute of Science and Technology, 4-7 July, (1977a).

Attewell, P.B. - Large ground movements and structural damage caused by tunnelling below the water table in a silty alluvial clay, Proc. I. Struct. E./U.W.I.S.T. Conf. on Large Ground Movements and Structures, University of Wales Institute of Science and Technology, 4-7 July (1977b).

Attewell, P.B. and Boden, B. - Development of stability ratios for tunnels driven in clay, Tunnels and Tunnelling 3 (1971) 195-198.

Attewell, P.B. and Farmer, I.W. - Determination and interpretation of surface and subsurface ground movements during construction of a tunnel in London Clay at Green Park, London, Report to Transport and Road Research Laboratory, Dept. of the Environment, Contract No. ES/LN/842/101, University of Durham (1972).

Attewell, P.B. and Farmer, I.W. - Ground deformations resulting from shield tunnelling in London Clay, Canadian Geotech. Journal 2 (1974) 380-395.

Attewell, P.B., Farmer, I.W., Glossop, N.H. and Kusznir, N.J. - A case history of ground deformation caused by tunnelling in laminated clay, Proc. Conf. on Subway Construction, Budapest-Balatonfured (1975) 165-178.

Bartlett, J.V. and Bubbers, B.L. - Surface movements caused by bored tunnelling, Proc. Conf. on Subway Construction, Budapest-Balatonfured (1970) 513-539.

Beaulieu, A.C. - Tunnelling experiences, City of Edmonton, Alberta, Canada, Proc. N.A. Rapid Exc. and Tunn. Conf., A.I.M.E. 2 (1972).

Beaumont, P. - Glacial deposits of East Durham, Ph.D. Thesis, University of Durham (1967).

Berry, D.S. - A discussion on the stochastic theory of ground movements, Rock Mech. and Eng. Geol. 2 (1964) 213-227.

Berry, D.S. - An elastic treatment of ground movement due to mining, J. Mech. and Phys. Solids 8 (1969) 280-292.

Bewick, J.E. - The measurement and analysis of ground movements associated with a tunnel driven in laminated clay at Hebburn, County Durham, M.Sc. Thesis, University of Durham (1973).

Boden, J.B. - Design aspects of tunnelling on Tyneside, U.K., Proc. I.C.E. 53 (1972) 275-284.

Broms, B.B. and Bennermark, H. - Stability of clay in vertical openings, J. Soil Mech. and Found. Div., ASCE, 93 (1967) 71-94.

Burland, J.B. and Moore, J.F.A. - Measurement of ground displacement around deep excavations, Symp. Field Inst., British Geotech. Soc. (1973) 70-84.

Burland, J.B. and Wroth, C.P. - Settlement of buildings and associated damage, Building Research Establishment Current Paper CP33/75 (1975).

Butterfield, R. and Howey, I.R. - A simple analogue for the rapid solution of general potential flow problems in two dimensions, Geotechnique 23 (1973) 13-21.

Cairncross, A.M. - Deformations around a tunnel in stiff clay, Ph.D. Thesis, University of Cambridge (1973).

Cedergren, U.R. - Seepage, drainage and flow nets, Wiley, N.Y. (1967).

Chan, H.T. and Kenney, T.C. - Laboratory investigation of permeability ratio of New Liskeard varved soil, Canadian Geotech. Journal 10 (1973) 453-472.

Chandrasekhar, S. - Stochastic problems in physics and astronomy, Review of Modern Physics, Am. Inst. of Phys. 15 (1943) 1-89.

Chaney, J.E. - Techniques and equipment using the surveyors level for accurate measurement of building movement, Symp. Field Inst., British Geotech. Soc. (1973) 85-99.

Cording, E.J. - Measurement of displacement in tunnels, Proc. 2nd Int. Cong. I.A.E.G. Sao Paulo 2 (1974).

Cording, E.J., Hansmire, W.H., MacPherson, H.H., Lenzini, P.A. and Vonderche, A.D. - Displacements around tunnels in soil, Final Report by the University of Illinois on Contract No. DOT FR 30022 to Office of the Secretary and Federal Railroad Administration, Dept. of Transportation, Wash., D.C. 20590, U.S.A. (1976).

Dawson, O. - Compressed air and its applications, in Tunnels and tunnelling, Pequignot, C.A. (ed.), Hutchinson (1963).

Deere, D.U., Peck, R.B., Monsees, J.E. and Schmidt, B. - Design of tunnel liners and support systems, Report for U.S. Dept. of Transportation, OHSGT, Contract 3-0152 (1969).

Dunnicliff, C.J. - Equipment for field deformation measurements, Proc. 4th Panam. Conf. on Soil Mech. and Found. Eng. 2 (1971) 319-332.

Drucker, M.A. - Determination of lateral passive earth pressure and its effect on tunnel stresses, J. Franklin Inst. (1943) 499-512.

El-Naga, N.M.A. - Measurement of ground-lining pressure distribution around two tunnels in stiff stony clay, M.Sc. Thesis, University of Durham (1976).

Francis, E.A. - Geology of Durham, Trans. Nat. Hist. Soc., Durham, Northumberland and Newcastle-on-Tyne 41 (1970) 1-78.

Girijavallabhan, C.V. and Reese, L.S. - Finite element method for problems in soil mechanics, J. Soil Mech. and Found. Div., ASCE 94 (1968) 473-496.

Glossop, N.H. and Farmer, I.W. - Ground deformation during construction of a tunnel in Belfast, Report to Transport and Road Research Laboratory, Dept. of the Environment, No. R6/77, University of Newcastle-upon-Tyne (1978).

Goldstein, M.N., Misumsky, V.A. and Lapidus, L.S. - The theory of probability and statistics in relation to the rheology of soils, Proc. 5th Int. Conf. on Soil Mech. and Found. Eng. 1 (1961) 123-126.

Gould, P. and Dunnicliff, C.J. - Accuracy of field deformation measurements, Proc. 4th Panam. Conf. on Soil Mech. and Found Eng. 1 (1971) 313-366.

Green, G.E. - Principles and performance of two inclinometers for measuring horizontal ground movements, Field Inst. in Geotech. Eng., British Geotech. Soc. (1973) 166-179.

Hackett, P. - An elastic analysis of rock movement caused by mining, Trans. I.M.E. 118 (1959) 421-433.

Halvorsen, G.T., Kesler, C.E. and Paul, S.L. - Fibrous concrete for the extruded liner system, Tunnels and Tunnelling 8 (1976) 42-46.

Hanna, T.H. - Foundation instrumentation, Series on rock and soil mechanics 1, Trans. Tech. Pub. (1973).

Hansmire, W.H. and Cording, E.J. - Performance of a soft ground tunnel on the Washington metro, Proc. 2nd N.A. Rapid Exc. and Tunn. Conf. A.I.M.E. 1 (1972) 371-390.

Jeppson, R.W. - Inverse solution to three dimensional flows, J. Eng. Mech. Div., ASCE 98 (1972) 789-812.

Kac, M. - Random walk and the theory of Brownian motion, American Mathematical Monthly, Math. Assn. of America, 14 (1947) 369-391.

Kell, J. - Tunnelling in soft ground, in Tunnels and Tunnelling, Pequignot, C.A. (ed.), Hutchinson (1963).

Kreyszig, E. - Introductory mathematical statistics, Wiley, N.Y. (1970).

Kuesel, T.R. - Soft ground tunnels for the Bart project, Proc. 1st N.A. Rapid Exc. and Tunn. Conf., A.I.M.E. 1 (1972) 287-313.

Lane, E.W., Campbell, F.B. and Price, W.H. - The flow net and the electrical analogy, Civil Engineering 4 (1934) 510-514.

Leach, B. - The effects of planar anisotropy on the consolidation and drained shear strength characteristics of a laminated clay, Ph.D. Thesis, University of Durham (1973).

Litwiniszyn, J. - On certain linear and nonlinear strata theoretical models, Proc. 1964 Int. Conf. on Strata Control and Rock Mech. (1964) 384-396.

Marshall, G.J. and Berry, D.S. - Calculation of the stress around an advancing longwall face in viscoelastic ground, Proc. 1st Cong., Int. Soc. of Rock Mech. 2 (1966) 379-384.

Milner, R.M. - Accuracy of measurement with steel tapes, Building (1969) 139-140.

Moretto, O. - In Deep excavations and tunnelling in soft ground, Proc. 7th Int. Conf. on Soil Mech. and Found. Eng., Mexico City 3 (1969) 325-328.

Muir Wood, A.M. - Civil engineers reference book: Sect. 30: Tunnelling Butterworths (1975).

Norgrove, W.B. and Staples, K.D. - The Tyneside sewerage scheme, J. Inst. Water Engrs. and Scientists 30 (1976) 9-24.

O'Rourke, T.D. - U.S. and U.K. tunnelling - developments, comparisons and trends, Tunnels and Tunnelling 10 (1978) 56-60.

Oakley, H.R. and Dyer, E.A. - Investigation of sea outfalls for Tyneside sewage disposal, Proc. I.C.E. 33 (1966) 201-230.

Parry, R.M.G. - Some properties of heavily overconsolidated Oxford clay at a site near Bedford, Geotechnique 22 (1972) 485-507.

Parzen, E. - Modern probability theory and its applications, Wiley, N.Y. (1960).

Peck, R.B. - Deep excavations and tunnelling in soft ground, Proc. 7th Int. Conf. on Soil Mech. and Found. Eng., Mexico City 3 (1969) 225-290.

Polshin, D.E. and Tokar, R.A. - Maximum allowable non-uniform settlement of structures, Proc. 4th Int. Conf. on Soil Mech. and Found. Eng. 1 (1957) 402-405.

Rebull, P.M. - Earth responses in soft ground tunnelling, Performance of Earth and Earth-Supported Structures, A.S.C.E. Speciality Conf. 1 (1972) 1517-1535.

Schofield, A. and Wroth, P. - Critical state soil mechanics, McGraw-Hill, London (1968).

Schmidt, B. - Settlements and ground movements associated with tunnelling in soil, Ph.D. Thesis, University of Illinois (1969).

Sizer, K. - The determination and interpretation of ground movements caused by shield tunnelling in silty alluvium at Willington Quay, N.E. England, M.Sc. Thesis, University of Durham (1976).

Skempton, A.W. and MacDonald, D.H. - Allowable settlement of buildings, Proc. I.C.E. 5 (1956) 727-768.

Smith, G.N. - Elements of soil mechanics for civil and mining engineers, Crosby Lockwood Staples, London (1974).

Smith, W. and Bevan, O.M. - Municipal tunnelling: a contractor's viewpoint, Tunnels and Tunnelling 4 (1972) 237-247.

Subsidence Engineers Handbook, National Coal Board Mining Department (1975).

Sweet, A.L. and Bogdanoff, J.L. - Stochastic model for predicting subsidence, J. Eng. Mech. Div., ASCE 91 (1965) 22-45.

Szechy, K. - Surface settlements due to the shield tunnelling method in cohesionless soils, Proc. Conf. on Subway Construction, Budapest-Balatonfured (1970) 615-625.

Terzaghi, K. - Influence of geological factors on the engineering properties of sediments, Harvard University, Soil Mech. Series 50 (1955).

Terzaghi, K. and Peck, R.B. - Soil mechanics in engineering practice, Wiley, N.Y. (1967).

Tomlin, G.R. - Seepage analysis through zoned anisotropic soils by computer, Geotechnique 16 (1966) 220-230.

Trotter, F.M. and Hollingsworth, S.E. - Correlation of northern drifts, Geologists' Magazine 69 (1932) 374-380.

Ullrich, Z. - Predicted surface settlements along planned n.s. metro line in Budapest, Melyip Tud Szemle 24 (1974) 519-523.

Voight, B. and Pariseau, W. - Strata of predictive art in subsidence engineering, J. Soil Mech. and Found. Eng. ASCE (1970) 721-750.

Walsh, T. and Biggart, A.R. - The bentonite tunnelling machine at Warrington, Paper presented at I.M.M. International Symp. "Tunnelling '76", London (1976).

Ward, W.H. - Precast concrete tunnel linings, Int. Cong. of Precast Industry (1966) 140-151.

Ward, W.H. - In Deep excavations and tunnelling in soft ground, Proc. 7th Int. Conf. on Soil Mech. and Found. Eng., Mexico City 3 (1969) 320-325.

Ward, W.H. and Thomas, H.S.H. - The development of earth loading and deformation in tunnel linings in London Clay, Proc. 6th Int. Conf. Soil Mech. and Found. Eng., Toronto 2 (1965) 432-436.

Wrigley, W. - The seepage of water into tunnel excavations, M.Sc. Thesis, University of Durham (1974).

Wyckoff, R.D. and Reed, D.W. - Electrical conduction models for the solution of water seepage problems, J. Applied Physics 6 (1935).

Zienkiewicz, O.C. and Cheung, Y.K. - The finite element method in structural and continuum mechanics, McGraw-Hill, London (1976).

Zienkiewicz, O.C., Mayer, P. and Cheung, Y.K. - Solution of anisotropic seepage by finite elements, J. Eng. Mech. Div., ASCE 92 (1966) 111-121.

APPENDICES

Appendix A

THE DRIFT MORPHOLOGY OF THE NORTH OF ENGLAND

Because the Tyneside area lies above a large buried valley, the great majority of civil engineering works in this locality are constructed in, or founded on, either glacial drift or post-glacial deposits such as alluvium or made ground. For example, of the 62 kilometers of interceptor sewer being constructed for the Northumbrian Water Authority, approximately 50 kilometres will be in this drift, the remainder being in the Coal Measures lying directly beneath it (Boden, 1967). All the tunnels on Tyneside which are described in this thesis are constructed in either glacial deposits of one kind or another or in more recent alluvium. The geological discussion here will therefore be confined to consideration of the drift deposits, and will only briefly mention the underlying rocks.

The surface drift deposits of the North-East of England were formed mainly as a result of glaciation occurring during the Pleistocene epoch. Estimates of the number of major glacial episodes that have occurred in this area vary from one (Francis, 1970) to five (Trotter and Hollingsworth, 1932). It is generally agreed, however, that the existing deposits have largely derived from the final stage of glaciation and date from the last few thousand years of the Weichselian, between 18,000 and 10,000 years before the present (Boden, 1972). Since it seems likely that some glacial deposits must have been layed down at an earlier stage than this, when, of course, glacial deposition is known to have been widespread elsewhere, it must be assumed that these

deposits were eroded away prior to the final glaciation by the advancing ice.

The general succession for the North-East of England is as follows:

Upper Till

Middle Sands

Lower Till

Hutton Henry Peat

Scandinavian Drift

Weathered Rockhead

The weathered rockhead in the Tyneside area consists almost entirely of Coal Measures rocks, typically sandstones, shales, mudstones, fireclay and coal, with localised Permian outliers in the south east.

The Scandinavian Drift dates from the first stage of the Weichselian, the Saalian. It is very localised in occurrence. Erratics in this deposit come, not only from Scandinavia, but also from Scotland, and the alternative name of Warren House Till has been proposed (Francis, 1970). The Hutton Henry Peat is likewise very uncommon. It is Eemian in age, dating from the middle, temperate stage of the Weichselian, and was deposited during an interglacial period.

The Lower Till (Wear Till or Blackhall Till) has been dated at about 18,500 years before the present (Francis, 1970) and is the major component of the succession. It is a stiff, sandy clay containing many erratics from the Lake District and Scotland. It represents the main stage of glaciation visible in this area, reaching a maximum thickness of 30 m. Overlaying this are localised sands known as the

Middle Sands. These are alluvial deposits and represent the second interglacial period of the Weichselian, corresponding with the Durham Complex to the south.

In general, in the North-East of England, the Middle Sands are directly superseded by the Upper Till. This is a brown stony clay for which the alternative names of Horden Till or Pelaw Till have been proposed by Francis (1970). It represents the final stage of glaciation in the area. The deposit tends to be thinner and less widespread than the Lower Till, but is found in most parts of the Eastern section of the area (i.e., East of Gateshead). It reaches a maximum of about 6 metres in thickness but in general is only 3 or 4 metres thick. It is normally or only very slightly overconsolidated, suggesting that the clay has never been subjected to a very large overburden such as an ice sheet. Beaumont (1967) suggests that this stony clay may represent a reworked boulder clay, probably the Lower Till, deposited as a turbidite, but if this were the case the clay would be expected to show well-graded bedding, which has in fact proved undetectable. Its lower boundary is highly irregular, suggesting that the stony clay was deposited after a period of erosion.

The above succession is complicated locally by the fact that the Tyne valley was considerably overdeepened during the interglacial period between the deposition of the Lower and Upper Tills. The Tyne valley is overdeepened by about 40 metres at its mouth, indicating that at this time the sea was at a much lower level than at present. The buried valley is filled with a complicated series of deposits known, not inappropriately, as the Buried Valley Deposits. These consist mainly of laminated clays with stony clays, silts, sands, and gravels,

often overlying varved clays. The silts, sands and gravels are often water-bearing. The varved clays at the bottom of the succession probably represent glacial lacustrine sediments resulting from the damming of the Tyne valley, at this time considerably deeper than at present, by the North-East ice sheet as the Western ice sheet withdrew during the late Weichselian stage, some 10,000 years before the present (Francis, 1970).

Above the varved clays the Buried Valley Deposits represent a much more changeable situation. They suggest a combination of simple lacustrine sedimentation (laminated clays), with periodic re-advances of the ice (stony clays), and much periglacial activity (sands, gravels, and like deposits).

The principal component of the Buried Valley Deposits is the laminated clay. This is generally regarded as a lacustrine deposit. Thin sections show both flocculated and roughly sub-parallel structures of the clay minerals (Bewick, 1973). The former suggests slightly saline conditions whilst the latter, found in the laminations, suggests fresh water. Hence the laminated clay was probably layed down in rather brackish conditions with periodic incursions of fresh water.

Some of the sediments making up the Buried Valley Deposits, particularly isolated units of stony clay, may, in fact, represent slumps or solifluction deposits (Francis, 1970).

The mode of origin of the Buried Valley Deposits has resulted not only in considerable vertical variation in material but also in marked horizontal changes in lithology, making correlations of successions extremely difficult, even between quite closely-spaced boreholes (Boden, 1972).

Uppermost in the succession are a number of localised occurrences of recent alluvium. These may rest on the Upper Till or may lie in valleys eroded deeper into the drift (as at Willington Gut). They consist largely of sand, silt, or gravel, sometimes containing considerable amounts of organic material and often with bands of peat or clay.

The drift, quite naturally, tends to be shallower over high ground, increasing in thickness as the rivers are approached. The maximum thicknesses of drift are found within the courses of the buried valleys. For example, in the Team Valley depths to rockhead as great as 60 metres have been recorded.

Details of the geotechnical properties of the particular materials encountered in the fieldwork described in this thesis are given in Chapter 4. A brief summary of the engineering properties of the drift in general is given below.

1. Lower Till

This is a stiff, hard, dark grey or brown sandy clay with scattered rounded pebbles and boulders. Its shear strength normally lies between 120 kN/m^2 and 170 kN/m^2, but may go as high as 400 kN/m^2 in places. This, combined with its uniform nature, makes it a good material for tunnelling. It is quite stable, and under most conditions would not require shield support (Boden, 1967), unless particularly wet.

2. Upper Till

This is a red or brown plastic clay containing a few small, generally angular, stones. Unlike the Lower Till it is not sandy. Its

shear strength is generally around 100 kN/m^2. It is also a good tunnelling medium but would usually require the use of a shield to avoid excessive surface settlements due to its more plastic nature.

Both of the tills are virtually impervious, as would be expected. Calculations based on consolidation tests from the site investigation reports suggest a coefficient of permeability for the tills of around 10^{-10} m/sec.

3. Buried Valley Deposits

Due to their lithological variation, the Buried Valley Deposits show marked changes in their geotechnical properties. The laminated clays are brown in colour and quite plastic. They generally have an undrained cohesion of around 50 kN/m^2, but this may go as low as 15 kN/m^2 or as high as 100 kN/m^2 in places. These values, obtained from the site investigation reports, are the result of many undrained tiraxial tests on 38 mm diameter samples cut axially at right angles to the laminations and are, therefore, representative of the strength of the clay itself. The laminae are silty or sandy, are frequently water-bearing, and much weaker than the surrounding clay. They make ideal slip planes and endow the laminated clay with anisotropic properties. Permeability in laminated clays can be highly anisotropic. Perpendicular to the laminations, the coefficient of permeability is around 10^{-9} m/sec, that is, it is practically impervious. Parallel to the laminations the coefficient of permeability may be much greater (Terzaghi, 1955). Chan and Kenney (1973), reporting on a Canadian varved clay, find a permeability ratio (the ratio between horizontal and vertical permeability) of only about 5, but this is for a clay with well-graded

layers rather than with distinct laminations. Kenney (1963) suggests that, in theory, soils with distinct laminations would be expected to show a higher permeability ratio. Parry (1972) reports on strongly-laminated Oxford Clay with a fine "dusting" of silt or sand along the laminations (i.e., a soil quite similar to the laminated clay in the North-East, although more highly overconsolidated). He finds a vertical permeability of 5×10^{-10} m/sec and a horizontal permeability of 3.5×10^{-8} m/sec (i.e., a permeability ratio of 70). This anisotropy may have a marked effect on the tunnelling properties of the soil, and is discussed further in Chapter 5.

The properties of the stony clays found amongst the Buried Valley Deposits are quite similar to those of the Upper Till, and they should therefore prove to be good tunnelling materials. Gravels and sands in the Buried Valley Deposits are uncemented and often water-bearing.

Appendix B

THE TYNESIDE SEWERAGE SCHEME

All the fieldwork carried out by the author and which forms the basis of this thesis was on various sections of the sewerage scheme at present being constructed in the Tyneside area. It is therefore considered appropriate to give a brief description of the scheme, its scope and its development.

B.1) History of the Tyneside Sewerage Scheme

In the early 19th century, industrialisation and population growth in the North-East of England began to cause pollution problems, particularly in the River Tyne. During the 19th century, migratory fish such as salmon disappeared from the Tyne due to pollution in the tidal estuary, and by 1920 the conditions in the river had become sufficiently bad to cause considerable public concern. A series of committees and investigations followed,but no significant result was achieved.

In 1966 the Tyneside Joint Sewerage Board was formed from a working party of representatives of the several public authorities on Tyneside, whose primary responsibility was the planning and construction of a new sewerage scheme. In 1974 this responsibility passed to the Northumbrian Water Authority.

At the present time, crude sewage from 88 percent of the population of Tyneside is discharged directly into the river. According to Norgrove and Staples (1976), the stratification of fresh water and sea water in the estuary results in an overall upstream movement of the

bottom layer of water, effectively trapping much organic waste in the estuary. At certain times of the year conditions in the Tyne become anaerobic and the smell may become offensive. The new sewerage scheme has therefore given priority to the removal of suspended organic solids from the river, with further treatment of the sewage as and when it is shown to be necessary.

Sewage from the area will be intercepted before it reaches the river and directed to treatment plants where the sludge can be separated and then dumped at sea.

B.2) Layout of the scheme

A map of the Tyneside drainage area is shown in Figure 1.1. This map shows the location of the north and south bank interceptor sewers, the treatment plants, the offshore spoil grounds and also gives the position of the three instrumentation sites described in this thesis. The drainage area covered by the scheme is a predominantly urban area of about 33,000 Ha including the City of Newcastle upon Tyne, together with industrial areas such as Gateshead, Hebburn, Jarrow, Howdon, and Wallsend. The scheme has been designed to serve a population of 1.3 million, which is the projected population of Tyneside in the year 2054.

The scheme will include three treatment plants at Dunston, Jarrow and Howdon,and approximately 62 km of interceptor sewer. These interceptor sewers, which are shown in Figure 1.1, run close to, and more or less parallel to the banks of the river with a spur at the North-East of the area running northwards parallel to the coast. The sewage from the North bank will flow South from Seaton Valley and Whitley Bay, and East from Newburn to the main treatment works at

Howdon. On the South bank, sewage from as far West as Gateshead and as far East as South Shields will converge on the preliminary treatment plant at Jarrow, and thence under the river via the Tyne siphon to Howdon. West of Gateshead a separate system carries the sewage from as far West as Ryton to be treated at the plant at Dunston. This separate system allows for a more flexible approach, necessary due to planning uncertainties concerning future population growth in the Southwest of the area, and also avoids the need for the construction of major sewers beneath the high ridge running north/south through Gateshead (Norgrove and Staples, 1976). The sewage is moved through the interceptors mainly by gravity. The depth of the interceptors is such that certain areas close to the river banks cannot be drained by gravity and these, producing relatively little sewage, are served by pumping stations and rising mains.

Eventually the area will have separate drainage and sewerage systems, the sewerage scheme being designed to accept the "foul flow" only of the projected 1.3 million population. However, the sewerage system will have to deal with stormwater runoff for the time being. Vortex type overflows have been installed at all major intercept points in order to make the most effective use of the interceptor sewers at all times.

According to Norgrove and Staples (1976) the estimated expenditure on the major construction programme is approximately 72 million. This expenditure is being phased over a long period, partly to spread the costs and partly to balance the demands on the industries' resources, the tunnelling industry in particular being "reasonably stretched" by the several projects running concurrently in the area.

Approximately 0.5 to 1.0 percent of the total estimated cost of the scheme has been spent on site investigation, principally on boreholes (about 1 per 120 m of sewer) and laboratory testing.

B.3) Sewage treatment

In 1964 it was decided, after a detailed investigation (Oakley and Dyer, 1966), to use sewage treatment works on the banks of the estuary rather than a sea outfall. This decision was partly economic, a cost comparison indicating that in the long term the cost of constructing and running the treatment works would be lower than that of constructing major sewers to a long sea outfall north of Whitley Bay, and also on the grounds of political pressure from the coastal authorities.

The main treatment plant is under construction at Howdon (see Figure 1.1). This plant will treat the sewage from the entire north bank and from the south bank east of Gateshead. Preliminary treatment consists firstly of screening the crude sewage through 100 mm and then 25 mm grids, followed by the removal of grit particles down to 0.2 mm diameter. Moisture is pressed out of the screenings which are then incinerated.

The sewage then flows into large settlement tanks (4 x 8000 m^3) on the south bank where most of the remaining sludge is allowed to settle out. This sludge is removed to storage tanks, and thence carried by barge to a dumping ground some 10-13 km offshore. Initially, this is the only treatment the sewage will receive. However, once the new system comes into operation, the quality of the river water will be monitored in order to assess the need for further treatment. Sufficient

land has been obtained to provide facilities for treatment up to Royal Commission standard, should that prove to be necessary. Preliminary treatment (screening and de-gritting) of the sewage from the south bank east of Gateshead will be carried out at the preliminary treatment works at Jarrow, prior to the passage of the effluent through the Tyne siphon to the plant at Howdon.

Effluent from the treatment works at Dunston will probably have to be treated to a higher standard than that from Howdon, since it will be retained in the estuary for a longer period. The design of this plant has not yet commenced, and the level of treatment has not yet been decided.

B.4) Sewerage

The scheme will involve the construction of approximately 62 km of interceptor sewer. About 50 km of this will be constructed in soft ground, the remainder in coal measures deposits (Boden, 1967). A large proportion of this construction will be underground. This is largely due to the fact that the route of the tunnel carries it through various types of urban and industrial development where the surface disturbance of cut and cover workings would be impossible or at least unacceptable.

The interceptors range in size from 0.6 m to 3.7 m internal diameter, the smaller diameters being constructed in timbered headings, the larger diameters in tunnel. For the soft ground tunnel construction a conventional bolted concrete segment primary lining has been used throughout, although a modern smooth-bore concrete lining was also considered.

The soft ground tunnels have been driven through a wide variety of deposits including boulder clay, laminated clay, soft organic silts, sands and gravels both below and above the water table (see Appendix A). This has provided a wide variety of tunnelling problems. At Neville St. in Newcastle, ground freezing was successfully used to stabilise a water-bearing fine sand through which a shaft was sunk. It has been necessary on a number of occasions, including one of the drives investigated in this thesis, to use compressed air in the tunnels to stabilise the tunnel face in very poor ground. Compressed air was used as a precautionary measure throughout the southbound drive of the Tyne siphon, due to the expected presence of water-bearing fissures beneath the bed of the river.

Many of the soft ground tunnel drives to the present time have used a shield, particularly those in the Buried Valley Deposits or alluvium and where the ground is either unpredictable or of poor quality. In better ground such as the stony clay, shields have proved to be unnecessary. Two of the case histories presented in the thesis, at Hebburn and Willington Quay were shield driven, the third, at Howdon, being in the stony clay.

Appendix C

FIELD INSTRUMENTATION

C.1) Main aims of the instrumentation

The main objectives of the measurement programme at all sites can be summarised as follows:

a. To measure the development of vertical settlement at the ground surface on the tunnel centre-line as the tunnel face progresses past the measurement points;

b. To delineate the shape and width of the surface settlement trough both while settlement is occurring and after it is complete;

c. To measure the development of vertical settlement with depth, both on the tunnel centre-line and at various distances away from the tunnel;

d. To measure the lateral displacement of the ground surface across the settlement trough perpendicular to the tunnel line of advance;

e. To measure lateral displacements of the ground at depth around the tunnel.

These measurements were carried out at all sites.

In some cases, measurements of pore water pressure, deformation of the tunnel lining, and direct measurement of ground movement into the face and onto the tunnel lining were carried out to supplement the main measurement programme. Laboratory tests, including extrusion tests (see Chapter 4), were also carried out on samples from certain sites to supplement the data available from the site investigation reports. Throughout the measurement programme the same methods and

equipment were used at all sites, making the results from each site consistent with one another and directly comparable. The methods used to attain the above five objectives were as follows:

a. In order to measure surface settlement, conventional levelling techniques were applied, using a surveyor level and staff, and surveying to semi-permanent levelling posts set in concrete or nails driven into the road surface.

b. Lateral surface movements were measured directly using a steel band and measuring between the surface levelling stations.

c. Magnetic-ring settlement gauges were installed in boreholes and used to monitor vertical movements below the ground surface.

d. The same boreholes contained aluminium inclinometer access tubes permitting measurement of lateral movement at depth both parallel to, and perpendicular to the tunnel centre-line, using a Soil Instruments inclinometer.

C.2) General layout of instrumentation

Site plans and details of the specific instrumentation layout at each site are given in Chapter 4. However, all the sites have several aspects in common, and these are detailed here. The principal instrumentation that was installed at each site consisted of surface levelling monuments and boreholes containing inclinometer access tubes and magnetic settlement rings.

Generally, the boreholes were set out in one or more lines perpendicular to the tunnel line of advance, with one borehole on the centre-line, one just outside the tunnel wall, and others at various distances further away for completing settlement profiles. The boreholes

were usually drilled to a depth 1 metre greater than that of the tunnel invert.* Inclinometer access tubes were installed in each of these boreholes, along with magnetic settlement rings at various depths.

C.3) Surface levelling stations

Since all sub-surface measurements of movement, both with the settlement rings and the inclinometer, were taken relative to datum points on the surface, the accuracy of these measurements is therefore limited by the accuracy of the surface surveying, which is itself limited by the stability of the surveying points themselves. The construction of these surveying monuments varied according to the particular site conditions (see Chapter 4). All were designed to be as rigid as possible, both in the vertical and horizontal sense. At all sites the levelling stations were installed several months prior to the commencement of the measuring programme, in order to allow time for them to stabilise.

At Hebburn and Howdon the ground surface was soft, being soil at Hebburn and ashy till at Howdon. At these sites the surveying monuments were constructed by excavating holes in the ground about 300 mm across and cementing steel pegs into them. The pegs were braced with steel cross pieces to keep them firmly in place in the cement. The Hebburn monuments, illustrated in Figure 4.8, were installed on public land by the side of a suburban street (see Figure C.1). It was therefore necessary to install the entire assembly below the ground surface and protect it with a box over the top. The holes were excavated down to the clay and the pegs were driven into this prior to

*Settlement measurements were referenced to surface surveying levels. Otherwise, these boreholes would have to have been taken much deeper to undisturbed ground.

cementing them in place.

The Howdon site was on a piece of waste ground adjacent to the railway sidings (see Figure 4.18). It was considered acceptable here to install the monuments with the tops of the pegs above ground surface, making surveying easier and more accurate. The ground consisted variously of ashy fill, ballast from the nearby railway tracks, and clay soil. Shorter pegs were used here and not set into the ground, which would have provided only a poor hold. Stability was ensured by using larger concrete blocks and building up the concrete almost to the tops of the pegs. The Howdon monuments are illustrated in Figure 4.22. In spite of the poor ground surface encountered at Howdon, the settlement stations gave consistent results throughout the monitoring period with little spread, and are considered to have performed adequately.

Surveying stations at Willington Quay were set out on a public highway (Gut Road) used extensively by heavy lorries servicing the Bridon ropeworks. It was therefore impossible to install any permanent instrumentation which would have stood appreciably "proud" of the road surface. Temporary stations were rejected because of their complexity and the probability of their silting up, a problem encountered with the boreholes. Instead, very simple permanent stations were constructed by driving nails into the road surface using a "Spit Gun." Nails of about 80 mm in length and 4 mm diameter were mounted, about 3 mm proud of the road surface, using steel washers. These stations had a sufficiently low profile to be harmless to vehicles, and despite the fact that some of them were subjected to the virtually continuous passage of heavy vehicles, they performed quite reliably and consistently.

The surveying monuments were installed in arrays running at right angles to the centre-line of the tunnel. These arrays were long enough to cover the whole width of the expected settlement trough, running from the centre-line to a distance of 2 to 3 times the depth of the tunnel. Surveying points were spaced evenly along this line, generally at 5 metre intervals, with extra points adjacent to the boreholes. A number of monuments was placed on the opposite side of the centre-line to check the symmetry of the trough. A temporary bench mark, of similar construction to the surveying monuments, was installed at sufficient distance from the centre-line to avoid any settlement, that is, more than 4 times the depth to the tunnel axis, but close enough to the array to maintain a high degree of accuracy, and all levelling was carried out relative to this point.

At all sites the surveying stations were used both for settlement measurements and for the monitoring of lateral movements. To facilitate lateral measurements the tops of the pegs were marked at the centre with a centre-punch.

C.4) Surface surveying procedures

As mentioned above, all surface surveying had to be as accurate as possible, since the sub-surface measurements were related to datum points at the surface. Offsetting this need for accuracy, however, was the need to be able to take sets of readings reasonably quickly, particularly when the tunnel face was close to the array, and the need for the monuments to be simple and robust enough to withstand the elements. At Willington Quay, for example, the settlement points were regularly driven over by heavy lorries, and at Howdon they were

vulnerable to contractors traffic and vandalism.

C.4.1) Surface levelling

Levelling was carried out using a Cooke 540 precise level and a heavy, one piece metric staff. The level was manual in operation and equipped with an internal optical micrometer. The staff used was graduated in 1/4 cm sections, the optical micrometer being used to interpolate between these markings to the nearest 0.05 mm.

Hanna (1973) suggests that a closing error of better than 0.5 mm is obtainable using this type of level. Similar results are reported by Cheney (1974). This is the closing error which should be obtainable over quite a long levelling traverse, but over the short distances involved in the surveying for tunnel settlement measurements, better accuracy can be expected. Levelling results taken over the period before any ground movement was detected at all instrumentation sites, indicated that the overall precision of the levelling procedure was around $\pm$ 0.2 mm, which is quite consistent with the observations of Hanna (1973) and Cheney (1974).

The levelling procedure was quite simple. The nearest settlement point was levelled to the temporary bench mark from two different level positions. The level was then moved to a position offset a few metres from the array but close to its centre. From here the remaining settlement points were levelled to the primary settlement station, with the level in two positions. The use of an intermediate level rather than levelling all points direct to the temporary bench mark introduces another source of error, but it is considered that this inaccuracy is outweighed by the increase in speed and precision from

placing the level closer to the surveying points. At Howdon, where the array was 55 m long, two intermediate levels were used to avoid levelling over excessive distances.

The arrays were levelled several times prior to the commencement of tunnel construction in order to establish an accurate set of datum levels. To improve the consistency of the results, levelling was carried out as far as possible using the same level operator and the same staff-man. On the occasions where this was not possible, a slight deterioration of the results became apparent, particularly where a different level operator was used, but in most cases the results were still acceptable.

C.4.2) Lateral surface measurements

In all cases measurements of lateral surface movements were taken using the surface settlement monuments. Movements were monitored by direct measurement using a 30 m (100 ft) graduated steel band. The band was held at a constant tension of 10 Kgf during measurement using a spring balance. At Howdon, where the measurement points projected well above ground level, this constant tension maintained a consistent catenery between the stations, and this was reproduced precisely each time measurements were taken. At the other sites, where the monuments were below, or flush with, the ground surface, the constant tension simply maintained identical conditions for each set of measurements.

Variations in the conditions at each site, coupled with problems such as ground irregularities where measurements were taken with the tape running along the ground surface meant that measurements of the absolute values of the distances between the settlement points

were not comparable. However, by taking care to ensure that the measurement technique and the conditions were identical for each set of readings, the relative movements between the stations could be found with reasonable precision.

It is important, where small relative movements are to be measured, to use as consistent a measurement technique as possible. This not only involves very careful observations, constant tape tension and care to ensure that the tape is straight and unobstructed throughout its length, but also means that the same personnel should be used to take all the measurements throughout a particular experimental programme. On the few occasions when it was necessary to take measurements using different personnel, the results were often found to be inconsistent and erratic. Generally, these results have been disregarded and are not presented in this thesis.

Since we are primarily interested in the relative movements of the surveying points rather than the actual distance between them, it was decided not to attempt to correct directly for changes in the temperature of the tape. These temperature changes were quite considerable, particularly at Willington Quay, where observations were made in hot summer conditions, with an air temperature of over 25° C, and in winter temperatures below freezing point. Although direct correction for these fluctuations would have been desirable, equipment for the accurate measurement of the temperature of the tape itself was unavailable. The use of air temperature was considered unsuitable since at times the tape experienced direct sunshine and would have been at a higher temperature than the surrounding air, while at other times it was submerged in water which would be expected to be below air temperature.

To correct indirectly for fluctuations in tape temperature, all readings at a given site were normalised to a nominal measurement right across the array, where no relative movement was expected, but where the tape conditions were precisely the same as for the other measurements. This normalisation process is bound to introduce small errors into the results, equal to the percentage error in measurement of the normalisation length, and the possibility of small movements between these primary points, but these errors are small compared with other errors inherent in the measurement system.

The tape was calibrated throughout its length in decimal feet, with marks at 0.01 ft (3 mm) intervals. Readings could be estimated to 0.001 ft (0.3 mm) at each station by practised observers. Under perfect conditions, the limit of accuracy of such a system is the sum of the observational errors at each point of measurement. Since readings were estimated to the nearest 0.33 mm the error should be $\pm$ 0.15 mm at each end, or a total error of 0.3 mm if the estimation procedure at each end is perfect and there is no tape movement between readings at either end. It should be noted that this represents the ultimate accuracy attainable for measurements of relative movements between the stations. The real accuracy obtainable with such a system is naturally rather less than this. Hanna (1973) suggests an optimum accuracy of $\pm$ 1 mm in 30 m when corrections for tape sag, tension, temperature and ground slope have been made, but the accuracy of relative measurements should be somewhat greater than this. Sources of error in tape measurement are discussed more fully by Milner (1969).

For all measurements of horizontal displacement, at least 3 sets of readings were taken at each station using different parts of

the tape. Anomalous readings were discarded and extra sets taken to give at least 3 sets of measurements within ± 0.002 ft (0.6 mm). The readings were averaged to give the final value. The observation procedure was kept as simple as possible and remained precisely the same throughout the three experiments. The tape was held tight along the line of measurement, one man holding the tape winder firmly against the ground, the other maintaining a constant 10 kgf in tension using a spring balance. The two observers read off the distance at their respective surveying stations simultaneously, to avoid as far as practicable the possibility of tape movement between observations.

Several complete sets of readings were taken over a period of several months before the commencement of tunnel construction in order to obtain a good datum value for the distance between each station. These datum values give a good indication of the overall accuracy of the system, and are generally within ± 0.5 mm of the average after all corrections have been made.

Measurements of lateral movement were also taken to the tops of the inclinometer access tubes, in order to ascertain whether the movement of the tubes corresponded to the movement of the ground surface. These observations were made using close-fitting steel plugs illustrated in Figure 4.17, readings being taken between punch marks at the tops of the rods. To ensure maximum accuracy the plugs were made an extremely close fit in the tubes, and required cleaning and oiling before insertion was possible.

C.5) Boreholes

Measurement of sub-surface movement at all sites was carried

out in boreholes set in arrays across the tunnel centre-line. The layout of the arrays is detailed in Chapter 4 and in Figures 4.6, 4.16 and 4.20. All boreholes were of 6" diameter and were drilled using conventional shell and auger methods. In bad ground at Willington Quay it was necessary to case the holes during drilling to prevent them caving in. The depths of the boreholes are shown in Tables 4.4, 4.8, and 4.10. The boreholes were generally drilled down to axis depth, with some, particularly on the centre-line down to a few metres below invert level. Ideally, where boreholes are to be used for the measurement of movement, for example, using inclinometers and settlement gauges, they should be drilled to a depth where no movement is expected and movements calculated relative to this point (in the same way that levels are measured relative to a bench mark beyond the zone of influence of the tunnel). This would improve the accuracy of the sub-surface measurements and also provide a check on the surface surveying. However, in the case of measurements around tunnels this would involve drilling the boreholes down to a considerable depth (at least 2 diameters below invert). This would, of course, increase the cost of the instrumentation considerably. In consequence, shallower boreholes were used and the movements in them were referred to the surveyed movement at the surface.

Soil Instruments inclinometer access tube was installed down the full length of each borehole. This consists of extruded aluminium tubing, 50 mm in internal diameter, with four orthogonal keyways running along its length. The tube is installed in 3 m lengths held together by telescopic joints. The joints are made up by "pop-riveting" a short length (200 mm) of slightly oversize tube over the

ends of the access tubes to be joined. The "pop-rivets" are designed to be weak enough to shear through any movement along two overlapping tube sections once the tube has been installed, thus permitting the tubes to move easily relative to one another. Magnetic rings were fixed around the inclinometer access tubes at various depths (see Table 4.4, 4.8 and 4.10) either by using small aluminium brackets riveted into place or by waterproof tape. This allows the rings to move freely relative to the tubes once installed. The entire assembly was surrounded by a bentonite-cement-water grout designed to possess similar geotechnical properties to those of the ground.

C.5.1) Ground coupling

In all field instrumentation procedures proper coupling between the ground and the instruments is of vital importance. Although coupling problems vary considerably with different forms of instrument, the basic aim is always the same: to install the instrument or probe in such a way that a) it measures correctly the conditions in the adjacent ground, and b) its presence does not affect the parameters it is designed to measure. These requirements often entail making the properties of the instrument as close as possible to those of the ground, for example, the elastic and plastic parameters, density and so on. In the case of boreholes used to measure ground displacement, it is necessary to ensure that a) the inclinometer access tubes and settlement rings move exactly the same amount as the surrounding ground, and b) that the ground movement is not distorted by the presence of the tube or the borehole. The first condition is fulfilled by ensuring that the magnetic rings are free to move axially along the tube and that the

inclinometer access tubes themselves are free to move in a lateral sense. Free movement of the magnetic rings is ensured by mounting them very weakly on the tubes, thus permitting them to slide freely up and down with movements in the surrounding grout. Movement of the tube itself is taken up by flexibility of the joints and to some extent of the tube itself. Although more flexibility of the tubing would be desirable this conflicts with the necessity for the tube cross section to remain absolutely uniform to permit smooth access for the inclinometer torpedo, and would also encourage twisting of the tube. This restriction of the movement to the joints is not very apparent from the inclinometer plots (Chapter 5) but may be more obvious where larger movements are involved. The telescopic joints also permit the tube sections to move in the vertical sense relative to each other, reducing the chance of interference between the tube and the settlement rings.

The second condition is fulfilled by designing the grout to possess a three month cohesion identical to that of the ground. A perfect match would mean that the grout behaved exactly like the ground, thus faithfully transmitting ground movements to the instrumentation. A stiffer grout would tend to resist the ground movement whereas a softer grout would tend to absorb some of it either elastically or plastically. Both effects mean that the resultant observations would be too low, and therefore the results presented in Chapter 5 should be regarded as minimum values. The loose flexible joints of the inclinometer access tubes should mean that they are flexible enough to offer negligible interference to movement of the grout.

C.5.2) Vandalism at Howdon

As was noted in Chapter 4, the instrumentation at Howdon was particularly vulnerable to vandalism. Since the boreholes were installed some months prior to the commencement of observations, these were effectively camousflaged in order to avoid this possibility. This proved to be rather over-effective since in the course of levelling the site the contractor inadvertently bulldozed over the borehole tops. Of the total of five boreholes four were recovered and the top sections replaced as shown in Figure 4. The top sections were concreted into place and caps padlocked over the tops. These padlocks were broken open and the tubes blocked with stones by vandals. Using a close fitting plug fixed to rigid rods it was possible to reclaim tubes 1 and 2 (see Figure 4.) but unfortunately tubes 3 and 4 remained firmly blocked at a depth of about 3 metres and therefore were not monitored.

C.6) The inclinometer

A Soil Instruments Mk 2 inclinometer with digital readout was used throughout the fieldwork described in this thesis. The torpedo consists of a tube with a pair of wheels, one sprung and one with its axle fixed, at either end. These wheels act to guide the torpedo down the keyways of the access tube, the spring permitting the torpedo to move smoothly past the joints in the tube, and also taking up a certain amount of distortion if necessary. The fixed wheels are either 0.5 m or 1.0 m apart, depending on the particular instrument, and it is between these that the measurements are made.

The principle of operation is as follows. The tube contains an oil-damped, high-density metal tapered bob-weight attached to a spring steel lead which is fixed at its top end to the body of the torpedo itself. Temperature matched resistance strain gauges are bonded to each side of the leaf spring forming a full bridge circuit. The whole assembly is sealed against the ingress of moisture. When the inclinometer torpedo is tilted, the bob-weight swings away from vertical causing the leaf spring to bend. The strain gauges respond to this distortion and this response is converted electronically into the value of the angle of tilt of the torpedo or the lateral displacement between the two fixed wheels. This is displayed as a digital readout at the surface. The facility is provided for the automatic summation of the displacements, giving a continuous profile down the hole. The system is reasonably insensitive to changes in temperature, the drift of an absolute reading being 2 secs/deg C (Green, 1973), but to ensure maximum accuracy it is advisable to ensure that the torpedo is immersed in water while readings are taken in order to provide a stable temperature. The readout unit is extremely sensitive to even slight amounts of moisture, becoming erratic and sometimes unusable in quite light rain. Several waterproofing devices were tried, the most successful being simply to cover the entire equipment, readout, cable drum and connectors, with a large plastic sheet. No method was entirely successful, however, and the most reliable results were obtained on dry days.

C.6.1) Accuracy of the inclinometer system

We must consider the accuracy of the inclinometer system in two parts: the accuracy of the instrument itself (torpedo, readout

and access tube assembly) in ideal conditions, and also the error due to "environmental" factors (installation, poor coupling, the effects of moisture, temperature changes, and so on). The accuracy of inclinometer systems has been discussed by several authors, most notably Dunnicliffe (1971), Gould and Dunnicliffe (1971), Green (1973), Hanna (1973) and Cording (1974).

The Soil Instruments Mk 2 system has a digital readout, reading to 0.0001 m (0.1 mm) displacement. This gives a maximum readable precision of $\pm$ 0.05 mm per $\frac{1}{2}$ m length for a half metre torpedo, resulting in a total error over a ten metre length of $\pm$ 1.0 mm. Green (1973) reported on the performance of two inclinometers, the Wilson 200 series slope indicator and the Soil Instruments Mk 1. The Wilson slope indicator uses a pendulum operated rheostat to derive an electrical analogue of inclination. The Soil Instruments Mk 1 is similar to the Mk 2 used by the author, but is only 12" (304.8 mm) in length and operates in plastic access tube of different cross section. Tests on the two instruments were carried out in the laboratory using 80' (24.38 m) lengths of access tubing calibrated against plumblines. These, of course, represent ideal conditions and give no indication of the system's compliance with the ground. The Mk 1 inclinometer uses a volt meter as its readout, reading to 0.5° and by estimation to 0.05°. This is equivalent to a deflection of 0.9 mm per metre. In practice the inclinometer was found to give an error in a single run of $\pm$ 0.15" (3.8 mm) over 80' (24.38 m) with a 4" (101 mm) deflection overall. For a deflection of 16" (0.406 m) the error is -0.1" to +0.5" (-2.54 mm to +12.7 mm). If an average of two runs is taken, one running down the tube and one running up it, the errors

reduce to ± 0.1" (2.54 mm) and ± 0.3" (7.62 mm) respectively. This would represent an error of ± 1.56 mm over 15 m (approximately 0.1 mm per metre for the best case). According to Green (1973), who was responsible for its design, the Soil Instruments Mk 2 inclinometer will read to an accuracy of 0.01^{o} which is equivalent to a deflection of 0.2 mm per metre or 3.0 mm in 15 m in the worst case when all errors sum together. In practice, since the Mk 2 has a resolution five times as great as the Mk 1 (0.01^{o} versus 0.05^{o}) we would expect its overall accuracy to be considerably improved. Green (1973) reports the field performance of the Mk 2 inclinometer in a 22 m length of casing. For a 3.3 mm registered displacement he finds a standard deviation of 0.3 mm over 16 sets of readings. The principal sources of error outside the instrument itself are spiralling of the casing (usually caused during the manufacture of the tube), and lack of repeatability of the reading position of the torpedo in the tube. The former was so small as to be immeasurable in the Soil Instruments tubing used and any twist present is probably restricted to the joints. Lengths of tubing 15 m in length were assembled in the laboratory and no twist could be measured between the ends. Green (1973) observed no twist in the aluminium tube, although in the plastic tubing used for the Soil Instruments Mk 1 instrument a cumulative twist of 16^{o} was observed.

Errors derived from inconsistency in the positioning of the torpedo are dependent partially on the accuracy of the cable markings, and partially on the skill of the operator. Careful technique and regular calibration of the cable should reduce these to a minimum.

"Environmental" errors, such as those due to temperature changes, can be avoided by careful operation. The consistency of the

datum values indicates that these are negligible. The datum values obtained at Willington Quay using a 1 metre torpedo show standard deviations of on average 0.075 mm for a series of four sets of observations. Occasional higher spreads indicate unstable measuring points, possibly due to distortions in the tubes or measurements taken close to joints. Proper grouting should ensure that the tube movements accurately reflect those of the ground, but, as previously noted, all sub-surface measurements should really be regarded as minimum values.

C.6.2) Measurement procedure

Measurements were taken at intervals from the top of the tube equal to the distance between the torpedo fixed wheels, both to attain the optimum accuracy and to simplify the data reduction procedure. The automatic summation facility was not used. A complete set of readings was taken with the torpedo moving down and then up the tube. This process was repeated with the unsprung wheels of the inclinometer in each of the four keyways. Thus four pairs of values were obtained for each level. Pairs of observations differing by more than 0.4 mm were rejected and the measurement repeated until consistent values were obtained, although normally the values differed by less than 0.2 mm. The data were then reduced and plotted out by computer (see Appendix D).

C.7) The magnetic settlement rings

In order to measure the vertical movement of the ground at depth, magnetic ring settlement gauges were installed around the

inclinometer access tubes at various depths, generally one at axis level and three or four rings equally spaced above this. The transducers themselves consist simply of radially polarised magnetic metal rings with an internal diameter about 5 mm greater than that of the inclinometer tubes. The rings were lightly attached to the access tubes at the required depths prior to their installation, using adhesive tape or small brackets "pop-riveted" in place. This ensured that the rings were free to move around the tubes with the surrounding grout. It must be emphasised that the settlement gauges are probably the most sensitive of all the instrumentation to poor ground coupling. It would be preferable to use gauges that couple directly into the soil rather than linking to it via the grout, such as are described by Burland and Moor (1973), but this type of equipment is unsuitable for installation around inclinometer access tubes. The rings used should perform satisfactorily provided that the grout is correctly matched to the soil, the rings are free to move and the strains to be measured are not too great. If the grout is poorly matched, then the magnetic rings, like the inclinometer, will give results which are too low. The subsurface settlements should thus be regarded as minimum values.

The position of each ring was monitored using a simple, magnetically-operated reed switch connected to a battery and buzzer at the surface. When the reed switch passes through a magnetic field of sufficient strength the circuit is closed, causing the buzzer to operate. The reed switch is sealed into a probe weighing about 0.5 kg which fits fairly closely into the inclinometer access tube. A steel tape, calibrated in millimetres throughout its length, is attached to the probe. The weight of the probe ensures that the tape is held

straight and under fairly constant tension throughout operations.

C.7.1) Method of operation

As the probe is lowered down the tube towards a magnetic ring, the magnetic field increases in strength until the reed switch closes and a note is heard from the buzzer. If the probe is lowered still further the field will decrease until the switch opens and the note stops. A similar sequence occurs as the probe is raised. To accurately locate the position of the ring, the opening and closing distances with the probe ascending and descending are averaged. Allowance must also be made for the distance between the reed switch and the end of the tape. Readings are taken to a mark at the top of the inclinometer tubes and are estimated to the nearest $\frac{1}{2}$ mm. As four readings are averaged to find the actual value the final accuracy should be rather better than this, provided that all the observations are made by the same operator. Readings taken by different operators proved to be so inconsistent that they were discarded.

As for the other instrumentation, a series of datum readings were taken prior to the construction of the tunnels. Tests on some of these observations show that they were normally distributed with a standard deviation of less than 0.5 mm.

The reed switches used throughout the measurement programmes were highly susceptible to the ingress of water and would endure only a couple of months use before a replacement became necessary. After repair it was necessary to re-calibrate the probe and for this purpose a simple laboratory rig was built. The calibration was checked regularly on this rig as a precaution against any movement of the tape

mounting.

C.8) The piezometers

At the Willington Quay and Howdon sites piezometers were installed in some of the boreholes (see Chapter 4). The piezometers were attached to the inclinometer access tubes at the required depths prior to their installation in the boreholes. The presence of the access tubes in the boreholes means that the normal type of open standpipe to the piezometer is impractical. Instead, a connection to the surface was made via two small diameter flexible plastic pipes. During installation it is imperative to ensure that the piezometers are not surrounded by grout. The boreholes were grouted to within 0.2 m of the base of the piezometer (checked by calculating the volume of grout required and then by dipping the boreholes with a plumbline). A metre of uniform sand was then added to cover the piezometer and ensure an uninterrupted flow of water followed by the rest of the grout as normal.

The piezometers were read using the simple tensometer shown in Figure C.1. The principle of operation is to pump de-aired water down one of the piezometer tubes and back through the tensometer until the entire system is free of any air locks. When the pump is detached, the water in that tube falls to balance the piezometric head at the piezometer, and the mercury in the tensometer is pulled up until it balances this drop in level. The mercury level is read to the nearest $\frac{1}{2}$ mm giving the piezometric head accurate to 7 mm. The system will only operate while the piezometric head is less than approximately 10 m (i.e., the tensometer cannot measure a pressure drop greater than one

atmosphere).

C.9) Other instrumentation

Various instrumentation methods were used for in-tunnel deformation measurements at the various sites to measure clay movements. Details of these are given in Chapter 4.

Appendix D

INCLINOMETER DATA PROCESSING

As described in Appendix C, the nature of the inclinometer's operation means that a certain amount of "data processing" is necessary before the results can be plotted. Four readings are taken at either 1 m or $\frac{1}{2}$ m intervals, depending upon the choice of recording instrument. These readings are averaged to give the displacement of the lower fixed wheel of the inclinometer relative to the top. The displacements are then summed to give the profile of the inclinometer tube and this is subtracted from the datum profile (obtained prior to the passage of the tunnel) to give the lateral displacement of the tube. This displacement can be found relative to either the top or the bottom of the tube. If the boreholes are deep enough, say to a depth of 2 or 3 tunnel diameters below invert level, it is reasonable to assume that there is no movement at the base of the tubes and in this case movements should be related to the base. For shallower boreholes, as described in this thesis, such an assumption cannot be made, and movements must therefore be related to the tops of the tubes. In this case it is necessary to monitor the movement of the tops of the tubes and add this to the "down-hole" displacements.

The above processing can best be carried out by computer. A program (INCPLOT) to do this and to plot the results is listed at the end of the thesis. It is written in Algol W, and was originated by Mr. A. Gowland in the Engineering Geology Laboratories at Durham University, but has since been extensively modified by the author. This program is

capable of plotting data from either $\frac{1}{2}$ m or 1 m inclinometers (or a combination of the two) relative to the surface or the base of the tubes.

The nature of the inclinometer readout makes it difficult to identify certain types of erroneous reading. Readings are only considered acceptable if both the upward and downward readings agree to with $\pm$ 0.2 mm. However, it is still possible to record erroneous observations if, when the inclinometer is turned through 180°, it is not parallel to its original position. This can arise when the fixed wheels are at a joint in the tube or due to distortion or dirt in the keyways. This point is perhaps clarified by reference to Figure 5.1. It is possible to detect "out of parallel" readings such as this quite simply since for parallel readings the sum of the four observations will be constant. Erroneous readings found in this way are replaced by the averages of the readings directly above and directly below. A program (CHECK) to carry out these corrections is listed at the end of the thesis.

In general it proved unnecessary to correct the data obtained from Hebburn or Willington Quay, although corrections were necessary to the data from Howdon.

The inclinometer plots presented in the main text of the thesis are tracings of the computer plots. Tracings are used both to improve the clarity of the plots as well as to reduce the large amount of computer output to more manageable proportions. An example of the computer output is presented along with the program listings.

Appendix E

THE NUMERICAL CALCULATION OF SETTLEMENT AND LATERAL DISPLACEMENT

The program (STOC) described in this Appendix and listed at the end of the thesis calculates settlement and lateral displacement using the source functions developed in Chapter 2. The program is written in PL1. The above parameters are calculated numerically for a tabular void and an annular void by summing the effects of infinitessimal point sources evenly distributed through the voids. These are plotted out along with the settlement and lateral displacement calculated directly for a single point source located at the centre of the tunnel.

Appendix F

THE FINITE DIFFERENCE PROGRAMS

F.1) The three-dimensional program

The first program presented in this Appendix (TUNPOT) calculates the potential at the nodal points of a cubic mesh around the tunnel as illustrated in Figure 3.1. The program is written in PL1. The finite-difference calculation itself is basically that described by Smith (1974), modified for three dimensions and to take account of different horizontal and vertical permeabilities. The tunnel is modelled as a cruciform-sectioned tube with a "radius" of 2 units. All other dimensions are scaled to this, thus restricting the models to only approximate representations of the originals. Any number of horizontal layers of differing permeabilities can be modelled, limited only by the mesh size.

Although for the examples shown a constant over-relaxation factor of 1.8 is used, it is possible to arrange for this to be changed during the calculation to improve convergence. Iterations are continued until the maximum change in potential at any point due to one iteration is exceeded by a pre-determined value.

The output consists of matrices of the node potentials representing sections in the plane of the face and the centre-line, alone with a horizontal section at axis-level. These are contoured and plotted using a Fortran program written by F.J. Rens of the Geography Department of the University of Durham.

F.2) The two-dimensional program

The second program presented in this Appendix (SECTION) calculates the potential field around a lined tunnel of infinite length. It is also written in PL1. It operates in a similar way to TUNPOT but simply calculates potentials in a plane perpendicular to the centre-line. In consequence its operation is considerably more rapid than the three-dimensional equivalent. The output is contoured and plotted in the same way as that from the three-dimensional program. Both programs are listed at the end of the thesis.

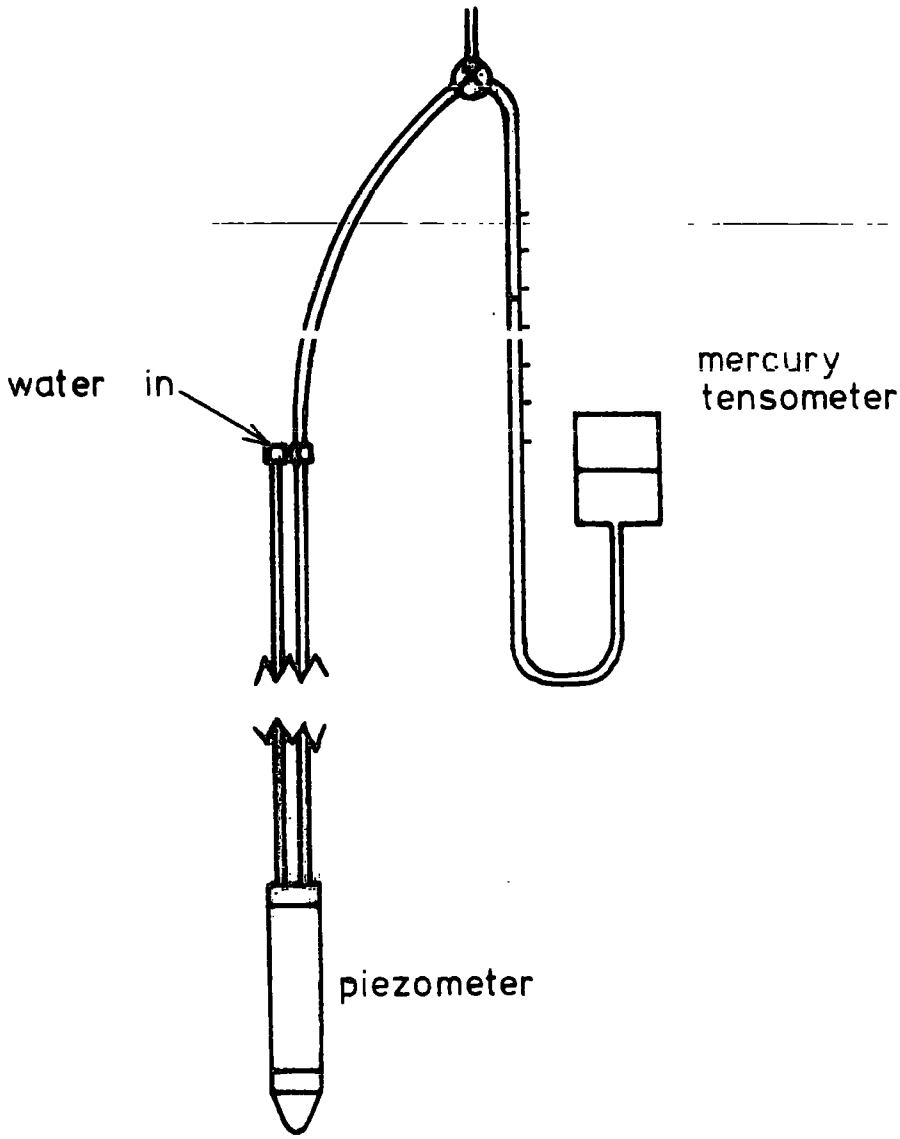

Figure C.1

```
1       SECTION:PROCEDURE OPTIONS(MAIN);
1.02    /*    THIS PROGRAM CALCULATES THE POTENTIAL FIELD IN A PLANE PERPENDICULAR
1.04          TO AN INFINITELY LONG TUNNEL USING THE FINITE DIFFERENCE METHOD. A
1.06          SQUARE MESH IS SET UP WITH DIMENSIONS "WIDTH" AND "HEIGHT" UNITS,
1.08          SCALED TO GIVE A TUNNEL DIAMETER OF 4 UNITS. THE TUNNEL IS LOCATED
1.1           AT A DEPTH "Z". A NUMBER OF LAYERS OF DIFFERING PERMEABILITY MAY
1.12          BE MODELLED AND THESE MAY BE ANISOTROPIC.    */
2       DCL (HEIGHT,WIDTH,INVERT,SOFFIT,UJ,SWITCH,
3       TEST,TEST2) FIXED BIN;
4       DCL CONTOUR ENTRY(CHAR(7),CHAR(40),CHAR(8) VARYING,FIXED BIN,FIXED BIN,
5            FIXED BIN,(*,*) FLOAT);
6       DCL (PERMUP,PERMDN,PERMH,PMAX,PREC,ORFACTOR,FACINC) FLOAT;
7       DCL (P(0:HEIGHT+1,-1:WIDTH+1),
8       P2(0:HEIGHT2,0:WIDTH2)) FLOAT CONTROLLED;
9       DCL (V(LAYERNO),H(LAYERNO)) FLOAT CONTROLLED;
10      DCL D(LAYERNO) FIXED BIN CONTROLLED;
11      DCL (VE(10),HE(10)) FLOAT;
12      DCL DE(10) FIXED BIN;
13      DCL BOUND FILE OUTPUT;
14      DCL (HEIGHT2,WIDTH2,Z,DIA,NIT,KOUNT) FIXED BIN;
15      DCL IDNUM CHAR(8) VARYING;
16      DCL (TA(0:500),TB(0:500)) FLOAT;
17      DCL GUESS FLOAT;
18       ON ENDFILE(SYSIN) GO TO FINISH;
18.02   /*    ID NUMBER (FOR OUTPUT IDENTIFICATION), MAXIMUM POTENTIAL (ARBITRARILY
18.04         100), AND TUNNEL DIAMETER ARE SET.    */
19      IDNUM='MNH8';
19.1    PMAX=100;
19.11   DIA=4;
19.2    /*    DATA IS READ IN.    */
20      START:GET DATA;
21      ALLOCATE V,H,D;
22      DO I=1 TO LAYERNO;
23        GET LIST(V(I),H(I),D(I));
24      END;
25            KOUNT=0;
25.2    /*    POTENTIAL FIELD IS ALLOCATED A CONSTANT, GUESSED VALUE.    */
26      ALLOCATE P;
27            P=GUESS;
28            P(0,*)=0;
29            P(*,-1)=0;
30      SOFFIT=Z-DIA/2;
31      INVERT=Z+DIA/2;
32      UJ=WIDTH-DIA/2;
33      TEST2=1;
33.2    /*    THE FOLLOWING SERIES OF DO LOOPS ASSIGNS THE BOUNDARY
33.4          CONDITIONS.    */
34      LOOP:TEST,A,B=0;
35            N=1;
35.02   /*    TA AND TB PROVIDE A RUNNING CHECK ON THE PROGRESS OF
35.04         THE ITERATIONS.    */
36      TA(KOUNT)=P(5,12);
37      TB(KOUNT)=P(14,12);
37.2    /*    PERMEABILITIES ARE ASSIGNED TO EACH LAYER.    */
38            DO I=1 TO HEIGHT;
39             PERMUP,PERMDN=V(N);
40             PERMH=H(N);
41             IF I=D(N) THEN DO;
42             PERMDN=V(N+1);
43             PERMH=MAX(H(N),H(N+1));


44             N=N+1;
45             END;
46        DO J=WIDTH BY -1 TO 0;
47             A,B=0;
48        IF I=HEIGHT THEN DO;
49          A=A+PERMDN*P(I+1,J)-PERMUP*P(I-1,J);
50          B=B+PERMDN-PERMUP;
51          END;
52           IF J=WIDTH THEN
53            A=A+PERMH*(P(I,J+1)-P(I,J-1));
54           IF J=UJ & (I=SOFFIT | I=INVERT) THEN GO TO CALC;
55           ELSE IF J>=UJ & I>=SOFFIT & I<=INVERT THEN DO;
56              P(I,J)=PMAX*I/INVERT;
57              GO TO END;
58           END;
58.2    /*    FINITE DIFFERENCE CALCULATION.    */
59      CALC: TEMP=P(I,J)+((PERMUP*P(I-1,J)+PERMDN*P(I+1,J)+PERMH*
60            (P(I,J-1)+P(I,J+1))-A)/(PERMUP+
61            PERMDN+2*PERMH-B)-P(I,J))*ORFACTOR;
62      IF P(I,J)=0 THEN ACC=1;
63      ELSE ACC=TEMP/P(I,J);
63.2    /*    CONVERGENCE IS CHECKED.    */
64      IF ACC>1+PREC|ACC<1-PREC THEN TEST,TEST2=1;
65      P(I,J)=TEMP;
66      END: A,B=0;
67        END2:END;
68      END;
69           KOUNT=KOUNT+1;
70            IF TEST=0 THEN DO;
71             IF TEST2=0 THEN GO TO DETAIL;
72             TEST2=0;
72.2    /*    OVER-RELAXATION FACTOR IS CHANGED.    */
73             ORFACTOR=ORFACTOR+FACINC;
74           END;
75           IF KOUNT<NIT THEN GO TO LOOP;
76      DETAIL:TA(KOUNT)=P(5,12);
76.02   /*    OUTPUTS POTENTIAL FIELD CLOSE TO TUNNEL INTO FILE "BOUND".    */
77      TB(KOUNT)=P(14,12);
78      HEIGHT2=3*DIA+1;
79      WIDTH2=3*DIA/2+1;
80      ALLOCATE P2;
81      DO I=0 TO HEIGHT2;
82        DO J=0 TO WIDTH2;
83           P2(I,J)=P((Z-3*DIA/2),(J+UJ-DIA));
84        END;
85      END;
86      J=1;
87      DO I=1 TO LAYERNO;
88        IF D(I)<=Z-3*DIA/2 THEN GO TO ENDLAYER;
89        IF D(I)>=Z+3*DIA/2 THEN DO;
90          DE(J)=3*DIA+1;
91          I=LAYERNO;
92          GO TO LAYEROUT;
93        END;
94        DE(J)=D(I)-Z+3*DIA/2;
95        LAYEROUT:VE(J)=V(I);
96        HE(J)=H(I);
97        LN=J;
98        J=J+1;
99      ENDLAYER:END;


100     OPEN FILE(BOUND) OUTPUT;
101     PUT FILE(BOUND) LIST(DIA,LN,PMAX,ORFACTOR,PREC,SWITCH);
102     DO J=1 TO LN;
103       PUT FILE(BOUND) LIST(VE(J),HE(J),DE(J));
104     END;
105     PUT FILE(BOUND) LIST(P2);
106     CLOSE FILE(BOUND);
107     FREE P2;
107.2   /*    PRINTED OUTPUT.    */
108     F1:  FORMAT(X(5),A,F(2),A);
109     F2:  FORMAT(X(5),A,F(5,2));
110     F3:  FORMAT(R(F2),A);
111     DO I=0 TO KOUNT;
112       PUT SKIP DATA(TA(I),TB(I));
113     END;
114     OPUT:PUT PAGE EDIT('INPUT DETAILS')(X(40),A);
115          PUT SKIP(6) EDIT('BLOCK DIMENSIONS-')(X(5),A);
116          PUT SKIP(4) EDIT('DEPTH OF SECTION=',HEIGHT,' UNITS')(R(F1));
117          PUT SKIP(2) EDIT('WIDTH OF SECTION=',WIDTH,' UNITS')(R(F1));
118          PUT SKIP(6) EDIT('TUNNEL DIMENSIONS-')(X(5),A);
119          PUT SKIP(4) EDIT('DEPTH TO AXIS=',Z,' UNITS')(R(F1));
120          PUT SKIP(2) EDIT('DIAMETER OF TUNNEL=',DIA,' UNITS')(R(F1));
121     DO N=1 TO LAYERNO;
122     PUT SKIP(4) EDIT('LAYER ',N)(X(10),A,F(2));
123     PUT SKIP(2) EDIT('HORIZONTAL PERMEABILITY=',H(N),'UNITS')(R(F3));
124     PUT SKIP(2) EDIT('VERTICAL PERMEABILITY=',V(N),'UNITS')(R(F3));
125     PUT SKIP(2) EDIT('THICKNESS OF LAYER=',D(N)-D(N-1),'UNITS')(R(F1));
126     END;
127          PUT SKIP(6) EDIT('Z/D=',INVERT/DIA)(R(F2));
128          PUT SKIP(2) EDIT('Z/H=',INVERT/HEIGHT)(R(F2));
129          PUT SKIP(2) EDIT('NUMBER OF ITERATIONS=',KOUNT)(X(5),A,F(2));
130        PUT SKIP EDIT('(ITERATION CONTINUED TO A PRECISION OF ',
131     PREC*100,'%)')(X(6),A,F(5,2),A);
132          PUT SKIP(2) EDIT('OVER RELAXATION FACTOR=',ORFACTOR)
133     (X(5),A,F(5,2));
134     PUT PAGE EDIT('POTENTIAL ARRAY. VERTICAL SECTION PERPENDICULAR TO',
135     ' TUNNEL CENTRE-LINE.')(X(5),A,A);
136          PUT SKIP(4);
137       PX: DO I=0 TO HEIGHT;
138             PUT SKIP(3);
139             DO J=WIDTH BY -1 TO 0;
140               PUT EDIT(P(I,J))(F(7,3));
141             END PX;
142     IF SWITCH=2 | SWITCH=3 THEN
143       CALL CONTOUR('SECTION','SECTION PERPENDICULAR TO CENTRE-LINE',IDNUM,
144       10,WIDTH+1,HEIGHT+1,P(*,*));
145     A13: GO TO FINISH;
146     CONTOUR:PROC (TI,TITLE,USERID,INC,PLOTLENGTH,ROW,P);
146.02  /*    OUTPUTS SECTION THROUGH POTENTIAL FIELD INTO FILE "FNAME"
146.04        IN A FORM SUITABLE FOR PROCESSING BY CONTOURING PROGRAM.    */
147     DCL FNAME FILE,
148         TI CHAR(7),
149         TITLE CHAR(40) VARYING,
150         USERID CHAR(8) VARYING,
151         FORM CHAR(28) INITIAL('10F8.4/10F8.4/10F8.4/10F8.4/'),
152         FORMAT CHAR(28) VARYING,
153         (INC,ROW,PLOTLENGTH,X,Y) FIXED BIN,
154         P(100,100) FLOAT;
155     LOWCON=0;
156     HICON=100;


157     PLOTWIDTH=8;
158     DENOM=1;
159     OPEN FILE(FNAME) OUTPUT TITLE(TI);
160     PUT FILE(FNAME) EDIT('12      1.0E0      1.0E0      0.2E0')(A)
161         (TITLE)(SKIP,A)('12      1.0E0      1.5E0      0.2E0')(SKIP,A)
162         (USERID,'15',LOWCON,INC,HICON,'19')(SKIP,A,SKIP,A,3 F(10),SKIP,A);
163     X=7*TRUNC(ROW/10);
164     Y=MOD(ROW,10);
165     IF Y=0 THEN DO;
166       FORMAT=SUBSTR(FORM,1,X-1);
167       PUT FILE(FNAME) SKIP EDIT('(',FORMAT,')')(A,A,A);
168       END;
169     ELSE DO;
170     FORMAT=SUBSTR(FORM,1,X);
171     PUT FILE(FNAME) SKIP EDIT('(',FORMAT,Y,'F8.4)')(A,A,F(1),A);
172     END;
173     PUT FILE(FNAME) EDIT('01',PLOTLENGTH,ROW,PLOTWIDTH,DENOM)
174     (SKIP,A,4 F(10));
175     C5: DO J=0 TO PLOTLENGTH-1;
176     PUT FILE(FNAME) SKIP;
177       DO I=ROW-1 BY -1 TO 0;
178        PUT FILE(FNAME) EDIT(P(I,J))(F(8,4));
179     END C5;
180     PUT FILE(FNAME) EDIT('20','13')(SKIP,A);
181     CLOSE FILE(FNAME);
182     RETURN;
183     END CONTOUR;
184     FINISH: END SECTION;
185     /*                  INPUT FORMAT
186     HEIGHT=<HEIGHT OF BLOCK (UNITS)>,
187     WIDTH=<WIDTH OF BLOCK (UNITS)>,
191     Z=<DEPTH TO AXIS (UNITS)>,
192     LAYERNO=<NUMBER OF LAYERS>,
193     GUESS=<ESTIMATED POTENTIAL>,
194     ORFACTOR=<OVER-RELAXATION FACTOR>,
195     FACINC=<OVER-RELAXATION FACTOR INCREMENT>,
196     PREC=<PRECISION AT WHICH ITERATION TERMINATES>,
197     NIT=<MAXIMUM PERMITTED NUMBER OF ITERATIONS>,
198     SWITCH=<1=NUMERICAL OUTPUT ONLY
199             2=OUTPUT TO CONTOURING FILES ONLY
200             3=1+2>;
201     <HORIZONTAL PERMEABILITY>  <VERTICAL PERMEABILITY>  <DEPTH
202          TO BASE OF LAYER>,  (REPEAT FOR EACH LAYER)    */
END OF FILE
```

```
BEGIN COMMENT THIS PROGRAM CALCULATES GROUND MOVEMENTS FROM INCLINOMETER
                                    DATA;
PROCEDURE TOLP(INTEGER VALUE I;
               REAL VALUE XX,DEINT,DIST;
               REAL ARRAY DISP,DEPTH(*);
               REAL VALUE XFACT,YFACT,ZFACT);
  BEGIN REAL X,YSTART,YSTOP;
    X:=XX+DIST/XFACT;
    YSTART:=3;
    YSTOP:=YSTART-I*DEINT/YFACT;
    PLTSCLE(0.0,ZFACT,0.0,-YFACT,X,YSTART);
    MOVETO(X,YSTART);
    DRAWTO(X,YSTOP);
    PLOTLINE(DISP,DEPTH,I+1,1.1,4.1);
  END;
PROCEDURE PLTNUM(REAL VALUE X0,Y0,HEIGHT;
                 LONG REAL VALUE NUMB;
                 REAL VALUE THETA;
                 STRING(7) VALUE FMT;
                 REAL VALUE SC);
      FORTRAN "PRFNMBR";
PROCEDURE PLOTAXIS(REAL VALUE X0,Y0;
                   STRING(10) VALUE BCD;
                   INTEGER VALUE NCHAR;
                   REAL VALUE AXLTH,THETA,XMIN,SC,DIST);
      FORTRAN "PAXIS";
PROCEDURE PLOTLINE(REAL ARRAY X,Y(*);
                   INTEGER VALUE N,K,J,L;
                   REAL VALUE SC);
      FORTRAN "PLINE";
 PROCEDURE DRAWTO(REAL VALUE X0,Y0);
      FORTRAN "PENDN";
PROCEDURE MOVETO(REAL VALUE X0,Y0);
      FORTRAN "PENUP";
PROCEDURE PLTSCLE(REAL VALUE XMIN,XFACT,YMIN,YFACT,XORG,YORG);
      FORTRAN "PLTOFS";
PROCEDURE SYMBOL(REAL VALUE X0,Y0,HEIGHT;
                 STRING(80) VALUE BCD;
                 REAL VALUE THETA;
                 INTEGER VALUE NCHAR);
      FORTRAN "PSYMB";
PROCEDURE PLOTEND;
      FORTRAN "PLTEND";
PROCEDURE PAPERMAX(REAL VALUE X);
      FORTRAN "PLTXMX";
PROCEDURE PLOTDASH(REAL ARRAY X,Y(*);
                   INTEGER VALUE N,K;
                   REAL VALUE DSLTH,SC);
      FORTRAN "PDSHLN";
REAL PROCEDURE SYMLNTH(REAL VALUE HGHT;
                       INTEGER VALUE NCHAR);
      FORTRAN "PSYMLN";
PROCEDURE SKIP(INTEGER VALUE N);
BEGIN FOR I:=1 UNTIL N DO
        BEGIN WRITE(" ");
        END;
END;
PROCEDURE F(INTEGER VALUE N,D);
BEGIN R_FORMAT:="A";R_W:=N;R_D:=D
END;


PROCEDURE E(INTEGER VALUE N);
BEGIN R_FORMAT:="S";  R_W:=N+7;
END;
PROCEDURE I(INTEGER VALUE N);
BEGIN I_W:=N;
END;
PROCEDURE B(INTEGER VALUE N);
BEGIN FOR I:=1 UNTIL N DO
    WRITEON(" ");
END;
PROCEDURE NEWPAGE; IOCONTROL(3);
INTEGER PROCEDURE LENGTH(STRING(256) VALUE WORDS);
  BEGIN INTEGER I; I:=256;
  CYC: I:=I-1;
       IF WORDS(I|1)=" " THEN GO TO CYC;
       I+1
  END;
PROCEDURE STRETCH(INTEGER VALUE RESULT IDSUB;
                  REAL VALUE RESULT DINTSUB;
                  REAL ARRAY TSUE,ASUB(*,*));
  BEGIN DINTSUB:=1.0;
  IDSUB:=TRUNCATE(IDSUB/2);
  FOR L:=1 UNTIL IDSUB DO
    BEGIN TSUB(L,1):=-(TSUB(2*L-1,1)+TSUE(2*L,1));
    TSUB(L,2):=-(TSUB(2*L-1,2)+TSUE(2*L,2));
    ASUB(L,1):=-(ASUB(2*L-1,1)+ASUB(2*L,1));
    ASUB(L,2):=-(ASUB(2*L-1,2)+ASUB(2*L,2));
    END;
  END;
PROCEDURE NEG(INTEGER VALUE ID;
              REAL ARRAY HORB,HORD,HORS(*);
              REAL ARRAY T,A(*,*));
  BEGIN FOR L:=0 UNTIL ID DO
    BEGIN HORB(L):=-HORB(L);
    HORD(L):=-HORD(L);
    HORS(L):=-HORS(L);
    FOR K:=1 UNTIL 2 DO
      BEGIN REAL TEMP;
      TEMP:=T(L,K);
      T(L,K):=A(L,K);
      A(L,K):=TEMP;
      END;
    END;
  END;
S_W:=0;
BEGIN
COMMENT MB IS THE NUMBER OF BOREHOLES
        MD IS THE MAXIMUM NUMBER OF READINGS OF ANY BOREHOLE
        HORDAT ARE THE DATUM VALUES
        T & A ARE THE RAW DATA;
  INTEGER MB,MD;
  REAL DATDINT;
  READ(MB,MD,DATDINT);
    BEGIN
    REAL ARRAY T,A(0::100,1::2);
    REAL ARRAY HORBAR,HORDIS,HORSUM,DEPTH,SUM(0::100);
    REAL ARRAY HORDAT(2::100,1::MB,1::2);
    REAL ARRAY TDISP,TDEPTH(1::101);
    FOR J:=1 UNTIL MD DO
    FOR K:=1 UNTIL MB DO


    FOR L:=1 UNTIL 2  DO READCN(HORDAT(J,K,L));
      BEGIN
      INTEGER ID,ICCN,JB,LB,LE;
      REAL BH,DINT,DIST,EPS,SCALE,GAP,HMIN,XX,XY,XO,YX,LX,LY,SH;
      REAL PLENGTH,SCALEX,SCALEY,SCALEZ;
      LONG REAL XL,YL;
      INTEGER XMIN,XMAX;
      STRING(80) TITLE,XLAB;
      STRING(10) USERID;
      STRING(3) BHC;
      READ(TITLE);
      READ(XLAB);
      READ(USERID);
      READ(BHC);
      READ(EPS);
      READ(SCALEX,SCALEY,SCALEZ);
      READ(XMIN,XMAX);
      SCALEX:=SCALEX*2.54;
      SCALEY:=SCALEY*2.54;
      SCALEZ:=SCALEZ*2.54;
      PLENGTH:=6.4*(XMAX-XMIN)/SCALEX;
      PAPERMAX(PLENGTH);
      LB:=LENGTH(TITLE);
      XX:=3.-XMIN/SCALEX;
      SKIP(4);
      SYMBOL(0.5,2.,0.2,USERID,90.,LENGTH(USERID));
      NEWPAGE;
      WRITE(B((90-LB) DIV 2+1),TITLE);
COMMENT BH IS THE BOREHOLE NUMBER & ORIENTATION AS X,Y
        X IS THE BOREHOLE NUMBER & Y THE ORIENTATION EITHER 1 OR 2;
      READ(BH);
COMMENT ID IS THE NUMBER OF READINGS FOR THE BOREHOLE
        DINT IS THE DEPTH INTERVAL 0.5 OR 1.0M.
        ICON CHANGES THE DIRECTION OF THE PLOT IF NON-ZERO
        DIST IS THE TUNNEL ADVANCE
        SH IS THE LATERAL SURFACE DISPLACEMENT;
      WHILE BH > 1.0 DO
        BEGIN
        READCN(ID,DINT,ICCN,DIST,SH);
        JB:=TRUNCATE(BH);
        LB:=ROUND((BH-JB)*10.);
        HORSUM(0):=SH;
        DEPTH(0):=0;
        HORBAR(0):=0;
        HORDIS(0):=0;
        T(0,1):=0; T(0,2):=0; A(0,1):=0; A(0,2):=0; SUM(0):=0;
        FOR L:=1 UNTIL ID  DO
          READ(T(L,1),T(L,2),A(L,1),A(L,2));
        IF DINT<>DATDINT THEN
        STRETCH(ID,DINT,T,A);
        FOR L:=1 UNTIL ID DO
          BEGIN
          DEPTH(L):=L*DINT;
          HORBAR(L):=(T(L,1)+T(L,2)-A(L,1)-A(L,2))/40.;
          HORDIS(L):=HORDAT(L,JB,LB)-HORBAR(L);
          HORSUM(L):=HORSUM(L-1)+HORDIS(L);
          SUM(L):=T(L,1)+T(L,2)+A(L,1)+A(L,2);
        END;
          IF ICCN=0 THEN
      NEG(ID,HORBAR,HORDIS,HORSUM,T,A);


          SKIP(2);
          WRITE(3(40),F(4,1),BH,B(2),F(7,2),DIST);
          SKIP(1);
          WRITE(B(30),"SURFACE DISPLACEMENT=",F(5,2),SH);
          SKIP(1);
          WRITE(B(17),"ORIGINAL DATA");
          WRITE(B(2),"DEPTH",F(6),"TOWARDS",B(10),"AWAY",B(8),"SUM"
            ,B(9),"DEPTH",B(6),"AVERAGE",B(5),"DIFFERENCE",B(5),
            "DISPLACEMENT");
          FOR L:=0 UNTIL ID DO BEGIN
          WRITE(B(2),F(4,1),DEPTH(L),B(3),F(6,0),T(L,1),T(L,2),B(3),
          A(L,1),A(L,2),B(3),SUM(L),B(5),F(4,1),DEPTH(L),B(5),F(8,3),
          HORBAR(L),B(5),HORDIS(L),B(7),F(10,3),HORSUM(L));
            TDISP(L+1):=HORSUM(L);
            TDEPTH(L+1):=DEPTH(L);
            END;
          TOLP(ID,XX,DINT,DIST,TDISP,TDEPTH,SCALEX,SCALEY,SCALEZ);
          READ(BH);
        END;
    IF XMIN REM 2=-1 THEN XMIN:=XMIN-1;
    IF XMAX REM 2=1 THEN XMAX:=XMAX+1;
      HMIN:=XMIN;
    FOR J:=XMIN STEP 2 UNTIL -2 DO
      BEGIN
      REAL HT;
      HT:=0.14;
      IF SCALEX>5 THEN
      HT:=0.7/SCALEX;
      XL:=-J;  XO:=XX-0.2+J/SCALEX;
      PLTNUM(XO,9.1,HT,XL,0.,"F3.0 ",0.);
    END;
      SYMBOL(XX,9.1,.14,"0",0.,2);
    FOR J:=2 STEP 2 UNTIL XMAX DO
      BEGIN
      REAL HT;
      HT:=0.14;
      IF SCALEX>5 THEN
      HT:=0.7/SCALEX;
      XL:=J;  XO:=XX-0.2+J/SCALEX;
      PLTNUM(XO,9.1,HT,XL,0.,"F3.0 ",0.);
    END;
    LX:=(XMAX-XMIN)/SCALEX+0.01;
    LY:=BPD/SCALEY;
    SYMBOL(3+(LX-SYMLNTH(.12,LENGTH(XLAB)))/2.,9.4,.12,XLAB,0.,
    LENGTH(XLAB));
    SYMBOL(3+(LX-SYMLNTH(.14,LE))/2.,9.75,.14,TITLE,0.,LE);
    SYMBOL(XX-0.2,9-10/SCALEY,.12,"DEPTH(0.5M)",90.,11);
    SYMBOL(3+(LX-0.5)/3.,8-LY,.14,BHC,0.,3);
    PLOTAXIS(3,9.," ",1.-LX,0.,HMIN,SCALEX,2/SCALEX);
    PLOTAXIS(-XX,9.," ",1.-LY,270.,0.,SCALEY,1.0);
      END;
  END;
    PLOTEND;
  END
END.
COMMENT      INPUT FORMAT.
             EACH LINE REPRESENTS ONE CARD.
  MB  MD  DATDINT
  (DATUM VALUES FOR ALL BOREHOLES. EACH CARD REPRESENTS A SINGLE DEPTH)
  "TITLE"



  "XLAB"
  "USERID"
  "BHC"
  BPD
  SCALEX  SCALEY  SCALEZ
  XMIN XMAX
  (THE FOLLOWING CARDS ARE ENTERED FOR EACH BOREHOLE)
  BH  ID DINT ICCN DIST SH
  (RAW DATA FROM INCLINOMETER, ONE CARD FOR EACH LEVEL)

WHERE:
  MB=NUMBER OF BOREHOLES
  MD=MAX NUMBER OF READINGS AT ANY BOREHOLE
  DATDINT=LENGTH OF INCLINOMETER USED FOR DATUM READINGS
  TITLE=TITLE OF PLOT OUTPUT
  USERID=USER'S ID NUMBER
  BHC=BOREHOLE IDENTIFICATION
  BPD=CODE FOR PRINT SIZE (NORMALLY 16)
  SCALEX=OVERALL HORIZONTAL SCALE (UNITS PER CM)
  SCALEY=OVERALL VERTICAL SCALE (METRES PER CM)
  SCALEZ=DISPLACEMENT SCALE (MM PER MM)
  XMIN=MINIMUM FACE ADVANCE
  XMAX=MAXIMUM FACE ADVANCE
  BH=BOREHOLE NUMBER AND ORIENTATION
  ID= NUMBER OF READINGS FROM BOREHOLE
  DINT=SIZE OF INCLINOMETER (0.5M OR 1.0M)
  ICCN=0.0 (IF NON ZERO=DIRECTION OF PLOT REVERSED)
  DIST=TUNNEL ADVANCE
  SH=SURFACE DISPLACEMENT;
END OF FILE
```

```
STOC:PROC OPTIONS(MAIN);
/*   THIS PROGRAM CALCULATES THE SETTLEMENT AND LATERAL DISPLACEMENTS
     AROUND A TUNNEL USING A MODIFIED VERSION OF THE 'SWEET AND
     BOGDANOFF' STOCHASTIC MODEL. THE TUNNEL IS MODELLED AS A POINT
     SOURCE, A TABULAR SEAM OR AN ANNULUS.  THE GEOMETRY OF THE
     TUNNEL IS ENTERED AS AXDEPTH, RAD AND VOLUME. SETTLEMENTS ARE
     CALCULATED AT A NUMBER OF LEVELS ABOVE THE TUNNEL GOVERNED BY
     'LEVNO' WHILE DISPLACEMENTS ARE CALCULATED FOR A NUMBER OF
     VERTICAL LINES OR BOREHOLES GOVERNED BY 'BHNO'. THE ABOVE PARAMETERS
     ARE ENTERED IN THE 'DATA' MODE. THE LAST TWO LINES OF DATA, INPUT
     IN THE 'LIST' MODE,  ARE THE DEPTHS OF THE SETTLEMENT LEVELS FROM
     THE GROUND SURFACE, AND THE DISTANCES OF THE BOREHOLES FROM THE
     CENTRE-LINE.    */
DCL(AXDEPTH,RAD,VOLUME,SCALE) FLOAT,
    (LEVNO,BHNO) FIXED BIN,
    (LEVEL(LEVNO),BOREHOLE(BHNO)) FLOAT CONTROLLED,
    (SEAMT,ANNT) FLOAT,
    (TEMP(101),DIST(101),DEPTH(101)) FLOAT CONTROLLED,
    (SETS(LEVNO,101),SETT(LEVNO,101),DISPS(BHNO,101),DISPT(BHNO,101),
    SETP(LEVNO,101),DISPP(BHNO,101)) FLOAT CONTROLLED;
/*   DATA IS READ IN.   */
INPUT:GET DATA(AXDEPTH,RAD,VOLUME,LEVNO,BHNO,SCALE);
IF LEVNO>0 THEN DO;
  ALLOCATE LEVEL;
  DO I=1 TO LEVNO;
    GET LIST(LEVEL(I));
  END;
END;
IF BHNO>0 THEN DO;
  ALLOCATE BOREHOLE;
  DO I=1 TO BHNO;
    GET LIST(BOREHOLE(I));
  END;
END;
START:ALLOCATE TEMP;
/*   DIST=DISTANCE FROM CENTRE-LINE.   */
IF LEVNO>0 THEN DO;
  ALLOCATE DIST,SETS,SETT,SETP;
  DO I=1 TO 101;
    DIST(I)=2*AXDEPTH*(I-1)/100.;
  END;
DO I=1 TO 10;
END;
/*   CALCULATE SETTLEMENTS FOR SEAM, ANNULUS AND POINT SOURCE.   */
  DO M=1 TO LEVNO;
    CALL SEAMSET(RAD,VOLUME,AXDEPTH-LEVEL(M),DIST,TEMP);
    SETS(M,*)=TEMP(*);
    CALL TUNSET(RAD,VOLUME,AXDEPTH-LEVEL(M),DIST,TEMP);
    SETT(M,*)=TEMP(*);
    CALL POINTST(VOLUME,AXDEPTH-LEVEL(M),DIST,TEMP);
    SETP(M,*)=TEMP(*);
END;
/*   PRINT TABLES OF RESULTS.   */
  CALL TABLE('SEAM','SETTLEMENT','DIST TO CL(M)',LEVNO,LEVEL,DIST,
             SETS);
  PUT SKIP(10);
  CALL TABLE('TUNNEL','SETTLEMENT','DIST TO CL(M)',LEVNO,LEVEL,DIST,
             SETT);
PUT SKIP(10);
CALL TABLE('POINT SOURCE','SETTLEMENT','DIST TO CL(M)',LEVNO,LEVEL,
             DIST,SETP);
END;
IF BHNO>0 THEN DO;
  ALLOCATE DEPTH,DISPS,DISPT,DISPP;
  DO I=1 TO 101;
    DEPTH(I)=(AXDEPTH+RAD)*(I-1)/100.;
  END;
/*   CALCULATE LATERAL DISPLACEMENTS DUE TO SEAM, ANNULUS AND
     POINT SOURCE.   */
  DO M=1 TO BHNO;
    CALL SEAMDSP(AXDEPTH,RAD,VOLUME,BOREHOLE(M),DEPTH,TEMP);
    DISPS(M,*)=TEMP(*);
    CALL TUNDISP(AXDEPTH,RAD,VOLUME,BOREHOLE(M),DEPTH,TEMP);
    DISPT(M,*)=TEMP(*);
    CALL POINTDP(AXDEPTH,VOLUME,BOREHOLE(M),DEPTH,TEMP);
    DISPP(M,*)=TEMP(*);
  END;
/*   PRINT TABLES OF RESULTS.   */
  CALL TABLE('SEAM','DISPLACEMENT','DEPTH(M)',BHNO,BOREHOLE,DEPTH,
             -DISPS);
  PUT SKIP(10);
  CALL TABLE('TUNNEL','DISPLACEMENT','DEPTH(M)',BHNO,BOREHOLE,
             DEPTH,-DISPT);
  PUT SKIP(10);
  CALL TABLE('POINT SOURCE','DISPLACEMENT','DEPTH(M)',BHNO,BOREHOLE,
             DEPTH,-DISPP);
END;
PUT SKIP;
/*   PLOT RESULTS.   */
IF LEVNO>0 THEN DO;
  IF BHNO<1 THEN CALL PLTXMX(28.0E0);
  IF BHNO>0 THEN CALL PLTXMX(30+12*BOREHOLE(BHNO)/(AXDEPTH+
                 RAD));
  CALL PLOT('SETTLEMENT',AXDEPTH,RAD,SETS,SETT,LEVEL,DIST,LEVNO,SCALE,
            0.0E0);
END;
IF BHNO>0 THEN DO;
  IF LEVNO<1 THEN DO;
    SH=0.0;
  IF 12*BOREHOLE(BHNO)/(AXDEPTH+RAD)>16 THEN
    CALL PLTXMX(12*BOREHOLE(BHNO)/(AXDEPTH+RAD));
  END;
  ELSE SH=3.0+12*DIST(101)/(AXDEPTH+RAD);
  CALL PLOT('DISPLACEMENT',AXDEPTH,RAD,DISPS,DISPT,BOREHOLE,DEPTH,BHNO,
            SCALE,SH);
END;
CALL PLTEND;
SEAMSET:PROC(R,V,LEV,W,SS);
/*   CALCULATES THE SETTLEMENT DUE TO A SEAM OF WIDTH R AND
     VOLUME V.   */
DCL (R,V,LEV) FLOAT,
    (W(101),SS(101)) FLOAT,
    (X,X1,Z,EX) FLOAT;
SS=0;
DO I=1 TO 100;
  X1=((I-50.5)/49.5)*R;
  DO J=1 TO 101;
    X=W(J)-X1;
    IF 2*X*X/(LEV*LEV)>100 THEN GO TO F;
    EX=EXP(-2*X*X/(LEV*LEV));
    SS(J)=SS(J)+V*EX*8/LEV;
F: END;
  END;
END SEAMSET;
TUNSET:PROC(R,V,LEV,W,ST);
/*   CALCULATES THE SETTLEMENT DUE TO AN ANNULAR VOID OF RADIUS
     R AND VOLUME V.   */
DCL (R,V,LEV) FLOAT,
    (W(101),ST(101)) FLOAT,
    (X,X1,Z,EX) FLOAT;
ST=0;
DO I=1 TO 100;
  X1=R*SIN(I*0.0628319);
  Z=LEV-R*COS(I*0.0628319);
  DO J=1 TO 101;
    X=W(J)-X1;
    IF 2*X*X/(Z*Z)>100 THEN GO TO E;
    EX=EXP(-2*(X*X)/(Z*Z));
    ST(J)=ST(J)+(V*EX*8/Z);
E:END;
END;
END TUNSET;
POINTST:PROC(V,LEV,W,SP);
/*   CALCULATES THE SETTLEMENT DUE TO A POINT SOURCE OF
     VOLUME V.   */
DCL (V,LEV,EX) FLOAT,
    (W(101),SS(101)) FLOAT;
SS=0;
DO I=1 TO 101;
  IF 2*W(I)*W(I)/(LEV*LEV)>100 THEN GO TO G;
  EX=EXP(-2*W(I)*W(I)/(LEV*LEV));
  SS(J)=SS(J)+(V*EX*8/LEV);
G:END;
END POINTST;
SEAMDSP:PROC(Z0,R,V,X,Z,DT);
/*   CALCULATES THE LATERAL DISPLACEMENT DUE TO A SEAM OF
     WIDTH R AND VOLUME V.   */
DCL (Z0,R,V,X) FLOAT,
    (X1,X2,Z1,Z2,Z3,EX,ST) FLOAT,
    (Z(101),DT(101)) FLOAT;
  DT=0;
  DO I=1 TO 100;
    X1=((I-50.5)/49.5)*R;
    X2=X-X1;
    DO J=1 TO 101;
      IF Z(J)<Z0 THEN DO;
        ON UNDERFLOW EX=0;
        ON OVERFLOW EX=0;
        Z3=Z0-Z(J);
        EX=EXP(-2*(X2*X2)/(Z3*Z3));
        ST=(8*V*EX/Z3);
        DT(J)=DT(J)-X2/Z3*ST;
      END;
    END;
  END;
END SEAMDSP;
TUNDISP:PROC(Z0,R,V,X,Z,DT);
/*   CALCULATES THE LATERAL DISPLACEMENT DUE TO AN ANNULAR VOID OF
     RADIUS R AND VOLUME V.   */
DCL (Z0,R,V,X) FLOAT,
    (X1,Z1,Z2,Z3,EX,ST) FLOAT,
    (Z(101),DT(101)) FLOAT;
  DT=0;
  DO I=1 TO 100;
    X1=X-R*SIN(I*0.0628319);
    Z1=Z0-R*COS(I*0.0628319);
    DO J=1 TO 101;
      IF Z(J)<Z1 THEN DO;
        ON UNDERFLOW EX=0;
        ON OVERFLOW EX=0;
        Z3=Z1-Z(J);
        EX=EXP(-2*(X1*X1)/(Z3*Z3));
        ST=(8*V*EX/Z3);
        DT(J)=DT(J)-X1/Z3*ST;
      END;
    END;
  END;
END TUNDISP;
POINTDP:PROC(Z0,V,X,Z,DS);
/*   CALCULATES THE LATERAL DISPLACEMENT DUE TO A POINT SOURCE
     OF VOLUME V.   */
DCL (Z0,V,X) FLOAT,
    (Z(101),DP(101)) FLOAT,
    (EX,SP,Z2) FLOAT;
  DP=0;
  DO I=1 TO 101;
    IF Z(I)<Z0 THEN DO;
      ON UNDERFLOW EX=0;
      ON OVERFLOW EX=0;
      Z2=Z0-Z(I);
      EX=EXP(-2*X*X/(Z2*Z2));
      SP=(8*V*EX/Z2);
      DP(J)=DP(J)-X/Z2*SP;
    END;
  END;
END POINTDP;
TABLE:PROC(TITLE,MODE,DATUM,NO,L1,L2,X);
/*   PRINTS TABLE OF RESULTS.   */
DCL (TITLE,MODE,DATUM) CHARACTER(20) VAR,
    NO FIXED BIN,
    L2(101) FLOAT,
    (L1(20),X(20,101)) FLOAT;
PUT SKIP(5) EDIT(TITLE)(X(35),A);
PUT SKIP EDIT(MODE,'(MM) AT')(X(30),A,A);
PUT SKIP EDIT('')(X(11));
DO I=1 TO NO;
  PUT EDIT(L1(I),'M')(X(6),F(4,1),A);
END;
PUT SKIP EDIT(DATUM)(X(3),A);
DO I=1 TO 11;
  J=(I-1)*10+1;
  PUT SKIP EDIT(L2(J))(X(6),F(5,2),X(2));
  DO L=1 TO NO;
    PUT EDIT(X(L,J))(X(5),F(6,2));
  END;
END;
END TABLE;
PLOT:PROC(MODE,Z0,R,X1,X2,L1,L2,NO,SC,SHIFT);
/*   PLOTS RESULTS ON NUMAC GRAPHICAL HARDWARE.   */
DCL (SHIFT,SC,Z0,R) FLOAT,
    NO FIXED BIN,
    L2(101) FLOAT,
    (L1(NO),X1(NO,101),X2(NO,101)) FLOAT CONTROLLED,
    TX(101) FLOAT,
    MODE CHARACTER(20) VAR,
    (SCALEX,SCALEY,XLTH,A) FLOAT,
    SCX FIXED DEC(5,2),
    NCHAR FIXED BIN(31),
    CHPAR CHARACTER(80) VAR,  BCD FLOAT DEFINED CHPAR;
SCALEX=25.4/SC;
SCX=SCALEX;
SCALEY=(Z0+R)/6.;
IF MODE='SETTLEMENT' THEN DO;
  XLTH=2*L2(101)/SCALEY;
  XMIN=-L2(101);
END;
ELSE IF MODE='DISPLACEMENT' THEN DO;
  XLTH=2*L1(NO)/SCALEY;
  XMIN=-L1(NO);
END;
A=SHIFT+2.0+XLTH/2.;
NCHAR=18;  CHPAR='DIST FROM C.L. (M)';
CALL PAXIS(SHIFT+2.0E0,8.0E0,BCD,NCHAR,XLTH,
           0.0E0,XMIN,SCALEY,1/SCALEY);
NCHAR=-8;  CHPAR='DEPTH(M)';
CALL PAXIS(A,8.0E0,BCD,NCHAR,6.0E0,-90.0E0,0.0E0,
           SCALEY,1/SCALEY);
CHPAR=SUBSTR(MODE,1,4)||' SCALE='||CHAR(SCX)||' MM PER IN';
NCHAR=LENGTH(CHPAR);
CALL PSYMB(A-2.0,1.0E0,-0.2E0,BCD,0.0E0,NCHAR);
CALL PENUP(A,8.0-Z0/SCALEY);
CALL PENDN(A-R/SCALEY,8.0-Z0/SCALEY);
CALL PCIRCL(A,8.0-Z0/SCALEY,90.0E0,-90.0E0,R/SCALEY,R/SCALEY,
            0.0E0,0.0E0);
DO I=1 TO NO;
  TX(*)=X1(I,*);
  IF MODE='SETTLEMENT' THEN DO;
    DO J=1 TO 101;
      IF TX(J)>2*SCALEX THEN TX(J)=2*SCALEX;
    END;
  CALL PSETT(TX,L2,-SCALEY,SCALEX,A,L1(I));
  END;
  ELSE IF MODE='DISPLACEMENT' THEN
  CALL PDISP(TX,L2,-SCALEX,SCALEY,A,-L1(I));
END;
DO I=1 TO NO;
  TX(*)=X2(I,*);
  IF MODE='SETTLEMENT' THEN DO;
  DO J=1 TO 101;
    IF X2(I,J)>2.0*SCALEX THEN X2(I,J)=2.0*SCALEX;
  END;
  CALL PSETT(TX,L2,SCALEY,SCALEX,A,L1(I));
END;
  ELSE IF MODE='DISPLACEMENT' THEN
  CALL PDISP(TX,L2,SCALEX,SCALEY,A,L1(I));
END;
END PLOT;
PSETT:PROC (SETSUB,XSUB,SUBX,SUBY,SUBAX,ISUB);
/*   PLOTS SETTLEMENT AND DISPLACEMENT CURVES.   */
DCL (SETSUB(101),XSUB(101)) FLOAT,
    (SUBX,SUBY,SUBAX,YORG) FLOAT,
    ISUB FLOAT,
    (NSUB,KSUB) FIXED BIN(31);
YORG=8.0-ABS(ISUB/SUBX);
CALL PLTOFS(0.0E0,SUBX,0.0E0,-SUBY,SUBAX,YORG);
CALL PENUP(SUBAX,YORG);
CALL PENDN(SUBAX+XSUB(101)/SUBX,YORG);
NSUB=101;  KSUB=1;
CALL PLINE(XSUB(1),SETSUB(1),NSUB,KSUB,0.0E0,0.0E0,1.0E0);
END PSETT;
PDISP:PROC (DSUB,ZSUB,SUBX,SUBY,SUBAX,ISUB);
DCL(DSUB(101),ZSUB(101),SUBX,SUBY,SUBAX,XORG) FLOAT,
    ISUB FLOAT,
    (NSUB,KSUB) FIXED BIN(31);
XORG=SUBAX+ISUB/SUBY;
CALL PLTOFS(0.0E0,SUBX,0.0E0,-SUBY,XORG,8.0E0);
CALL PENUP(XORG,8.0E0);
CALL PENDN(XORG,2.0E0);
NSUB=101;  KSUB=1;
CALL PLINE(DSUB(1),ZSUB(1),NSUB,KSUB,0.0E0,0.0E0,1.0E0);
END PDISP;
END STOC;
/*                 INPUT FORMAT
     AXDEPTH=<DEPTH TO AXIS (M)>,
     RAD=<TUNNEL RADIUS (M)>,
     VOLUME=<SETTLEMENT VOLUME AS % OF TUNNEL VOLUME>,
     LEVNO=<NUMBER OF LEVELS TO PLOT SETTLEMENT>,
     BHNO=<NUMBER OF 'BOREHOLES' TO PLOT DISPLACEMENT>,
     SCALE=<SETTLEMENT AND DISPLACEMENT SCALE (1=LIFESIZE)>;
<L(1)>  <L(2)>  ...  <L(LEVNO)>,    (DEPTH TO EACH LEVEL)
<BH(1)>  BH(2)>  ...  <BH(BHNO)>,     (DISTANCE FROM TUNNEL C.L.
                                        TO EACH 'BOREHOLE')    */
END OF FILE
```

```
TUNPOT:PROCEDURE OPTIONS(MAIN);
/*    THIS PROGRAM CALCULATES THE POTENTIAL FIELD AROUND A TUNNEL USING
      THE FINITE DIFFERENCE METHOD. A CUBIC MESH IS SET UP WITH DIM-
      NENSIONS 'MLENGTH','MWIDTH',AND 'MHEIGHT' UNITS, SCALED TO GIVE A
      TUNNEL DIAMETER OF 4 UNITS. THE TUNNEL IS LOCATED AT A DEPTH 'MZ'. A
      NUMBER OF LAYERS OF DIFFERING PERMEABILITY MAY BE MODELLED AND
      THESE MAY BE ANISOTROPIC.    */
DCL (HEIGHT,WIDTH,LENGTH,INVERT,SOFFIT,UJ,TUNLENGTH,LINEDLENGTH,SWITCH,
TEST,TEST2) FIXED BIN;
DCL CONTOUR(4) CHAR(4),CHAR(40),CHAR(8) VARYING,FIXED BIN,FIXED BIN,
    FIXED BIN,(*,*) FLOAT);
DCL (PERMUP,PERMDN,PERMH,PMAX,PREC,ORFACTOR,FACING,GUESS) FLOAT;
DCL (P(0:HEIGHT+1,-1:WIDTH+1,-1:LENGTH+1),
P2(0:HEIGHT2,0:WIDTH2,0:LENGTH2)) FLOAT CONTROLLED;
DCL (VE(LAYERNO),H(LAYERNO)) FLOAT CONTROLLED;
DCL (DLAYERNO,J) FIXED BIN CONTROLLED;
DCL (VE(10),HE(10)) FLOAT;
DCL DE(10) FLOAT BIN;
DCL (DEND,FILE,OUTPUT,
DCL (HEIGHT2,WIDTH2,LENGTH2,Z,DIA,SHIELDLENGTH,NIT,KOUNT) FIXED BIN;
DCL (TUNDIA,CHAR(8)) VARYING;
DCL (TA(0:100),TB(0:100)) FLOAT;
ON ENDFILE(SYSIN) GO TO FINISH;
/*    ID NUMBER (FOR OUTPUT IDENTIFICATION), MAXIMUM POTENTIAL (ARBITRARILY
      100), AND TUNNEL DIAMETER ARE SET    */
PMAX=100;
DIA=4;
IDNUM='MNH8';
/*  DATA IS READ IN.    */
START:GET DATA;
ALLOCATE V,H,D;
DO I=1 TO LAYERNO;
  GET LIST(VE(I),H(I),D(I));
END;
KOUNT=0;
/*    POTENTIAL FIELD IS ALLOCATED A CONSTANT, GUESSED VALUE.    */
ALLOCATE P;
        P=GUESS;
        P(0,*,*)=0;
        P(*,-1,*)=0;
        P(*,*,-1)=0;
        P(*,*,LENGTH+1)=0;
LINEDLENGTH=TUNLENGTH-SHIELDLENGTH;
SOFFIT=Z-DIA/2;
INVERT=Z+DIA/2;
UJ=WIDTH-DIA/2;
TEST2=1;
/*    THE FOLLOWING SERIES OF DO LOOPS ASSIGNS THE BOUNDARY
      CONDITIONS.    */
LOOP:TEST=1;A=99;
     N=1;
/*    TA AND TB PROVIDE A RUNNING CHECK ON THE PROGRESS OF
      THE ITERATIONS.    */
TA(KOUNT)=P(5,12,15);
TB(KOUNT)=P(14,12,7);
/*    PERMEABILITIES ARE ASSIGNED TO EACH LAYER.    */
      DO I=1 TO HEIGHT;
      PERMUP,PERMDN=V(N);
/*    PERMHH(N);
      IF I=D(N) THEN DO;
```

```
      PERMDN=V(N+1);
      PERMH=PMAX/H(N+1);
      N=N+1;
      END;
  DO J=WIDTH BY -1 TO 0;
  IF I>=SOFFIT & I<=INVERT & J>=UJ THEN GO TO LOOP2;
    DO K=0 TO LENGTH;
      A=1;
  IF I=HEIGHT THEN DO;
    A=A*PERMDN*P(I+1,J,K)-PERMUP*P(I-1,J,K);
    B=B+PERMDN-PERMUP;
    END;
    IF J=WIDTH THEN
      A=A+PERMH*(P(I,J+1,K)-P(I,J-1,K));
    IF TUNLENGTH=LENGTH THEN DO;
      IF K=0 THEN A=A+PERMH*(P(I,J,K-1)-P(I,J,K+1));
      IF K=LENGTH THEN A=A+PERMH*(P(I,J,K+1)-P(I,J,K-1));
    END;
/*  FINITE DIFFERENCE CALCULATION.    */
    TEMP=P(I,J,K)+((PERMUP*P(I-1,J,K)+PERMDN*P(I+1,J,K)+PERMH*(
    P(I,J-1,K)+P(I,J+1,K))+5(I,J,K-1)+P(I,J,K+1))-A)/(PERMUP+
    PERMDN+4*PERMH-B))-P(I,J,K))*ORFACTOR;
IF P(I,J,K)=0 THEN ACC=1;
ELSE ACC=TEMP/P(I,J,K);
/*    CONVERGENCE IS CHECKED.    */
IF ACC>1+PREC|ACC<1-PREC THEN TEST,TEST2=1;
P(I,J,K)=TEMP;
A=99;
    END;
GO TO END2;
LOOP2:DO K=0 TO LENGTH;
        A=B=0;
  IF TUNLENGTH=LENGTH THEN DO;
    IF K=0 THEN A=A+PERMH*(P(I,J,K-1)-P(I,J,K+1));
    IF K=LENGTH THEN A=A+PERMH*(P(I,J,K+1)-P(I,J,K-1));
  END;
  IF K<LINEDLENGTH THEN
    IF J=UJ THEN
      IF I=SOFFIT+2 THEN DO; A=A+PERMH*(P(I,J+1,K)-P(I,J-1,K));
          GO TO CALC;    END;
        ELSE GO TO CALC;
    ELSE IF J=UJ+1 THEN IF I=SOFFIT+1 THEN GO TO KS;
        ELSE IF I=INVERT-1 THEN GO TO KI;
        ELSE IF I=SOFFIT+2 THEN GO TO KA;
        ELSE GO TO CALC;
    ELSE IF J=UJ+2 THEN IF I=SOFFIT THEN GO TO KS;
        ELSE IF I=INVERT THEN GO TO KI;
        ELSE GO TO KA;
    ELSE GO TO CALC;
  ELSE IF K<TUNLENGTH
    THEN IF J=UJ & (I=SOFFIT | I=INVERT) THEN GO TO CALC;
      ELSE DO;
        P(I,J,K)=PMAX*I/INVERT;
        GO TO END;
      END;
    ELSE IF J=WIDTH THEN A=PERMH*(P(I,J+1,K)-P(I,J-1,K));
    GO TO CALC;
KS:   A=A+PERMH*(P(I,J+1,K)-P(I,J-1,K))+PERMDN*P(I+1,J,K)-PERMUP*
      P(I-1,J,K);
      B=B+PERMDN-PERMUP;
```

```
KI:   GO TO CALC;
      A=A+PERMH*(P(I,J+1,K)-P(I,J-1,K))+PERMUP*P(I-1,J,K)-PERMDN*
      P(I+1,J,K);
      B=B+PERMUP-PERMDN;
      GO TO CALC;
KA:   P(I,J,K)=5;
      GO TO END;
/*  FINITE DIFFERENCE CALCULATION.    */
CALC: TEMP=P(I,J,K)+((PERMUP*P(I-1,J,K)+PERMDN*P(I+1,J,K)+PERMH*
      (P(I,J-1,K)+P(I,J+1,K)+P(I,J,K-1)+P(I,J,K+1))-A)/(PERMUP+
      PERMDN+4*PERMH-B))-P(I,J,K))*ORFACTOR;
IF P(I,J,K)=0 THEN ACC=1;
ELSE ACC=TEMP/P(I,J,K);
/*    CONVERGENCE IS CHECKED.    */
IF ACC>1+PREC|ACC<1-PREC THEN TEST,TEST2=1;
P(I,J,K)=TEMP;
END: A=B=0;
     END;
  END2:END;
END:
    KOUNT=KOUNT+1;
      IF TEST=0 THEN DO;
        IF TEST2=0 THEN GO TO DETAIL;
        TEST2=0;
/*    CHANGES OVER-RELAXATION FACTOR.    */
        ORFACTOR=ORFACTOR+FACING;
      END;
      IF KOUNT<NIT THEN GO TO LOOP;
DETAIL:TA(KOUNT)=P(5,12,15);
/*    OUTPUTS POTENTIAL FIELD CLOSE TO TUNNEL INTO FILE "BOUND".    */
TB(KOUNT)=P(14,12,7);
HEIGHT2=3*DIA+1;
WIDTH2=3*DIA/2+1;
LENGTH2=SHIELDLENGTH+2*DIA+1;
ALLOCATE P2;
DO I=0 TO HEIGHT2;
  DO J=0 TO WIDTH2;
    DO K=0 TO LENGTH2;
      P2(I,J,K)=P((Z-3*DIA/2),(J+UJ-DIA),(K+LINEDLENGTH-DIA));
    END;
  END;
END;
J=1;
DO I=1 TO LAYERNO;
  IF D(I)<Z-3*DIA/2 THEN GO TO ENDLAYER;
  IF D(I)>Z+3*DIA/2 THEN DO;
    DE(J)=3*DIA+1;
    I=LAYERNO;
    GO TO LAYEROUT;
  END;
  DE(J)=D(I)-Z+3*DIA/2;
  LAYEROUT:VE(J)=V(I);
  HE(J)=H(I);
  L=J+1;
  J=J+1;
ENDLAYER:END;
OPEN FILE(BOUND) OUTPUT;
PUT FILE(BOUND) LIST(SHIELDLENGTH,DIA,LN,PMAX,ORFACTOR,PREC,SWITCH);
DO
  PUT FILE(BOUND) LIST(VE(J),HE(J),DE(J));
```

```
END;
PUT FILE(BOUND) LIST(P2);
CLOSE FILE(BOUND);
FREE P2;
/*    PRINTED OUTPUT    */
F1:  FORMAT(X(5),A,F(5,4));
F2:  FORMAT(X(5),A,F(5,2));
F3:  FORMAT(R(F2),A);
DO I=0 TO KOUNT;
  PUT SKIP DATA(TA(I),TB(I));
END;
OPUT:PUT PAGE EDIT('INPUT DETAILS')(X(40),A);
     PUT SKIP(6) EDIT('BLOCK DIMENSIONS=',X(5),A);
     PUT SKIP(4) EDIT('DEPTH OF BLOCK=',HEIGHT,' UNITS')(R(F1));
     PUT SKIP(4) EDIT('WIDTH OF BLOCK=',WIDTH,' UNITS')(R(F1));
     PUT SKIP(2) EDIT('LENGTH OF BLOCK=',LENGTH,' UNITS')(R(F1));
     PUT SKIP(6) EDIT('TUNNEL DIMENSIONS=')(X(5),A);
     PUT SKIP(4) EDIT('DEPTH TO AXIS=',Z,' UNITS')(R(F1));
     PUT SKIP(2) EDIT('DIAMETER OF TUNNEL=',DIA,' UNITS')(R(F1));
     PUT SKIP(2) EDIT('LENGTH OF TUNNEL=',TUNLENGTH-2*DIA,' UNITS')(R(F1));
     PUT SKIP(2) EDIT('UNLINED LENGTH=',SHIELDLENGTH,' UNITS')(R(F1));
DO N=1 TO LAYERNO;
PUT SKIP(4) EDIT('LAYER ',N)(X(10),A,F(2));
PUT SKIP(2) EDIT('HORIZONTAL PERMEABILITY=',H(N),'UNITS')(R(F3));
PUT SKIP(2) EDIT('VERTICAL PERMEABILITY=',V(N),'UNITS')(R(F3));
PUT SKIP(2) EDIT('THICKNESS OF LAYER=',DEN)=D(N-1),'UNITS')(R(F1));
END;
     PUT SKIP(6) EDIT('Z/DIA=',INVERT/DIA)(R(F2));
     PUT SKIP(2) EDIT('L/DIA=',SHIELDLENGTH/DIA)(R(F2));
     PUT SKIP(2) EDIT('Z/H=',INVERT/HEIGHT)(R(F2));
     PUT SKIP(12) EDIT('NUMBER OF ITERATIONS=',KOUNT)(X(5),A,F(2));
     PUT SKIP EDIT('(ITERATION CONTINUED TO A PRECISION OF ',
PREC*100,'%)')(X(6),A,F(5,2),A);
     PUT SKIP(2) EDIT('OVER RELAXATION FACTOR=',ORFACTOR)
(X(5),A,F(5,2));
     PUT PAGE EDIT('POTENTIAL ARRAY. VERTICAL SECTION ALONG TUNNEL CENTR
E-LINE.')(X(5),A);
     PUT SKIP(4);
     J=WIDTH;
PV:  DO I=0 TO HEIGHT;
       PUT SKIP(3);
       DO K=0 TO LENGTH;
         PUT EDIT(P(I,J,K))(F(7,3));
       END;
     END PV;
IF SWITCH=2 | SWITCH=3 THEN
  CALL CONTOUR('CENT',4,'VERT.SECTION ALONG TUNNEL CENTRE-LINE.',
  IDNUM,10,LENGTH+1,HEIGHT+1,P(*,WIDTH,*));
     PUT PAGE EDIT('POTENTIAL ARRAY. HORIZONTAL SECTION ALONG TUN
EL AXIS.')(X(5),A);
     PUT SKIP(4);
PH:  DO J=0 TO WIDTH;
       PUT SKIP(3);
       DO K=0 TO LENGTH;
         PUT EDIT(P(Z,J,K))(F(7,3));
       END;
     END PH;
A12:IF SWITCH=2 | SWITCH=3 THEN
  CALL CONTOUR('AXIS',4,'HORIZONTAL SECTION ALONG TUNNEL AXIS',IDNUM,
  10,LENGTH+1,WIDTH+1,P(Z,*,*));
PUT PAGE EDIT('POTENTIAL ARRAY. VERTICAL SECTION IN PLANE OF TUNNEL',
'FACE.')(X(5),A,A);
```

```
     PUT SKIP(4);
PX:  DO I=0 TO HEIGHT;
       PUT SKIP(3);
       DO J=WIDTH BY -1 TO 0;
         PUT EDIT(P(I,J,FLOOR(LENGTH/2)))(F(7,3));
       END PX;
PLAN=TUNLENGTH;
IF SWITCH=2 | SWITCH=3 THEN
  CALL CONTOUR('FACE',4,'VERTICAL SECTION PARALLEL TO TUNNEL FACE',IDNUM,
  10,WIDTH+1,HEIGHT+1,P(*,*,PLAN));
A13: GO TO FINISH;
CONTOUR:PROC (TI,TITLE,USERID,INC,PLOTLENGTH,ROW,P);
/*    OUTPUTS SECTION THROUGH POTENTIAL FIELD INTO FILE 'FNAME'
      IN A FORMAT SUITABLE FOR PROCESSING BY CONTOURING PROGRAM.    */
DCL FNAME FILE,
    TI CHAR(4),
    TITLE CHAR(40) VARYING,
    USERID CHAR(8) VARYING,
    FORM CHAR(20) INITIAL('10F8.4/10F8.4/10F8.4/10F8.4/'),
    FORMAT CHAR(20) VARYING,
    (INC,ROW,PLOTLENGTH,X,Y) FIXED BIN,
    P(1:ROW,1:COL) FLOAT;
LOWCON=0;
HICON=100;
PLOTWIDTH=8;
DENOM=1;
OPEN FILE(FNAME) OUTPUT TITLE(TI);
PUT FILE(FNAME) LIST('12      1.2E0      1.2E0      0.2E0')(A)
     PUT FILE(FNAME) LIST('12      1.2E0      1.2E0      0.2E0')(SKIP,A)
     (USERID,'15',LOWCON,INC,HICON,'19')(SKIP,A,SKIP,A,3 F(10),SKIP,A);
X=7*TRUNC(ROW/10);
Y=MOD(ROW,10);
IF Y=0 THEN DO;
  FORMAT=SUBSTR(FORM,1,X-1);
  PUT FILE(FNAME) SKIP EDIT('(',FORMAT,')')(A,A,A);
  END;
ELSE DO;
FORMAT=SUBSTR(FORM,1,X);
PUT FILE(FNAME) SKIP EDIT('(',FORMAT,Y,'F8.4)')(A,A,F(1),A);
END;
PUT FILE(FNAME) EDIT('(1)',PLOTLENGTH,ROW,PLOTWIDTH,DENOM)
(SKIP,A,4 F(10));
C5: DO J=0 TO PLOTLENGTH-1;
PUT FILE(FNAME) SKIP;
  DO I=ROW-1 BY -1 TO 0;
PUT FILE(FNAME) EDIT(P(I,J))(F(8.4));
END C5;
PUT FILE(FNAME) EDIT('26','13')(SKIP,A);
CLOSE FILE(FNAME);
RETURN;
END CONTOUR;
FINISH: END TUNPOT;
/*                    INPUT FORMAT
HEIGHT<HEIGHT OF BLOCK (UNITS)>,
WIDTH=<WIDTH OF BLOCK (UNITS)>,
LENGTH=<LENGTH OF BLOCK (UNITS)>,
TUNLENGTH=<TOTAL LENGTH OF TUNNEL (UNITS)>,
SHIELDLENGTH=<UNGROUTED LENGTH (UNITS)>,
Z=<DEPTH TO AXIS (UNITS)>,
LAYERNO=<NUMBER OF LAYERS>,
```

```
GUESS=<ESTIMATED POTENTIAL>,
ORFACTOR=<OVER-RELAXATION FACTOR>,
FACING=<OVER-RELAXATION FACTOR INCREMENT>,
PREC=<PRECISION AT WHICH ITERATION TERMINATES>,
NIT=<MAXIMUM PERMITTED NUMBER OF ITERATIONS>,
SWITCH=<1=NUMERICAL OUTPUT ONLY
        2=ADDITIONAL OUTPUT TO CONTOURING FILES ONLY
        3=1+2>;
<HORIZONTAL PERMEABILITY> <VERTICAL PERMEABILITY> <DEPTH
    TO BASE OF LAYER>,  (REPEAT FOR EACH LAYER)    */
END OF FILE
```

INCLINOMETER RESULTS. HOWDEN.

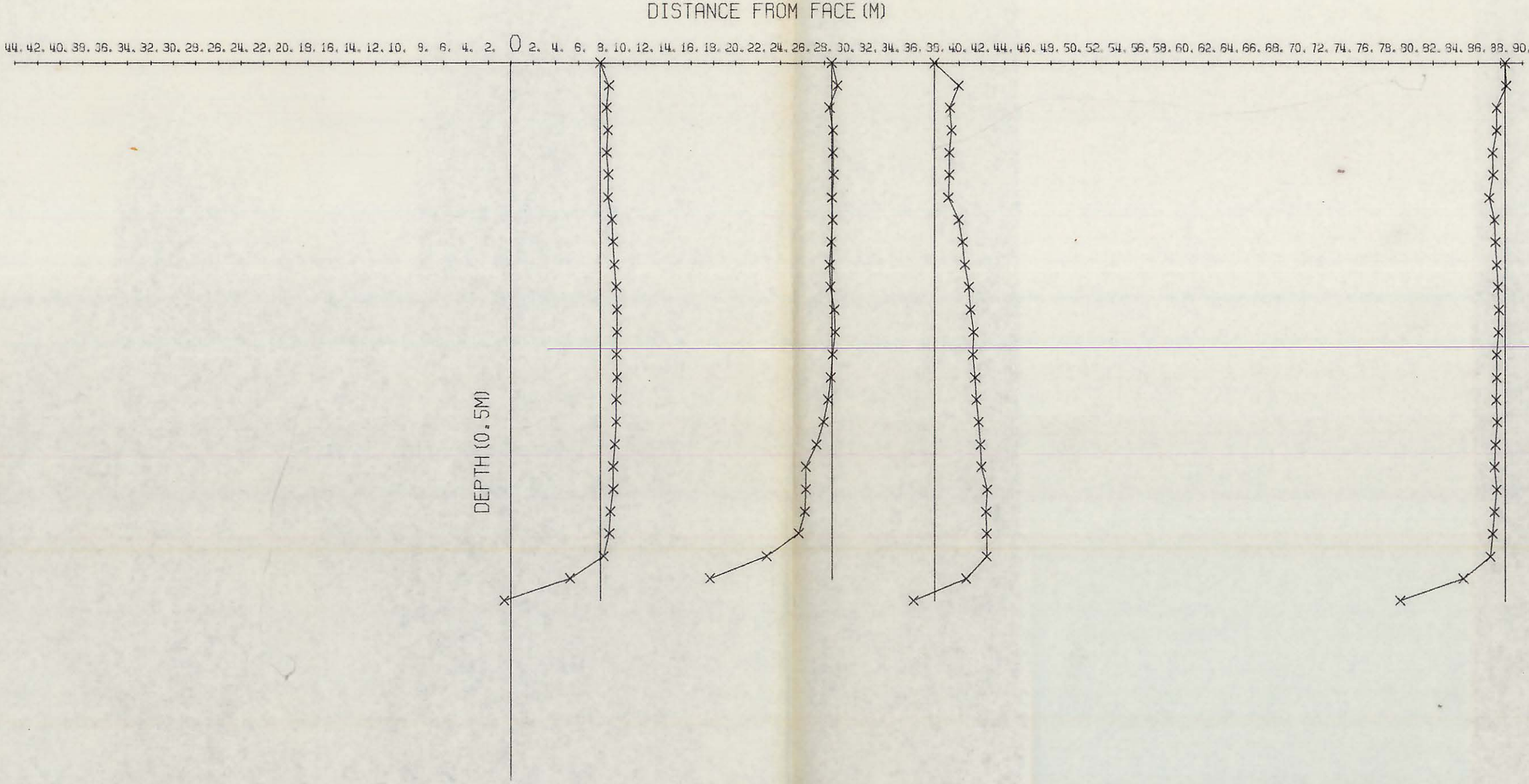

```
      CHECK:PROC OPTIONS(MAIN);
      /*  TO REMOVE ANOMALOUS INCLINOMETER DATA + REVERSE IT IF REQUIRED  */
      DCL (BH,DINT,DIST,SH,AV,TOTAL) FLOAT,
          MOD FILE OUTPUT,
          (ID,ICON,REV) FIXED BIN,
          (B,C,D,E) FLOAT,
          (S(0:ID),(T,A)(0:ID,2)) FIXED BIN CONTROLLED,
          CHPAR CHAR(80),
          (FLAG,KOUNT,TEST) FIXED BIN;
      READ:GET LIST(BH);
      IF BH<1.0 THEN GO TO FINISH;
        GET LIST(ID,DINT,ICON,DIST,SH);
        IF ID<0 THEN DO;
          ID=-ID;  REV=-1;
        END;
        ALLOCATE S,T,A;
        T(0,*),A(0,*)=0;
        DO I=1 TO ID;
          GET LIST(T(I,1),T(I,2),A(I,1),A(I,2));
        END;
      /*    IF REV=-1 THEN DATA IS REVERSED    */
        IF REV=-1 THEN DO;
          T=-T;  A=-A;
        END;
      /*    AVERAGE SUM FOUND, DISCOUNTING ERRONEOUS DATA    */
        TOTAL=0;
        DO I=1 TO ID;
          S(I)=T(I,1)+T(I,2)+A(I,1)+A(I,2);
          TOTAL=TOTAL+S(I);
        END;
        AV=TOTAL/ID;
        TOTAL,KOUNT,TEST=0;
        DO I=1 TO ID;
          IF ABS(S(I)-AV)<20 THEN DO;
            TOTAL=TOTAL+S(I);
            KOUNT=KOUNT+1;
          END;
        END;
        AV=TOTAL/KOUNT;
      /*    IF SUM DIFFERS FROM AVERAGE BY MORE THAN 20, DATA    */
      /*    REPLACED BY AVERAGE OF ADJACENT VALUES    */
        LOOP:FLAG=0;
        DO I=1 TO ID;
          IF ABS(S(I)-AV)>20 THEN DO;
            IF I=1 THEN DO;
              T(I,1)=T(I+1,1);  T(I,2)=T(I+1,2);
              A(I,1)=A(I+1,1);  A(I,2)=A(I+1,2);
            END;
            ELSE IF I=ID THEN DO;
              T(I,1)=T(I-1,1);  T(I,2)=T(I-1,2);
              A(I,1)=A(I-1,1);  A(I,2)=A(I-1,2);
            END;
            ELSE DO;
              T(I,1)=(T(I-1,1)+T(I+1,1))/2;
              T(I,2)=(T(I-1,2)+T(I+1,2))/2;
              A(I,1)=(A(I-1,1)+A(I+1,1))/2;
              A(I,2)=(A(I-1,2)+A(I+1,2))/2;
            END;
            S(I)=T(I,1)+T(I,2)+A(I,1)+A(I,2);
            IF ABS(S(I)-AV)>20 THEN FLAG=1;
          END;
        END;
        IF FLAG=1 THEN GO TO LOOP;
      /*    CORRECTED DATA OUTPUT INTO FILE MOD    */
        PUT FILE(MOD) EDIT(BH,ID,DINT,ICON,DIST,SH)(F(3,1),X(7),F(2,0),X(8),
                          F(3,1),X(7),F(1,0),X(9),F(6,2),X(4),F(3,1));
        DO I=1 TO ID;
          PUT FILE(MOD) SKIP EDIT(T(I,1),T(I,2),A(I,1),A(I,2))
                                 (4(F(4,0),X(6)));
        END;
        PUT FILE(MOD) SKIP;
        GO TO READ;
      FINISH:PUT FILE(MOD) EDIT(BH)(F(3,1));
      END CHECK;
      /*    INPUT FORMAT.
            INPUT FOR EACH BOREHOLE SAME AS FOR INCPLOT, I.E.
            CONTROL CARD FOLLOWED BY RAW DATA    */
END OF FILE
```